UNIVERSITA' DEGLI STUDI DI PARMA

Dottorato di ricerca in Scienze Chimiche

Ciclo XXI

Synthesis of multivalent glycoclusters for the selective inhibition of lectins and targeted imaging

Coordinatore:
Chiar.mo Prof. Alberto Girlando.....

Tutor:
Chiar.mo Prof. Rocco Ungaro
Prof. Alessandro Casnati.....

Dottorando: Gabriele Rispoli

2006-2008

Contents

Chapter 1

Multivalency and the glycoside cluster effect

1.1 General aspects of multivalency

In order to enhance the binding efficiency and selectivity of the designed ligands, chemists usually try to optimise the complementary matching (in terms of size and nature of binding forces) between the interacting species. However, quite recently they started to take advantage of a new powerful concept, multivalency, which is the ability of a particle (or molecule) to bind another particle (or molecule) via multiple simultaneous noncovalent interactions (**Fig. 1**).

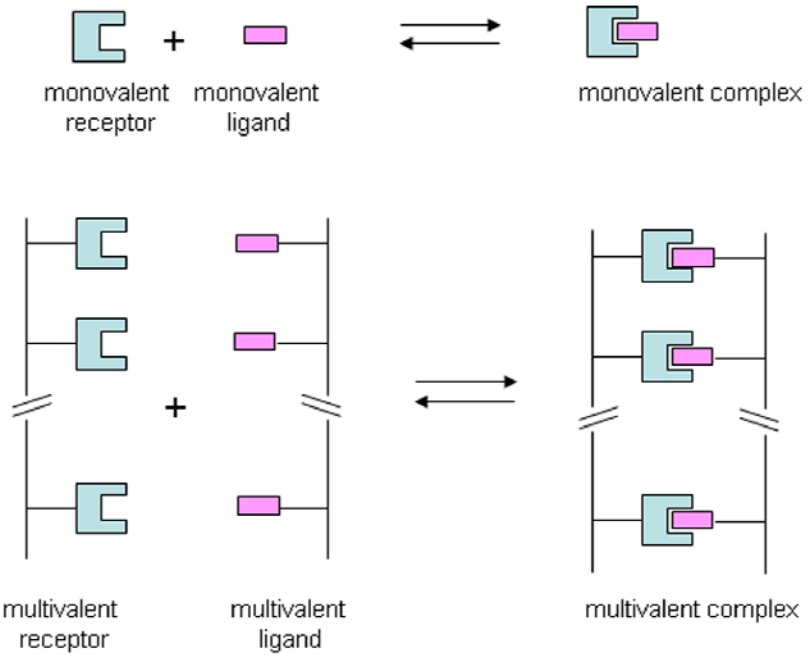

Fig. 1 Example of monovalent *vs* multivalent complexes. Taken from ref. 1

The *valency* is therefore the number of ligating functionalities of the same or similar types connected to each of these entities. Multivalent interactions usually result in high specificity and thermodynamic and kinetic stability (much higher than those arising from a simple monovalent interaction). Nature exploits multivalency to convert relatively weak interactions (*e.g.* carbohydrate-protein interactions) into strong and specific recognition events. In the biomimetic approach to Drug Design, multivalency has also been exploited to successfully obtain inhibitors of some of these pathogens, allowing to develop therapeutic agents able to neutralise bacterial toxins or to prevent viral or bacterial infections. In the last decade, also Supramolecular Chemistry became more and more interested in applying the multivalency concept to the recognition of biological important molecules and to nanotechnology. Multivalency, in fact, has different and attractive features common to the supramolecular concept of *self-assembly*, such as reversibility, self-sorting and self-repairing and the possibility to reach high thermodynamic and kinetic stability.[2] Virtually any of the noncovalent interactions can be used to form multivalent complexes. Moreover, supramolecular

systems, sometimes simpler than the natural ones, can help the understanding and quantitative description of the multivalent effect.[3] A multivalent ligand (**Fig. 2**) consists of a main core, called *scaffold*, bearing several covalent connections, *linkers* or *spacers*, to the peripheral *ligating* (binding) units.

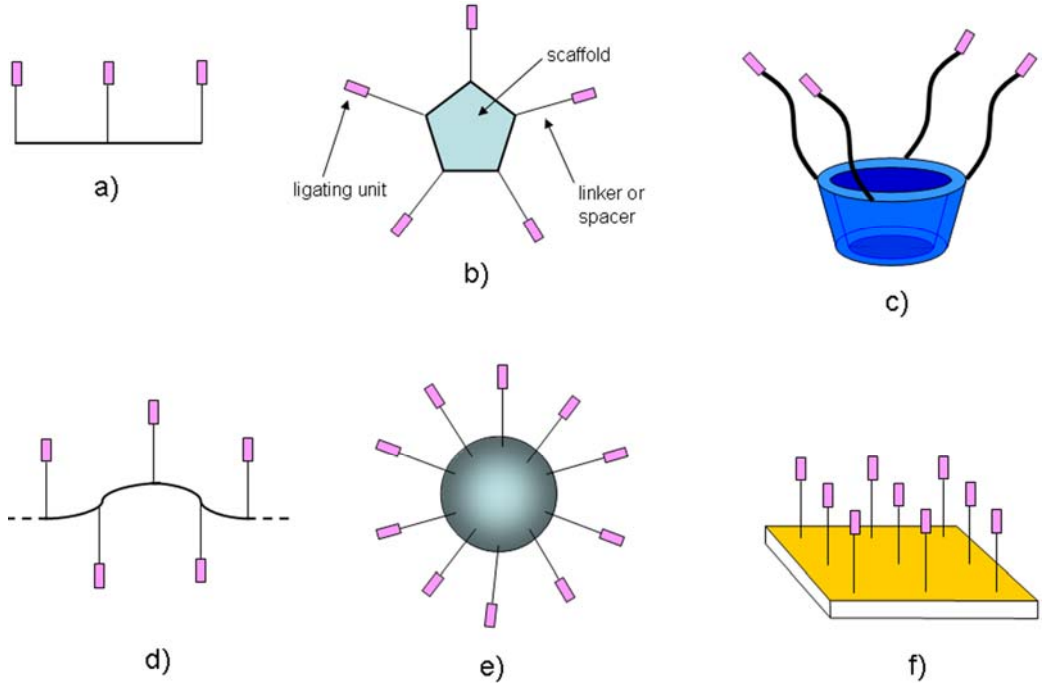

Fig. 2 Different topologies of multivalent ligands. a) 1-D linear arrangement, b) 2-D cyclic/macrocyclic; c) 3-D cavity containing scaffolds (cyclodextrins/calixarenes); d) polymers/peptoids; e) nanoparticles/dendrimers/liposomes; f) 2-D self-assembled monolayers (SAM) on Au/quartz. Taken from ref. 1

Any multivalent scaffold can in principle be used, from those having low valency such as benzene derivatives, monosaccharides, transition metal complexes, azamacrocycles, cyclodextrins or calixarenes (**Fig. 2a-c**) to high valency ones such as dendrimers, polymers, peptoids, proteins, micelles, liposomes, and self-assembled monolayers (SAMs) on nanoparticles or plane surfaces (**Fig. 2d-f**).

Often, the concept of *cooperativity*, generally intended as the influence of the binding of one ligand on the receptor's affinity toward further binding, is associated with multivalency[14]. However, as elegantly pointed out by Ercolani,[4] cooperativity in multivalent systems is extremely scarce. Moreover, although cooperativity can be easily and rigorously assessed by using Hill or Scatchard plots for the binding of monovalent ligands to a multivalent receptor (the most famous case being the binding of four O_2 molecules to tetrameric haemoglobin), much more difficult is to prove its existence when a multivalent ligand interacts with a multivalent receptor.

In general, to describe multivalent binding, an approach based on the additivity of the free energies[5,6] can be used. The standard binding free energy for multivalent binding ΔG°_{multi} is

$\Delta G^{\circ}_{multi} = n\Delta G^{\circ}_{mono} + \Delta G^{\circ}_{interaction}$

where ΔG°_{mono} is the standard binding free energy of the corresponding monovalent interaction, n is the valency of the complex and $\Delta G^{\circ}_{interaction}$ is the balance between favourable and unfavourable effects of tethering.

A rather qualitative but often useful parameter, β, has been introduced by Whitesides et al.,[14] as

$\beta = K_{multi}/K_{mono}$,

where K_{multi} and K_{mono} are the association constants for the multivalent and monovalent complexes, respectively. The parameter β, named *enhancement factor*, has been often used in the literature to compare the efficiency of ligands having different topology and/or valency: molecules with high β values are efficient ligands/inhibitors. Sometimes, if the valency n of the complex is know, this enhancement factor can be normalised to n, giving rise to the parameter β/n. Similarly a *relative potency* (r.p.) has been defined as $IC_{50}^{multi}/IC_{50}^{mono}$ which is often also normalised to the valency n giving rise to r.p./n, *relative potency per ligating unit.*

More rigorous approaches have been proposed to quantitatively describe the multivalent binding process. Kitov and Bundle,[6] for instance, developed a model where the standard free energy of multivalent interaction, $\Delta G^{\circ}_{avidity}$, is a function of three terms ΔG°_{inter}, ΔG°_{intra} (binding free energies for the first intermolecular and the second intramolecular process, respectively, *see* **Fig. 3**) and a statistical term $\Delta S^{\circ}_{avidity}$, namely *avidity entropy*, calculated on the basis of the topology of the complex. The avidity entropy can grow rapidly with the valency of the complex, always favouring binding, which explains why multivalency can overcome the loss of conformational entropy. By a nonlinear fitting of the measured binding energies for a series of multivalent ligands, ΔG°_{inter} and ΔG°_{intra} can be determined, thus allowing to design and maximise the avidity of multivalent ligands.

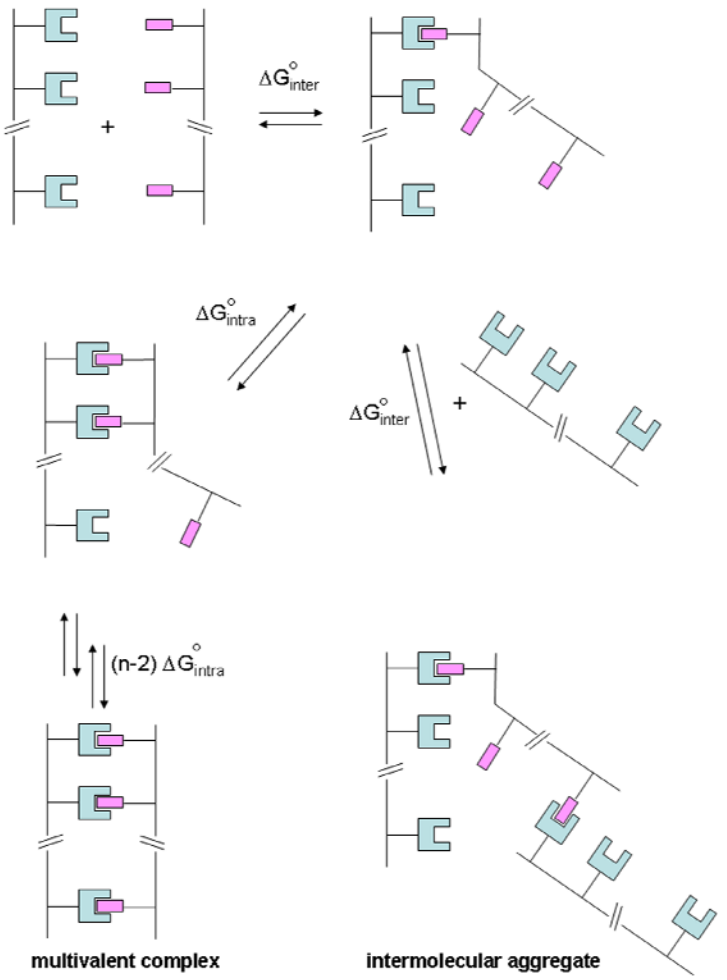

Fig. 3 *Inter*molecular and *intra*molecular processes for the formation of a multivalent complex or of an intermolecular aggregate. Taken from ref. 1

Very important is also the choice of the spacer which links the scaffold to the ligating units. It should be of the proper length to allow the simultaneous binding of all the ligating groups, without generating enthalphic unfavourable strains (enthalpically diminished binding).

Finally, the kinetics of multivalent interactions is usually characterised by a step-wise dissociation pathway having extremely low dissociation rates. This also explains why the use of very high concentration of monovalent competing species is necessary to avoid rebinding of the partially dissociated multivalent complex.

1.1. Glycobiology and the glycoside cluster effect

Glycobiology[7] is an interdisciplinary science, crossing the fields of chemistry, biology and medicine studying all the aspects of the structure, biosynthesis and functions of glycans widely distributed in nature. A very broad spectrum of functions have been revealed to glycans, besides the

well-known, energetic and structural role they have. In fact, it is now clear that carbohydrates are involved in many important cellular processes regarding interactions with different chemical or biological species as, for example, viruses, bacteria, proteins, nucleic acids, hormones and other cells (**Fig. 4**).[8] In almost all such processes a carbohydrate ligand usually binds to a protein receptor.[9,10] Therefore there is an increasing interest in the synthesis of new neoglycoconjugates or high affinity mimics of native saccharides which could interfere in these processes; such compounds have potential therapeutic value in the treatment of viral, parasitic, mycoplasmal and bacterial infections, and of a wide range of human tumours. The study and understanding of protein–carbohydrate interactions, is therefore of paramount importance in glycobiology.

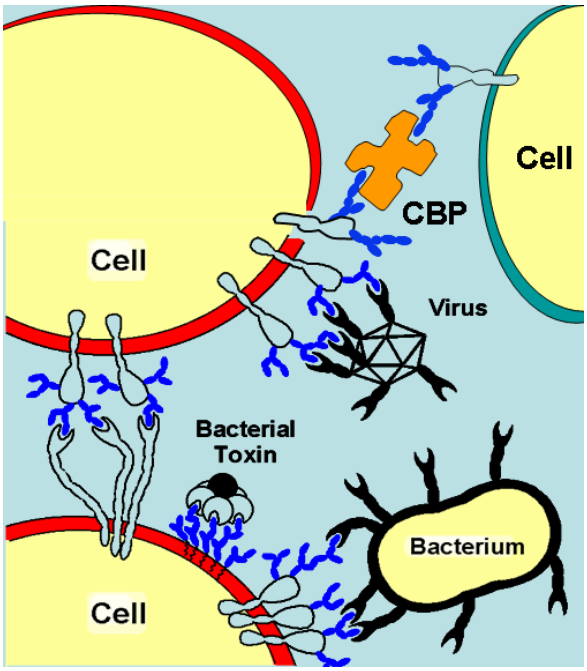

Fig. 4. Adapted from F. Stoddart's web page

http://www.chem.ucla.edu/dept/Faculty/stoddart/research/multivalency.htm

A reason for the difficulty in understanding completely the role of carbohydrates in all the physiological and pathological events of cell communication and trafficking lies in the structural complexity of oligosaccharides. While the other two classes of biopolymer, nucleic acids and proteins, have a linear arrangement of repeating units, carbohydrate building blocks have multiple points of attachment, leading to highly branched and stereochemically differentiated structures.[11] This structural complexity is further increased by post–synthetic modifications: hydroxyl groups can be sulphated, phosphorylated, acetylated, or oxidized to generate distinct biological activities[4]. All these elaborations of the sugars especially on the cell surface will equip the cells with a peculiar set of epitopes like a signature, distinguishing cell types from another. The mapping of the glycan profiles will at least provide an insight into the cell's individual activity pattern of the enzymatic

machinery for the production of words in the sugar code (glycocode)[11,12]. In analogy to genomics and proteomics this work to map glycan determinants has been named glycomics[13].

A second difficulty in studying carbohydrate-protein interactions is that binding affinities are weak, with dissociation constants in the milli-micromolar range;[9] however, the efficiency and selectivity of the *in vivo* control of events mediated by protein–carbohydrate binding requires significantly greater affinity. Nature overcomes this limitation by combining multiple simultaneous interactions between two or more carbohydrates of the glycoproteins organised in domains on the cell surface - "glycocalix" - and a corresponding multimeric protein (**Fig. 4**). This particular type of multivalent effect[14] has been also named "glycoside cluster effect".[9,15] These multivalent interactions have several mechanistic and functional advantages over their monovalent counterparts, the most relevant one probably being the ability to increase the specificity of binding.

1.3 The carbohydrate binding proteins: the lectins

There are several examples in nature of proteins which noncovalently interact with carbohydrates: the carbohydrate binding proteins (CBP). Important examples are carbohydrate-specific enzymes and anti-carbohydrate antibodies. However, recently, another class of such proteins, the lectins,[10,16,17] raised the interest of many bio-organic research groups. Lectins, in fact, bind mono- and oligosaccharides reversibly and with high specificity, but are devoid of catalytic activity, and in contrast to antibodies, are not the products of an immune response. Lectins contain typically two or more carbohydrate-combining sites and therefore bind to cell membrane oligosaccharide by exploiting the multivalent effect. When reacting with cells, for example erythrocytes, they bind not only the sugars of a single cell, but eventually cause cross-linking of the cells and their subsequent precipitation, a phenomenon referred to as cell agglutination. Lectins also form cross-links between polysaccharide or glycoprotein molecules in solution and induce their precipitation. Both the agglutination and precipitation reactions of lectins are inhibited by the sugar ligands for which the lectins are specific. Lectins are found in most organisms, ranging from viruses and bacteria to plants and animals. They represent a heterogeneous group of oligomeric proteins that vary widely in size, structure, molecular organization, as well as in the constitution of their combining sites. Although lectins were first described at the beginning of the 20th century, their started to catch remarkable attention in the 1960s, when it was demonstrated their role on cell surfaces during physiological and pathological processes, from cell differentiation to cancer.[18] The study of lectins and their role in cell recognition processes, as well as the application of these proteins for the study of carbohydrates

in solution and on cell surfaces, are giving important contributions to the advancement of glycobiology.[19]

Lectins are divided, according to their origin, in microbial, plant or animal[16] lectins. Initially they were classified, into five groups, depending on the specificity to the monosaccharide for which they exhibit the highest affinity:

i). D-mannose,

ii). D-galactose/*N*-acetyl-D-galactosamine,

iii). *N*-acetyl-D-glucosamine,

iv). L-fucose,

v). *N*-acetylneuraminic acid.

Relevant for the biological activities of lectins is the fact that of the numerous monosaccharides found in nature, only those listed above are typical constituents of surfaces of eukaryotic cells.

The classification of lectins according to their monosaccharide specificity, however, masks the fact that they often exhibit an exquisite specificity for di-, tri-, and tetrasaccharides (with association constants up to 1000-fold higher as compared with the monosaccharide) and that certain lectins interact only with oligosaccharides. Moreover, lectins of the same specificity group may differ markedly in their affinities for different oligosaccharides. From the functional point of view, binding of oligosaccharides is of special significance since, as mentioned earlier, they are most likely the natural ligands of lectins.

However, also thanks to the high-resolution X-ray crystallography of lectins and their complex with carbohydrates it was possible to identify the carbohydrate recognition domain (CRD): therefore, the more accepted current classification of lectins is based on the homology of their CRD and they are divided in C-type, I-type, S-type, P-type, pentraxins, wild-type and so on..

C-type lectins are, for example, calcium dependent lectins while I-type show an immunoglobulin-like CRD.

Animal lectins can be divided, according to the classification reported in Table 1, into 5 different families. Very important animal lectins are the galectins. They share a cation-independent binding capacity to β-galactosides and show the conservation of a series of amino acid residues with relevance for the topology of the CRD. The former designation S-type lectins should be abandoned due to a lack of precision. Members of other lectin families are also soluble without addition of detergent and Cys residues (sulfhydryl groups) are not essential for the activity of several galectins, as shown by site-directed mutagenesis and the natural occurrence of galectins without a Cys residue.[16]

Family	Structural motif	Carbohydrate ligand
C-type	CRD conserved	variable (mannose, galactose, fucose, heparin tetrasaccharide)
I-type	immunoglobulin-like CRD	variable (Man,GlcNAc,, HNK-1 epitope, hyaluronic acid, *a2,3/a2,6*-sialyllactose)
Galectins (S-type)	CRD conserved	β-galactoside
Pentraxine	pentameric subunit arrangement	4,6-cyclic acetal of β-galactose, galactose, sulfated and phosphorylated monosaccharides
P-type	CRD conserved	mannose-6-phosphate-containing glycoproteins

Table 1. Current categories for classification of various animal lectins.

Immunohistochemical fingerprinting had revealed, among galectin three subgroups (**Fig. 5**), that is, homodimeric proto-type (Gal-1), chimera-type (Gal-3), and tandem-repeat-type (Gal-4) proteins, an unfavourable relationship of galectin expression to prognosis in several tumor systems, for example in colon cancer for galectin-1, galectin-3, and galectin-4.[20]

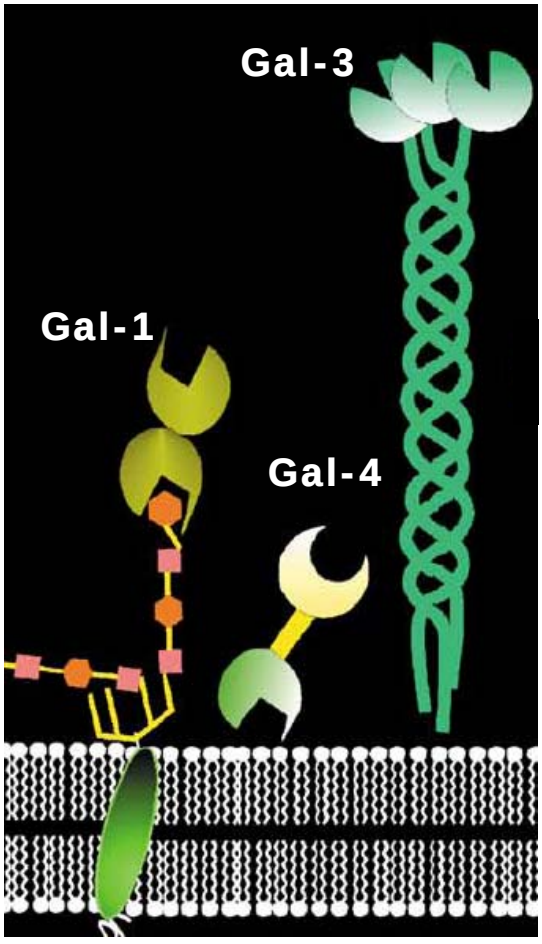

Fig. 5: The three different topologies of galectins: Gal-1 is binding to a membrane glycoprotein.

1.4 Inhition of biological processes by polyglycosylated ligands

This discovery of functional lectin–carbohydrate interactions and the possibility to inhibit them by using small polyglycosylated molecules offer enormous potential to the design of new drugs which could interfere with several pathological events (**Fig. 6**) such as intoxication by plant/bacterial toxins, viral and bacterial infections and tumor progression.

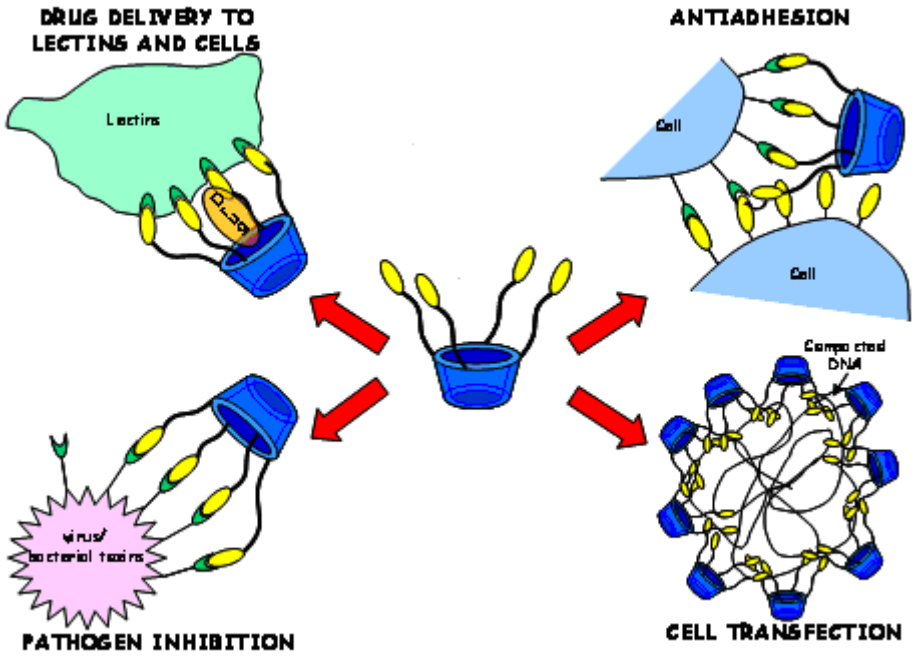

Fig. 6: Examples of multivalent ligands and their potential uses

If nature has circumvented the tight binding limitation through multivalency, it seems reasonable that multivalent ligands should bind with high affinity as well. On this basis many polyglycosylated molecules have been prepared and studied as multivalent ligands for a wide range of lectins. Most of these ligands show enhancements in activity compared to the corresponding monovalent ligand indicating that multivalency, *i.e.* the "glycoside cluster effect", is involved.

Several model systems have been developed to study multivalent carbohydrate-protein interactions.[21] The low valency model systems present less than 20 carbohydrate ligands while the high valency model systems (glycoproteins, glycosylated monolayers/nanoparticles) possess a larger number (often hundreds) of carbohydrate ligands and will be not considered in this brief survey.

Model systems with low valency have been important for defining the geometric and structural requirements for tight binding to polyvalent receptors[22]. While these models are reasonably well defined and readily modified using synthetic organic chemistry, it is often necessary to prepare a large number of compounds in order to identify polyvalent ligands that achieve significant binding enhancements.[23] Most of the polyvalent systems with low valency have been designed using detailed structural information of the carbohydrate binding protein. This approach, that is obviously limited to systems for which crystallographic or NMR structural data are available, significantly reduces the time required to develop a polyvalent system having ligands with the appropriate geometry and spacer length. Kiessling and co-workers[24] generated a series of ligands, possessing structural diversity, to explore the effects of architecture on the inhibition and clustering of a model protein, the lectin concavalin A (Con A); the structural parameters that were varied include scaffold shape, size, valency, and density of binding elements. The authors found that ligands with certain architectures are effective inhibitors: specifically, high molecular weight, polydisperse polyvalent ligands are effective inhibitors for Con A binding, whereas linear oligomeric ligands have structural properties that favour clustering. The shape of a multivalent ligand also influences specific aspects of receptor clustering.

In the following paragraphs few examples of multivalent synthetic ligand will be described, divided by type of scaffold used.

Clusters. Glycoclusters represent a large group of model systems that present a low number of carbohydrate ligands on a small molecular template. These low valency model systems have been extremely important in determining the optimal binding geometries and ligand to ligand distances for a particular multivalent protein; the success or failure of a particular model system depends on the nature of the scaffold and the length of the tether between the scaffold and the carbohydrate. Generally the conformational flexibility and the ligand to ligand spacing in multivalent interactions are very important in this type of compounds; moreover it is very difficult to design the appropriate polyvalent ligand for a particular system. Concerning the importance of maximize the interactions between the receptor and the ligand it is important to project and design a molecule that incorporates structural information of the multiple target sites. Recently Fan[25] prepared a pentavalent ligand of *Escherichia coli* heat-labile enterotoxin (LT) by a modular structure-based design. In this modular approach, the large pentavalent ligand is divided into three modules to mimic the symmetrical arrangement of the five B-subunits of the LT: a semirigid "core", a pentaazamacrocycle (15-N-5) that adopt a 5-fold symmetric structure and provides the basis for the generation of structural complementarity for the overall pentavalent ligand to LT, "linkers" of different length that project in the direction of the receptor binding sites, and "fingers" (galactose)

that fit into the binding sites. The success of this design depends critically on the possibility to change the length of the ligand by assembling a different number of linker units (n in **Fig. 7**): the result is an IC_{50} value of 0.56 μM versus a value of 0.01 μM for the natural receptor.

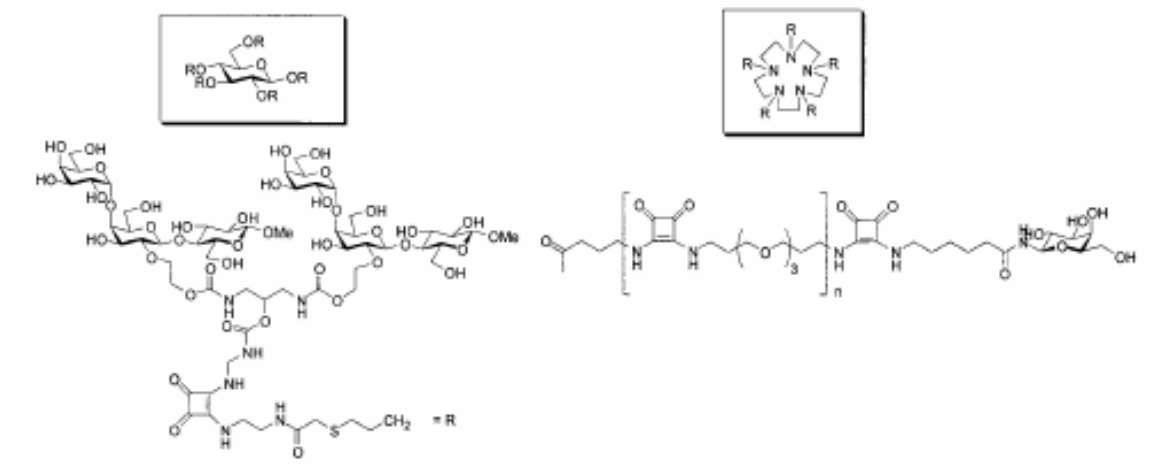

Fig. 7 Example of glycocluster for the inibition of pentameric lectins

Bundle et al.[26] recently prepared a decavalent sugar cluster for the inhibition of the binding of Shiga-like toxin, a member of the AB_5 family of bacterial toxins; these toxins consist of five identical carbohydrate-binding subunits (B) arranged around a core subunit (A) in a star-like fashion. The authors used D-glucose as scaffold for the attachment of ligands (trisaccharide Gal – Gal – Glc) and varied the length of the spacer arm to achieve optimal binding. The most successful inhibitor, named STARFISH, had an IC_{50} of $4x10^{-10}$ mol/l. This value is comparable to the estimated affinity of the natural (monovalent) ganglioside (GB3) – toxin interaction ($K_d = 10^{-9}$ mol/l) and is 10^6 more potent than the single trisaccharide ligand ($\beta \sim 10^6$).

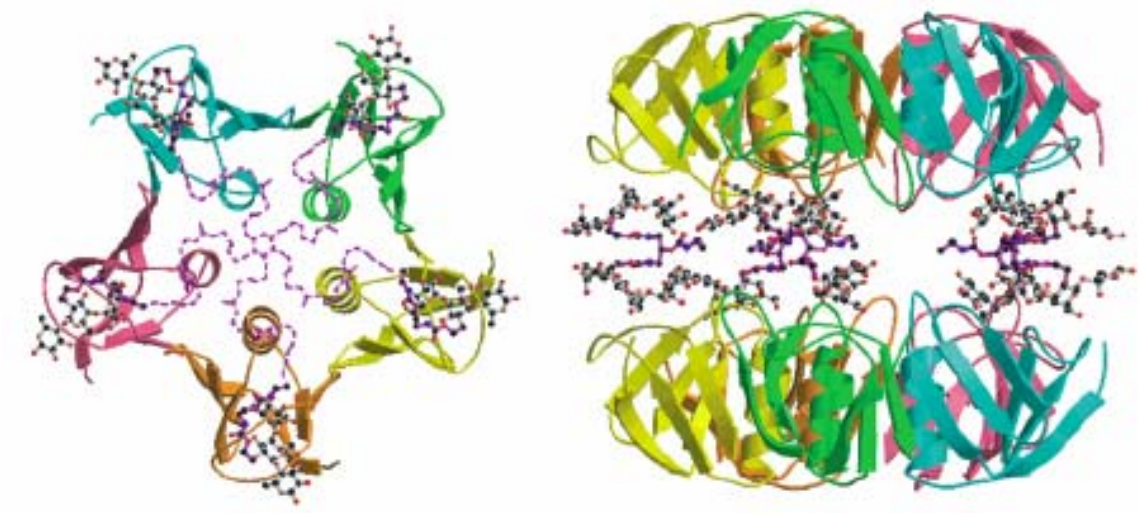

Fig. 8: Polar and equatorial view of the crystal structure of the complex between STARFISH and the two B_5 units of Shiga-like toxin.

The authors obtained a crystal structure of the toxin-inhibitor complex and found that each STARFISH ligand bound two toxin pentamers (**Fig. 8**).

Cyclodextrins. Cyclodextrins are cyclic oligosaccharides containing α-(1,4)-linked glucopyranosyl units. These structures present a hydrophobic interior that is capable of binding small organic molecules and a hydrophilic exterior. Hydroxyl groups on the exterior of the cyclodextrins can be modified so that ligands are presented on a single face of the structure with control over ligand to ligand spacing. Although several synthetic methods for the preparation of glycosylated cyclodextrins have been reported[27], few of these conjugates have been evaluated in terms of activity. Nishimura prepared a series of perglycosylated cyclodextrins and showed that a hexavalent *N*-acetylglucosamine conjugate inhibited the agglutination of human erytrocytes at a 240-fold lower concentration than its monomeric counterpart[28]. Defaye prepared a cyclodextrins derivatized with dendridic mannosides and showed that the hexavalent conjugate inhibited the binding of Con A to yeast mannan with an IC_{50} of 8 μmol/l, a 100-fold increase in potency over α-methyl mannoside[29]. Moreover, recently Mazzaglia and Darcy[30] prepared some nano-aggregates of amphiphilic β-cyclodextrins with alkylthio chains of differents length at the primary side and glycosylthio-oligo-(ethyleneglycol) units at the secondary side (**Fig. 9**).

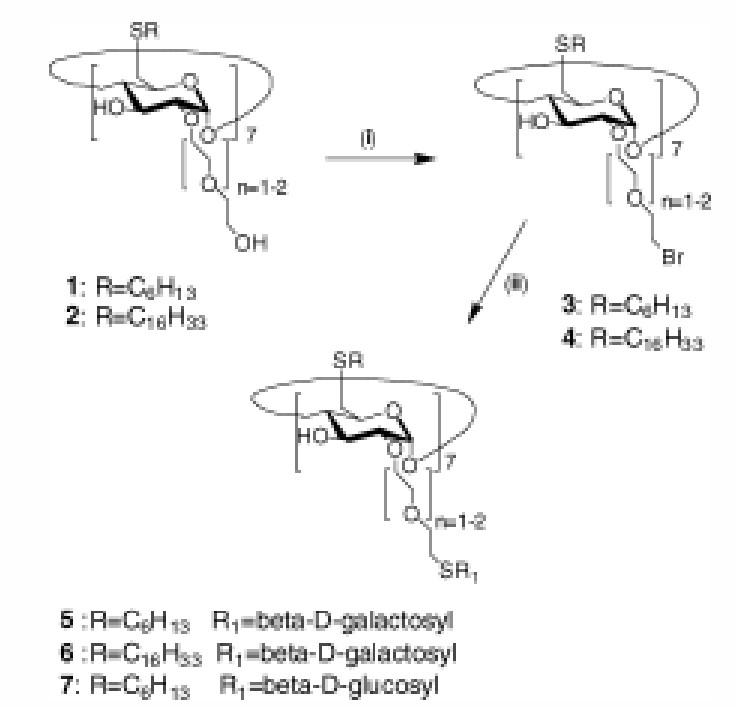

Fig. 9: Examples of perglycosylated amphiphilic cyclodextrins from ref. 30

These particular nanoparticles and vesicles targeted by galactosyl moieties showed multivalent effects in their binding to lectins.

Calixarenes. Calix[n]renes[31] (**Fig. 10**) are synthetic macrocycles derived from the condensation of phenol and formaldehyde.

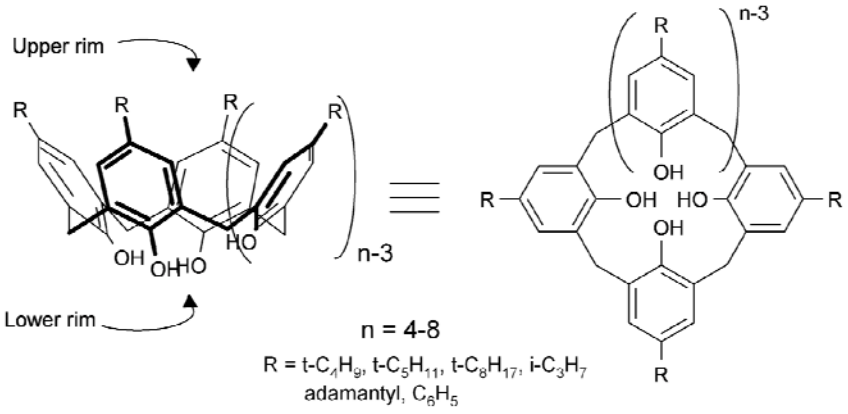

Fig. 10: General formulas of calix[n]arenes.

The shape, size and conformational properties of these molecules can be fine-tuned by varying the procedures used for their synthesis. Calix[4]arenes can therefore be fixed in four different structures named *cone, partial cone*, *1,3-alternate* and *1,2 alternate* (**Fig. 11**) which show very different molecular recognition properties. Like cyclodextrins, these scaffolds are able to bind hydrophobic organic molecules and can be modified with carbohydrate ligands on one of the two rims of the molecule with control over ligand to ligand spacing. Calixarenes are particularly attractive as glycoconjugate scaffolds and the derivatives functionalized with carbohydrates at the upper or lower rim are named glycocalixarenes.[1, 32] Furthermore, the calix[n]arenes blocked in the cone conformation can, to some extent, mimic a small portion of the cell surface presenting a series of glycosylated residues, projected all in the same direction, on the exterior of a lipophilic backbone (calixarene structure).

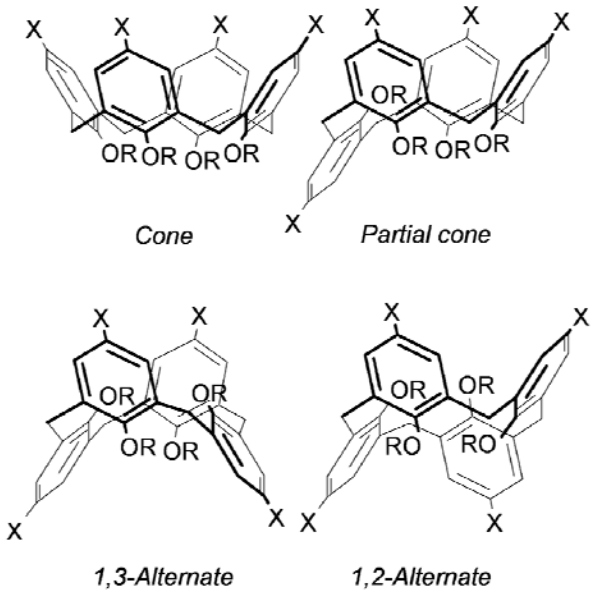

Fig. 11: The four limiting conformations of calix[4]arenes

These glycoconjugates have attracted attention also because they can be potentially used also for site-directed drug delivery. Aoyama, for example, prepared a resorcarene presenting eight galactoside (**Fig. 12a**) and showed that this glycoconjugate can selectively deliver a fluorescent dye to the surface of rat hepatoma cells[33]. Ungaro and co-workers showed that the tetraglycosylureido calix[4]arene (**Fig. 10b**) is able to efficiently and selectively bind to Concavalin A and to complex small organic and anionic guest.[34]

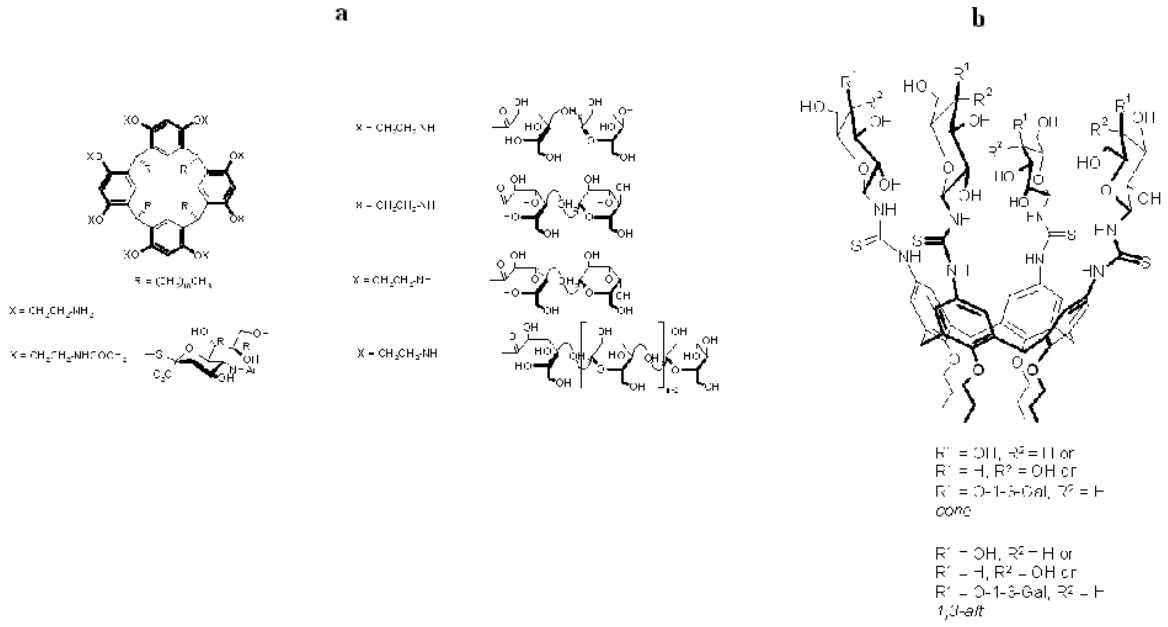

Fig. 12: a) Polyglycosylated resorcarenes and b) glycosylthioureidocalix[4]arenes.

The tetrasialosides[35] and the corresponding tetra-N-acetylgalactosides[36] synthesised by Roy and co-workers, through the conjugation of sugar units to a spacer present at the lower rim of calix[4]arenes, are able to efficiently crosslink and agglutinate carbohydrate binding protein specific for the saccharides present on the macrocycle. Calix[4]- and calix[8]arene glycoclusters were also prepared by Consoli et al.. Glycocalixarenes exposing N-acetylglucosamine (GlcNAc) units were successfully tested as ligands of the wheat germ agglutin, a GlcNAc binding protein, and as inhibitors of agglutination of human erytrocytes.[37] More recently, a divalent glycocalixarene (**Fig. 13**) bearing two pseudo-GM1 sugar units at the upper rim showed a remarkable enhancement factor (β = 2000 per sugar units) in the binding of pentameric Cholera Toxin B_5 (CTB_5). The binding of the glycocalix to CTB_5 (K_d = 48 nM) is even slightly better than that of the natural oligosaccharide GM1 (K_d = 219 nM).[38]

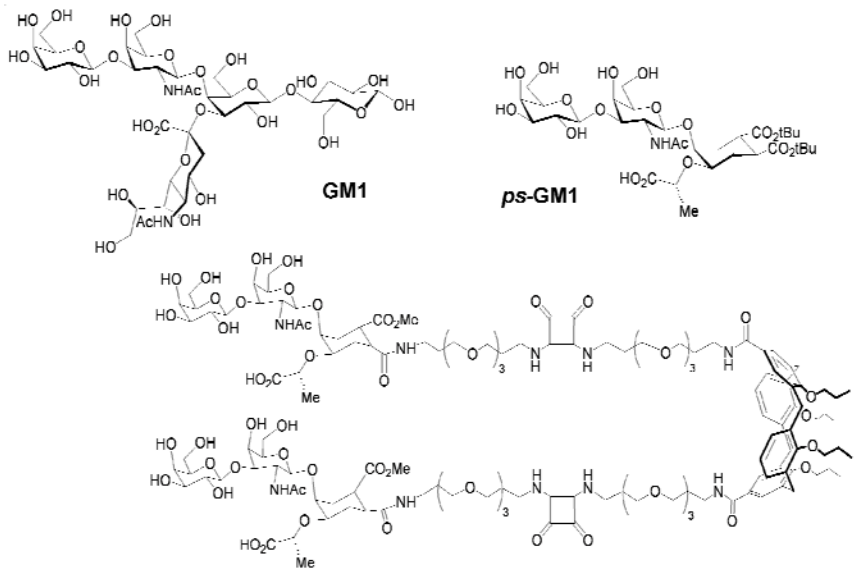

Fig. 13: The GM1 oligosaccharide, its ps-GM1 mimic and a divalent glycocalixarene for CTB_5 binding.

A small library of calix[n]arenes bearing lactosylthioureido moieties at the upper rim and having different valency and conformation have been shown to strongly inhibit the adhesion of galectins to the oligosaccharide of tumor cells.[39] Quite interestingly the inhibition depends not only on the valency of the glycoconjugate but also on its structure. The tetravalent calix[4]arene in the *cone* structure is selective for Gal3 while its stereoisomer in the *1,3-alternate* conformation inhibits both Gal1 and Gal4.

Dendrimers. At the borderline between systems with low valency and systems with high valency, one can find the dendrimer-based multivalent ligands. The term "dendrimer" derives from a greek word that means tree. In fact, dendrimers are macromolecular compounds that comprise a series of branches around an inner core just like in a tree[40] (**Fig. 14**).

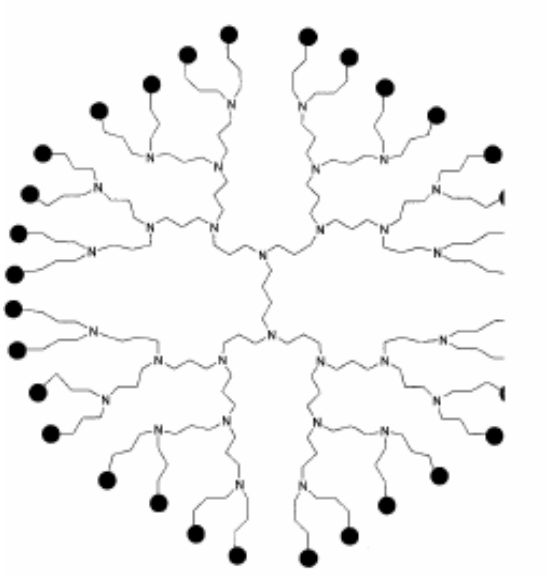

Fig. 14: Example of dendrimer

Dendrimers can be synthesised utilising two different approaches: a) starting from the central core and building up the branches toward the periphery (divergent synthesis), or b) joining the preformed branches to the inner core (convergent synthesis). Dendrimers are largely used for the study of biological systems because of their size and their ease of preparation and functionalization. Dendrimers that incorporate carbohydrates into their structures are named "glycodendrimers" and can be divided into three main categories: a) glycodendrimers that simply have saccharide residues on their outer surface, b) glycodendrimers containing a sugar unit as the central core where all branches are attached, and c) glycodendrimers with carbohydrates constituting the branches. Bernardi and Pieters, have recently prepared a series of glycodendrimers based on the 3,5-di-(2-aminoethoxy)-benzoic acid branching unit for inhibition of pentavalent cholera toxin[41]. The tetravalent compound was shown to be 440-fold more potent than its monovalent counterpart. More recently, it has been shown that the octavalent glycodendrimers of **Fig. 15**, bearing galactose[42] units or GM1 oligosaccarides[43] in the periphery, have spectacular relative potency (per sugar units) of 2500 and 47500, respectively.

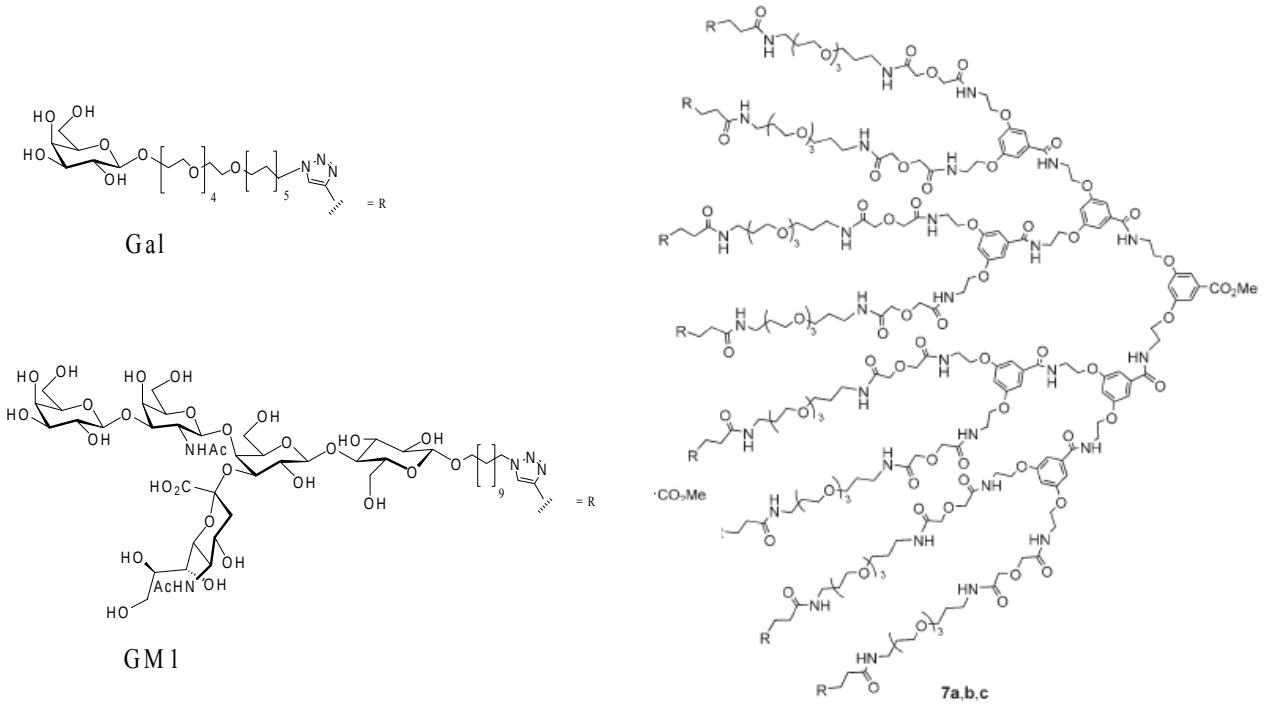

Fig. 15: The octavalent dendrimers bearing galactose or GM1 oligosaccharides at the periphery.

Dendrimers bearing 8 or 16 sialic acid at the periphery (**Fig. 16a**) as inhibitors of human erythrocyte hemagglutination by *Influenza* viruses have been recently designed and synthesised.[44] Stoddart and coworkers developed a series of dendrimers having from 3 to 36 α-mannose units as carbohydrates and found the most pronounced binding to Concanavalin A for the 9-mer and 18-mer.[45] Other interesting examples of glycodendrimers are those derived from polyamidoamine (PAMAM), that are constituted by a polyamide core (**Fig. 16**).[46]

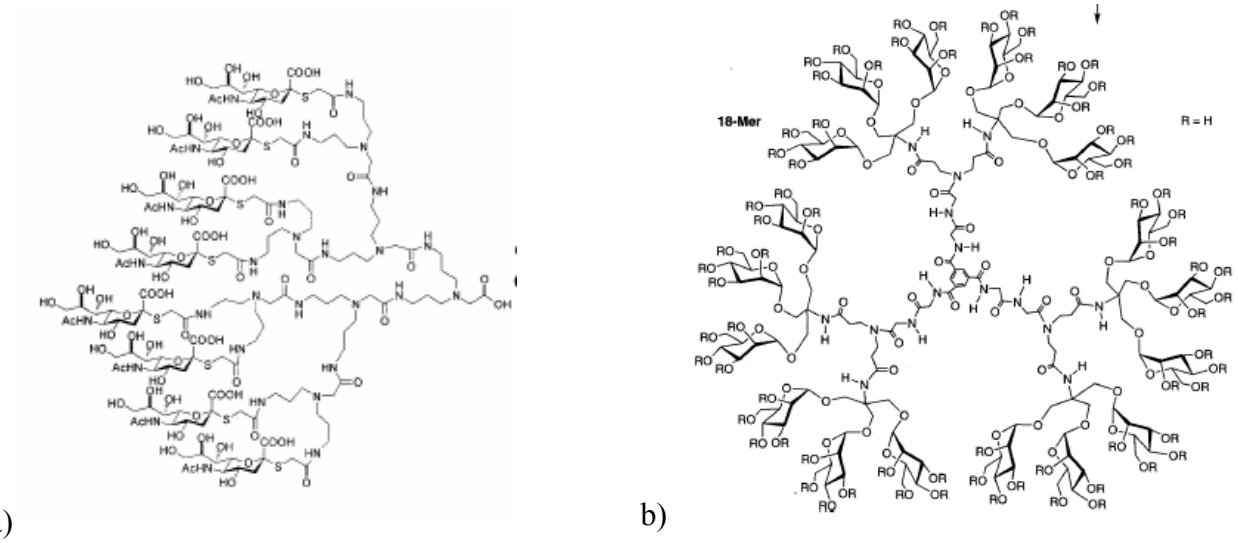

Fig. 16: Examples of glycosylated dendrimers bearing a) sialic acid and b) mannose units at the periphery

An interesting self-assembling dendrimer has recently been developed by Thoma and co-workers, They have synthesize some glycodendrimers able to self-assemble into nanoparticles and thus behaving as polyvalent ligands[47]. If the self-assembly is a dynamic process, natural polyvalent receptor could serve as templates optimizing size and shape of their own polyvalent inhibitors.

Generally, dendrimers are useful scaffolds for the design of polyvalent ligands for two reasons. First, they allow to obtain a valency between that of glycoclusters and model systems that present very large numbers of carbohydrates. Secondly, synthetic chemistry allows a wide flexibility in adjusting the valency, size and even shape of the molecule. However, despite this flexibility in design, they sometimes fail to display large enhancement factors in the binding to polyvalent proteins. Many authors reason that the poor binding enhancements observed reflect an incorrect spacing or geometry of the carbohydrates presented on these scaffolds.

1.4 References

[1] L. Baldini, A. Casnati, F. Sansone, R. Ungaro *Chem. Soc. Rev.*, **2007**, *36*, 254–266.

[2] A. Mulder, J. Huskens and D. N. Reinhoudt, *Org. Biomol. Chem.*, 2004, **2**, 3409-3424.

[3] S.-K. Choi, *Synthetic Multivalent Molecules*, S.-K. Choi, John Wiley & Sons, Inc., Hoboken, New Jersey, 2004.

[4] G. Ercolani, *J. Am. Chem. Soc.* **2003**, *125*, 16097-16103.

[5] W. P. Jenks, *Proc. Natl. Acad. Sci. U. S. A.* **1981**, *78*, 4046-4050

[6] P. I. Kitov and D. R. Bundle, *J. Am. Chem. Soc.* **2003**, *125*, 16271-16284.

[7] T. W. Rademacher, R. B. Parekh, R. A. Dwek *Annu. Rev. Biochem.* **1988**, *57*, 785-838.

[8] A. Varki *Glycobiology* **1993**, *3*, 97-130

[9] Y. C. Lee, R. T. Lee *Acc. Chem. Res.* **1995**, *28*, 321-327.

[10] H. Lis, N. Sharon *Acc. Chem. Res.* ***1998***, *98*, 637̃674.

[11] H.-J. Gabius *Naturwissenschaften* **2000**, *87*, 108-121.

[12] H.J. Gabius, H.C. Siebert, S. Andre, J. Jimenez-Barbero, H. Rudiger, *ChemBioChem* **2004**, *5*, 740– 764.

[13] J. Hirabayashi, K.-I. Kasai *Trends Glycosci. Glycotechnol.* **2000**, *12***,** 1-5.

[14] M. Mammen, S.-K. Choi, G. M. Whitesides *Angew. Chem. Int. Ed. Engl.* **1998**, *37*, 2754-2794.

[15] J. J. Lundquist, E. J. Toone *Chem. Rev.* **2002**, *102*, 555-578.

[16] H.-J. Gabius *Eur. J. Biol.* **1997**, *243*, 543-576

[17] H.-J. Gabius Eukaryotic Glycosylation and Lectins: Hardware of the Sugar Code (Glycocode) in Biological Information Transfer, Eurekah, 2001.

[18] H. Lis, N. Sharon In *The Lectins: Properties, Functions and Applications in Biology and Medicine*; Liener, I. E., Sharon, N., Goldstein, I. J., Eds.; Academic Press, Inc.: Orlando, 1986; p 293

[19] R. A. Dwek *Chem. Rev.* **1996**, *96*, 683-720.

[20] a) K.-I. Kasai, J. Hirabayashi, *J. Biochem.* **1996**, *119*, 1–8; b) H.-J. Gabius, Eur. *J. Biochem.* **1997**, *243*, 543–576; c) K. Kayser, D. Hoeft, P. Hufnagl, J. Caselitz, Y. Zick, S. André, H. Kaltner, H.-J. Gabius, *Histol. Histopathol.* **2003**, *18*, 771–779; d) N. Nagy, H. Legendre, O. Engels, S. Andrè, H. Kaltner, K. Wasano, Y. Zick, J.-C. Pector, C. Decaestecker, H.-J. Gabius, I. Salmon, R. Kiss, *Cancer* **2003**, *97*, 1849–1858; e) S. Langbein, J. Brade, J. K. Badawi, M. Hatzinger, H. Kaltner, M. Lensch, K. Specht, S. André, U. Brinck, P. Alken, H.-J. Gabius, *Histopathology* **2007**, *51*, 681–690.

[21] R. Roy *Top Curr Chem* **1997**, *187*, 241-274.

[22] D. Duchene, G. Ponchel, D. Wouessidjwew *Adv. Drug Deliv. Rev.* **1999**, *36*, 29-40.

[23] D. A. Fulton, J. F. Stoddart *Bioconj. Chem.* **2001**, *12*, 655-672.

[24] J. E. Gestwicki, C. W. Cairo, L.E. Strong, K. A. Oetjen, L.L. Kiessling *J. Am. Chem. Soc.*, **2002**, *124*, 14922-14933

[25] E. Fan, Z. Zhang, W. E. Minke, Z. Hou, C. L. M. Verlinde, W. G. J. Hol *J. Am. Chem. Soc.* **2000**, *122*, 2663-2664.

[26] P.I. Kitov, J.M. Sadowska, G. Mulvey, G. D. Armstrong, H. Ling, N. S. Pannu, R. J. Read, D. R. Bundle *Nature*,**2000**, *403*, 669-672.

[27] D. A. Fulton, J. F. Stoddart *Bioconj. Chem.* **2001**, *12*, 655-672.

[28] T. Furuike, S. Aiba, S. I. Nishimura *Tetrahedron* **2000**, *56*, 9909-9915.

[29] I. Baussanne, H. Law, J. Defaye, J. M. Benito, C. O. Mellet, J. M. Garcia Fernandez, *Chem. Comm.* **2000,** 1489-90.

[30] A. Mazzaglia, D. Forde, D. Garozzo, P. Malvagia, B. J. Ravoo, R. Darcy *Org. Biomol. Chem.* **2004**, *2*, 957-960.

[31] C. D. Gutsche, In Calixarenes Revisited; J. F. Stoddart Ed.; The Royal Society of Chemistry: Cambridge, 1998; In Calixarenes in Action; L. Mandolini, R. Ungaro Eds.; Imperial College Press: London, 2000. In Calixarenes 2001; Z. Asfari, V. Böhmer, J. Harrowfield, J. Vicens Eds.; Kluwer Academic Publishers: Dordrecht, The Netherlands, 2001.

[32] A. Casnati, F. Sansone, R. Ungaro *Acc. Chem. Res.* **2003**, *36*, 246-254

[33] T. Fujmoto, T. Miyata, Y. Aoyama *J. Am. Chem. Soc.* **2000**, *122*, 3558-559.

[34] F. Sansone, E. Chierici, A. Casnati, R. Ungaro *Org. Biomol. Chem.* **2003**, *1*, 1802-1809.

[35] S. J. Meunier, R. Roy *Tetrahedron Lett.* **1996**, *37,* 5469-5472.

[36] R. Roy, J. M. Kim *Angew. Chem. Int. Engl. Ed.* **1999**, *38,* 369-372.

[37] G. M. L. Consoli, F. Cunsolo, C. Geraci, V. Sgarlata *Org. Lett.* **2004***, 6*, 4163-4166.

[38] D. Arosio, M. Fontanella, L. Baldini, L. Mauri, A. Bernardi, A. Casnati, F. Sansone, R. Ungaro *J. Am. Chem. Soc.* **2005**, *127*, 3660–3661.

[39] S. André, F. Sansone, H. Kaltner, A. Casnati, J. Kopitz, H.-J. Gabius, R. Ungaro *ChemBioChem* **2008**, 9, 1649 – 1661.

[40] D. A. Tomalia, H. D. Durst *Top. Curr. Chem.* **1993**, *165*, 193-313.

[41] D. Arosio, I. Vrasidas, P. Valentini, R. M. J. Liskamp, R. J. Pieters, A. Bernardi *Org. Biomol. Chem.* **2004**, *2*, 2113-2124.

[42] H. M. Branderhorst, R. M. J. Liskamp, G. M. Visser, R. J. Pieters *Chem. Commun.* **2007**, 5043–5045.

[43] A. V. Pukin, H. M. Branderhorst, C. Sisu, C. A. G. M. Weijers, M. Gilbert, R. M. J. Liskamp, G. M. Visser, H. Zuilhof, R. J. Pieters *ChemBioChem* **2007**, *8*, 1500 – 1503.

[44] D. Zanini, R. Roy *J. Org. Chem.* **1996,** *61,* 7348-7354.

[45] P. R. Ashton, E. F. Hounsell, N. Jayaraman, T. M. Nilsen, N. Spencer, J. F. Stoddart, M. Young *J. Org. Chem.*, **1998**, *63,* 3429-3437.

[46] T. K. Lindhorst, C. Kieburg *Angew.Chem. Int. Ed. Eng.* **1996**, *135*, 1953-1956.

[47] G. Thoma, A. G. Katopodis, N. Voelcker, R. O. Duthaler, M. Streiff *Angew. Chem. Int. Ed.***2002**, *41*, 3195-3198.

Chapter 2

Synthesis of inhibitors of the lectin *LecB* from *Pseudomonas Aeruginosa*

2.1 Introduction

Pseudomonas Aeruginosa (PA), a Gram-negative bacterium, is an opportunistic pathogen that causes a variety of diseases, including respiratory tract infections in patients suffering from cystic fibrosis. Cystic fibrosis (CF) is a genetic disease developed by mutations in the gene encoding the CF transmembrane conductance regulator (CFTR). CFTR regulates ion transporter across the lung epithelia, and patients with CF suffer impaired ion transport and a depletion of airway surface liquid volume. The poor lung hydration leads to the deterioration of lung hygiene as much secretions become refractory to mucociliary clearance. Despite the particularly physiotherapy and antibiotics, the median age for survival is about 37 years. The cystic fibrosis patients gets several combination of physiotheraphy, postural drainage and antibiotics, that help them to remove mucus from lungs, improve their ability to breathe, and treat chronic lung infections. Therapeutic treatment of *Pseudomonas Aeruginosa* bacteria is still very difficult because they exhibit high intrinsic resistance against a variety of different antibiotics. The vilurence is associated with their ability to adhere to host cell surface, to form a stable biofilms in the human lung and to secrete hydrolytic enzymes and toxic compounds. The *P. aeruginosa* covers the lipopolysaccharides (LPSs) that protect the cells thus avoiding the diffusion of antibiotics. The host polysaccharides act as specific targets for the pathogen binding and are involved in the establishment of infection. The bacterium host selectivity depends on the carbohydrate specificity of its lectins and adhesins, which is part of its virulence factors. Several virulence factors are produced by *P. aeruginosa,* among which the two lectins, LecA (PA-IL) and LecB (PA-IIL), that exert different cytotoxic effects on respiratory epithelial cells and are believed to be the mediators of biofilm formation in the airway mucosa. In cystic fibrosis patients, the bacteria exist mainly as biofilms, adopting an aerobic metabolism and encapsulating themselves in extracellular matrix, which protects them from different antibiotics[1]. Lectins (see also chapter 1) are specific carbohydrate-binding proteins different from enzymes and antibodies. They are found in a wide range of organisms as viruses, bacteria, plants and animals, and are believed to play an important role in cell-cell interactions. Lectins play also an important role in human infections. It was demonstrated that a *P. aeruginosa*-induced otitis externa diffusa as well as respiratory tract infections can be strongly depressed by application of a solution containing LecA and LecB-specific sugars which inhibit adhesion of these bacteria on the cell LPSs.

2.2 Biochemical properties of the Lectins PA-IL and PA-IIL

The lectin PA-IL (51 kDa) is a multimeric protein composed of four subunits of 121 amino acids and binds D-galactose and its derivatives[2]. Lectin PA-IIL (47 kDa) which is also multimeric, is composed of four subunits of 114 amino acids and specifically binds L-fucose together with few other monosaccharides[3]. Both PA lectins were shown to be located mainly in the cytoplasm of planktonic cells[4]. After their purification from the planktonic cell extracts[5], they behave as Ca^{++}-dependent tetrameric plant lectins, displaying haemagglutinating activity and relative resistance to heating, proteolysis and extreme pH. Biochemical studies also indicated the additional presence of Mg^{2+} ions in PA-IL and Mg^{2+} and Zn^{2+} ions in PA-IIL. These lectins were demonstrated to act directly in *vitro* and in *vivo* as cytotoxic compounds. When looking more particularly at respiratory epithelial cells, PA-IL was shown to be strongly cytotoxic for these cells. The PA-IL gene was isolated from *P. aeruginosa* ATCC 27853 genomic library[6], whereas the PA-IIL gene was identified in the *P. aeruginosa* PAO1 genomic sequence thanks to the sequence of its 33 N-terminal amino acids[3]. The genes also referred to as *lec*A and *lec*B, are widely separated (about 867.5 kb) on the *P. aeruginosa* chromosome. Both mature proteins lack the initiator methionine and display acidic characters, but PA-IIL differs from PA-IL in lacking cysteine, methionine and histidine.

2.3 Affinity and specifity in Carbohydrate binding of the *P. aeruginosa* lectins

The PA-IL lectin has medium affinity for D-galactose with an association constant (K_a) of 3.4×10^4 M^{-1} as reported from equilibrium dialysis study[7]. Among monosaccharides, the specificity is strictly for galactose, but there is also binding at lower affinity with N-acetyl-D-galactosamine. Affinity enhancements where observed when a hydrophobic group is present on the sugar anomeric position, either in α or β configuration and the tightest binding was obtained with phenyl- β-thiogalactoside[8] (see tab. 1). Among the disaccharides, only those containing a terminal α-D-galactose residue are recognised like αGal1-3Gal, αGal1-4Gal, and αGal1-6Gal that display the highest affinity for the lectin[8,9].

The PA-IL lectin binds several glycoproteins[9] and glycosphingolipids[8,10] amongst which the glycoconjugates with terminal non-substituted αGal1-4Gal disaccharide, *i.e.*, the human P1 and Pk blood group antigens, present on either red blood cell glycosphingolipidis and αGal1-3Gal disaccharide, the human blood group antigen and the xeno-antigen present on non-human tissues.

Carbohydrate specificity of PA-IL and PA-IIL

PA-IL		PA-IIL	
Inhibitor	Potency	Inhibitor	Potency
Phenyl-β-Gal	57.1	Lacto-*N*-fuco (Le^a pentasaccharide)	5
αGal1-6Glc (melibiose)	13.3	Sialyl Lewis a	3.5
αGal1-3αGal-*O*-Me	4.7	Lewis a	2.8
αGal-*O*-Me	2.7	3′Fucosyllactose	1.4
βGal-*O*-Me	2.2	L-Fucose	1.0 [a]
αGal1-4Gal	1.8	L-Galactose	0.41
D-Galactose	1.0 [b]	Lewis x	0.17
αGal1-3Gal	0.8	Sialyl Lewis x	0.13
D-GalNAc	0.5	D-Arabinose	0.08
βGal1-4Glc	0.5	D-Fructose	0.05
D-Fucose	0.02	D-Mannose	0.04

Table 1 Table selected from A. Imberty et al. *Microbs and Infection 6* **(2004)** 221-228

[a] Taken as reference value of 1.0 for an IC_{50} of 0.25 nM for inhibition of PA-IIL-binding to human group H and Le^b active glycoprotein.
[b] Taken as reference value of 1.0 for an IC_{50} of 40 nM for inhibition of PA-IL-binding to hydatid cyst glycoprotein.

The lectin PA-IIL has high affinity for L-fucose with association constant (Ka)[11] of 1.6 x 10^6 M^{-1} in the hemagglutination inhibition test. Among monosaccharides it shows the strongest affinity for p-nitrophenyl-α-L-fucose, followed in order by L-fucose > L-galactose > D-arabinose > D-fructose > D-mannose while D-galactose is not bound significantly.

The ability of different complex oligosaccharides to inhibit the binding of PA-IIL to human blood group H and to Le^b active glycoprotein was also measured[12]. The Le^a pentasaccharide and Le^x trisaccharide (not shown in tab. 1) are the most potent inhibitors with 5 and 30 times higher activity than L-fucose respectively. These polysaccharides are isomeric structures that differ in the linkage of the galactose to the GlcNAc residue. It seems that the orientation of the GlcNAc N-acetyl group plays a major role in the binding.

2.4 Crystal structure of the PA-IL and PA-IIL lectins

In the literature several examples of PA-IL crystal structures have been reported: the native lectin with one calcium ion per monomer[13], the calcium-free lectin and the lectin with both calcium ion and bound galactose[14].In all these cases the PA-IL has a quaternary structure with a tetramer arranged around a pseudo C222 axis of symmetry.

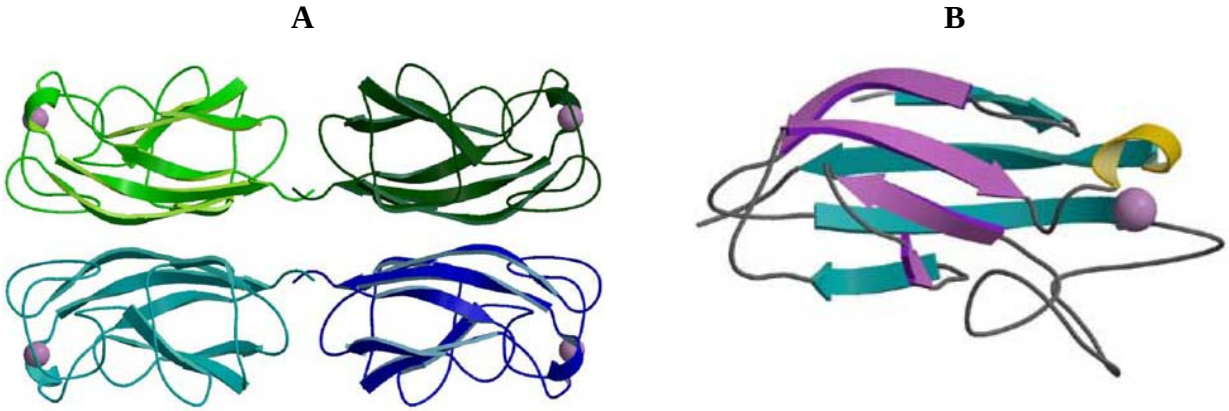

Fig.1 PA-IL Picture from A. Imberty et al. *Microbs and Infection 6* **(2004)** 221-228

X-Ray crystal structure of PA-IL lectin with calcium ion in its (A) tetrameric and (B) monomeric arrangement.

For the PA-IIL lectin there are two crystallographic studies[12 15] the first one concerns the native lectin and the calcium-free protein, while the second study reports the X-ray crystal structure of the complexes with three different monosaccharides L-fucose, D-mannose, and D-fructopyranose.

For PA-IIL a tetrameric association also occurs around a pseudo C222 axis of symmetry, resulting in a spherically formed quaternary structure (see fig. 2), like the PA-IL, but more compact.

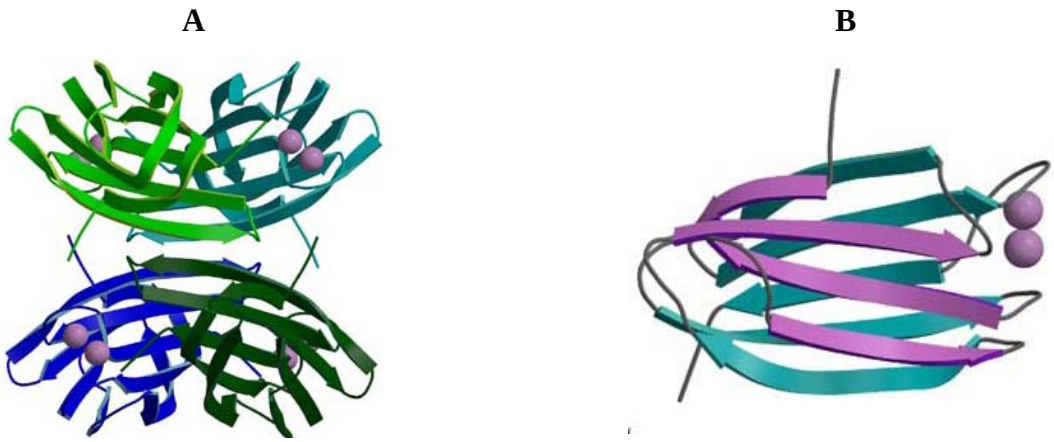

Fig.2 PA-IIL Picture from A. Imberty et al. *Microbs and Infection 6* **(2004)** 221-228

X-Ray crystal structure of PA-IIL lectin with calcium ions in its (A) tetrameric and (B) monomeric arrangement.

In both lectins the monosaccharide-binding is mediated by calcium ion. The sugar-binding site of PA-IL involves one calcium ion, whereas that of PA-IIL involves two calcium ions. In the complex between PA-IL and galactose[14] one carbohydrate residue is inserted in each monomer, sitting on the calcium atom. The coordination sphere of the calcium ion directly involves the atoms O3 and O4 of the galactose (see **Fig. 3**). There are also six direct hydrogen bonds between the protein and the carbohydrate hydroxyl groups and there is one additional interaction mediated by a water molecule. Moreover, weak contacts between the apolar face of the galactose residue and some hydrophobic amino acid residues were observed.

In the PA-IIL/fucose complex[12] there is a peculiar situation since the fucose residue is locked on the two calcium ions. In the picture (**Fig. 3**) one can observe three hydroxyl groups of the fucose binding to those calcium ions indeed: O2 with the first calcium, O4 with the second one and O3 with both of them. Besides these interactions, hydrogen bonds between three hydroxyl groups of the monosaccharide and carboxylic groups of the calcium-binding site can be observed. The pyranose oxygen of the fucose is involved in an hydrogen bond with the main peptide chain. In conclusion there are seven hydrogen bonds between the sugar and the protein with an additional hydrogen bond mediated by a water molecule. In position 6 of the fucose, the methyl group is important because it is located in a hydrophobic pocket of the lectin. In the literature, X-ray crystal structures of the PA-IIL complexes with fructose and mannose[15] have been also reported. The fructose in its D-configuration uses a $^{2}C_{5}$ chair conformation which is similar to the $^{1}C_{4}$ chair of the L-fucose and has the same distribution of equatorial and axial hydroxyl groups. Considering that fructose binds the lectin using the same conformation of fucose but has no methyl group at the C6 position, the lower affinity to PA-IIL for fructose compared to fucose could be explained by the lacking of

hydrophobic interactions. Mannose is different from fucose in its $^4C_1$ chair conformation and in axial configuration at O2. Fucose and Mannose binds isosterically but adopt different orientations of their rings in the binding site, with O2, O3, and O4 of fucose being sterically equivalent to O4, O3 and O2 of mannose.

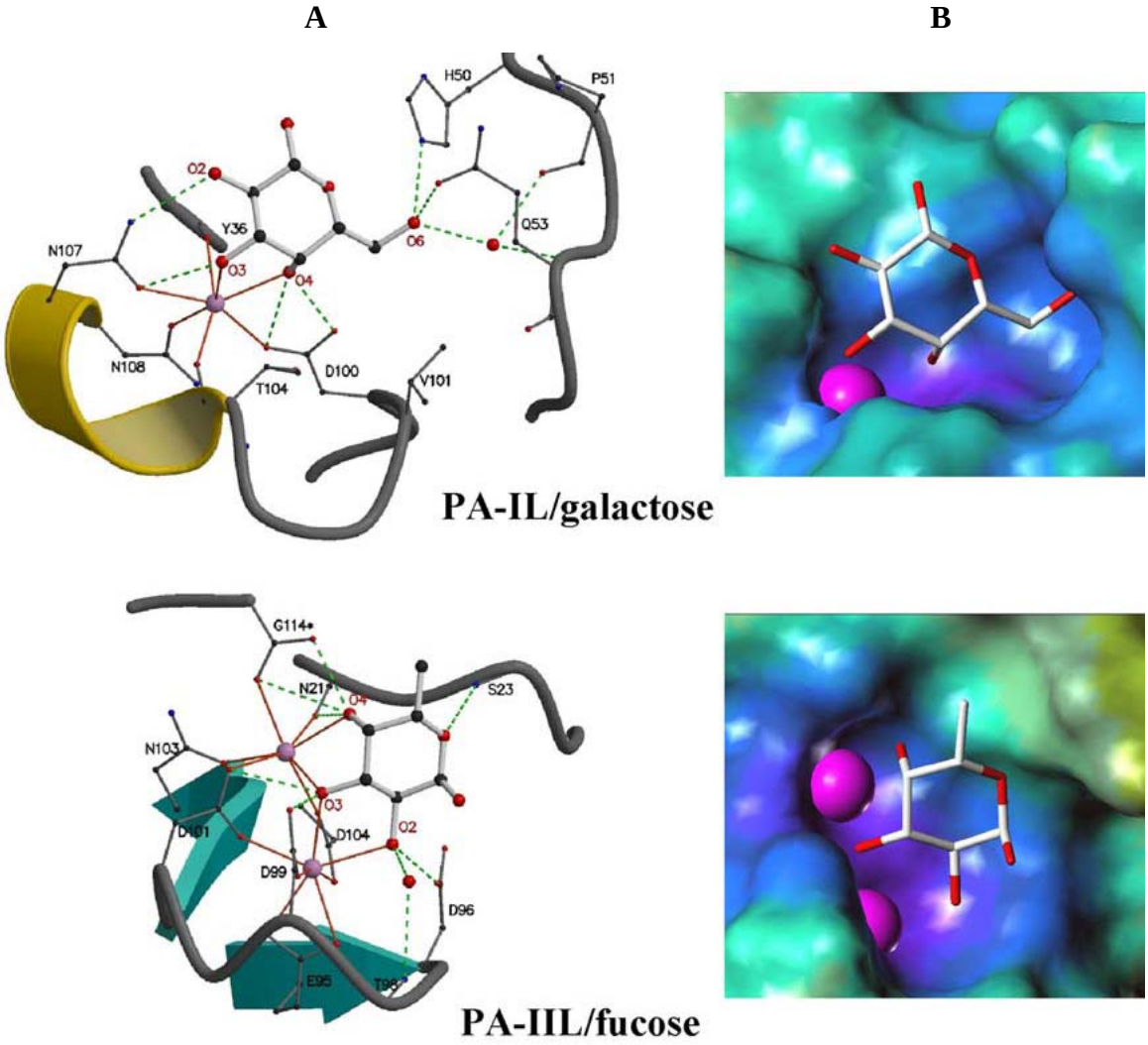

Fig. 3 Picture from A. Imberty et al. *Microbs and Infection 6* **(2004)** 221-228

Binding sites of the X-ray crystal structures of PA-IL/galactose and PA-IIL/fucose complexes.

(A) Stick representation of the amino acids involved in binding. Ca^{2+} coordination bonds are shown as solid orange lines; hydrogen bonds as dashed green lines. Colour coding: red, oxygen; blue, nitrogen; black, carbon; pink, $Ca^{2+.}$ (B) Electrostatic surface representation (colour-coding from violet for negative to orange for positive) of the protein-binding site, with Ca^{2+} as large magenta spheres and monosaccharides as stick models.

2.5 Roles of PA-IL and PA-IIL in infection

Today, the exact biological roles of the two *Pseudomonas Aeruginosa* lectins have not yet been completely understood, but hypotheses have been considered. It is sure that PA-IL and PA-IIL are two lectins which bind specific glycans and that display multivalent effects. Most of their activity is stored intracellularly, although small but significant fractions are present on the cytoplasmic membrane, on the outer membrane and in periplasmic space[16]. The higher intracellular activities of the lectins are only released from the bacteria following their lysis. The distribution may change, in fact recent studies have reported that the PA-IIL is present in higher amount on the bacterial outer membrane[15]. These protein are therefore very important, because they play an important role in the interaction of the bacteria with the environment.

The cell surface of the intact bacteria was shown to strongly agglutinate human erythrocytes and therefore may be involved in the bacterial adhesion to host cells[16]. It has been demonstrated that these lectins could have a role also in inducing agglutination of other bacteria or uni- and oligocellular eukaryotic organisms[6].

The role of bacterial-lectin interactions with host glycans is well established in symbiosis and pathogenicity[17]. The *Pseudomonas Aeruginosa* is a saprophytic bacterium which can become an aggressive pathogen if in contact with damaged and inflamed tissues like burn wounds and lungs of cystic fibrosis patients because in these cases the host cell surfaces present altered glycosylations. In several studies of the CF the important point is the mutations in the cystic fibrosis transmembrane conductance regulator (CFTR) gene which results in altered ion movements and also influences the N-glycosylation of the CFTR protein and other cell surface glycoproteins. The fucosylation increase, the sialylation decrease with higher levels of $Lewis^x$ and $Lewis^a$ epitopes were demonstrated to correlate with PA specific binding[18]. In addition, both the mucus (with mainly mucins, glycoproteins containing 70-80 % carbohydrates) covering the airway epithelia of CF patients and their salivary mucins that show higher levels of sialylated and sulphated Lewis x oligosaccharides[19], attract *P. Aeruginosa*[20]. One can correlate these data with the biochemical and modelling studies and prove that PA-IIL has high affinity for oligosaccharides of the Lewis series[12].

The studies on the crystal structure, and on the biochemical properties of PA-IL and PA-IIL, together with the discover of their high affinity ligands opened the way to design new carbohydrate compounds for an efficient inhibition of bacterial adhesion and biofilm formation derived from *Pseudomonas Aeruginosa* infection.

2.6 Glycopeptide dendrimer libraries for lectin P.A. inhibition

One of the main pharmaceutical strategies aimed at avoiding PA infection and removing or reducing the formation of biofilms originating from these bacterial strain is to find efficient inhibitors of PA-IL and PA-IIL. For this purpose, multivalent ligands (see chapter 1) have already demonstrated to be superior Different multivalent inhibitors based on the multiple display of glycosides, in particularly mannose and galactose[21], and having a scaffold based on dendrimers[22], oligosaccharides[23], or glycopeptides[24] are known. Moreover in the literature, no synthetic multivalent ligands were reported for fucose-specific lectins. Among all the different multivalent scaffold which can be used, dendrimers have been deeply studied. The field of dendrimer[25] chemistry has undergone a rapid development and has evolved from the discovery and the establishment of efficient synthetic procedures to the characterization of dendrimer properties and the design of functional dendrimers[26]. Also combinatorial chemistry has recently developed very rapidly with the aim at discovering synthetic compounds useful in biomedical applications where combinatorial chemistry was used. The Reymond's group recently linked combinatorial to dendrimer chemistry and reported the synthesis of peptide dendrimer[27] combinatorial libraries[28] together with their use in the discovery of synthetic enzyme models and in drug delivery[29]. The use of neoglycopeptide dendrimer combinatorial libraries was also applied to the discovery of lectin inhibitors[30].

In particular this method was exemplified by the selection of a strong ligand for fucose-specific lectins UEA-I from the plant *Ulex europeaeus*[31] and for PA-IIL. The advantage of using of peptide dendrimer libraries is two-fold. First solid phase peptide synthesis (SPPS) can be used, ensuring high yields and purity of the products; moreover, identification of the most active members of the library can be easily obtained simply by sequencing its amino acids and without the use of any tag. Solid phase peptide synthesis was therefore used to prepare a library of peptide dendrimer containing alternating α-amino acids with the branching diamino acids (Lys). At the end of the peptide synthesis, L-fucose units were conjugated to the four terminal amino groups thus obtaining tetravalent glycopeptides dendrimers of up to 37 amino acids in 11 coupling steps (**scheme 1**).

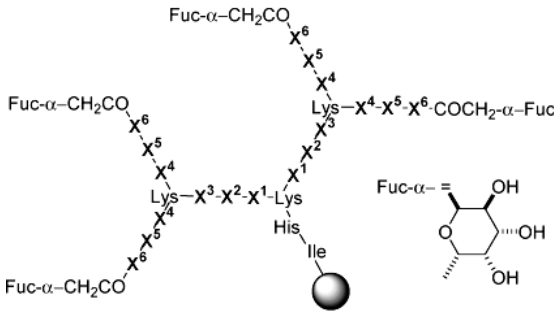

X^6	X^5	X^4	X^3	X^2	X^1
Lys	Arg	Leu	Tyr	Lys	Ala
Phe	Ala	Val	Phe	Arg	Thr
Ser	Pro	Asp	Ser	Pro	Leu
Glu	Thr	Tyr	Glu	Val	Asp
Gly	His	Ile	His	Gly	Ile

Scheme 1 Combinatorial Library of Neoglycopeptide Dendrimer (5^6 = 15 625 sequence)

Picture from Org. Lett., vol. 9, No. 8, 2007

For the synthesis of the solid supported combinatorial libraries the "split-and-mix" metod[32]was used , which allows the simultaneous preparation of a large number of compounds in very few steps[33]. This synthesis is carried out on a solid phase support consisting of millions of microscopic beads, and results in the so-called one-bead-one-compound (OBOC) libraries in which each of the beads carries only one of the possible compounds.

A large library (15 625-member) with a second-generation dendrimer was prepared on tentagel beads (0.5 g, 0.30 mmol/g diameter bead of 90 μm). Each dendrimer was funcionalized at the N-terminus with L-fucose. The combinatorial library was carried out with amino acids placed in six variable positions to allow positive, negative, hydrophobic, small and polar or aromatic residues during all the sequence (**Scheme 2**). Each dendrimer was checked by amino acid analysis of randomly selected beads, providing the expected statistical distribution of amino acids at the variable positions.

The library was assayed for binding to biotinylated UEA-I lectin and stained with an alkaline-phosphatase-conjugated antibiotin antibody and 5-bromo-4-chloro-3-indolyl phosphate/ nitro blue tetrazolium (BCIP/NBT) as a chromogenic substrate as described for a related on-bead assay for wheatgerm hemaglutinin[34]. While the N-acetylated control library gave less than 1% of stained beads in the assay, over 90% of the beads in the fucosylated library were darkly stained. Addition of 3 M fucose during the lectin binding step reduced staining to less than 2% of the beads. Darkly stained beads were manually picked, and their sequence was determined by amino acid analysis. A strong consensus for positively charged lysines at the terminal positions X^6 and at position X^2 was

observed and therefore the eight dendrimers of **Table 2** were independently synthesised by SPPS, fucosylated and cleaved from the resin.

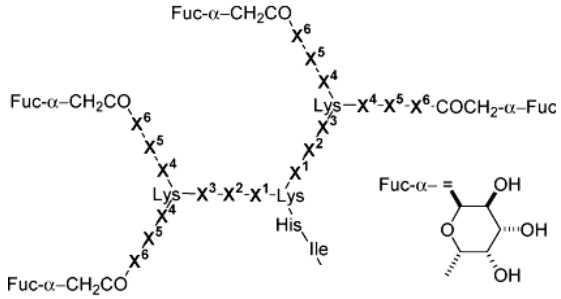

X^6	X^5	X^4	X^3	X^2	X^1
Lys	Arg	Leu	Tyr	Lys	Ala
Phe	Ala	Val	Phe	Arg	Thr
Ser	Pro	Asp	Ser	Pro	Leu
Glu	Thr	Tyr	Glu	Val	Asp
Gly	His	Ile	His	Gly	Ile

Scheme 2 Combinatorial Library of Neoglycopeptide Dendrimer (5^6 = 15 625 sequence)

Picture from Org. Lett., vol. 9, No. 8, 2007

Dendrimer	X6	X5	X4	X3	X2	X1
FD1	Lys	His	Val	His	Gly	Ala
FD2	Lys	Pro	Leu	Phe	Lys	Ile
FD3	Lys	His	Leu	Glu	Lys	Ile
FD4	Lys	Arg	Asp	Ser	Arg	Ala
FD5	Lys	Thr	Ile	Ser	Arg	Leu
FD6	Lys	Thr	Leu	His	Lys	Ala
FD7	Lys	Ala	Ile	His	Lys	Thr
FD8	Lys	Thr	Val	Ser	Arg	Ile

Table 2 Sequences from the Dendrimer Combinatorial Library

Every dendrimer from the library were tested in lectin binding by enzyme-linked lectin assay (ELLA) as described in literature[35]. This test measures the competition between the ligand and a biotinylated polymeric fucose reagent in the binding with the lectin. This test has identified the **FD2** dendrimer as the most potent (**Tab. 3**) ligand with an IC_{50} = 11 μM and a relative potency of 115 in reference to L-fucose. The other three dendrimers (**FD1, FD3,** and **FD4**) showed relative potencies in the range 20-40, which is similar on a per residue basis to the α-*C*-allyl fucoside (**5**).

To study the role played by the dendrimeric structure in these multivalent ligands, the terminal arm **2G0** and the outer branch **2G1** (**Fig 4**) were also synthesized and tested. A gradual increase in relative potency per fucose unit was observed in the series **2G0** (r.p./n. = 4) → **2G1** (r.p./n. = 11) → **FD2** (r.p /n. = 29).

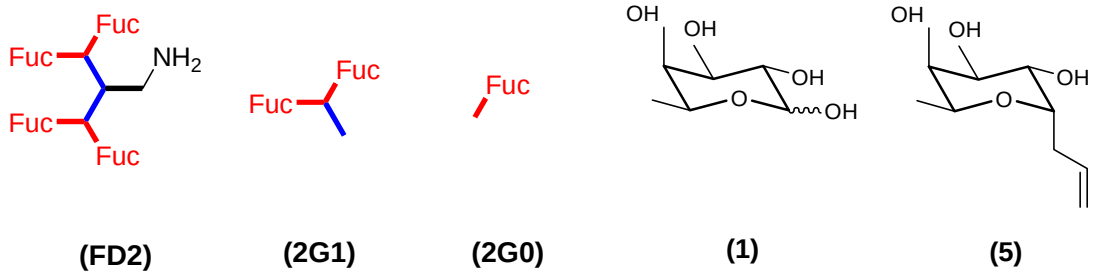

(FD2) **(2G1)** **(2G0)** **(1)** **(5)**

FD2 = (Fuc-Lys-Pro-Leu)$_4$-(Lys-Phe-Lys-Ile)$_2$-Lys-His-Ile-NH$_2$
2G1 = (Fuc-Lys-Pro-Leu)$_2$-Lys-Phe-Lys-Ile-NH$_2$
2G0 = Fuc-Lys-Pro-Leu-NH$_2$

Fig. 4 Structures of glycopeptide dendrimers FD2 and lower-generation analogues 2G1 and 2G0

No.	IC_{50} (μM)	r. p.[a]	n[b]	r. p./n[c]
1	1265±5	1	1	1
5	261±13	5	1	5
FD1	67±4	19	4	5
FD2	11±0.35	115	4	29
FD3	72±9	18	4	4
FD4	31.5±9	40	4	10
2G0	290±40	4	1	4
2G1	56±6	23	2	11

Tab. 3 IC_{50} in ELLA test against UEA-I lectin

[a] r.p. = relative potency to fucose IC50 (fucose)/IC50 (ligand). [b] *n* = number of fucosyl units per dendrimer. [c] Relative potency per fucose residue.

The high potency observed for the **FD2** dendrimer seems therefore be due to the multivalent effect, while there is almost no increase in the r.p./n. values for the other tetravalent dendrimers **FD1**, **FD3**, and **FD4.** The strong affinity of **FD2** toward UEA-I is therefore deeply dependent on its structure and amino acid sequence. Besides the multivalent presentation of fucosyl units, **FD2** probably gives rise also to attractive secondary interactions of its peptide backbone with the lectins. In fact there could possibly be electrostatic interactions between the 6-fold positively charged

dendrimer and the negatively charges found close to the fucose binding site in UEA-I which can improve the binding. Also inhibition lectin PA-IIL test with **FD2** gave a high result of IC_{50} of 0.14±0.035μM that corresponds to a 80 fold relative potency. As for UEA-I, also in PA-IIL negatively charged residues are found close to the fucose binding site[36].

2.7 Synthesis of new fucosylated peptide dendrimers with high proteolytic stability

Results obtained by the library of dendrimers have shown that the best inhibitor of PA-IIL are tetravalent dendrimers featuring positively charged amino acids (Lys) at the outer layers having a terminal C-fucoside residue mediating the binding to the lectin. The aim of my project, carried out during a six-months leave at the University of Berne in the group of Prof. J. L. Reymond, was to developed peptide dendrimers showing high proteolytic stability. In fact, in order to study and use the fucosylated peptide dendrimers in *in vivo* applications, a high stability to enzyme is to be seek. All the peptide dendrimers previously synthesized in Berne were based on L-amino acids and therefore, theoretically highly unstable in the presence of proteolytic enzymes. Given the structure of the most potent L-amino acid base peptide dendrimer **FD2** we have planned to synthesize its counterpart based on D-amino acids which, being not recognised by natural proteases, should be much more stable. Therefore during my stay in Berne I resynthesized the **FD2** L-dendrimer, named Ile-GAR- L, a related L-dendrimer but having a L-Leu as the first amino acid, and therefore named Leu-GAR-L (see **Fig. 4**) and the D-dendrimer, Leu-GAR- D, having only as branching L-Lys and all D-amino acids instead of L-amino acids. Therefore, my research work in Berne started with the synthesis of C-fucosyl-acetic acid building block from L-fucose via the known C-allyl fucoside **3** (see **scheme 3**). A C-fucosyl derivative was chosen instead of an O-fucosyl one since the latter are know to be easily cleaved by glycosidases.

The C-fucosyl-acetic acid **(4)** group was obtained by L-fucose **(1)** in a three steps procedure as reported in literature (Scheme 1)[37]. L-fucose **(1)** was acetylated with acetic anhydride in pyridine to give **2** in quantitative yield. In this step the complete removal of the toxic pyridine, which is used as solvent, was obtained performing several washes of the organic phase with a saturated aqueous solution of copper sulphate. This salt forms a water soluble complex with pyridine which is dark blue. So the organic phase was washed with the $CuSO_4$ aqueous solution until the colour of the water layer becomes light blue. After evaporation of the solvent, compound **2** was obtained pure without further purification. The peracetylated L-fucose **(2)** was subsequently alkylated in the anomeric position with allyl trimethyl silane, boron trifluoride and trimethyl silyl triflate. In this step two parameters are very important: the time of the reaction which must be sufficiently long to

ensure a complete conversion and the temperature that needs to be maintained between 0 and -18° C for all the time of the reaction. In this way we could obtain only the α-allyl compound pure. The final step was the conversion of the allyl group of **3** in the corresponding acetic acid moiety. The reaction was performed at room temperature in aqueous mixture of CCl_4 and acetonitrile with ruthenium(III) chloride and sodium meta periodate under vigorous stirring. After work-up and trituration of the crude product with ethyl ether very pure compound **4** was obtained and used without further purification. The C-fucosyl-acetic acid was therefore synthesized from L-fucose in 84% overall yield.

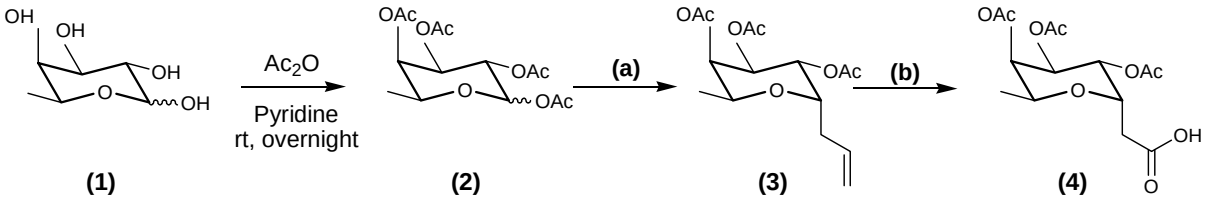

(a) 1) $(CH_3)_3SiCH_2CH=CH_2$ 0°C, 5 min. 2) BF_3-OEt_2 TMSOTf 0°C 5h, -18°C overnight, 0°C 5h, CH_3CN dry
(b) $NaIO_4$ $RuCl_3$, $CCl_4/CH_3CN/H_2O$ overnight

Scheme 3 Synthesis of C-fucosyl acetic acid **4**

The dendrimer synthesis was performed through the Solid Phase Peptide Synthesis (SPPS) manual procedure, in plastic syringes. Nova Syn TGS RAM resin was used as solid support.(**scheme 4**) The F-moc protected resin (see **scheme 5**), after swelling with dichlorometane, was deprotected with a solution of piperidine/DMF 20/80 (**a scheme 4**). The deprotection was checked with Trinitrobenzenesulfonic Acid (TNBS) (**b scheme 4**) which is a reagent used in qualitative tests for free amine. In fact, one can see at the microscope the beads red coloured if the amine is free and colourless when the amine is still protected.

The resin was then coupled with the amino acid using PyBOP and di-isopropyl-ethylamine (DIEA) (**c**). Generally, in the synthesis of first generation dendrimers the reaction time is 1 h and 30 min, but one needs 3 h reaction time after the first generation. After each coupling the resin was checked again with the TNBS test. If the TNBS test indicated the presence of some free amino groups, the coupling was repeated. In any case after each coupling, the remaining free amino groups were capped with acetic anhydride/CH_2Cl_2 (**c**$^{\mathbf{1}}$). The Fmoc protecting groups of each amino acid were then removed with a solution of 20% piperidine in DMF and steps (**c**) and (**c**^{1}) repeated until the desired peptide structure was obtained. At the end of the sequence the resin was coupled with fucose **4** in the presence of DIEA and HCTU (**d**) overnight. In this step a large excess of carbohydrate was used and the coupling was repeated two more times. It was observed that

conjugation of the sugar is hard to be quantitative and often dendrimer minus one fucose unit were obtained. The glycodendrimer was then deacetylated using a solution of MeOH/NH_4/H_2O (v/v 8:1:1) for 24 h for two times (step 1 in **scheme 4**) The resin was then dried and the dendrimer cleaved from the resin with TFA/TIS/H_2O (95:2.5:2.5) for 4 h (step 2 in **scheme 4**) The peptide was precipitated with methyl *tert*-butyl ether and dissolved in a water/acetonitrile mixture.

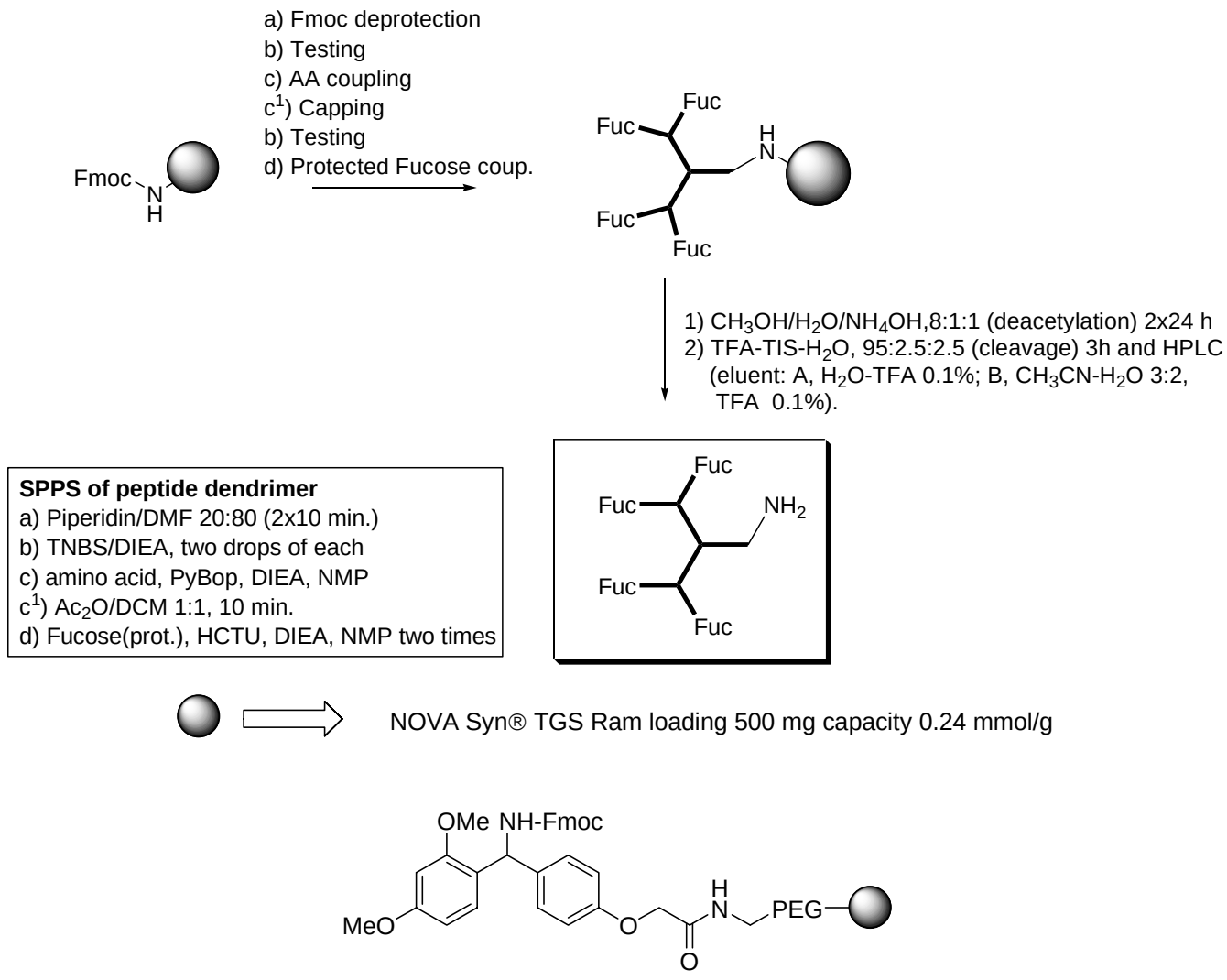

Scheme 4 Solid Phase Peptide Synthesis general procedure

All dendrimers were purified by preparative HPLC with detection at λ= 214 nm on a chromolith performance RP-C18, 4.6 x 100 mm column flow rate 3 mL $min,^{-1}$ eluent A: water and TFA (0.1%); eluent B: acetonitrile, water and TFA (3/2/0.1%). After purification, the structure of the dendrimer was confirmed by ESI-MS. Lectin binding was assessed with an Enzyme-Linked Lectin assay (ELLA). As reported above, this assay measures, through absorbance (read at 415 nm), the competition between the ligand and a biotinylated polymeric fucose reagent, toward the lectin (PA-

IIL). The logarithm of the concentration of the dendrimer was plotted vs the % of inhibition. The sigmoidal curve was fitted and the concentration at 50% of inhibition (IC_{50}) was determined.

Ile - GAR- L

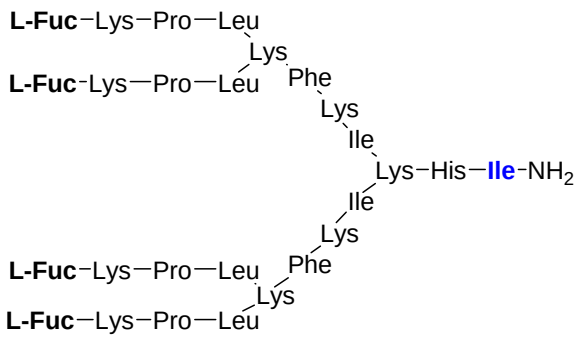

ES-MS = 3535.0
Y = 8% isolated after prep. HPLC

Leu - GAR- D

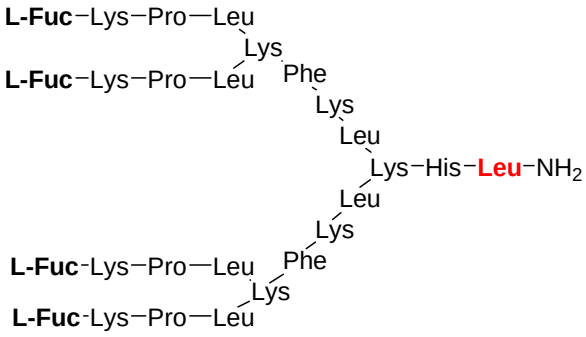

ES-MS = 3535.0
Y = 12% isolated after prep. HPLC

Leu - GAR- L

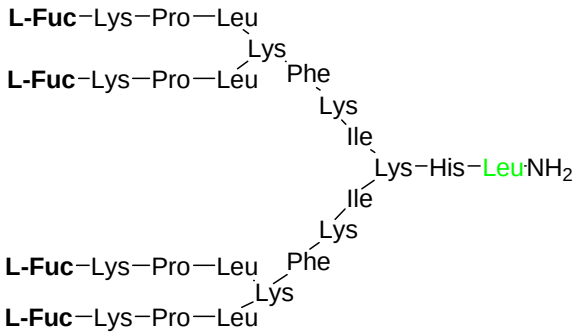

ES-MS = 3535.0
Y =10% isolated after prep. HPLC

Ile - GAR- L dendrimer with L-amino acid sequence and Ile as first
Leu - GAR- L dendrimer with L-amino acid sequence and Leu as first
Leu - GAR- D dendrimer with D-amino acid sequence, L-Lys as branch and Leu as first

Fig. 4 Glycopeptide dendrimers synthesized in Berne

The results of IC_{50} obtained by the ELLA test (see **Tab. 4**) indicate that Ile GAR-L and Leu GAR-L having all L-amino acids are the most potent ligands against PA-IIL lectin, with an IC_{50} = 0.14 µM and 0.15 µM respectively, which corresponds to a relative potency of 80 and 73 relative to L-fucose. No differences, within experimental errors, between the two amino acid based dendrimers was observed, indicating that the presence of a L-Ile or a L-Leu as first amino acid is not significant. Concerning Leu-GAR-D dendrimer, ELLA test against PA-IIL lectin shown an IC_{50} = 0.66 µM and a relative potency of 17 relative to L-fucose. As could be expected, Leu-GAR-D has a

different IC_{50} value than its L-amino acid counterparts, but is only 4-fold less active. In any case, Leu-GAR-D is 17 times (ca 4 times per sugar units) more potent than the monovalent L-fucose, thus showing that also for this ligand, a multivalent effect is operating.

No.	IC_{50} (μM)	r.p[a].	n[b]	r.p./n[c]
L-fucose	11	1	1	1
Ile-GAR-L	0.14 ± 0.035	80	4	20
Leu-GAR-L	0.15±0.082	73	4	18
Leu-GAR-D	0.66±0.12	17	4	4.2

Table 4. IC_{50} Values with PA-IIL lectin as measured by ELLA test

[a] r.p. = relative potency to fucose = IC_{50} (fucose)/IC_{50} (ligand). [b] n. = number of fucosyl units per dendrimer.
[c] Relative potency per fucose residue.

After having demonstrated that Leu-GAR-D is able to inhibit PA-IIL, we undertook studies aimed at evaluating its proteolytic stability. All dendrimers were incubated with two proteins, Trypsin and Chymotrypsin, with human serum and bacteria PAO1 at 37 °C. The stability of each dendrimer was monitored by HPLC injection at 10, 30, 60 min and after 24 h. (see **Tab 5**). The dendrimers Ile-GAR-L and Leu-GAR-L are, as expected, not stable under these proteolytic conditions. In the presence of the proteolytic Trypsin or Chymotrypsin, more than 95% of the dendrimer is decomposed after only 30 min. of incubation. These L-dendrimers are slightly more stable in the presence of human serum or bacteria PAO1, but also in these cases an extended decomposition can be observed. Especially in the presence of bacteria PAO1, after 1 h, 20-50% of the dendrimer is decomposed, and after 24 h no traces of the inhibitor could be found in the incubation liquor.
Remarkably different is the situation observed with the D-peptide dendrimer Leu-GAR-D, since it is resistant to proteolytic conditions in human serum, PAO1 bacterial strains and even enzymes. In all cases also after prolonged incubation time Leu-GAR-D can be found completely integer.

Cond.	Leu-GAR-L	Ile-GAR-L	Leu-GAR-D
Trypsin 10 min	68	17	100
Trypsin 30 min	6	1	100
Trypsin 1h	1	0	100
Trypsin 24 h	0	-	100
Chymotrypsin 10 min	49	2	100
Chymotrypsin 30 min	1	0	100
Chymotrypsin 1h	0	0	100
Chymotrypsin 24 h	-	-	100
Serum 30 min	100	100	100
Serum 4h	100	~90	100
Serum 24 h	57	49	Not determ.
PAO1 10 min	92	100	100
PAO1 30 min	90	65	100
PAO1 1h	78	54	100
PAO1 24 h	0	0	not determ.

Tab.5 Percentage (%) of integer fucosylated peptide dendrimer detected by HPLC after the delay of time indicated in different proteolytic conditions (T = 37° C).

2.8 Conclusions

The neoglycopeptide dendrimers are a new class of synthetic macromolecules that can be prepared by standard peptide coupling chemistry with an efficient solid phase peptide synthesis. Every The experiments reported in this chapter show that ligands for fucose-binding lectins can be selected by affinity screening of combinatorial libraries of such dendritic ligands. A new approach to dendrimer property tuning is demonstrated by combinatorial variation of dendrimer branch length and multivalency level, using a large self-encoded glycopeptides dendrimer library. The preparation of a different arm-length combinatorial dendrimer library is an important extension of the self-encoded dendrimer library principle, that allow to prepare a large combinatorial libraries using the exact same number of synthetic operations, and relying as before on the simple amino acid analysis for sequence determination. After the screening of a large number of dendrimers Reymond's group has identified a potent tetravalent *C*-fucosyl peptide dendrimer **FD2** with 100-fold higher potency than fucose for binding to the lectins UEA-I and PA-IIL. This is the first example of a multivalent ligand of these lectins. During the research activity carried out at Bern University, three glycopeptide dendrimers bearing L-Fuc at the periphery were synthesised. They strongly inhibit the adhesion of glycoproteins to LecB of *Pseudomanos Aeruginosa*, showing promises for their therapeutical applications against the formations of biofilms. Remarkablys, the Leu-GAR-D dendrimer, composed of D-amino acids, is stable to proteolysis, without loosing its activity. Further optimization of **FD2** and **Leu-GAR-D** are in progress to increase binding affinity toward PA-IIL with regards to the possible therapeutic relevance of lectin ligands as inhibitors of biofilm formation in the *Pseudomonas aeruginosa* pathogen.

2.9 Experimental section

Materials and reagents. Amino acids were used as the following derivatives: Fmoc-Ala-OH, moc Asp(O*t*-Bu)-OH, Fmoc-Arg(Pbf)-OH, Fmoc-His(Boc)-OH, Fmoc-Leu-OH, Fmoc-Phe- OH, Fmoc-Ser(*t*-Bu)-OH, Fmoc-Thr(*t*-Bu)-OH, Fmoc-Ile-OH, Fmoc-Gly-OH, Fmoc-Tyr(*t*- Bu)-OH, Fmoc Pro-OH, Fmoc-Lys(Boc)-OH, Fmoc-Lys(Fmoc)-OH, Fmoc-Glu(OtBu)-OH, Fmoc-Val-OH and FmocDapFmoc-OH. NovaSyn® TGR (loading: 0.18-0.29 mmol/g), and Rink amide NovaGel (loading: 0.63 mmol/g), was purchased from Novabiochem (Switzerland). Lectin UEA-I was purchased from Sigma and lectin PA-IIL was provided through collaborations. All solvents used were of analytical grade. Analytical RP-HPLC was performed in Waters (996 Photo diode array detector) chromatography system using a chromolith performance RP-C18, 4.6 x 100 mm, flow rate 3 mL.min-1 column. Compounds were detected by UV absorption at 214 nm. Preparative RPHPLC was performed with HPLC-grade acetonitrile and MilliQ deionized water in a Waters prepak cartridge 500 g (RP-C18 20 mm, 300 Å pore size) installed on a Waters Prep LC4000 system from Millipore (flow rate 100 mL.min^{-1}, gradient 1 or 1.25 %.min^{-1} CH_3CN). MS spectra were provided by the Service of Mass Spectrometry of the Department of Chemistry and Biochemistry, University of Bern.

2-(Tri*-O-*acetyl*-α-*L-fucopyranosyl)acetic acid* (4).** The known 3-(Tri-*O*-acetyl-α- L -fucopyranosyl)-1-propene **3**, prepared as described in Uchiyama, T.;Woltering, T. J.;Wong,W.; Lin, C.-C.; Kajimoto, T.; Takebayashi, M.; Weitz-Schmidt, G.; Asakura, T.; Noda, M.;Wong, C.-H. *Bioorg. Med. Chem.* **1996**, ***7, 1149-1165, (3.8 g, 12.0 mmol) was dissolved in $H_2O/CCl_4/CH_3CN$ (30:14:14, *v/ v,* 116mL). Sodium(meta)periodate (10.1 g, 48.0 mmol, 4.0 eq) and $RuCl_3$ (0.1 g, 0.48 mmol, 0.04 eq) were added. The resulting solution was stirred at r.t. for 4 h and partitioned between water (50 mL) and dichloromethane (100 mL). The aqueous phase was extracted with dichloromethane (2×50 mL) and the combined organic phases were washed with water (2×50 mL), extracted with saturated aqueous $NaHCO_3$ (2×50 mL). The aqueous phase was then acidified to pH 4 by addition of conc. HCl and reextracted in dichloromethane. The organic phase was washed with brine (100mL), then dried over $MgSO_4$. The solvent was removed under reduced pressure to give **4** as a white foamy solid (2.6 g, 67%). 1H NMR (400 MHz, [d]chloroform): δ = 1.17 (d, *J* = 6.4 Hz, 3 H, H-6), 2.01, 2.04, 2.15 (each: s, 3H, OAc), 2.66 (dd, *J* = 15.5, 5.6 Hz, 1 H, H-1'a), 2.76 (dd, *J* = 15.5, 8.8 Hz, 1 H, H-1'b), 4.04 (dq, *J* = 2.0, 6.4 Hz, 1 H, H-5), 4.70 (dt, *J* = 9.0, 5.5 Hz, 1 H, H-1), 5.16 (dd, *J* = 9.7, 3.3 Hz, 1 H, H-3), 5.28 (dd, *J* = 3.3, 2.2 Hz, 1 H, H-4), 5.38 (dd, *J* = 9.8, 5.5 Hz, 1 H, H-2). 13C NMR (75 MHz, [d]chloroform): δ = 16.0; 20.8; 33.0; 67.2; 67.6; 68.6; 69.5; 70.3;

169.8; 170.2; 170.6; 175.5. ESI-MS: *m/z* 355.09 ([M + Na]$^+$). HRMS (ESI-MS): calc. for [C14H20O9+Na]: 355.1005; found: 355.1014.

Dendrimer synthesis, general procedure. Peptide syntheses were performed manually in a glass reactor or plastic syringes (5 or 10 mL). The resin NovaSyn® TGR (loading: 0.18-0.29 mmol/g) was acylated with each amino acid or diamino acid (3 eq) in the presence of BOP or PyBOP (3 eq) and DIEA (5 eq) for 1 h and 30 min, 3 h after the first generation. After each coupling the resin was successively washed with NMP, MeOH, and CH_2Cl_2 (3× with each solvent), then checked for free amino groups with the TNBS test. If the TNBS test indicated the presence of free amino groups, the coupling was repeated. After each coupling the potential remaining free amino groups were capped with acetic anhydride/CH_2Cl_2 for 10 min. The Fmoc protecting groups were removed with a solution of 20% piperidine in DMF (2×10 min) and the solvent was removed by filtration. In the end of the sequence the resin was capped with carbohydrate **4** (5 eq) in the precence of DIC (5 eq) and HOBt (5 eq) or DIEA (5 eq) and HCTU (3 eq) in NMP overnight. The carbohydrate was deacetylated with a solution of MeOH/NH_4/H_2O (v/v 8:1:1) for 24 h. The resin was dried and the cleavage was carried out with TFA/TIS/H_2O (95:2.5:2.5) for 4 h. The peptide was precipitated with methyl *tert*-butyl ether then dissolved in a water/acetonitrile mixture. All dendrimers were purified by preparative HPLC with detection at λ = 214 nm. Eluent A: water and TFA (0.1%); eluent B: acetonitrile, water and TFA (3/2/0.1%). Dendrimers were obtained as colorless foamy solids after cleavage from the resin and preparative RP-HPLC purification.

Dendrimer GAR 1-5-1: (Fuc-α-CH_2CO-Lys-Pro-Leu)$_4$(Lys-Phe-Lys-Ile)$_2$Lys-His-Ile-NH_2 with L amino acid : (Yield = 8.0 %) MS (ES+) calc for $C_{172}H_{290}N_{35}O_{43}$ [M+H]$^+$: 3536.34, found: 3536.0. Preparative RP-HPLC: (A/B = 80/20 to A/B = 40/60 in 50 min). Deletion side product with MS 3439.0 = [M$^+$] – 97 (proline residue).

Dendrimer GAR 1-20-1: (Fuc-α-CH_2CO-Lys-Pro-Leu)$_4$(Lys-Phe-Lys-Ile)$_2$Lys-His-Leu-NH_2 with L-amino acid : (Yield = 10.0 %) MS (ES+) calc for $C_{172}H_{290}N_{35}O_{43}$ [M+H]$^+$: 3536.34, found: 3536.0. Preparative RP-HPLC: (A/B = 80/20 to A/B = 40/60 in 50 min). Deletion side product with MS 3439.0 = [M$^+$] – 97 (proline residue).

Dendrimer GAR 1-13-1: (Fuc-α-CH_2CO-Lys-Pro-Leu)$_4$(Lys-Phe-Lys-Ile)$_2$Lys-His-Leu-NH_2 with D-amino acid and only L-Lys as branching : (Yield = 12.0 %) MS (ES+) calc for $C_{172}H_{290}N_{35}O_{43}$ [M+H]$^+$: 3536.34, found: 3536.0. Preparative RP-HPLC: (A/B = 80/20 to A/B =

40/60 in 50 min). Deletion side product with MS 3347.0 = $[M^+]$ – 188 (minus one fucose residue dendrimer).

Proteolytic stability test with PAO1

Inocula of *P. aeruginosa* strains PAO1 were prepared from 5 ml overnight cultures grown in LB broth and the optical density (600 nm) was adjusted to 0.1 and aliquots of 20 µL were mixed with 20 µL dendrimer solution (2 mM) in tris buffer (100mM, pH 7.5). The mixture was incubated at 37˚C for 10 min, 30 and 60 min and the proteolysis was stopped by addition of 100 µL of H_2O (1 % TFA). The solution was filtered and analyzed by RP-HPLC. Flowrate: 1.5 $mL \cdot min^{-1}$ (AD 80/20 to 0/100 in 15 min). Conversions were calculated by comparing integrals of starting material left after the test with a blank.

Proteolytic stability test with Human serum

20 µL human serum to 20 µL of dendrimer solution, 2 mM in tris buffer (100mM, pH 7.5). The proteolysis was stopped by addition of 100 µL MeOH (1% TFA), filtered and then analyzed by RP-HPLC. Flowrate: 1.5 $mL \cdot min^{-1}$ (AD 80/20 to 0/100 in 15 min). Conversions were calculated by comparing integrals of starting material left after the test with a blank.

Proteolytic stability test in solution with Trypsin and Chymotrypsin

The proteolysis was started by an addition of 5 µL of a freshly prepared stocksolution of the protease (2.4 mg/mL of trypsin and 1 mg/mL of chymotrypsin) to a mixture of 50 µL dendrimer solution (2 mM in tris buffer (100mM, pH 7.5)) and 45 µL of tris buffer (100mM, pH 7.5). The reaction mixture was analysed after 10, 30, 60 min and 48 hours by RP-HPLC. Flowrate: 1.5 $mL \cdot min^{-1}$ (AD 80/20 to 0/100 in 15 min). Conversions were calculated by comparing integrals of starting material left after the test with a blank.

2.10 References

[1] P. K. Singh. A. L. Schaefer, M. R. Parsek, T. O. Moninger, M. J. Welsh, E. P. Greenberg, *Nature* **2000** 407 762-764.

[2] N. Gilboa-Garber, L. Mizrahi, N. Garber, *FEBS Lett*. **1972,** 28,93-95.

[3] N. Gilboa-Garber, D. J. Katcoff, N. C. Garber, *FEBS Immunol. Med. Microbiol*. **2000,** 29,53-57.

[4] Glick, J.& Garber, N. *J. Gen. Microbiol*. **1983.** 129,3085-3090.

[5] N. Gilboa-Garber, *Methods Enzymol*. **1982** 83,378-385.

[6] D. Avichezer, D. J. Katcoff, N.C. Garber, N. Gilboa-Garner, *J. Biol. chem*. **1992** 267, 23023-23027.

[7] N. Garber, U. Guempel, A. Belz, N. Gilboa-Garber, R: J. Doyle, *Biochim. Biophys. Acta* **1992** 1116, 331-333.

[8] B. Lanne, J. Ciopraga, J. Bergstrom, C. Motas, K. A. Karlsson, *Glycoconj. J.* **1994** 11, 292-298.

[9] C. P. Chen, S. C. Song, N. Gilboa-Garber, K. S. Chang, A. M. Wu, *Glycobiology* **1998** 8, 7-16.

[10] N. Gilboa-Garber, D. Sudakevits, M. Sheffi, R. Sela, C. Levene, *Glycoconj. J.* **1994** 11, 414-417.

[11] N. Garber, U. Guempel, N. Gilboa-Garber, R. J. Doyle, *FEMS Microbiol. Lett.* **1987** 49, 331-334.

[12] E. Mitchell C. Houles, D. Sudakevitz, M. Wimmerova, C. Gautier, S. Pèrez, A. M. Wu, N. Gilboa-Garber, A. Imberty, *Nature Struct. Biol.* **2002** 9, 918-921.

[13] Z. J. Liu, W. Tempel, D. Lin, K. Karaveg, R. J. Doyle, J. P. Rose, B. C. Wang, *Am. Cryst. Assoc.* **2002** 29, 98 Abstr. Papers (Annual Meeting).

[14] G. Cioci, E. P. Mitchell, C. Gautier, M. Wimmerova, D. Sudakevitz, S. Pèrez, N. Gilboa-Garber, A. Imberty, FEBS *Lett.* **2003** 297-301.

[15] R. Loris, D. Tielker, K.-E. Jaeger, L. Wyns, *J. Mol. Biol.* **2003** 331, 861-870.

[16] J. Glick, N. C. Garber, *J. Gen. Microbiol.* **1983** 9,3085-3090.

[17] L. V. Hooper, J. I. Gordon, *Glycobiology* **2001** 11, 1R-10R.

[18] L. Imundo, J. Barasch, A. Prince, Q. Al-Awqati, *Proc. Natl. Acad. Sci.* USA **1995** 92, 3019-3023.

[19] G. Lamblin, S. Degroote, J. M. Perini, P. Delmotte, A. Scharfman, M. Davril, J. M. Lo-Giudice, N. Houdret, V. Dumur, A. Klein, P. Roussel, *Glycoconj. J.* **2001** 18, 661-684.

[20] A. Scharfman, S. Degroote, J. Beau, G. Lamblin, P. Roussel, J. Mazurier, *Glycobiology* **1999** 9, 757-764.

[21] (a) Lee, Y. C.; Lee, R. T. *Acc. Chem. Res.* **1995**, *28*, 321-327. (b) Mammen, M.; Choi, S.-K.; Whitesides, G. M. *Angew. Chem., Int. Ed.* **1998**, *37*, 2754-2794. (c) Bertozzi, C. R.; Kiessling, L. L. *Science* **2001**, *291*, 2357-2364. (d) Kitov, P. I.; Sadowska, J. M.; Mulvey, G.; Armstrong, G. D.; Ling, H.; Pannu, N. S.; Read, R. J.; Bundle, D. R. *Nature* **2000**, *403*, 669-672. (e) Gabius, H.-J.; Siebert, H.-C.; Andre´, S.; Jime´nez-Barbero, J.; Ru¨diger, H. *ChemBioChem* **2004**, *5*, 740-764. (f) Ambrosi, M.; Cameron, N. R.; Davis, B. G. *Org. Biomol. Chem.* **2005**, *3*, 1593-1608. (g) Kiessling, L. L.; Gestwicki, J. E.; Strong, L. E. *Angew. Chem., Int. Ed.* **2006**, *45*, 2348-2368.

[22] (a) Roy, R. *Trends Glycosci. Glycotechnol.* **2003**, *15*, 291-310. (b) Ro¨ckendorf, N.; Lindhorst, T. K. *Top. Curr. Chem.* **2001**, *217*, 201- 238.

[23] Oligosaccharide libraries on tentagel: (a) Liang, R.; Yan, L.; Loebach, J.; Ge, M.; Uozumi, Y.; Sekanina, K.; Horan, N.; Gildersleeve, J.; Thompson, C.; Smith, A.; Biswas, K.; Still, W. C.; Kahne, D. *Science* **1996**, *274*, 1520-1522. (b) Liang, R.; Loebach, J.; Horan, N.; Ge, M.; Thompson, C.; Yan, L.; Kahne, D. *Proc. Natl. Acad. Sci. U.S.A.* **1997**, *94*, 10554-10559

[24] Glycopeptide libraries (no fucose): (a) Halkes, K. M.; St. Hilaire, P. M.; Crocker, P. R.; Meldal, M. *J. Comb. Chem.* **2003**, *5*, 18-27. (b) Ying, L.; Liu, R.; Zhang, J.; Lam, K.; Lebrilla, C. B.; Gervay-Hagues, J. *J. Comb. Chem.* **2005**, *7*, 372-384. (c) Wittmann, V.; Seeberger, S. *Angew. Chem., Int. Ed.* **2004**, *43*, 900-903

[25] a) G. R. Newkome, C. N. Moorefield, F. Vögtle, *Dendritic Molecules: Concepts, Synthesis, Perspectives,* VCH, Weinheim, **1996**; b) A. W. Bosman, H. M. Jansen, E. W. Meijer, *Chem. Rev.* **1999** 99, 1665-1688; c) M. Fischer, F. Vögtle, *Angew. Chem.* **1999**, 38, 885-905; d) J. P. Majoral, A.-M. Caminade, *Chem. Rev.* **1999**, 99, 845-880; e) O. A. Matthews, A. N. Shipway, J. F. Stoddart, *Prog. Polym. Sci*. **1998**, 23, 1-56; f) H. Frey, C. Lach, K. Lorenz, *Adv. Matrr.* **1998**, 10, 279-293.

[26]a) H. F. Chow, T. K.-K. Mong, M. F. Nongrum, C.-W. Wan, *Tetrahedron* **1998**, 54, 8543-8660; b) J. M. J. Frèchet, *Science,* **1994**, 263, 1710-1715; c) D. K. Smith, F. Diederich, *Chem. Eur. J.* **1998**, 4, 1353-1361; d) A. Archut, F. Vögtle, *Chem. Soc. Rev.* **1999**, 27, 233-240.

[27] Crespo, L.; Sanclimens, G.; Pons, M.; Giralt, E.; Royo, M.; Albericio, F. *Chem. Re*V. **2005**, *105*, 1663-1681.

[28] (a) Clouet, A.; Darbre, T.; Reymond, J.-L. *Angew. Chem., Int. Ed.* **2004**, *43*, 4612-4615. (b) Clouet, A.; Darbre, T.; Reymond, J.-L. *Biopolymers (Pept. Sci.*) **2006**, *84*, 114-123.

[29] (a) Esposito, A.; Delort, E.; Lagnoux, D.; Djojo, F.; Reymond, J.-L. *Angew. Chem., Int. Ed.* **2003**, *42*, 1381-1383. (b) Lagnoux, D.; Delort, E.; Douat-Casassus, C.; Esposito, A.; Reymond, J.-L. *Chem.-Eur. J.* **2004**, *10*, 1215-1226. (c) Clouet, A.; Darbre, T.; Reymond, J.-L. *Ad*V. *Synth. Catal.* **2004**, *346*, 1195-1204. (d) Douat-Casassus, C.; Darbre, T.; Reymond, J.-L. *J. Am. Chem. Soc.* **2004**, *126*, 7817-7826. (e) Delort, E.; Darbre, T.; Reymond, J.-L. *J. Am. Chem. Soc.* **2004**, *126*, 15642-15643. (f) Kofoed, J.; Reymond, J.-L. *Curr. Opin. Chem. Biol.* **2005**, *9*, 656-664. (g) Lagnoux, D.; Darbre, T.; Schmitz, M. L.; Reymond, J.-L. *Chem.-Eur. J.* **2005**, *11*, 3943-3950. (h) Delort, E.; Nguyen-Trung, N.-Q.; Darbre, T.; Reymond, J.-L. *J. Org. Chem.* **2006**, *71*, 4468-4480. (i) Kofoed, J.; Darbre, T.; Reymond, J.-L. *Org. Biomol. Chem.* **2006**, 3268-3281. (j) Darbre, T.; Reymond, J.-L. *Acc. Chem. Res.* **2006**, *39*, 925-934.

[30] E. Kolomiets, E. Johansson, O. Renaudet, T. Darbre and J.-L. Reymond, *Org. Lett.,* **2007,** vol. 9, 1465-1468.

[31] (a) Audette, G. F.; Vandonselaar, M.; Delbaere, L. T. J. *J. Mol. Biol.* **2000**, *304*, 423-433. (b) Loris, R.; De Greve, H.; Dao-Thi, M.-H.; Messens, J.; Imberty, A.; Wyns, L. *J. Mol. Biol.* **2000**, *301*, 987-1002.

[32] (a) Furka, A.; Sebestye´n, F.; Asgedom, M.; Dibo´, G. *Int. J. Pept. Protein Res.* **1991**, *37*, 487-493. (b) Lam, K. S.; Salmon, S. E.; Hersh, E. M.; Hruby, V. J.; Kazmierski, W. M.; Knapp, R. J. *Nature* **1991**, *354*, 82- 84. (c) Houghten, R. A.; Pinilla, C.; Blondelle, S. E.; Appel, J. R.; Dooley, C. T.; Cuervo, J. H. *Nature* **1991**, *354*, 84-86. (d) Lam, K. S.; Lebl, M.; Krchnak, V. *Chem. Re*V. **1997**, *97*, 411-448.

[33] A. Furka, F. Sebestye´n and M. Asgedom, *Int. J. Pept. Protein Res.*, **1991**, 37, 487–493; (b) K. S. Lam, S. E. Salmon, E.M. Hersh, V. J. Hruby, W. M. Kazmierski and R. J. Knapp, *Nature,* **1991,** 354, 82–84; (c) R. A. Houghten, C. Pinilla, C. S. E. Blondelle, J. R. Appel, C. T. Dooley and J. H. Cuervo, *Nature,* **1991**, 354, 84–86; (d) K. S. Lam, M. Lebl and V. Krchnak, *Chem. Rev.,* **1997**, 97, 411–448

[34] Glycopeptide libraries (no fucose): (a) Halkes, K. M.; St. Hilaire, P. M.; Crocker, P. R.; Meldal, M. *J. Comb. Chem.* **2003**, *5*, 18-27. (b) Ying, L.; Liu, R.; Zhang, J.; Lam, K.; Lebrilla, C. B.; Gervay-Hagues, J. *J. Comb. Chem.* **2005**, *7*, 372-384. (c) Wittmann, V.; Seeberger, S. *Angew. Chem., Int. Ed.* **2004**, *43*, 900-903.

[35] Perret, S.; Sabin, C.; Dumon, C.; Pokorna´, M.; Gautier, C.; Galanina, O.; Ilia, S.; Bovin, N.; Nicaise, M.; Desmadril, M.; Gilboa-Garber, N.; Wimmerova´, M.; Mitchell, E. P.; Imberty, A. *Biochem. J.* **2005**, *389*, 325- 332

[36] (a) Mitchell, E.; Houles, C.; Sudakevitz, D.; Wimmerova, M.; Gautier, C.; Pe´rez, S.; Wu, A. M.; Gilboa-Garber, N.; Imberty, A. *Nat. Struct. Biol.* **2002**, *9*, 918-921. (b) Loris, R.; Tielker, D.; Jaeger, K.-E.; Wyns, L. *J. Mol. Biol.* **2003**,

331, 861-870. (c) Tielker, D.; Hacker, S.; Loris, R.; Strathmann, M.; Wingender, J.; Wilhelm, S.; Rosenau, F.; Ja¨ger, K.-E. *Microbiology* **2005**, *151*, 13131-1323

[37] Uchiyama, T.; Woltering, T. J.; Wong, W.; Lin, C.-C.; Kajimoto, T.; Takebayashi, M.; Weitz-Schmidt, G.; Asakura, T.; Noda, M.; Wong, C.-H. *Bioorg. Med. Chem.* **1996**, *7*, 1149-1165.

Chapter 3

Lanthanide (III) chelates in Magnetic Resonance Imaging (MRI)

3.1 Magnetic Resonance Imaging (MRI)

Magnetic resonance imaging (MRI), or Nuclear magnetic resonance imaging (NMRI), is primarily a medical imaging technique most commonly used in radiology to visualize the structure and function of the body[1]. It provides detailed images of the body in any plane. MRI provides much greater contrast between the different soft tissues of the body than computed tomography (CT) does, making it especially useful in neurological (brain), musculoskeletal, cardiovascular, and oncological (cancer) imaging. Unlike CT, it uses no ionizing radiation, but uses a powerful magnetic field to align the nuclear magnetization of (usually) hydrogen atoms in water in the body. MRI is a relatively new technology, which has been in use for little more than 35years (compared with over 110 years for X-ray radiography). The first MR Image was published[2] in 1973 and the first study performed on a human took place on July 3, 1977. Magnetic resonance imaging was developed from knowledge gained in the study of nuclear magnetic resonance. In its early years the technique was referred to as nuclear magnetic resonance imaging (NMRI). However, as the word *nuclear* was associated in the public mind with ionizing radiation exposure it is generally now referred to simply as MRI. Scientists still use the term NMRI when discussing non-medical devices operating on the same principles. The term Magnetic Resonance Tomography (MRT) is also sometimes used. One of the contributors to modern MRI, Paul Lauterbur, originally named the technique *zeugmatography*, a Greek term meaning "that which is used for joining"[2]. The term referred to the interaction between the static, radiofrequency, and gradient magnetic fields necessary to create an image, but this term was not adopted. The MRI technique is based on the possibility of generating images through the spatial localization of the water protons in the tissues[1] Compared to a traditional NMR experiment the spatial information is decoded through the application of magnetic field gradients in such a way that the proton resonance becomes dependent on the position (**Fig.1**).

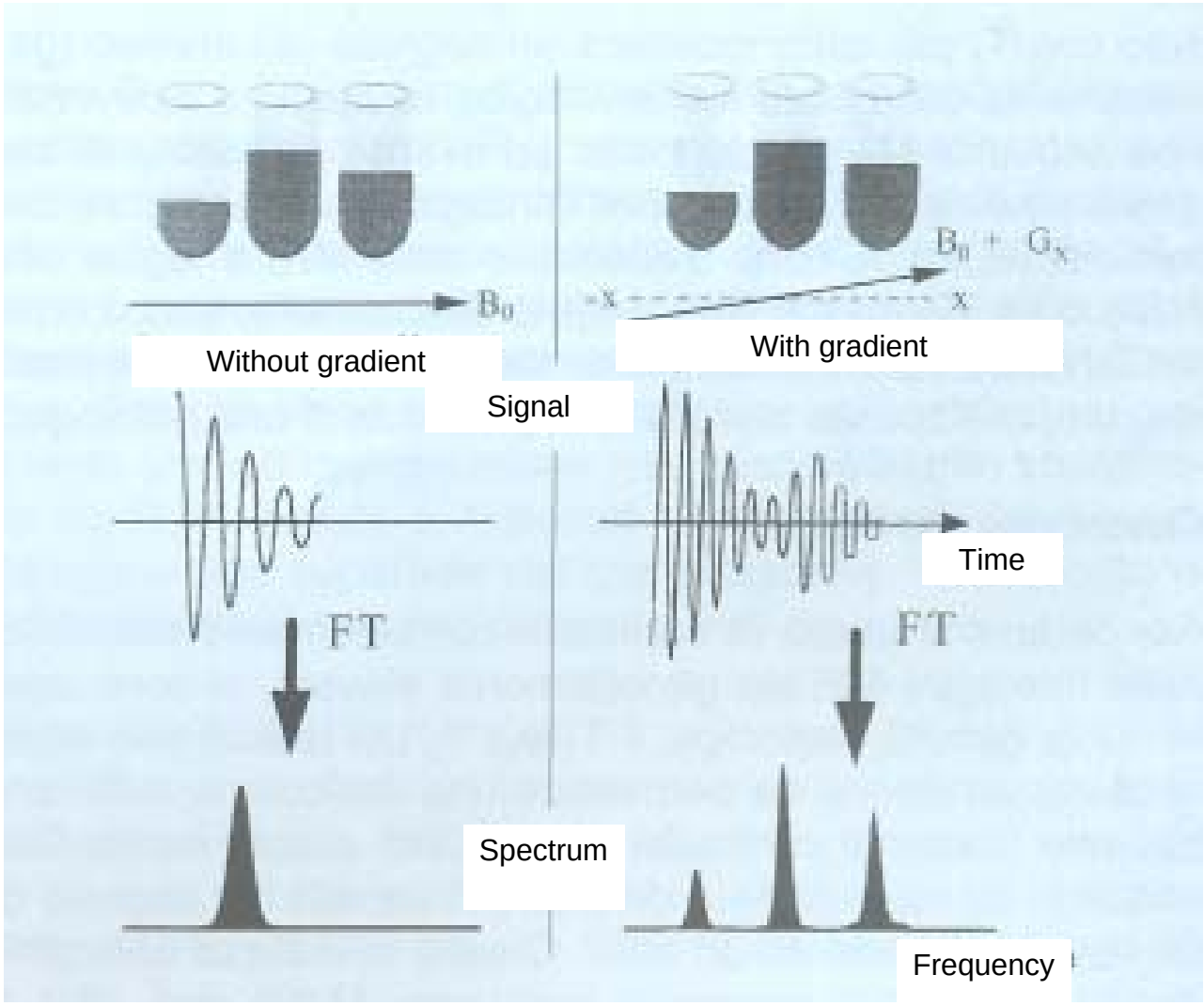

Fig. 1. Signals and spectra obtained from three water samples in different positions along the x axis without and with the application of a field gradient along the x axis. In the presence of the gradient the signals of the three samples are resolved and the separation between the signals is dependent on their spatial separation in the x direction and on the intensity of the field gradient.

MRI gives the maps of local chemico-physical properties such as the proton density, the longitudinal (T_1) and transverse (T_2) relaxation times, which become images once the relation between these parameters and the anatomy and pathology of the tissues has been established. The quality of an image depends on the degree of contrast which can be obtained and, in this case, it derives from the differences in the water concentration and in the relaxation times of the protons in the different biochemical environments[3]. Careful design of the imaging pulse sequence allows one contrast mechanism to be emphasized while the others are minimized. The ability to choose different contrast mechanisms gives MRI tremendous flexibility. In the brain, T_1-weighting causes the nerve connections of white matter to appear white, and the congregations of neurons of gray matter to appear gray, while cerebrospinal fluid (CSF) appears dark. The contrast of white matter,

gray matter and cerebrospinal fluid is reversed using T_2 imaging, whereas proton-density-weighted imaging provides little contrast in healthy subjects. Additionally, functional parameters such as cerebral blood flow (CBF), cerebral blood volume (CBV) or blood oxygenation can affect T_1, T_2 and so can be encoded with suitable pulse sequences. The body is mainly composed of water molecules which each contain two hydrogen nuclei or protons. When a person goes inside the powerful magnetic field of the scanner these protons align with the direction of the field. A second radiofrequency electromagnetic field is then briefly turned on causing the protons to absorb some of its energy. When this field is turned off the protons release this energy at a radiofrequency which can be detected by the scanner. The position of protons in the body can be determined by applying additional magnetic fields during the scan which allows an image of the body to be built up. These are created by turning gradients coils on and off which creates the familiar knocking sounds during an MR scan. Diseased tissue, such as tumors, can be detected because the protons in different tissues return to their equilibrium state at different rates. By changing the parameters on the scanner this effect is used to create contrast between different types of body tissue.

Fig. 2 MRI Scanner (courtesy from NASA)

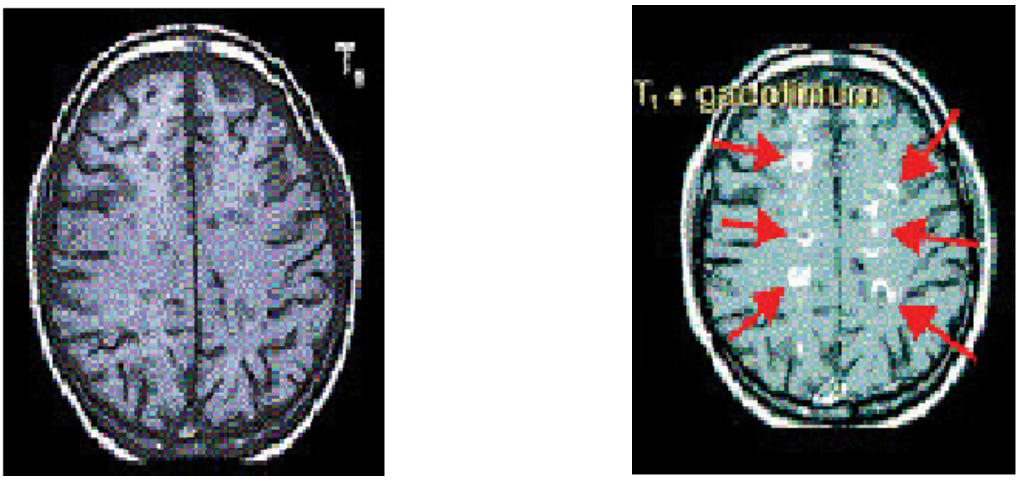

A **B**

Fig. 3 MRI image of a brain of the Schlerosis multiple patient; **A)** without contrast agent, **B)** with contrast agent

from web: /www.sclerosi-multipla.com

3.2 Gd (III) complexes as contrast agents for MRI

In some situations it is not possible to generate enough image contrast to adequately show the anatomy or pathology of interest by adjusting the imaging parameters alone, in which case a contrast agent may be administered. This can be as simple as water, taken orally, for imaging the stomach and small bowel. However, most contrast agents(CA) used in MRI are selected for their specific magnetic properties. Paramagnetic substances are usually used for increasing and controlling the magnetic relaxation of water protons[4]

Fig. 4: MR image in the presence of a contrast agent

Most studies have been performed on complexes of Gd (III) since this metal ion with a *S* ground state electronic structure couples a large magnetic moment with a long electron spin relaxation time ($\approx 10^{-9}$ s at the magnetic field strengths for MRI applications) two properties that ensure an optimum efficiency for nuclear spin relaxation of the interacting nuclei.

Other general requirements of CA for MRI are low toxicity, rapid excretion after administration, good water solubility and low osmotic potential of the solutions clinically used. Moreover, since the free metal ions are toxic they must be coordinated by a strong binding ligand that occupies most of the available coordination sites. Eventually, the preferred metal complexes, in addition to showing high thermodynamic (and possibly kinetic) stability, should present at least one water molecule in the inner coordination sphere, in rapid exchange with the bulk solvent, in order to affect strongly the relaxation of all solvent protons. The anionic complexes Gd(DTPA)$^{2-}$ (MAGNEQUIST^{R} , Schering AG, Germany) and Gd(DOTA)$^{-}$ (DOTAREM^{R} , Guerbert SA, France) were the first complexes entered into clinical practice and they represent the reference compounds for the development and evaluation of new agents. Gd(DTPA-BMA) (OMNISCAN^{R}, Nycomed Imaging

AS, Norway) and GdHPDO3A (PROHANCE^{R}, Bracco, Italy), have been introduced with the aim of providing systems with reduced osmotic potential for applications requiring high doses of CA. **Fig. 5** reports the schematic structure of the four ligands and the thermodynamic stability constants of their Gd (III) complexes measured at 25 °C and $\mu = 0.1$.

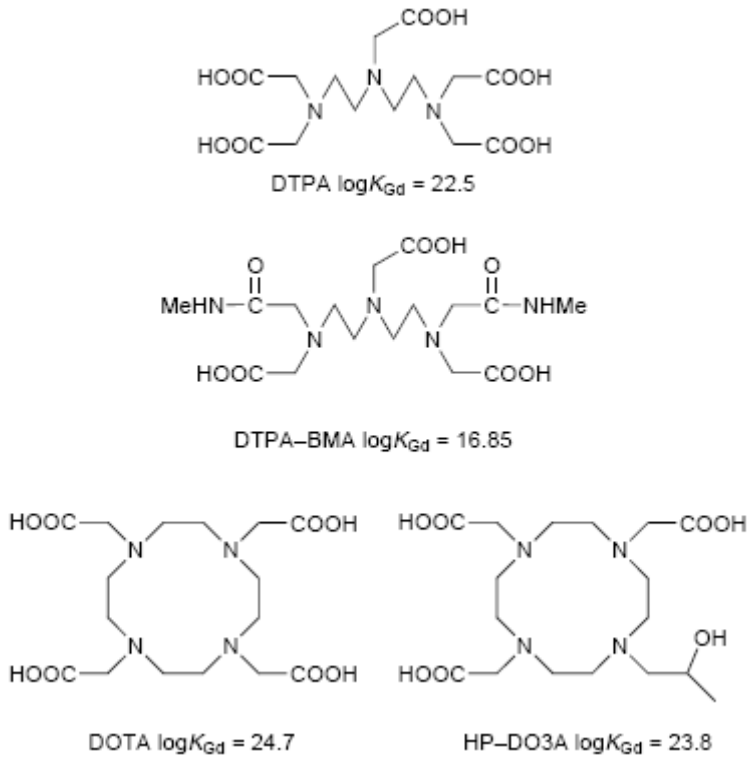

Fig 5 Schematic representation of the four ligands whose Gd(III) complexes are currently used as CA for MRI. Thermodynamic stabilities of the complexes in water at 25 °C and $\mu = 0.1$ M are reported. (Adapted from ref 5)

It may be surprising to find out that a complex like Gd(DTPA-BMA), whose stability constant is more than five orders of magnitude lower than Gd(DTPA)$^{2-}$ is considered safe enough for its clinical use. However, it has been pointed out that the toxicity[6] *in vivo* of Gd(III) complexes with polyaminocarboxylate logands does not correspond to the overall thermodinamic stability. Rather, the lack of displacement of Gd(III) by endogenous Ca(II) and the selectivity towards Ln(III) ions introduced by the two amide substuituents are effective in setting off the net loss in the overall thermodynamic stability.

These agents catalytically shorten the relaxation time of nearby water molecules , thereby enhancing the contrast with background tissues. In 1999, approximatively 30% of all MRI scans

used a contrast agent, most of which were based on gadolinium complexes. By now, this number has probably increased to between 40 and 50 %.

This utility has prompted research on improved Gd-based contrast agent, about which several reviews have recently been published. [5-20]

Current MRI agents require gram quantities of Gd in order to obtain satisfactory contrast in the resulting image. With such large doses required for reasonable image enhancement, current contrast agents (CA) are limited to targeting sites where they can be expected to accumulate in high concentrations, such as the blood stream. Ideally, second generation agents will be site-specific; much higher relaxivities will be required to account for the decrease in concentration that accompanies increased tissue specificity. The image-enhancing capability of a contrast agent is directly proportional to its relaxation of neighbouring water molecules by the paramagnetic ion; that is, to the relaxation rate increase either longitudinal ($1/T_1$) or transverse ($1/T_2$). This effect includes both inner-sphere contributions (from water molecules directly coordinated to the Gd) and out-sphere contributions (from nearby, H-bonded waters). The latter are usually relatively small and are usually neglected. The overall paramagnetic relaxation enhancement referred to by a 1mM concentration of a given Gd(III) chelate is called its proton *relaxivity* (r_{1p}), whose unity is $mM^{-1}s^{-1}$

For Gd(III) complexes, the inner sphere relaxivity primarily results from a dipolar contribution (through-space interaction due to the random fluctuations of the electronic field) and can be described by the Solomon-Bloembergen-Morgan theory[21]. According to the SBM theory to increase the relaxivity, r_{1p}, of a Gd contrast agent, one has to design a ligand that will enable the complex to have a greater number of inner sphere water molecules, q ; an optimally short water residence time τ_M ; and a slow tumbling rate, $1/\tau_R$ (**Fig. 6**) , while maintaining sufficient thermodynamic stability. This is quite a challenge ! The water residence time, τ_M , is probably the least understood and most important parameter that affects relaxivity. Indeed it has been demonstrated that the relaxivity of a gadolinium complex will increase upon slowing down its molecular tumbling (increasing its molecular weight) insofar as its water residence time is close to optimal. [22-25]

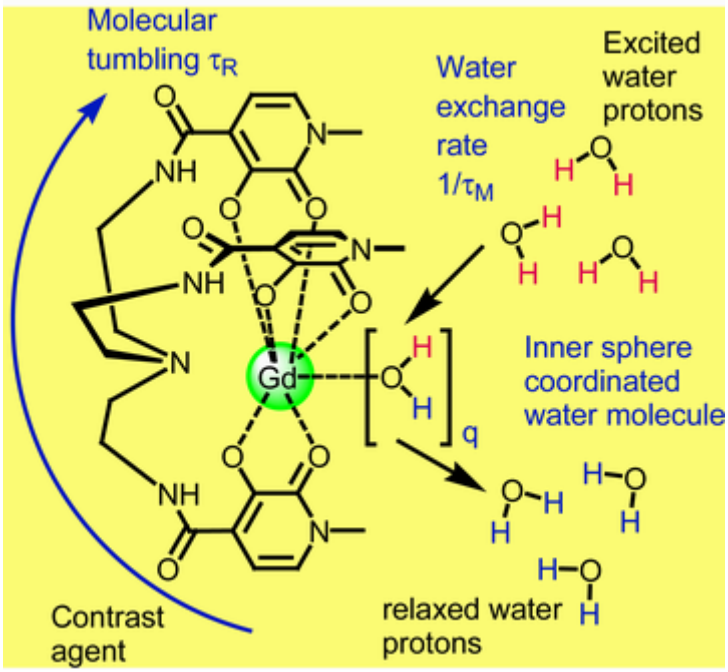

Fig. 6 Parameters influencing relaxivity

(taken from : http://www.cchem.berkeley.edu/knrgrp/mri.html)

In order to evaluate the relaxation parameters it is necessary to study the dependence of the relaxivity upon magnetic field. This is made possible through an instrumentation called field-cycling NMR relaxometer . The technique, called Nuclear Magnetic Relaxation Dispersion (NMRD) gives the so called *dispersion profile* by measuring, over a large frequency interval (0.01-50 MHz), the longitudinal relaxation time (T_1) of water molecules in a solution containing the paramagnetic complex (**Fig. 7**).The quantitative analysis of the *dispersion profile* allows a more accurate evaluation of all parameters which determine relaxivity.

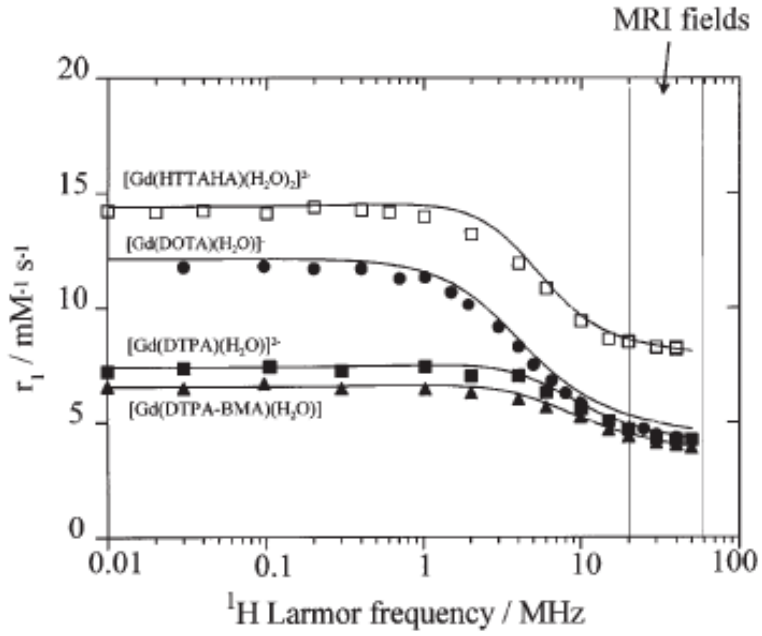

Fig. 7 Typical NMRD profiles of low molecular weight Gd(III) complexes

(adapted from ref. 18)

Considering the aforementioned properties, current commercial poly(amino-carboxylate) complexes (**Fig. 7**) have several disadvantages. They have only one coordinated water molecule and fast tumbling rates due to their small size. Attempts to increase their relaxivities by grafting them on macromolecules (slowing τ_R) have led to mixed success due to the accompanying particularly slow water exchange rates[1 26 27], $1/\tau_M$, typically 0.5-5x10^{-6} s^{-1} . These water exchange rates are several orders of magnitude slower than the rate for $Gd(H_2O)_8^{3+}$ and far below levels necessary to achieve high relaxivity ($\tau_M \approx 20$ ns at 20 MHz). Because the fundamental properties of current commercial contrast agents are far from optimal, their resulting relaxivities are very low (≈ 5 $nM^{-1}s^{-1}$), just a few percentage points of what is theoretically possible. Recent attempts to increase their water exchange rates by destabilizing their nine-coordinate ground state have resulted in less stable complexes[26 27].

3.3 DOTA and its Lanthanide Complexes

We will give here some details on 1,4, 7,10-tetraazacyclododecane-N,N', N'',N'''-tetraacetic acid (DOTA) and its Gd (III) complex (Gadoterate), since our contrast agents are based on this macrocycle.

Gadoterate has been the first macrocyclic gadolinium complex which entered the market ((DOTAREM^R , Guerbert SA, France). DOTA is considered a derivative of a macrocyclic

tetramine, called cyclen, which can be synthesized through different routes[28 29 30 31 32 33 34]. The first one is illustrated in **scheme 1** in which the cyclization of the tosylates **1** and **2** is performed in high yields, since the hydrocarbon segments between the heteroatoms are short, and relatively equal segnments of the target macrocycle are condensed. After detosilation of **3** the cyclen **4** is obtained. For the production of cyclen on a large scale, the tetramerization of N-benzylaziridine **6** seems to be preferential (**Scheme 2**). Tetrabenzylcyclen **7** has been prepared in nearly quantitative yield by refluxing a mixture of **6** and p-toluenesulfonic acid in alcohol for 6 hours. Debenzylation of **7** can be carried out by treatment with 10% Pd-C under hydrogen. Cyclen **4** is obtained in high yield. Alkylation with chloro- or bromoacetic acid leads to the ligand DOTA **9**, which is subsequently complexed with gadolinium chloride or gadolinium oxide to yield Gd-DOTA **5**[33] (**Scheme 3**)**.**

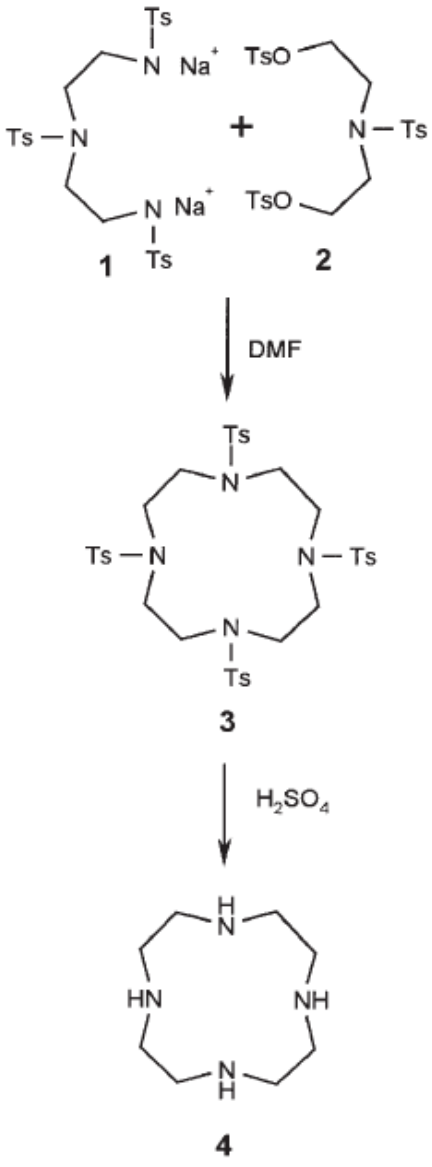

Scheme 1. Synthesis of cyclen by cyclization

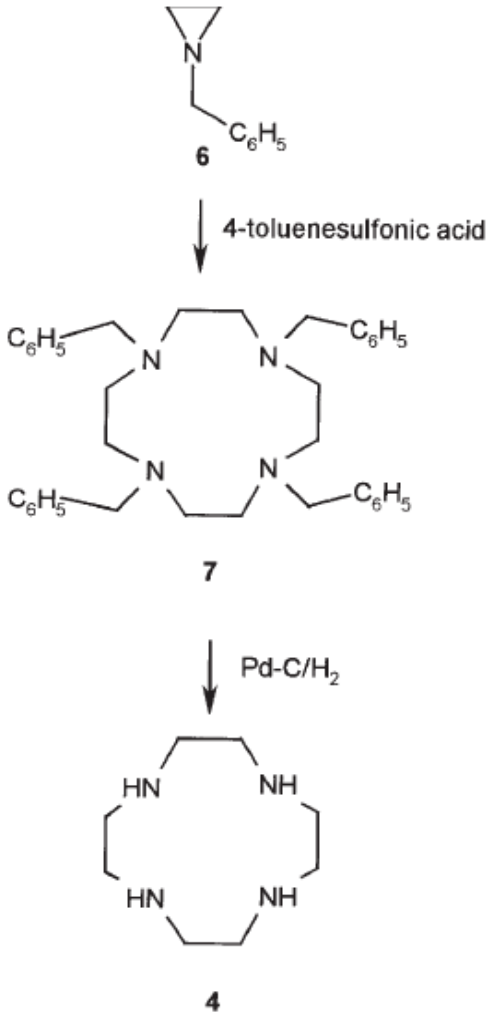

Scheme 2. Synthesis of Cyclen by tetramerization

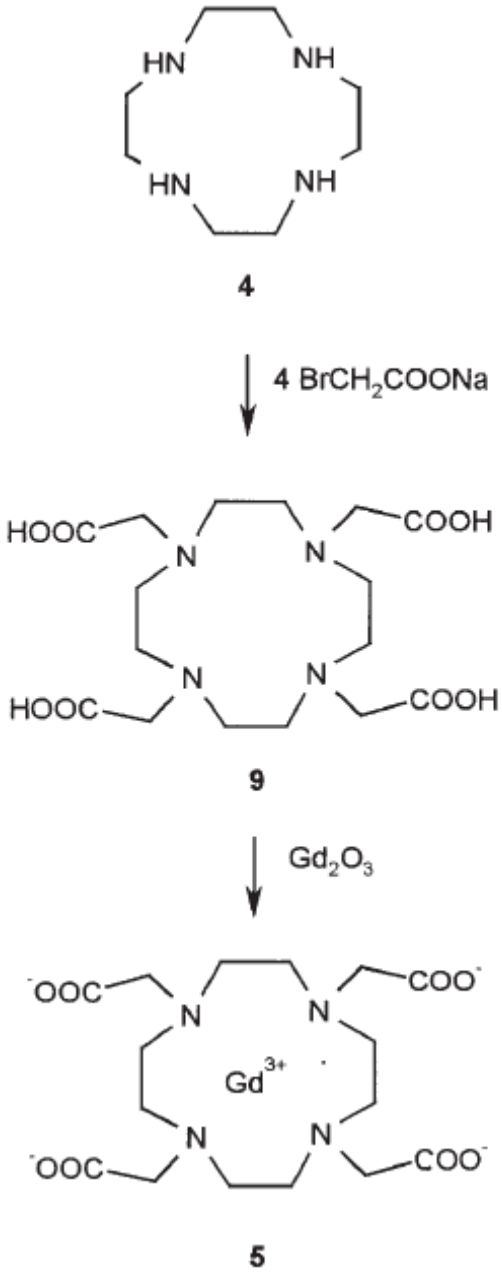

Scheme 3 Synthesis of gadoterate (Gd-DOTA) from cyclen

Due to the macrocyclic nature of the ligand the Gd (III) complex is endowed with high thermodynamic and kinetic stability *in vivo*[35 36]. The formulations of Dotarem (Gd-DOTA) consist of gadoterate as its N-methylglucamine salt in concentration of 0.5 and 1.0 mol/l. The latter solution displays relatively high osmolarity (4.02 osmol/kg water) and viscosity (11.3 cP)[37].

Several cyclen-based macrocyclic ligands similar to DOTA have been synthesized, in order to improve the relaxivity properties of their gadolinium complexes or for other purposes. A list is reported in **Scheme 4.**

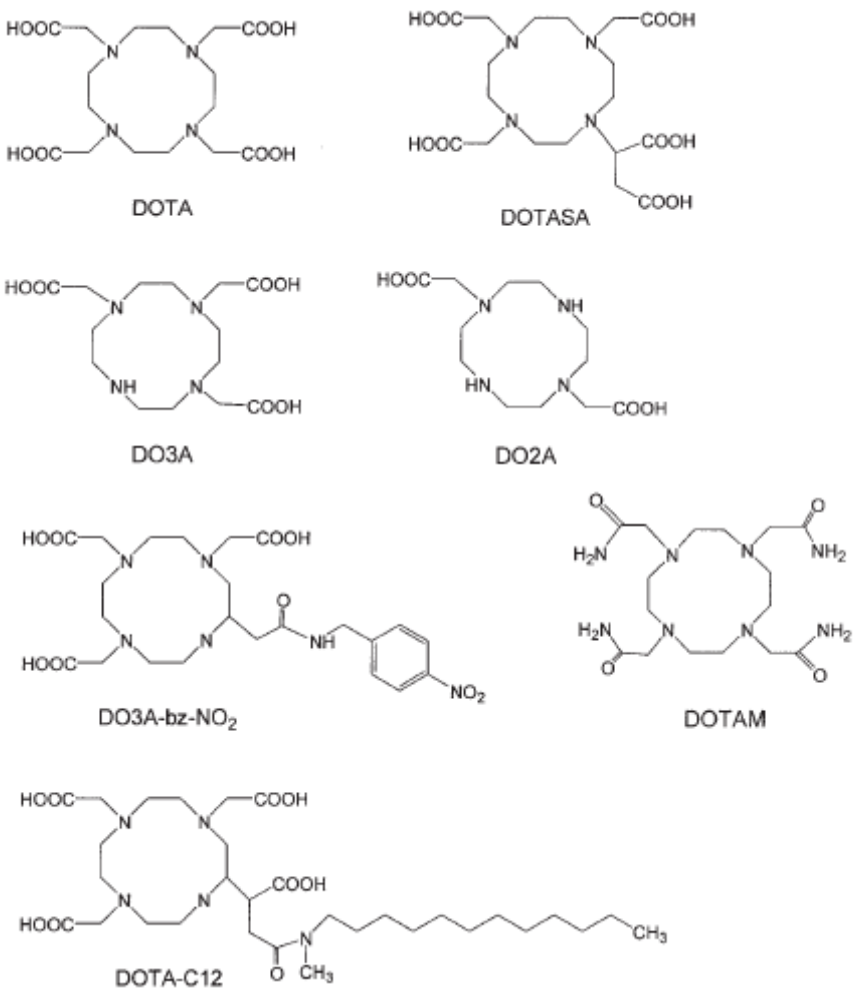

Scheme 4 Some representative examples of DOTA analogues

(from ref 18)

DOTA, having four carboxylate groups, forms with Gd(III) a negatively charged complex having one coordinated water molecule. The structure and dynamics in solution of the Lanthanide complexes of DOTA depends on many factors which has been elucidated (**Fig. 8**) through the combined use of several techniques (mainly 2D NMR)[16].

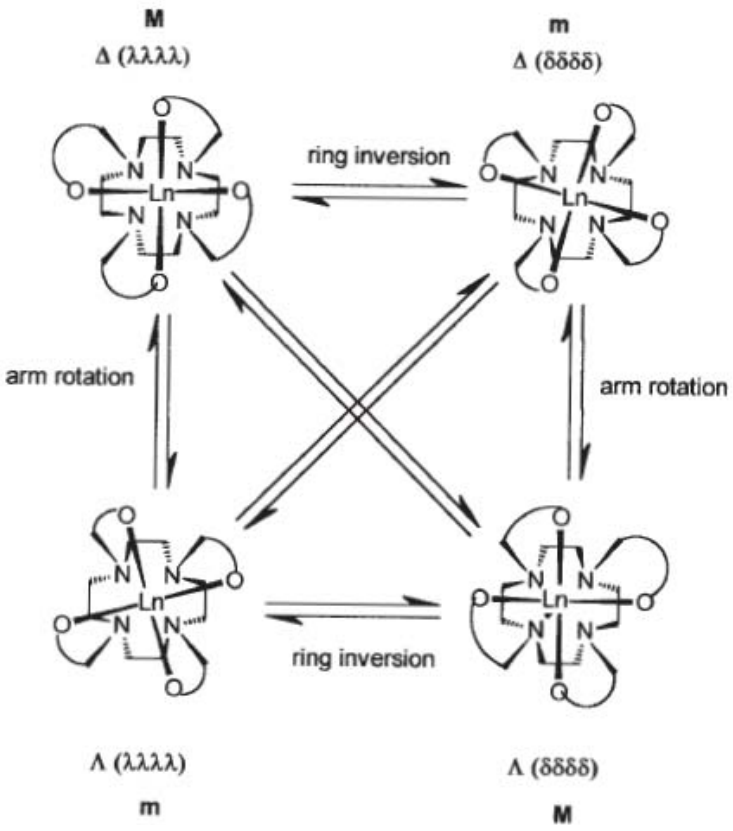

Fig. 8 Schematic representation of the structures and dynamics of $[Ln(DOTA)]^-$ complexws, looking down along the Ln-water O bond. The water ,olacule is omitted for clarity.

As briefly pointed out in the previous sections of this chapter, the research in the field of contrast agents (CA) for Magnetic Resonance Imaging has taken two main directions:

1) design and synthesis of kinetically stable lanthanide complexes in which the number of coordinated water molecules is higher and their exchange rates is increased compared to the known CAs, in order to enhance relaxivity (especially at the higher magnetic field strengths of current and future clinical MRI scanners);
2) attach to the selected gadolinium complexes recognition motives in order to deliver the paramagnetic complex to a specific organ or a biological target (**site-specific MRI)**.

Along the first line interesting new results have been recently reported by the group of K. N. Raymond[38], who synthesized a series of hydroxypyridone-based Gd(III) complexes (**Fig. 9**) which show significantly improved properties compared to the commercial agents.

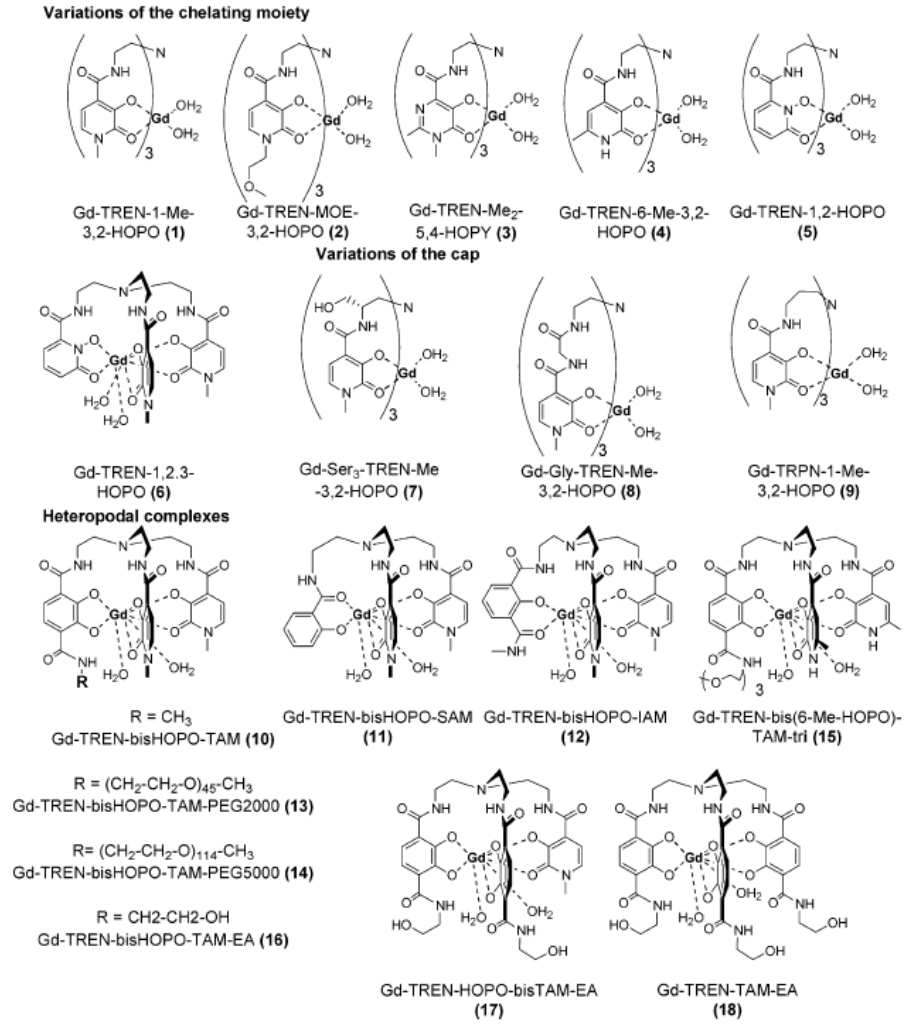

Fig.9: Structures of hydroxypyridone-based Gd(III) complexes

The X ray crystal structure of the gadolinium (III) complex of one of these ligands, called **Tren-tris HOPO** shows that it is 8-coordinate.The organic ligand is coordinated in an hexadentate fashion through the hydroxypyridone O-atoms and two water molecules complete the coordination sphere (**Fig. 10**). The relaxivity appears to be 2.5 times as high as that of [Gd (DTPA)]$^{-}$.

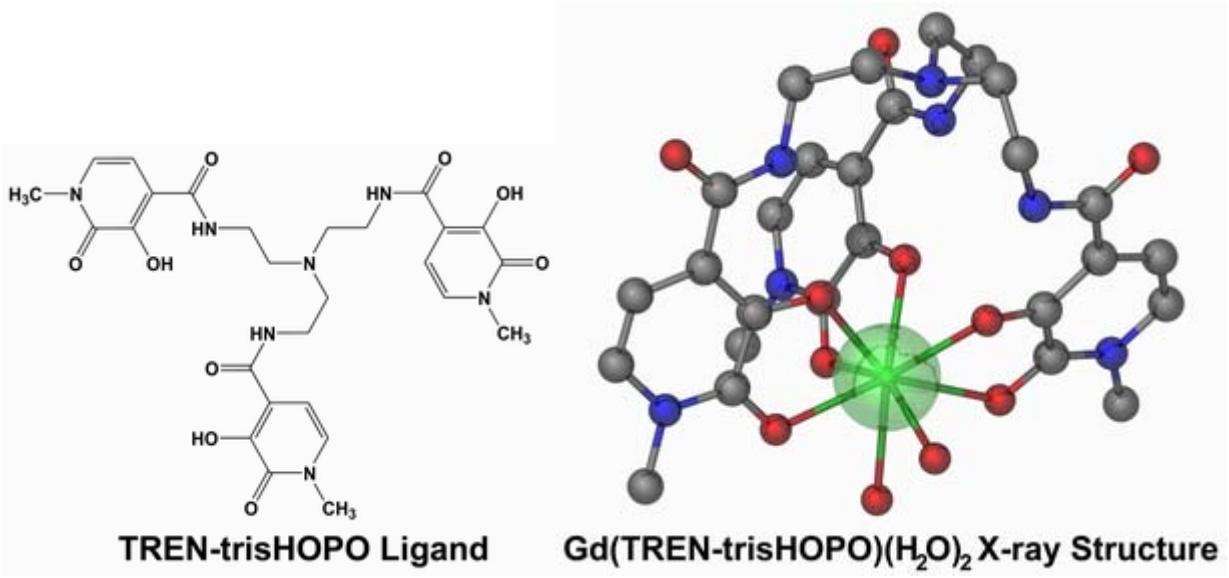

Fig. 10 (taken from : http://www.cchem.berkeley.edu/knrgrp/mri.html)

Although the organic ligand is only hexadentate, the thermodynamic stability of the complex is good (log β_{110}= 20.3), which may be ascribed to some degree of preorganization and stability due to internal hydrogen bonds.

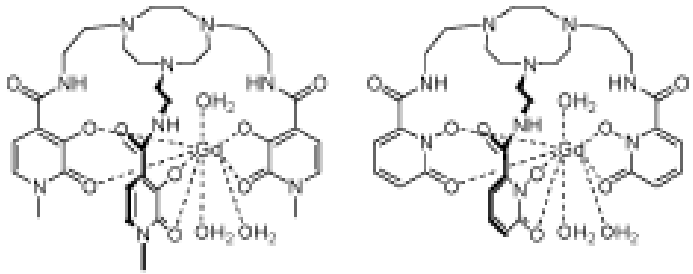

A **B**

Fig. 11

More recently the same group reported[39] two other examples (**A and B Fig 11**) of water soluble tris-hydroxypiridonate Gd(III) complexes in which the TREN cap has been replaced by a trazacyclononane (TACN) derivative. These two complexes shows an increased hydration number (q=3), a fast water exchange and a slow electronic relaxation which results in one of the highest relaxivity observed for a low molecular weight CA (r_{1p} = 13.1 and 12.5 mM^{-1} s^{-1} for A and B respectively at 20 MHz and 298 K, whereas this value is around 4-5 mM^{-1} s^{-1} for commercial agents in the same conditions. Concerning point 2, several examples of targeting using non sugar DOTA-conjugates will be given below (**3.4),** whereas the carbohydrate-based site specific MRI contrast agents will be discussed in more details in Chapter 4.

3.4 Site-specific MRI.

Typical clinical MRI contrast agents such as Gd-DTPA or Gd-DOTA are small molecules that distribute evenly through-out the extracellular space. These agents are well suited for vascular imaging applications, such as angiography and perfusion imaging. However, there is an increasing interest in achieving high MRI contrast and resolution especially in those regions or organs affected by diseases. New contrast agents are therefore needed which could reach this selectivity goal. The strategy, which has been named **targeted** or **site-specific MRI** tries to reach this goal *via* molecular imaging of the pathologic (or physiologic) biomarkers (**Fig. 12**) which can lead to early recognition of diseases, better therapeutic management, and improved monitoring for recurrence.[40,41,42] Although biomolecules are much too small (nm size) and in far too low of a concentration (pM range) to be directly imaged by MRI - which has a typical resolution of µm and detection limit of µM - by selective accumulation of site-directed contrast agents on molecular epitopes of pathologic or biomarkers it would be possible to visualise specific organs or tissues.

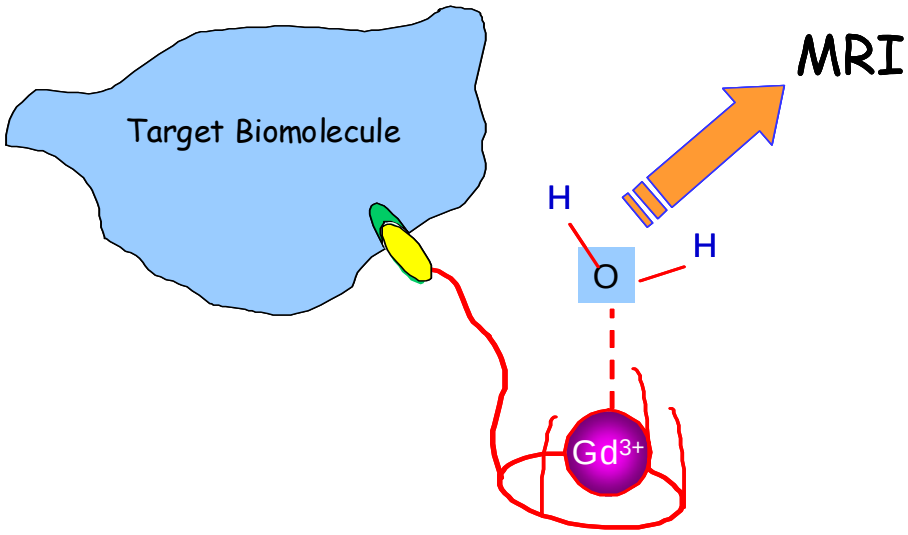

Fig. 12: Schematic representation of site-specific contrast agent in molecular imaging.

The design of site-specific contrast agents (also named molecular imaging contrast agent) implies the conjugation of a Gd(III) chelate to a proper ligand which shows selectivity for the biomarker of interest, generally genes or proteins which are linked directly or indirectly to human diseases. In this way, thanks to the selective ligand-receptor interaction, the Gd-chelate can be targeted directly and specifically, thus allowing the imaging of a receptor-rich tissue. Imaging of proteins or protein functions is more feasible, given the much larger number of such targets per cell compared with the number of DNA or mRNA targets per cell.[43]

Following this design, several molecular imaging contrast agents conjugated to monoclonal antibodies (mAb), antibody fragments (Fab), (recombinant) proteins, peptides, peptidomimetics, sugars and small molecules[44] were synthesised and tested.

Historically, the first example of *in vivo* MRI of cell surface molecular targets in solid tumors with site-specific contrast agents was obtained in 1985 when a Gd-DTPA chelate was conjugated to a mAb.[45] It was however recognised that one of the major problems associated to this contrast agent was the low sensitivity of MR detection. That is also the reason why the use of dendrimers, polymerised vesicles, liposomes or polypeptides carrying hundreds of Gd-chelates or nanoparticles resulting in a massive accumulation of paramagnetic probes in close proximity to the receptor is a strategy pursued by different research groups.[42,46]

By coupling Gd-chelates to lipoprotein HDL and LDL it was possible to image atherosclerosis plaques since these contrast agents appear to accumulate in the resident macrophages of the plaque.[47] Moreover, since LDL receptors are over expressed in many type of malignant tumors, magnetically labelled LDL was also used to assess the expression of this receptor *in vitro* on melanoma cells.[48]

Other examples of site-specific contrast agents were obtained by coupling a fibrin-avid small peptide to a Gd-DTPA complex. In this way, it was possible to induce a substantial image enhancement of advanced atherosclerosis plaques which are rich in fibrin and thrombus.[49] Even more remarkable enhancement were obtained using paramagnetic perfluorocarbon nanoparticles coupled with antifibrin antibodies.[50]

On the other hands, early atherosclerosis is associated with increased angiogenesis in the vessel wall for which the $\alpha_V\beta_3$-integrins are general markers. Therefore $\alpha_V\beta_3$-integrin-targeted paramagnetic perfluorocarbon nanoparticles were used to specifically detect and characterise early stage atherosclerosis.[51] Moreover, since $\alpha_V\beta_3$-integrins and selectins are highly expressed at tumor vasculatures, paramagnetic polymerised vescicles were coupled to proper $\alpha_V\beta_3$-integrin antibodies to target tumor angiogenesis.[52] Another ligand very specific for the $\alpha_V\beta_3$-integrins, a cyclic peptide containing the RGD sequence of amino acids, was also incorporated into liposomes containing a Gd-DTPA attached to two stearyl chains and a fluorescent rhodamine lipid. This bimodal targeted liposomal contrast agent is able to detect angiogenic endothelium in mouse tumor both at anatomical level *in vivo* by MRI, and at subcellular level *ex vivo* by fluorescence microscopy (**Fig. 13**).[53]

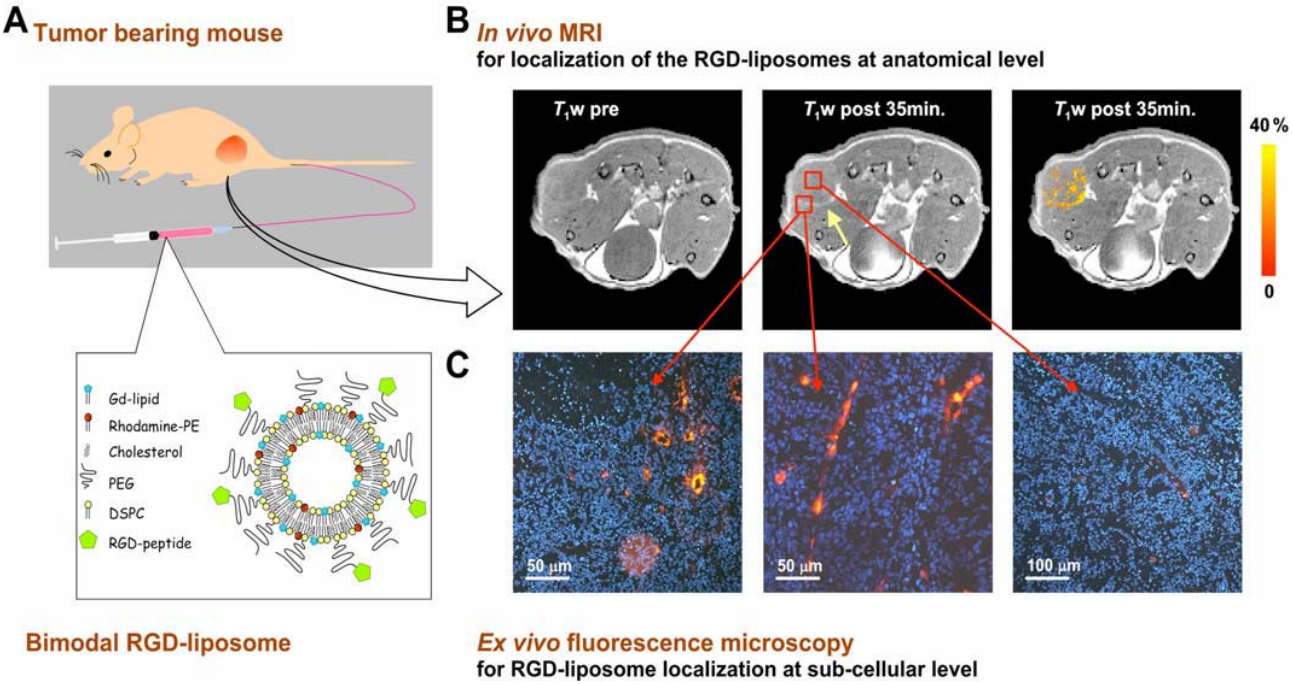

Fig. 13. Bimodal liposomal contrast agent is used to identify angiogenic endothelium in mouse tumor. Picture taken from ref. 53

Bile acid moieties such as cholic acid, cholylglycine, and cholyltaurine were also conjugated to DTPA or DOTA chelating groups and their Gd(III) complexes showed high biliary elimination as well as good tolerabilities. Noticeably, the conjugate **1** seems to play a peculiar role in addressing the Na+/taurocholate transport system.[54]

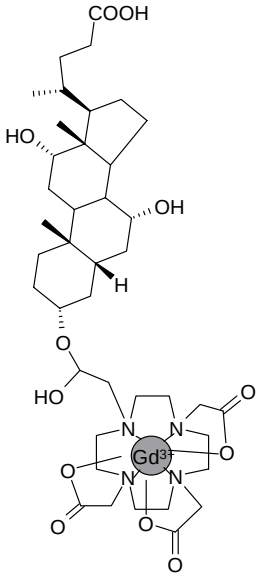

1

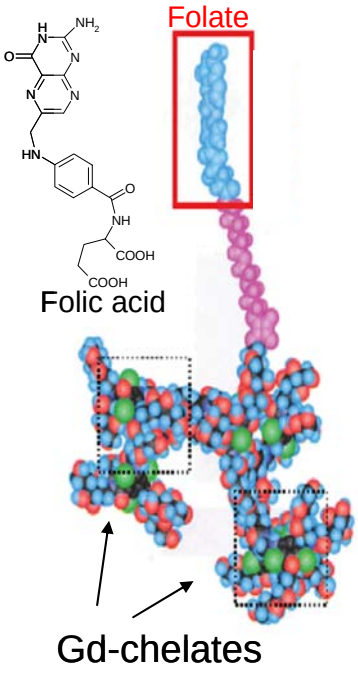

2

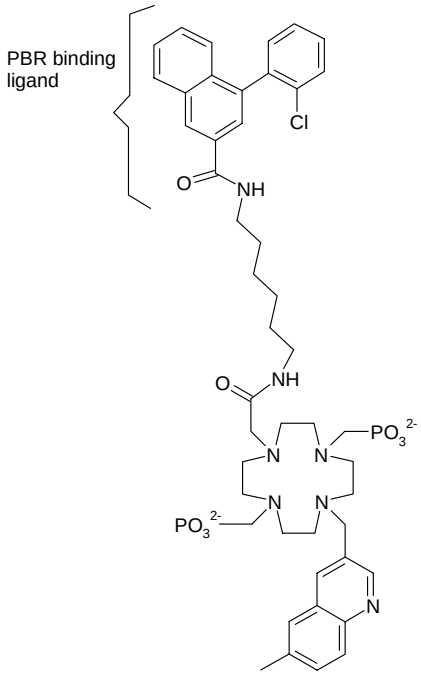

3

Rather studied is also the folate receptor targeting. In fact, folate receptors are overexpressed by several types of cancer cells including ovarian, breast, colorectal and nasopharyngeal carcinomas in adults as well as pediatric tumors, and show high affinity ($K_d \sim 10^{10}$ M) for the folate ligand. The uptake of a Gd polyamidoamine (PAMAM) folate dendrimer in ovarian cancers was observed[55,56] while more recently, the specific accumulation to an ovarian tumor of a folic acid conjugate **2** with a high relaxivity dimeric Gd-chelate was obtained.[57,58]

Another candidate receptor for MRI is the so-called peripheral benzodiazepine receptor (PBR), overexpression of which has been observed in certain cancers.[59] The Gd-complex of **3** yielded a contrast enhancement of 1.7 : 1 in the localization of glioblastoma (brain cancer) cells.

3.5 References

[1] P.A. Rinck, *Magnetic Resonance in Medicine*, Blackwell Scientific Pubblications, Oxford. **1993.**

[2] P.C. Lauterbur *Nature* **1973,** 242 190–191.

[3] M. F. Tweedle, in *"Lanthanide Probes in Life, Chemical and Earth Science (Theory and Practice)"*, J. C. G. Bünzli, G. R. Choppin Eds. Elsevier, New York, **1989**.

[4] R.B. Lauffer, *Chem. Rev.* **1987**, 87, 901- 927.

[5] S. Aime, M.Botta, M. Fasano, and E. Terreno, *Chem. Soc. Rev.* **1998**, 27, 19-29.

[6] C. Paul-Roth and K.N. Raymond, *Inorg. Chem.* **1995**, 34 1408-1412.

[7] P. Caravan, J. J. Ellison, T.J. Mc Murry, R. B. Lauffer, *Chem. Soc. Rev.* **1999,** 99 2293-2352.

[8] D. Parker, J. A. Williams, *J. Chem. Soc. Dalton Trans.* **1996,** 3613-3628.

[9] S. Aime, M. Botta, M. Fasano, E. Terreno, *Coord. Chem. Rev.,* **1999,** 186321-333.

[10] V. Comblin, D. Gilsoul, M. Hermann, V. Humblet, V. Jacques, M. Mesbahi, *Coord. Chem. Rev.,* **1999,** 186 451-470.

[11] L. Thunus, R. Lejeune, *Coord. Chem. Rev.* **1999,** 184, 125-155.

[12] M. Botta, *Eur. J. Inorg. Chem.,* **2000,** 399-407**.**

[13] S. Aime, C. Cabella, S. Colombatto, S.G. Crich, E. Gianolio, F. Maggioni, *J. Magn. Res. Imaging,* **2002,** 16, 394-406.

[14] E. Brucker, *Top. Curr. Chem.,* **2002**, 221, 103-122.

[15] L. Frullano , J.Rohovec , J. A. Peters, C. F.G.C. Geraldes , *Top. Curr. Chem.* **2002,** 221, 26-60.

[16] H. Gries, *Top. Curr. Chem.* **2002**, 221, 1-24.

[17] V. Jacques, J.F. Desreux, *Top. Curr. Chem.* **2002,** 221, 123-164.

[18] E. Tóth, L. Helm, A.E. Merbach, *Top. Curr. Chem.* **2002,** 221, 61-101.

[19] T.J. Meade, A.K. Taylor, S.R. Bull, *Curr. Opinion Neurobiol.,* **2003,** 13, 597-602.

[20] S.R. Zhang, M. Merritt, D.E.Woessner, R.E. Lenkinski, A.D. Sherry, *Acc. Chem. Res.,* **2003,** 36, 783-790.

[21] N. Bloembergen, E.M. Purcell, R. V. Pound, *Phys. Rev.,* **1948,** 73, 678; I. Salomon, *Phys. Rev.,* **1955,** 99, 559; I. Solomon, N. Bloembergen, *J. Chem. Phys.,* **1956,** *25,* 261; N. Bloembergen, *J. Chem. Phys.,* **1957,** 27, 572**;** N. Bloembergen, L.O. Morgan**,** *J. Chem. Phys., ,* **1961,** 34, 842; R.E. Connick, D.J. Fiat, *Chem.Phys., 44,* 4103.

[22] G.M. Nicolle, E. Toth, H. Schmitt-Willich, B. Raduchel, A.E. Merbach, *Chem. Eur. J.,* **2002,** 2, 10040-1048.

[23] E. Tóth, D. Pubanz, S. Vauthey, L. Hem, A.E.Merbach, *Chem. Eur. J.,* **1996**, 2, 1607-1615.

[24] E.C. Wiener, M.W. Brechbiel, H.Brothers, R.L. Magin, O.A. Gansow, D.A. Tomalia, P.C. Lauterburg, *Magn. Res. Med. ,* **1994,** 311-8.

[25] E. Tóth, A.E.Merbach, *ACH Models Chem.,* **1998**, 135, 873-884.

[26] T.H. Cheng, Y.M. Wang, K.T. Lin, G.C. Liu, *J. Chem. Soc.Dalton Trans.* **2001,** 3357-3366.

[27] S. Laus , R. Ruloff , E. Tóth, A.E.Merbach, *Chem. Eur. J.,* **2003**, 9, 3555-3566.

[28] J.E. Richman, T.J. Atkins, *J. Am. Chem. Soc.* **1974,** 96, 2268-2270

[29] H. Stetter, E.E. Roos , *Chem. Ber.,* **1954,** 87, 566.

[30] H. Stetter, J. Marx, *Justus Liebig Ann. Chem.,* **1957,** 607, 607.

[31] H. Stetter, K.H. Mayer, *Angew. Chem.,* **1961,** 88, 760.

[32] K. Tsuboyama, S. Tsuboyama, J. Uzawa, K. Kobayashi, T. Sakurai, *Tetrahedron Lett.* **1977,** 52, 4603

[33] H. Stetter, W. Frank, *Angew. Chem.,* **1976,** 88, 760.

[34] G.R. Hansen, T.E. Burg , *J. Heterocycl. Chem.,* **1968,** 5, 305.

[35] D.K. Cabbiness, D.W. Margerum, *J. Am. Chem. Soc.,* **1969,** 91, 6540- 6441

[36] R.M. Clay, S. Corr, M. Micheloni, P. Paoletti, *Inorg. Chem.,* **1984,** 24,3330

[37] M.F. Tweedle, *Invest. Radiol.,* **1992,** 27,52.

[38] K.N. Raymond, V.C. Pierre *Bioconjugate Chem.* **2005,** 16, 3-8, and references therein.

[39] E.J. Werner, S. Avedano, M. Botta, B.P. Hay, E.G. Moore, S. Aime, K.N. Raymond, *J. Am. Chem. Soc.*, *129* , **(2007),** 1870-1871.

[40] P.M. Winter; S.D. Caruthers; S.A. Wickline; G.M. Lanza *Curr. Card. Rep.* **2006**, *8*, 65-69.

[41] D. Artemov, Z. M. Bhujwalla; J.W.M. Bulte *Curr. Pharmaceut. Biotech.* **2004**, *5*, 485-494.

[42] G.J. Strijkers, W.J.M. Mulder, G. A. F. van Tilborg, K. Nicolay *Anti-cancer Agents in Med. Chem.* **2007***, 7*, 1-15.

[43] M. Atri *J.Clin.Onol.* **2006**, *24*, 3299-3308.

[44] T. Storr, K. H. Thompson, C. Orvig *Chem. Soc. Rev.* **2006**, *35*, 534-544.

[45] W. T. Anderson-Berg, M. Strand, T. E. Lempert, A. E. Rosenbaum, P. M. Joseph *J. Nucl. Med.* **1986**, *27***,** 829-833.

[46] P. Caravan *Chem. Soc. Rev.* **2006**, *35*, 512-523.

[47] J. C. Frias, M. J. Lipinski, S. E. Lipinski, M. T. Albelda *Contrast Media Mol. Imaging* **2007**, *2*, 16–23.

[48] H. Li, B. D. Gray, I. Corbin, C. Lebherz, H. Choi, S. Lund-Katz, J. M. Wilson, J. D. Glickson, R. Zhou, *Acad. Radiol.,* **2004**, *1*, 1251-1259.

[49] M. Sirol, J.G.S. Aguinaldo, P.B. Graham, R. Weisskoff, R. Lauffer, G. Mizsei, I. Chereshnev, J.T. Fallon, E. Reis, V. Fuster, J.-F. Toussaint, Z.A. Fayad *Atherosclerosis* **2005**, *182***,** 79–85.

[50] S. Flacke, S. Fischer, M. J. Scott, R. J. Fuhrhop, J. S. Allen, M. McLean, P. Winter, G. A. Sicard, P. J. Gaffney, S. A. Wickline, G. M. Lanza. *Circulation* **2001**, *104***,** 1280–1285

[51] P. M. Winter, A. M. Morawski, S. D. Caruthers, R. W. Fuhrhop, H. Zhang, T. A. Williams, J. S. Allen, E. K. Lacy, J. D. Robertson, G. M. Lanza,; S. A. Wickline *Circulation* **2003**, *108***,** 2270–2274.

[52] D. A. Sipkins, D. A. Cheresh, M. R. Kazemi, L. M. Nevin, M. D. Bednarski, K. C. Li, *Nat. Med.,* **1998**, *4*, 623-626.

[53] W. J. Mulder, G. J. Strijkers, J. W. Habets, E. J. Bleeker, D. W. van der Schaft, G. Storm, G. A. Koning, A. W. Griffioen, K. Nicolay, *FASEB J.,* **2005**, *19*, 2008-2010.

[54] P. L. Anelli, L. Lattuada, V. Lorusso, G. Lux, A. Morisetti, P. Morosini, M. Serleti, F. Uggeri *J. Med. Chem.* **2004,** *47,* 3629-3641.

[55] S. D. Konda, M. Aref, M. Brechbiel, E. C. Wiener *Invest. Radiol.* **2000**, *35*, 50–57

[56] E. C. Wiener, S. Konda, A. Shadron, M. Brechbiel, O. Gansow *Invest. Radiol.* **1997**, *32*, 748–754

[57] Z. J. Wangm S. Boddington, M. Wendland, R. Meier, C. Corot, H. Dalrup-Link *Pediatr. Radiol.* **2008**, *38*, 529-537.

[58] C. Corot, P. Robert, E. Lancelot, P. Prigent, S. Ballet, I. Guilbert, J.-S. Raynaud, I. Raynal, M. Port *Magn. Res. Med.* **2008**, *60*, 1337–1346.

[59] F. Delavoie; H. Li; M. Hardwick, J. C. Robert, C. Giatzakis, G. Oeranzi, Z. X. Yao, J. Maccario, J. J. Lacapere, V. Papadopoulos *Biochem.* **2003**, *42*, 4506-4519.

Chapter 4

Synthesis and properties of polyglycosylated-DOTA ligands

4.1 Sugar-Gd.chelate conjugates as MRI contrast agents.

Few examples of contrast agents with appended sugar units at the periphery have been reported in the literature.

A functional MRI agents was reported by Meade and co-workers who developed a Gd-DOTA derivative capped by a β-galactosyl residue **(I)**. The sugar, blocks the close approach of water molecules to the metal centre and therefore limits the contrast enhancement to outer-sphere relaxation. However, in the presence of β-galactosidase enzyme, galactose is cleaved causing a transition from a weak to a strong relaxivity state.[1] This "smart contrast agent" may find application in monitoring several processes which this enzyme is involved in.[2] More recently a similar approach was used to detect oncologically relevant enzyme β-glucoronidase.[3] Enzymatic hydrolysis of the β-glucoronic acid from **(II)** allowed to switch on relaxivity of the Gd chelate demonstrating the potential of this approach for imaging cancer cells *via* changes in enzyme levels.

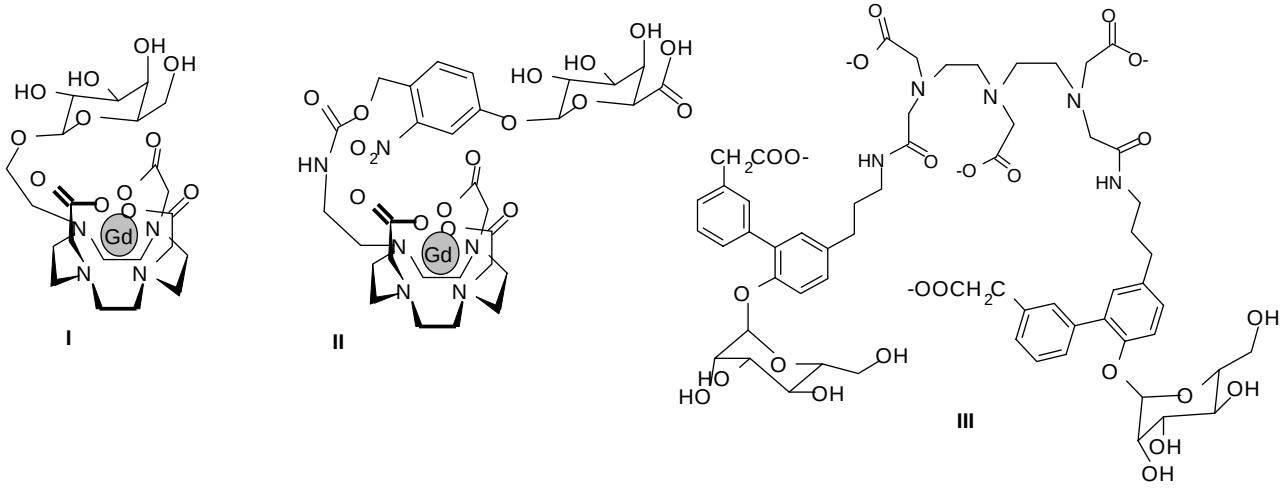

Other site-specific MRI contrast agents may have potential for molecular imaging of tumor related cell surface receptors. Gd-DTPA-B(sLex)A, for example, is a Gd-DTPA based MRI contrast agent (**III**) specific for the E-selectin receptor obtained by conjugation to a Sialyl Lewis^X mimic.[4] Although this contrast agent has only been applied in inflammatory models it is potentially useful for staining the tumor vasculature where the cell surface receptors (E-selectins) are expressed.

With the idea to exploit the cluster glycoside effect[5] and to target carbohydrate binding proteins (lectins)[6] biomarkers of many inflammatory and tumor processes, recently few glycoclusters functionalised with DOTA or DTPA have been synthesised.

A tetragalactosylated DOTA derivative (**IV**)[7] and a tetra-galactosylated DTPA analogues **(V)**[8] for the targeting of hepatic asyaloglycoprotein receptor were reported. Cell internalization and animal studies on both $^{153}Sm^{3+}$ and Gd^{3+} complexes were carried out with γ-scintigraphy and MRI,

respectively. *In vitro* studies showed superior activity of the multivalent derivatives **(IV-V)** compared to monovalent ones in the uptake of their radiolabelled Sm (III) complexes by hepatocyte carcinoma cells line Hep G2 containing the asialoglycoprotein receptor. Also *in vivo* biodistribution of the radiolabelled polygalactosylated derivative **(IV)** looked promising with interesting specificity for the liver uptake and superior activity especially when compared to the polyglucosylated counterparts.

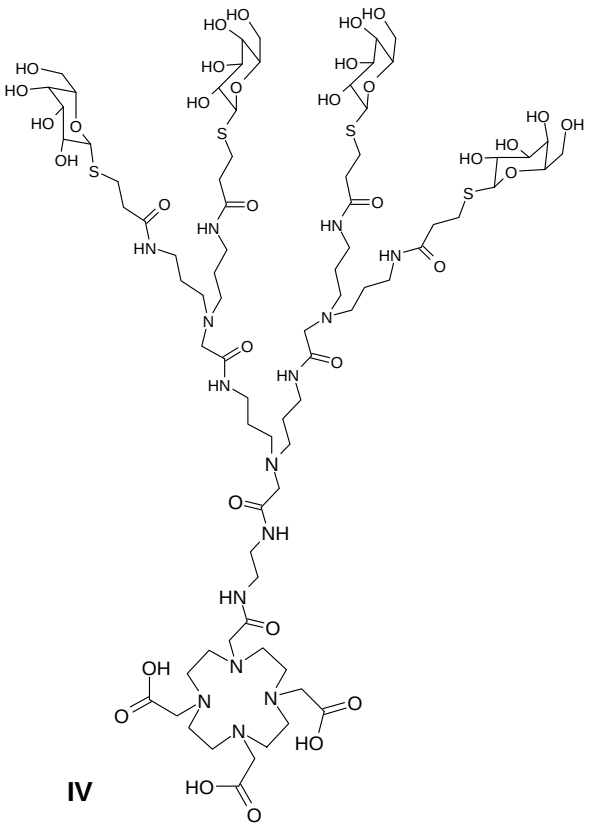

IV

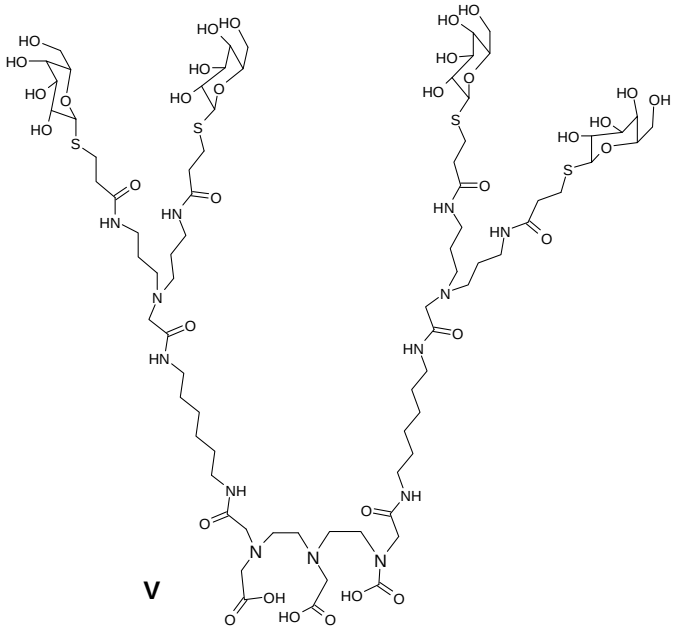

V

However, despite this specific liver uptake of the radiolabelled galactose-bearing multivalent compounds, the animal MRI assessment of the corresponding Gd^{3+} chelates showed liver-to-kidney contrast effects which are not significantly better than those shown by aglycono-Gd-DTPA. This has been attributed by the authors to a quick wash-out from the liver of these hydrophilic complexes, before they can be sufficiently concentrated within the hepatocytes via receptor-mediated endocytosis.[9]

Dendritic DTPA **(VI)** or DOTA **(VII)** Gd complexes bearing 12 glycosyl units at the periphery were also independently prepared by Takahashi[10] and Parker and Aime.[11] While **VI** was only prepared and characterised, the glucosyl complex **VII** was also studied in details and compared directly with ProHance, at the same doses, in preliminary imaging experiments with mice. The Gd complex **(VII)** gave rise to a longer-lived signal enhancement, maintaining a 50-60% overall increase over the period 5 to 45 min post-injection and a significant gain compared to the enhancement of ProHance. Unluckily, a study carried out with a galactosyl anologue of **VII** to seek

liver targeting based on the recognition of one or multiple β-galactosyl residues by asialoglycoprotein receptor, gave no significant enhancement in this organ.

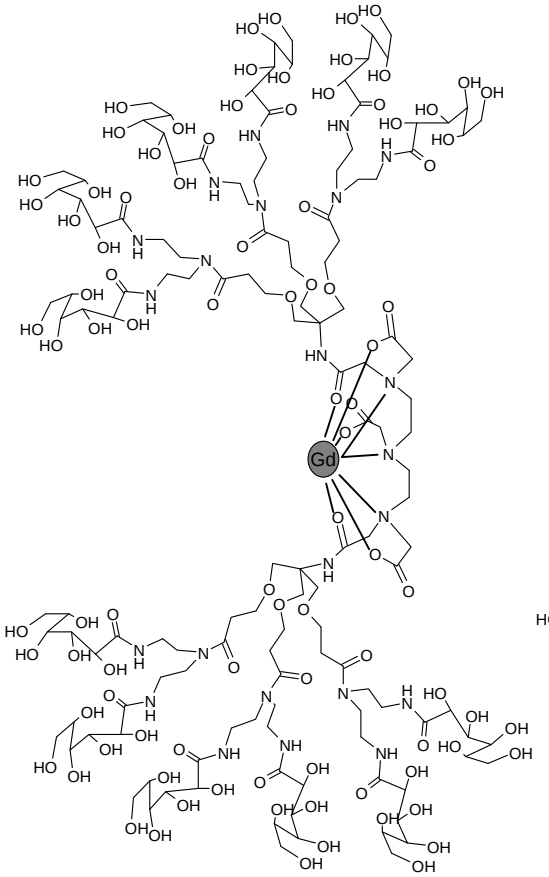

VI

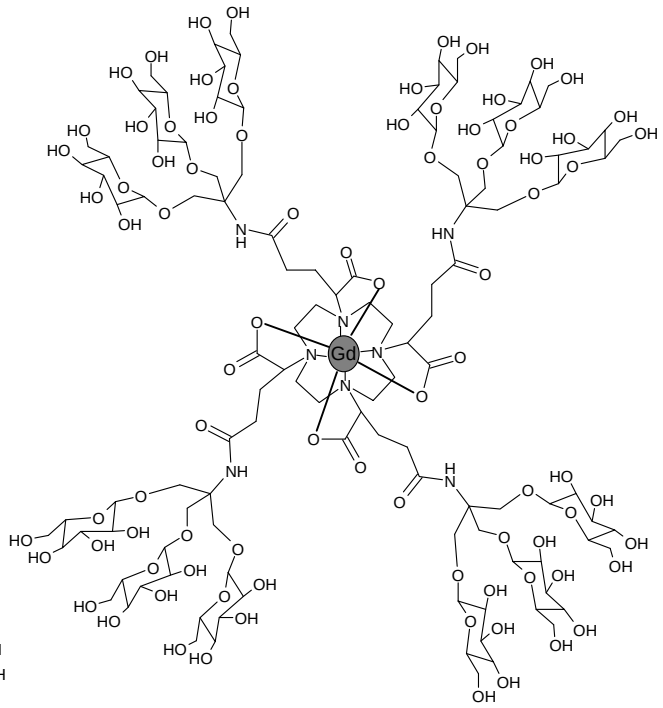

VII

4.2 Methods of ligand conjugation to chelating units.

Different strategies for the conjugation of the sugar units to the moiety devoted to Gd(III) complexation have been used. They can be grouped in three different categories: *i*) covalent methods; *ii*) biotin/(strept)avidin coupling; *iii*) noncovalent approach.

The covalent methods, which can be considered the most classical and used strategies, aim at forming a covalent bond between the ligand and the chelating unit possibly separating them with a linker of proper length. The reaction which are mostly used are those forming amide bonds also because Gd(III) chelating units such as DOTA or DTPA presents carboxylic acid groups which might be used for this purpose. Quite common is the use of coupling reagents such as HATU, HBTU or PyBOP which have shown to be so successful in peptide synthesis. In general, very efficient reactions should be chosen like those between amino groups and iso(thio)cyanates in order

to form (thio)urea bonds. The selection of very efficient reactions is particularly crucial when the synthesis of multivalent ligands has to be carried out. This is also the reason why, in the latest years, an important success has been obtained by the "Click Chemistry" methodology which exploits the 1,3-dipolar cycloaddition reaction also know as Huisgen reaction.

The 1-3 –dipolar cycloaddition reactions have been the subject of intensive research, most notably by Rolf Huisgen, whose work led to formulation of the general concepts of 1,3-dipolar cycloadditions[12]. This cycloaddition chemistry found many of applications in organic synthesis and has been the subject of several reviews. In a few years since its discovery, the Cu-catalyzed azide-alkyne 1,3-dipolar cycloaddition (CuAAC) has been established as one of the most reliable procedure for the covalent assembly of complex molecules. It has enabled a number of applications in synthesis, medicinal chemistry, molecular biology and materials science. The 1,2,3-triazole finds several application because it has many advantageous properties: a) high chemical stability, it is inertness to severe hydrolytic, oxidizing, reducing conditions and at high temperature, b) a strong dipole moment (5.2-5.6 D), c) aromatic character, d) good hydrogen-bond-accepting ability[13 14].

The 1,2,3-triazole reaction has been thoroughly investigated by Huisgen and co-workers in 1950s to 1970s[15,16]. This reaction is thermodynamically favoured ($\Delta H°$ = -45 to -55 Kcal/mol) due to the high potential-energy content of the two reaction components, and the kinetic-energy barrier is relatively high (ca. 26 Kcal/mol for methyl azide and propyne[17]), so the reaction is very slow at room temperature for unactivated reactants. The uncatalyzed thermal cycloaddition of azides to alkynes requires prolonged heating and one can obtain a mixture of 1,4- and 1,5-disubstituted regioisomers. Today the efficient route, CuAAC leads only to 1,4-disubstituted-1,2,3-triazoles at room temperature in good yields. In this reaction one can use different Cu(I) sources: copper(I) salts (CuI, CuBr) and coordination complexes like $[Cu(CH_3CN)_4]PF_6$,[18] $(EtO)_3P$ x CuI,[19] and $[Cu(PPh_3)_3]Br$[20 21] can be used. The latter catalyst is very efficient in organic solvent where the cuprous salts have limited solubility. However the Cu(I) is thermodinamically unstable and can be easily oxidized to inactive Cu(II). Aqueous alcohols like methanol, ethanol, tert-butanol, THF and DMSO can be used as solvent. The discovery that catalytic Cu(I) increases the reaction rate and controls the regioselectivity to give the 1,4-di-substituted triazole group while suppressing the formation of the 1,5-regioisomer was made independently in recent years by Sharpless[22], Meldal[23] and their co-workers.

The biotin/(strept)avidin approach is quite often used for the conjugation of different types of labels to antibodies[2]. It exploits the extraordinary high avidin-biotin binding affinity ($K_d = 10^{-15}$ M) that results in a practically irreversible binding under physiological conditions. It offers also the

advantage that the biotinylated (or avidin conjugated) Gd complex can be also administered after the avidin conjugated (or biotinylated) antibody has reached his molecular target thus preventing any negative influence of the contrast agent on the recognition process between the antibody and the target (**Fig. I**).

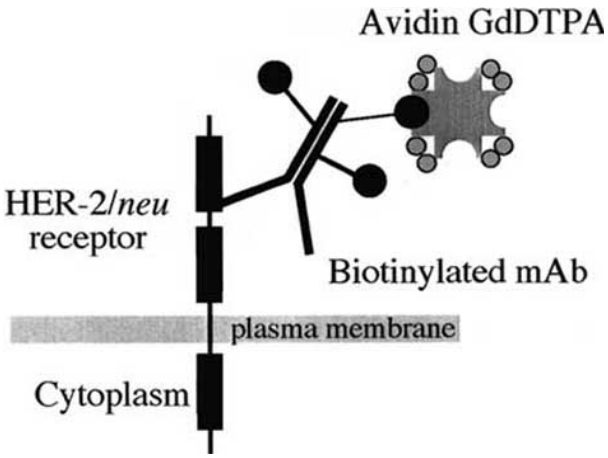

Fig. I: The two-step labelling scheme with receptor pretargeting by biotinylated antibody and avidin-based Gd contrast agent. From ref. 2.

Biotin-avidin (streptavidin) linker system will, however, have limited application *in vivo* because both avidin and streptavidin are foreign proteins and may induce host immune response. This significantly limits the successful applications of this technique *in vivo* especially when repetitive imaging is required.

The noncovalent approach, exploits the possibility of generating a stable supramolecular complex between the Gd-complexes and the ligand, without carrying out a real chemical reaction thus avoiding purification steps. A nice example of this supramolecular approach was obtained by mixing a cyclodextrin-grafted chitosan with a Gd-DTPA derivative bearing either an hydrophobic bis-phenyl-cyclohexyl-phosphate or a lithocholic acid residue (**Fig. IV**). Thanks to hydrophobic interactions between the lipophilic residues of the Gd complexes and the cyclodextrin cavities, stable adducts, showing important relaxivity values, were observed. This system thus appears promising as carrier for the *in vivo* vehiculation of Gd(III) complexes.[24]

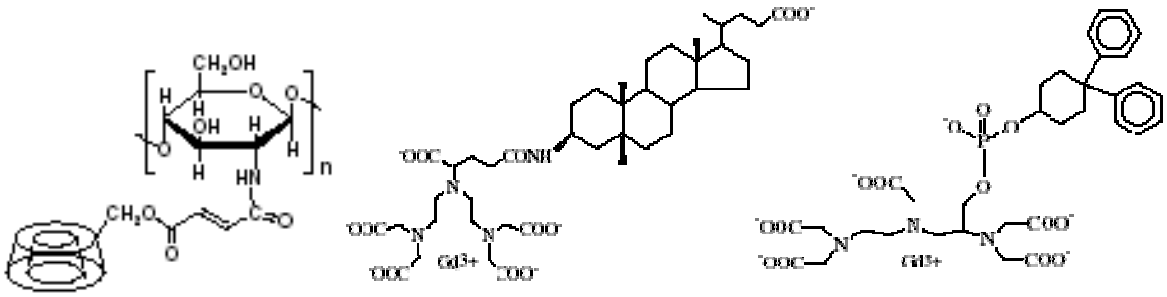

Fig. II: The noncovalent approach for the preparation of stable adducts between a biopolymer and a contrast agent. In the figure the chitosan-cyclodextrin conjugate and two different lipophilic Gd-DTPA complexes are represented (from ref. 24).

Another possibility, exploited in this noncovalent approach, is to assemble the Gd chelate and the ligand in a supramolecular structure like a liposome, a micelle or a nanoparticle[25].

4.3 Synthesis of site specific contrast agents using a calix[4]arene scaffold

The first goal of this project was the synthesis of polyglycosylated site specific contrast agent based on the calixarene scaffold and featuring four units of the same saccharide at the upper rim for polyvalent interactions with the lectins and the 1,4,7,10- tetraazacyclododecane-N,N',N'',N'''-tetraacetic acid (DOTA) at the lower rim for gadolinium complexation (**Fig. 1 B**)

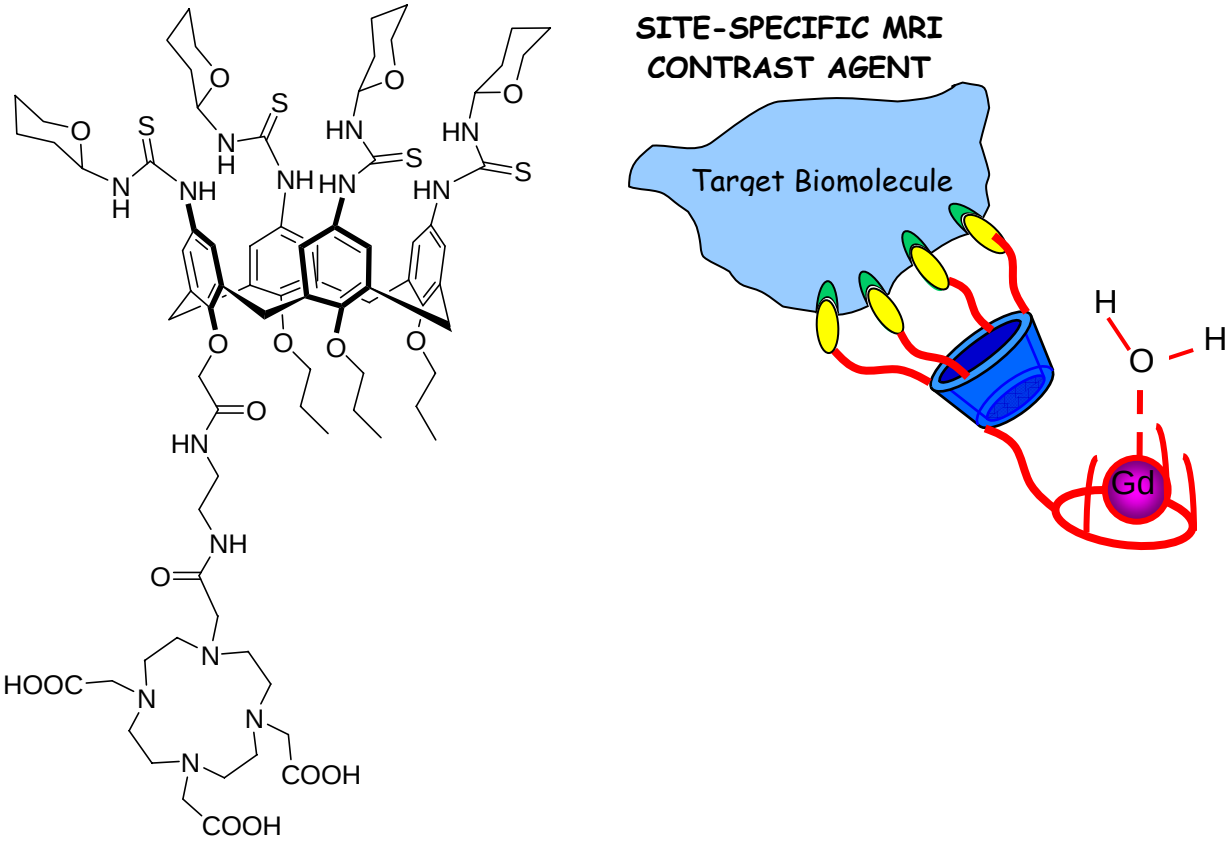

A **B**

Fig. 1

Taking advantage of the previous experience of glycosylation reactions on calixarene scaffolds carried out in our research group[26 27 28 29 30 31], we planned to conjugate the sugars at the upper rim of the calix using thiourea bonds. The coupling reaction between p-amino calixarenes and peracetylated-β-glycosyl isothiocyanates is, in fact, always nearly quantitative. Moreover in this coupling reaction the same stereochemistry at the sugar anomeric position is maintained. This conjugation method is also quite convenient since different β-glycosyl isothiocyanates are commercially available, although we usually prefer to synthesise then by ourselves.

We originally planned to synthesize compounds of type A (**Fig.1**) following a convergent strategy preparing separately the calix[4]arene having four amino groups at the upper rim and one carboxy unit at the lower rim (by reducing the nitroderivative **5**) the mono functionalized DOTA derivative **12** and the peracetylated-β-glycosyl isothiocyanates (**C**). The DOTA derivative **12** and the saccharide unit (**C**) were also synthesised.

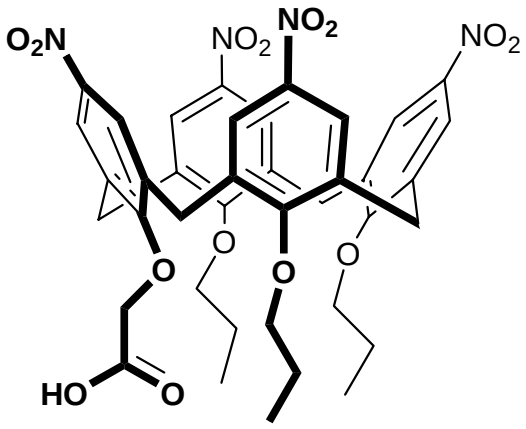

5

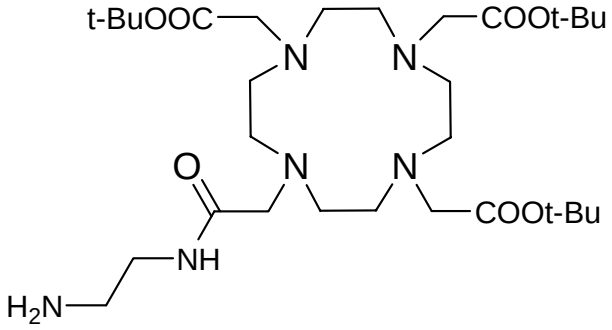

12

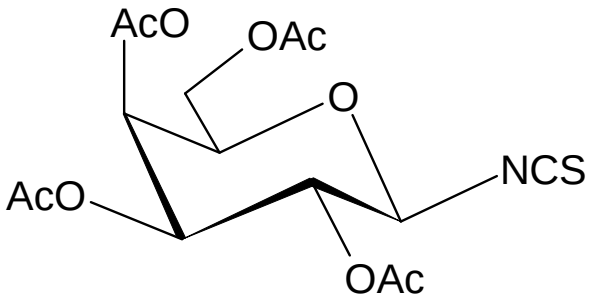

C

The synthesis of the lower rim monofunctionalized-p-nitro calix[4]arene (**5**) has been carried out in four steps, from p-tert-butyl calix[4]arene (1). In the first step, cesium fluoride and a stechiometric amount of ethyl bromo-acetate in dry DMF under nitrogen atmosphere were used to obtain a selective monoalkylation at lower rim (**scheme 1**). The cesium fluoride being a weak base, can deprotonate only one of the phenolic hydroxyl group. It has been demonstrated, in fact, that there is a wide difference between the first and the second pKa values in calix[4]arenes[32] When the first phenolic hydroxyl group is deprotonated, the resulting phenolate can be stabilized by two H-bonds from the adjacent phenolic OH's. The reaction time is quite important. The reaction was monitored by TLC and after 24 hs the starting material disappeared and a new spot of the target compound

appeared. The reaction was quenched immediately after traces of a new spot corresponding to the 1,3-dialkylated compound appeared. After acidic extraction, the crude material was purified by flash-chromatography to get compound **2** with 60% yield. The ^{1}H-NMR spectrum of compound **2** (**fig. 2**) showed the characteristic peaks of compound having only one symmetry plane. Particularly diagnostic of the mono functionalization are the signals of the hydroxyl groups which give rise to two singlets at δ = 10.23 ppm and at δ = 9.25 ppm in the integration ratio 1:2. Rather typical of the monosubstitution are also the two doublets for the axial methylene protons at 4.48 ppm and 4.30 ppm. The singlet at δ = 4.89 ppm, the quadruplet at δ = 4.41 ppm and the triplet at δ = 1.41 ppm show the presence on calixarene of only one ethyl acetate group.

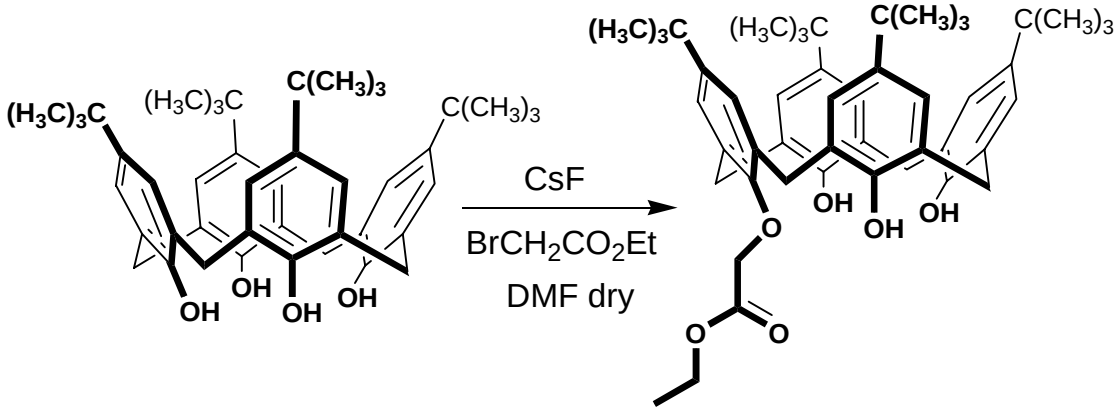

1 **2**

Scheme 1

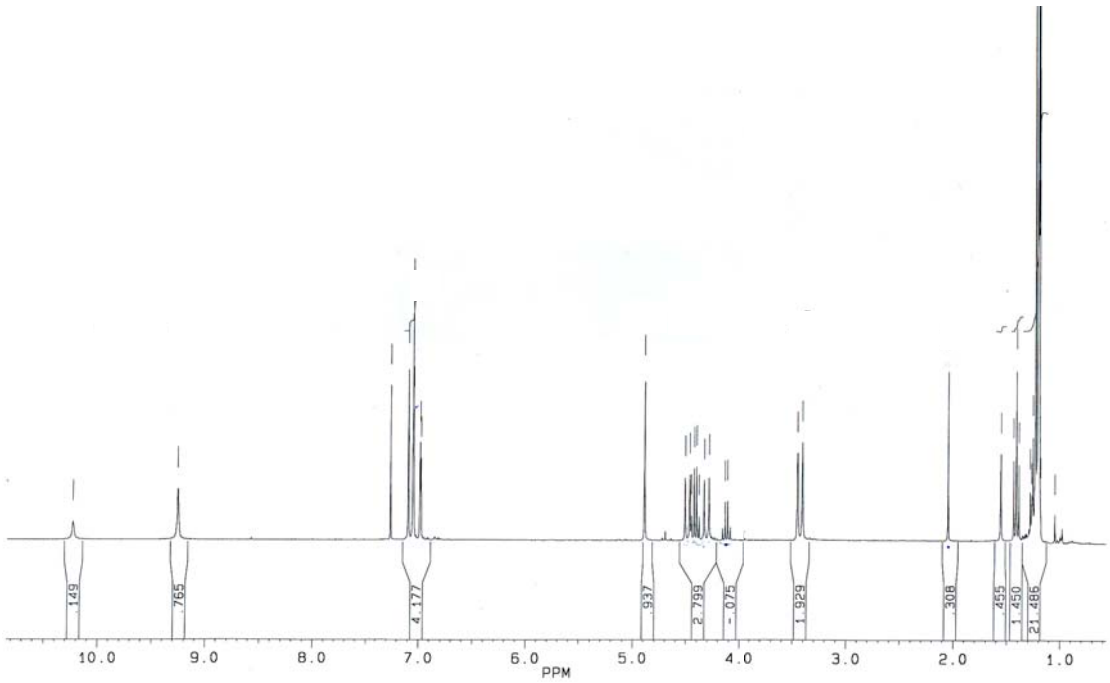

Fig. 2 ^{1}H NMR Spectrum ($CDCl_3$, 300 MHz, 298 K) of the compound **2**.

Compound **2** was then submitted to exhaustive alkylation ,by stirring it in the presence of sodium hydride and five equivalents of iodo-propane to get the corresponding triproproxy-monoester **3** (**Scheme 2**). After the work-up, recrystallization with acetonitrile allowed to isolate the pure product. The size of the annulus of calix[4]arenes is too small to allow a propoxy group to pass inside and therefore different fixed conformations are formed depending on the synthetic procedure used[33]. In the ^{1}H-NMR spectrum (**Fig. 3**) the typical signals of the propoxy groups were observed, while no hydroxyl signal could be detected. However, there are signals (▼) which can be attributed to the corresponding acid compound **4.** This was also confirmed by ESI-MS that showed three different peaks: one peak at m/z 884.3 of the ion $[M + Na]^+$ corresponding to the monoester derivative **3** and two peaks at m/z 877.5 and 855.5 respectively of the ions $[M - H + 2 Na]^+$ and $[M + Na]^+$ of the carboxylic acid compound **4.** Probably, due to the not completely dry conditions, the hydrolysis of the ethyl ester also took place. However, we did not proceed in the elimination of monoacid **4** from the reaction mixture, since in the following step the hydrolysis of the ester group was anyhow required.

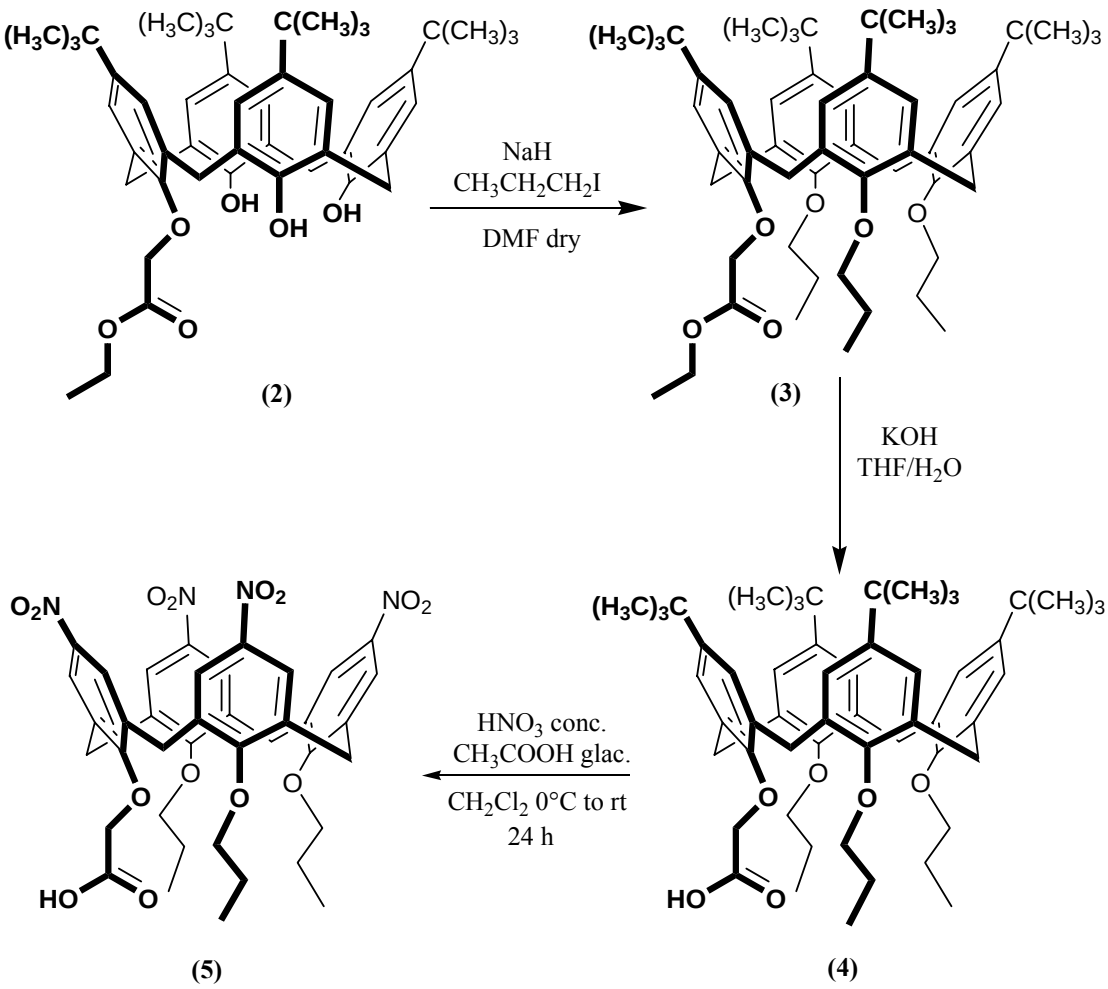

Scheme 2

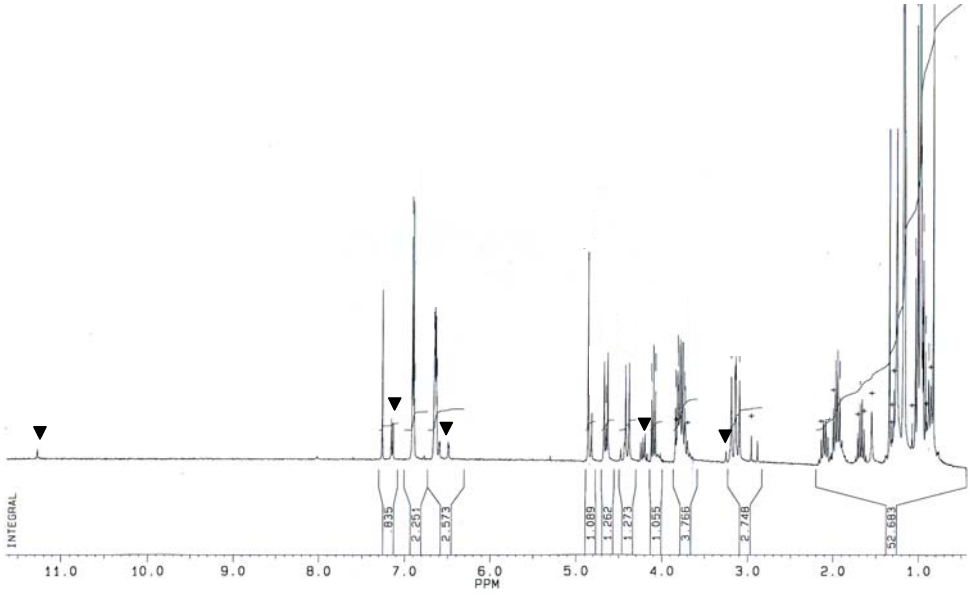

Fig. 3 ^{1}H NMR spectrum ($CDCl_3$, 300 MHz, 298 K) of the compound **3**. (▼) signals of the monoacid compound **4**.

Therefore the mixture of acid and ester was stirred at reflux with potassium hydroxide in THF and water, overnight.

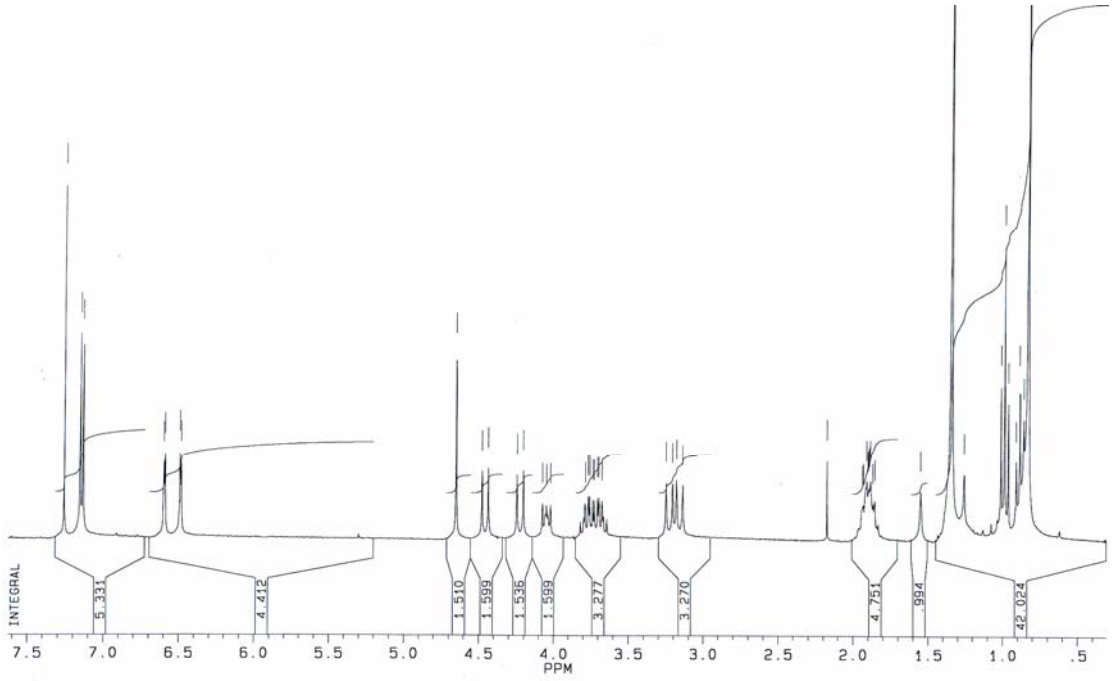

Fig. 4 ^{1}H NMR spectrum ($CDCl_3$, 300 MHz, 298 K) of the compound **4**

After the work-up of the reaction, the crude product was triturated in methanol to obtained the mono acid in 83 % yield. In the ^{1}H-NMR spectrum (**Fig. 4**) it is possible to see the disappearance of the characteristic signals of the ester, the quadruplet to δ = 4.41 ppm and the triplet to δ = 0.98 ppm. Again, the ^{1}H-NMR spectrum is quite characteristic of a compound fixed in the cone conformation and having one symmetry plane. There are two singlets at 7.15 and 7.13 ppm which are respectively, the aromatic protons of the phenolic unit bringing the acetic acid moiety and that diametrically opposite; two doublets with *J* meta (2.4 Hz) at δ = 6.59 and 6.48 ppm correspond to the protons of the others two aromatic rings. The chemical shift difference between the two groups of signals suggests that the calixarene is in flattened cone conformation: in particular the ring with the acetic acid group and the opposite one are more opened, shielding the protons of the other two rings which are in a nearly parallel disposition. The two low field doublets at δ = 4.45 ppm and δ = 4.22 ppm are originated by the axial protons of the $ArCH_2Ar$ groups whereas the two high field doublets at δ = 3.22 and 3.15 ppm are generated by the equatorial $ArCH_2Ar$ protons. This chemicals shift difference is quite peculiar indicating mono substitution at lower rim. To carry out the following nitration of the upper rim, classical conditions developed for the ipso-nitration of calixarenes were used.

Compound **4** was stirred at room temperature with a mixture of concentrated nitric acid and glacial acetic acid for three days. The reaction was monitored by mass spectrometry since it is not very

easy to separate the product of partial nitration from the final tetra-nitro compound by TLC. After this time we obtained the tetra-nitro calyx[4]arene **5** in 81% yield without the need of further purification. In the ^{1}H-NMR spectrum (**Fig. 5**) it is possible to see that there is no signal of the tert-butyl groups at high field and the aromatic protons are shifted to lower field (δ = 8.01 ppm and δ = 7.22 ppm) due to the presence of the electronwithdrawing NO_2 groups. We also have tried this reaction in different nitration conditions, with trifluoroacetic acid and sodium nitrate, but we obtained compound **5** in only 35% yield.

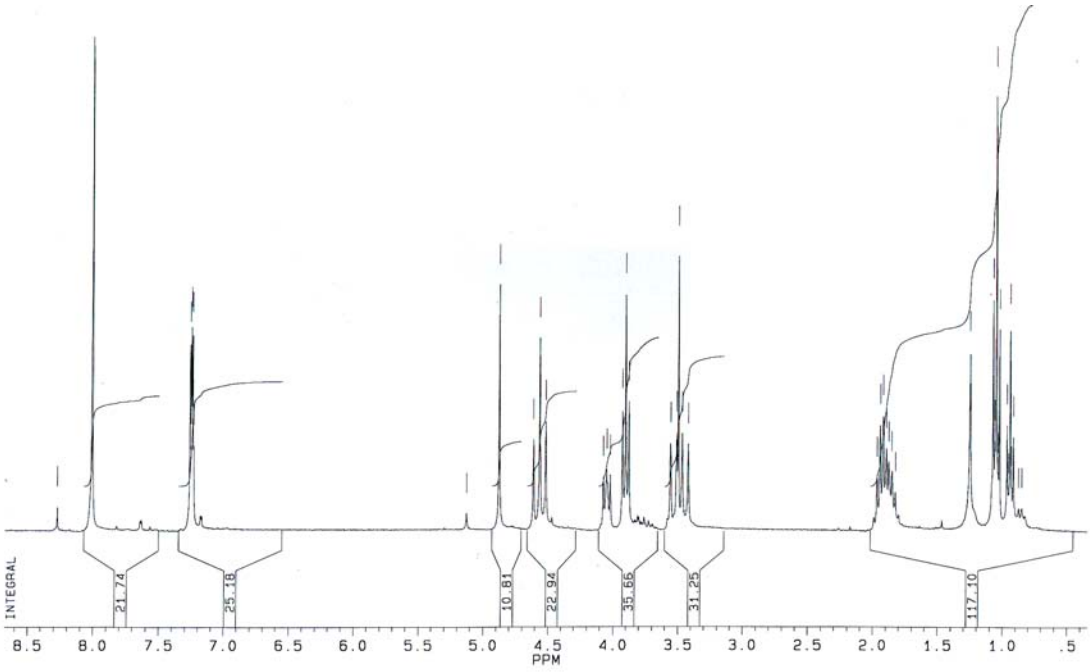

Fig. 5 ^{1}H NMR spectrum ($CDCl_3$, 300 MHz, 298 K) of the compound **5**.

The synthesis of the monofunctionalised DOTA derivative **12** was carried out in several steps following procedures which are reported in the literature. We started from cyclization reaction between ethylene glycol ditosylate **7** and triethylene tetraamine tetratosylate[34] **6 (scheme 4)** which yields tetratosylated cyclen. In this reaction is very important the heating time since if it is shorter than three hours a considerable amount of the acyclic mono condensation product is formed. After work-up, the crude reaction product was recrystallized from toluene to obtained a white solid powder of pure compound **8**. This compound was characterized by ^{1}H-NMR and shows the typical signals of the tosyl and of the methylene groups.

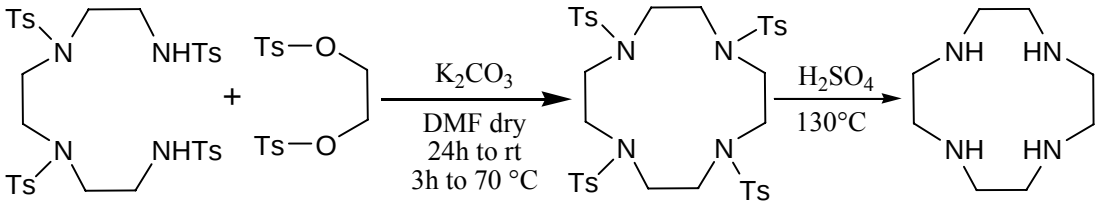

(6) **(7)** **(8)** **(9)**

Scheme 4

We proceeded in the removal of the tosyl groups by using sulfuric acid at 130° C to obtained the corresponding cyclen (**9**) after trituration of the crude product in ethyl ether. For the work-up we followed the procedure reported in literature[35]. In the ^{1}H-NMR spectrum we have observed the disappearance of the tosyl groups and the presence of only one peak at 2.67 ppm of the methylene protons.

The cyclen (**9**) was subsequently reacted with three equivalent of tert-butyl bromoacetate (**scheme 5**). to obtained the triester compound[36] (**10**) in 62% yield after recrystallization from toluene which allows to eliminate a small amount of the tetra-alkylated cyclen. In the ^{1}H-NMR spectrum of **10** it is possible to observe three singlets of the tert-butyl groups at δ = 1.46, 1.45, 1.44 ppm while at δ = 3.28 and 3.36 ppm there are two characteristic signals of the NCH_2CO groups (1:2 ratio). Moreover a broad signal at 10.00 ppm is evident which is attributed to the endocyclic amine proton. In the following step, we again alkylated the remaining secondary amine groups of cyclen using ethyl bromoacetate and potassium carbonate as base, in order to obtain an ester group orthogonal to the other three already present. Compound (**11**) was obtained in 92% yield after trituration with ethyl ether (**scheme 5**).

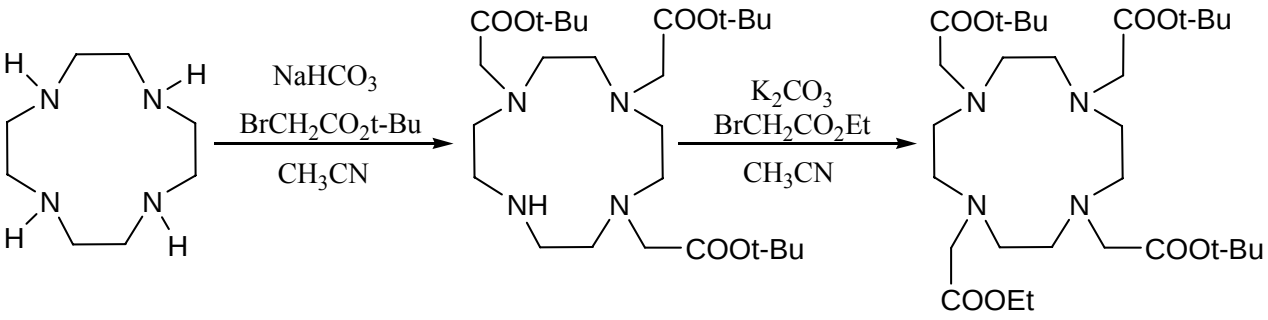

(9) **(10)** **(11)**

Scheme 5

The ^{1}H-NMR spectrum in $CDCl_3$ confirms the presence of the compound (**11**): in fact one can observed at δ = 4.15 ppm and at 1.26 ppm the typical signals of the ethyl group, a quartet and a triplet respectively.

For the synthesis of compound **11** we also, tried to follow a different procedure which was reported in literature which inverts the alkylation steps. This approach consists in the mono-alkylation of compound **9** with ethyl-bromoacetate, followed by trialkylation with tert-butyl bromoacetate. During this procedure, however, we encountered some difficulty since in the first step the reaction is not very selective and we observed a mixture of compounds (mono-, di-, tri- and tetraalkylated) which was very difficult to be separated by flash chromatography. Therefore this strategy was abandoned and we followed the one reported above (**scheme 5**) which gave good yields.

The last steps to complete the synthesis and prepare a DOTA derivative **12** which could be easily attached to the calixarene carboxylic acid consisted in the selective amide formation between the ethyl ester (**11**) and ethylenediamine for 72 h (**scheme 6**).

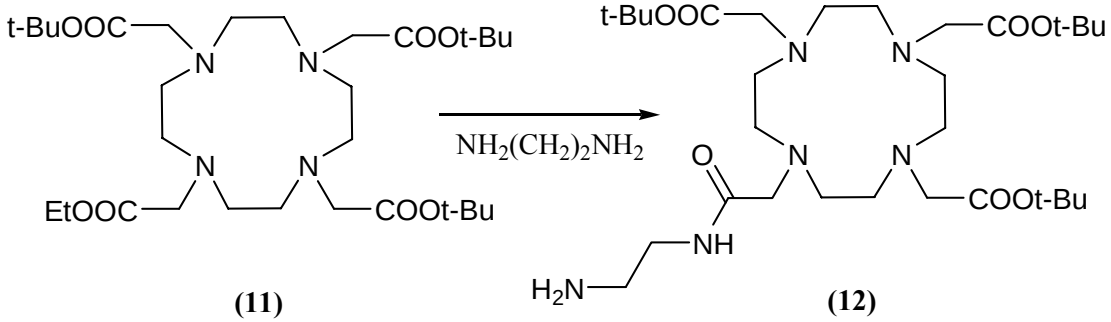

(11) **(12)**

Scheme 6

In this reaction we used ethylendiamine as solvent in order to prevent the coupling of two molecules of compound **11** with both ends of the diamine. The reaction was stirred at room temperature for three days. After complete conversion of the starting material (monitored by TLC) we evaporated the solvent to obtained pure compound **12**. The ^{1}H-NMR spectrum (**Fig. 6**) in $CDCl_3$ shows the disappearance of the ethyl ester signals and the appearance of a triplet at 8.76 ppm (NH amidic) and a quadruplet at 3.36 ppm plus a triplet at 2.90 ppm attributable to the methylene groups of ethylene diamine. Moreover, a singlet at 1.45 ppm of the tert-butyl groups and a broad signals of the endocyclic methylenes can be observed between 2 and 4 ppm. These signals are rather broad since the macrocycle possess a reduced conformational mobility at room temperature.

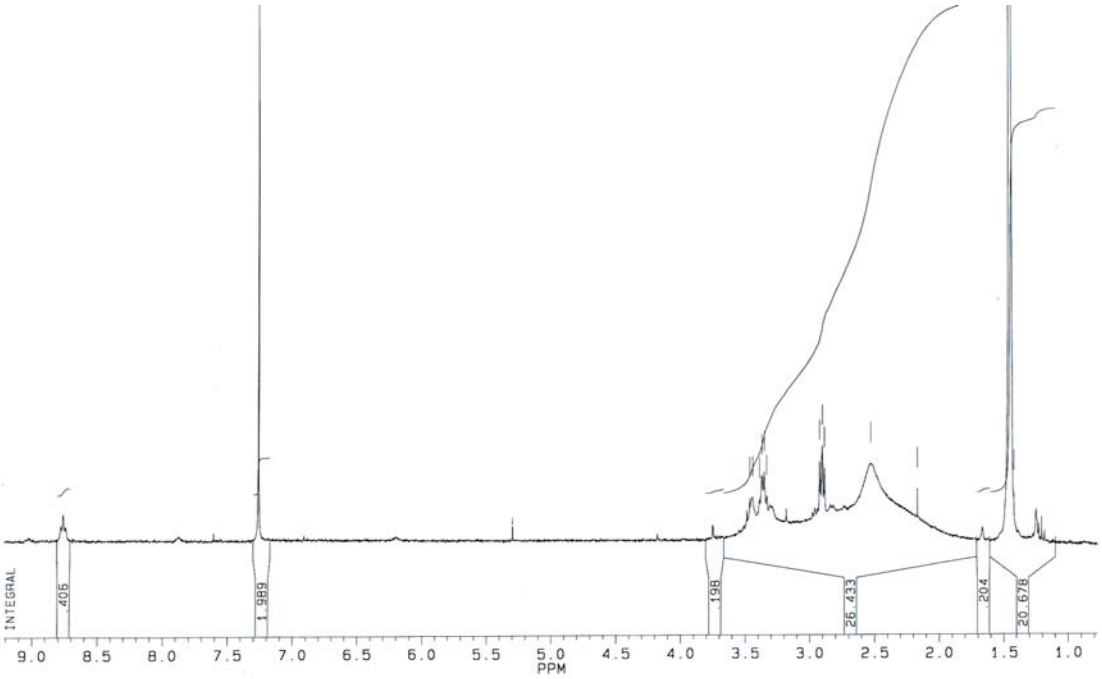

Fig.6 ^{1}H NMR spectrum ($CDCl_3$, 300 MHz, 298 K) of the compound 12

Compound 12 was then coupled to the tetranitro-calixarene mono-carboxylic acid (**5**). The reaction was performed using hydroxy benzotriazole (HOBt) and dicyclohexylcarbodiimide DCC (**scheme 7**) to form the active ester which was reacted *in situ* with a slight excess of the DOTA amine derivative (**12**). We tried to purify the compound from dicyclohexyl urea by crystallization using several solvents but without success and therefore we had to use the flash chromatography which gave compound (**13**) in very pure form. The ^{1}H-NMR spectrum (**fig. 7**) shows two broad peaks at 8.80 and 8.85 ppm for the amide groups, two singlet for the aromatic protons of the nucleus bearing the DOTA derivative and of the opposite one, while the protons of other two aromatic rings give rise to two doublets at 7.80 and 7.77 ppm. Again, very broad signals between 2 and 3 ppm were attributed to the methylene proton of cyclen.

The position of the aromatic signals suggests that the phenolic nucleus functionalized with the DOTA derivative and the one in opposite position are in a nearly parallel situation in the shielded zone created by the other two rings. The structure of compound (**13**) was also confirmed by mass spectrometry where the peak at m/z = 1407.6 corresponding to $[M+Na]^+$ was observed

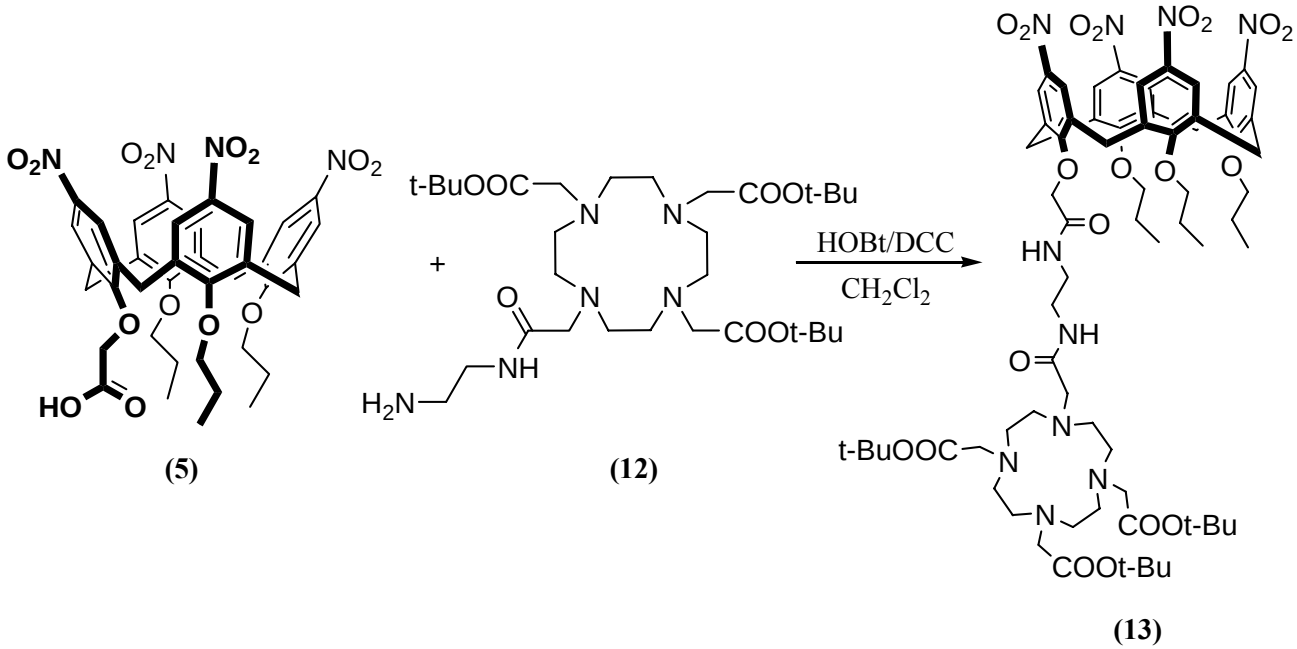

(5) **(12)** **(13)**

Scheme 7

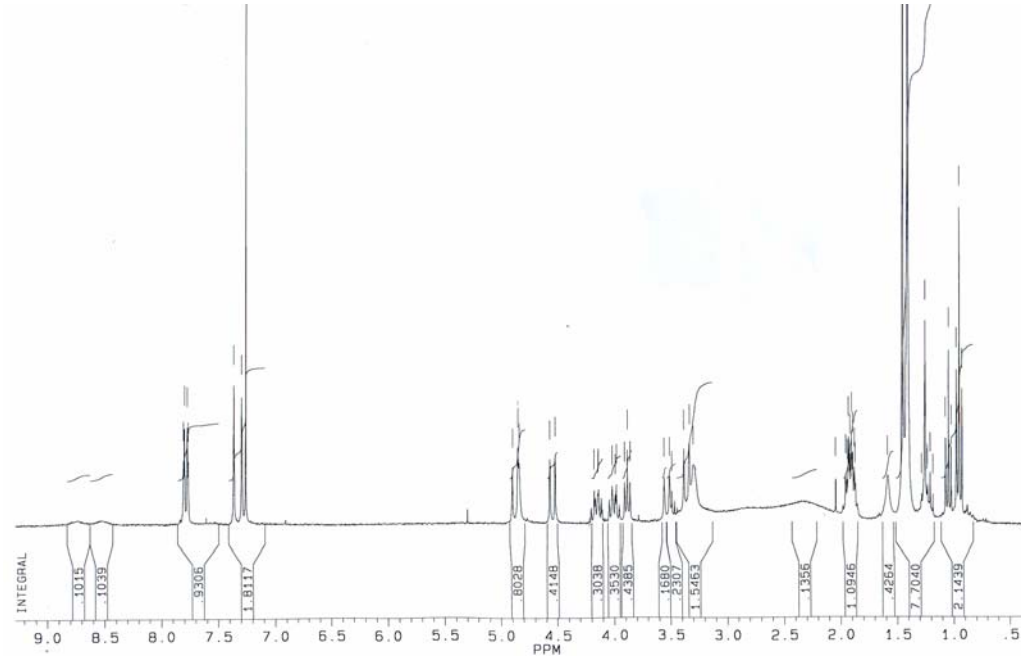

Fig. 7 ^{1}H NMR spectrum ($CDCl_3$, 300 MHz, 298 K) of the compound **13**

The reduction of the nitro groups in calixarene **13,** was carried as reported in **scheme 8**. Compound **13** was dissolved in methanol and then a catalytic amount of Pd/C was added. The mixture was stirred at room temperature under hydrogen (1 atm) in the Parr apparatus. The reaction was rather slow and still after one day of reaction we obtained only a partial reduction of our compound. We have assessed that the reaction needs five days to give the compound **14**, completely reduced as ascertained by ESI-MS analysis.

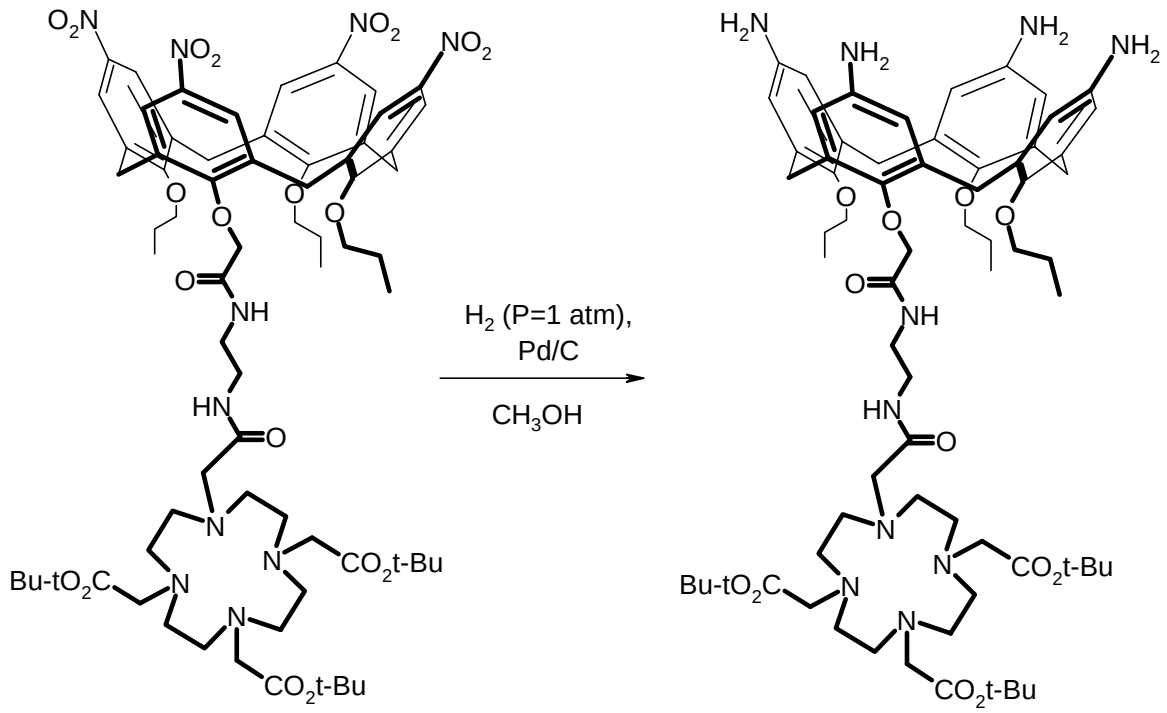

Scheme 8

Even if the ^{1}H-NMR spectrum of compound **14** showed only very broad signals we nevertheless decided to proceed with the conjugation of the carbohydrate units using a procedure well consolidated in our group and reported in **scheme 9.** Compound **14** was solubilised in dichloromethane and then 1.5 equivalent for each amino group, of tetraacetyl D-galactosyl β-isothiocyanate, was added using DIPEA as base in order to be sure that all the amino groups are deprotonated. After three days stopped the reaction evaporated the solvent and tried to purify the crude product by crystallization from ethyl ether, to eliminate the carbohydrate in excess. However, both the ^{1}H-NMR spectrum, which shows very broad peaks for all the signals, and the ESI-MS spectrum, in which the molecular peak is not present, suggest that the coupling reaction was not successfully. The incomplete conjugation of the saccharides to the calixarene scaffold, might

probably originates from a not complete reduction of the p-nitrocalixarene **13** to the p-amino derivative **14**. Moreover quite recently, in our group, it has been observed that amino calixarenes can be easily carbonatated to carbamic acids, also by atmospheric CO_2.It might be that this effect had also concurred in the degradation of our p-amino calixarene derivative **14** preventing a complete conjugation of the sugar moieties. We tried to force the reaction conditions increasing the reaction time and the amount of reagents in the last two steps, but without any success, therefore we decided to change our of glycoconjugation strategy.

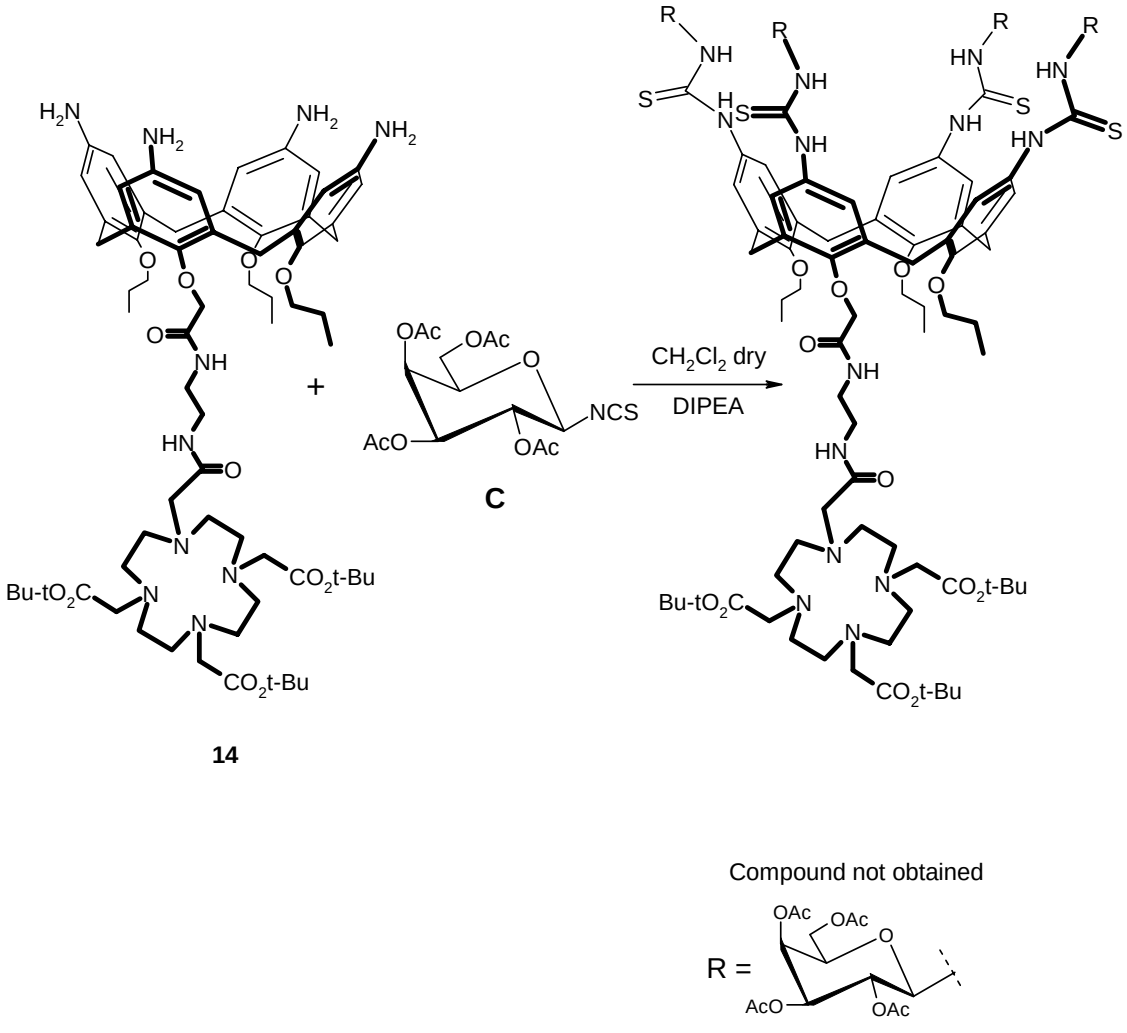

Scheme 9

We devoted our attention to the 1,3-dipolar cycloaddition reactions of azides with alkynes to give 1,2,3-triazoles[37], which is a very efficient ligation technique, often referred as "Click Chemistry"[38]. This reaction, first proposed in 1960s was usually carried out at high temperature to give a 1:1 mixture of two regioisomers, the 1,4 and 1,5 disubstituted triazole ring. Nowadays, with the use of

copper(I) as catalyst one can selectively obtain the 1,4-disostituted triazole[39] in very high yields and excellent purity, often without the need of any purification. That is the main reason why this conjugation reaction is often used for multivalent ligands[40]. We therefore planned to use this strategy to conjugate the sugar units to the calixarene scaffold.

Our first idea was to synthesise the tetra alkynyl calix[4]arene (**21**) and then to react it with the 2-azido *O*-glycosyl tetraacetyl-D- galactose (**23**) using the "Click Chemistry"[41].

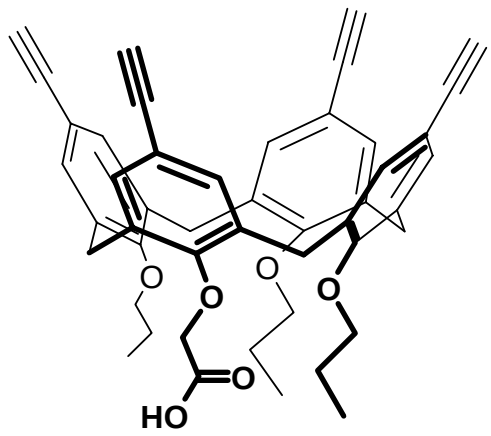

(21)

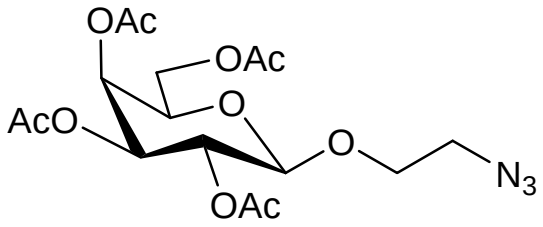

(23)

Fig. 8

For the synthesis of compound (**21**), we started from p-H calix[4]arene and functionalized it at the lower rim as reported in literature[42] thus obtaining the desired monoester-tripropoxy derivative **17.** We then functionalized compound **17** at the upper rim as reported in **scheme 8**. Bromination or iodination of calixarenes can be conveniently performed by direct substitution with the appropriate halogen and the halogenated macrocycles used for further functionalization. So we reacted compound **17** with silver acetate and, after 30 min., iodine was added and the suspension was stirred to 60°C for 1h. The reaction was monitored by TLC and after complete conversion of the starting material was quenched. We thus obtained the corresponding p-iodocalixarene **18** in high yield and without further purification.

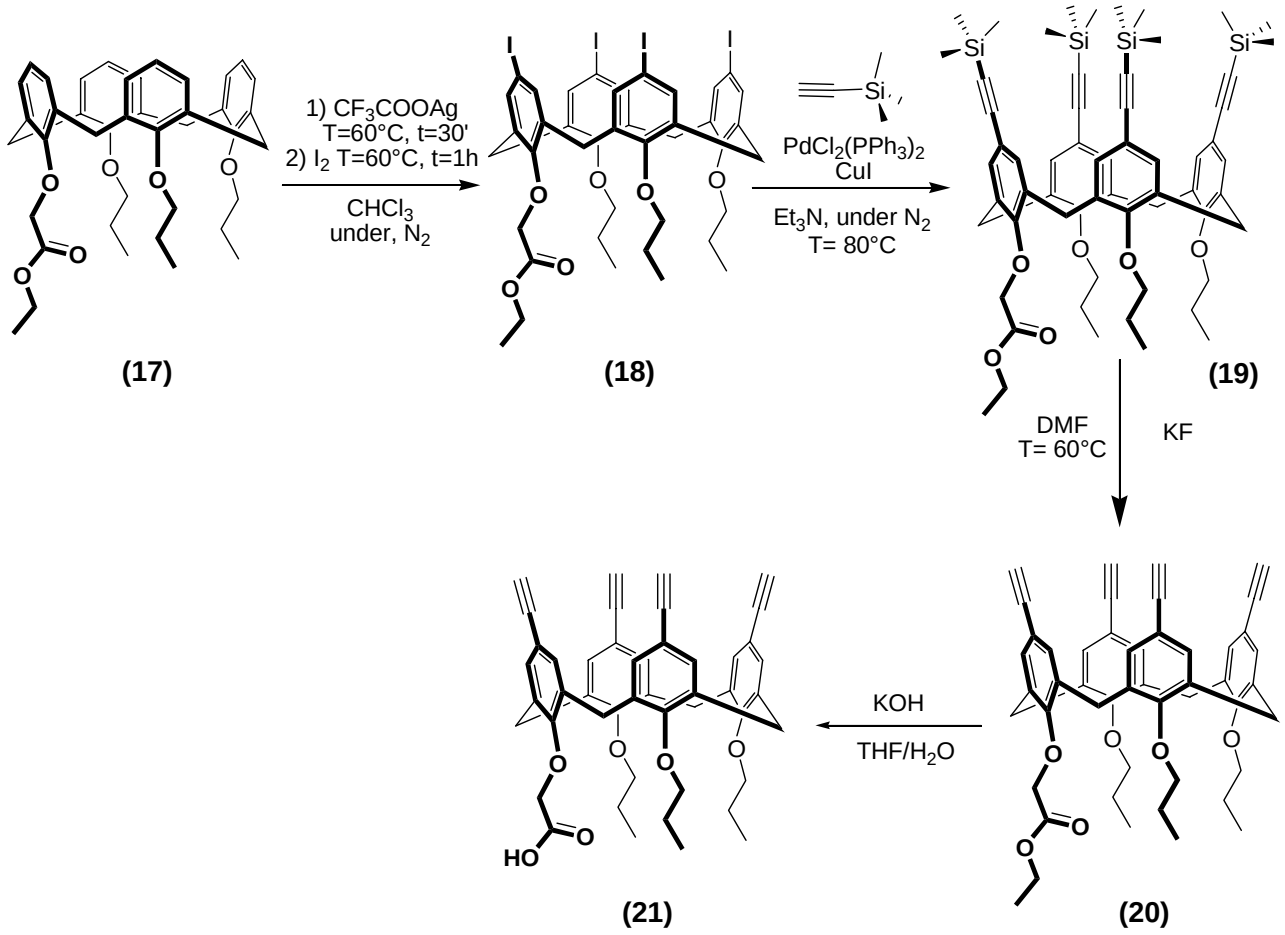

Scheme 8

The following step is a Pd-catalyzed cross-coupling reaction of the aryl halides with terminal alkynes, named *Sonogashira coupling*[43 44]. The reaction was performed under Argon atmosphere in degassed triethylamine since it has been was demonstrated that the oxygen promotes the coupling between two alkyne moieties. Although we used Pd(II), it is reduced *in situ* by Cu(I) to Pd(0) which is the active species in the catalytic cycle. This reaction is very sensitive to the presence of oxygen and to reaction conditions not completely dry, so that sometimes we also obtained as by-products partially substituted calixarenes which had to be eliminated by flash chromatography. The ^{1}H-NMR spectrum (**Fig. 9**) showed beside the characteristic signal at δ = 0.2 ppm of the trimethylsilane groups, also some minor signals around 5.5 ppm which seems to indicate the presence of alkene protons. Moreover, also in the aromatic region and around the signals of the OCH_2CO groups other signals shows the presence of minor compounds, which, however could not be eliminated by flash chromatography.

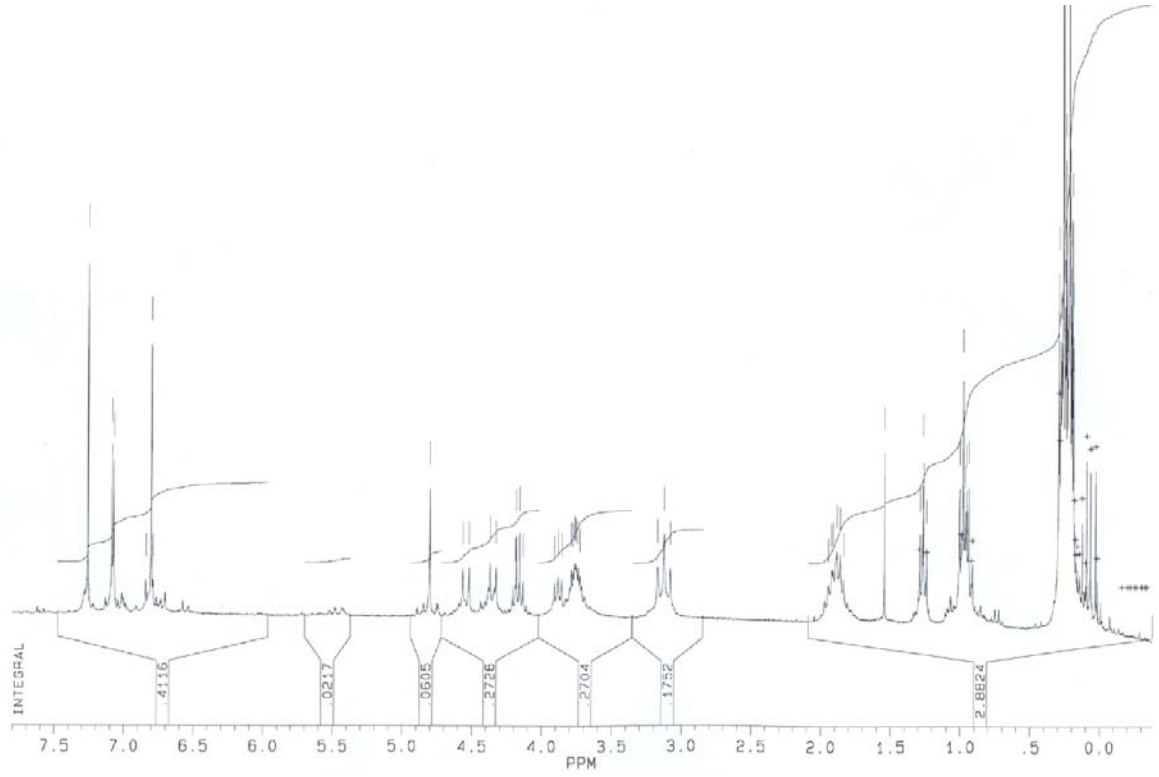

Figure 9 : ^{1}H NMR spectrum (300 MHz, $CDCl_3$, 300 K) of compound **19**

In the following reaction, the tri-methylsilyl groups were removed with potassium fluoride in DMF at 60° C. The reaction was quenched after 24 h to give the compound **20** in 98% yield without further purifications. The compound **20** was characterized by mass spectrometry, where the molecular peak $[M+Na]^+$ at m/z = 755.41 and two other peaks at m/z = 781.29 and at m/z = 807.47 could be observed. Moreover the ^{1}H-NMR spectrum (**Fig 10**) shows the absence of the signals of the trimethylsilyl groups and the appearance of the signals of the protons of the alkynes confirming the complete deprotection. However, still around 5.5 ppm some signals possibly due to vinylic protons could be observed. Looking to the literature[45], we found that in Sonogashira coupling there is often the possibility that trimethylsilyl acetylene reacts also with the alkyne bound to the aromatic group to form an addition product having a double bond as reported in **scheme 9**. This hypothesis is confirmed by the presence of the peaks at m/z = 781.29 and 807.47 in the mass spectrum which are attributed to the addition of one and two -C≡CH groups, respectively (**Fig. 11**). Luckily, at this stage the by-products could be eliminated by flash chromatography. The formation of the above mentioned by-products are probably facilitated by the fact that we have used an excess of trimethyl silyl acetylene and a long the reaction time, needed to substitute all the four iodine atoms at the upper rim of the calix[4]arene.

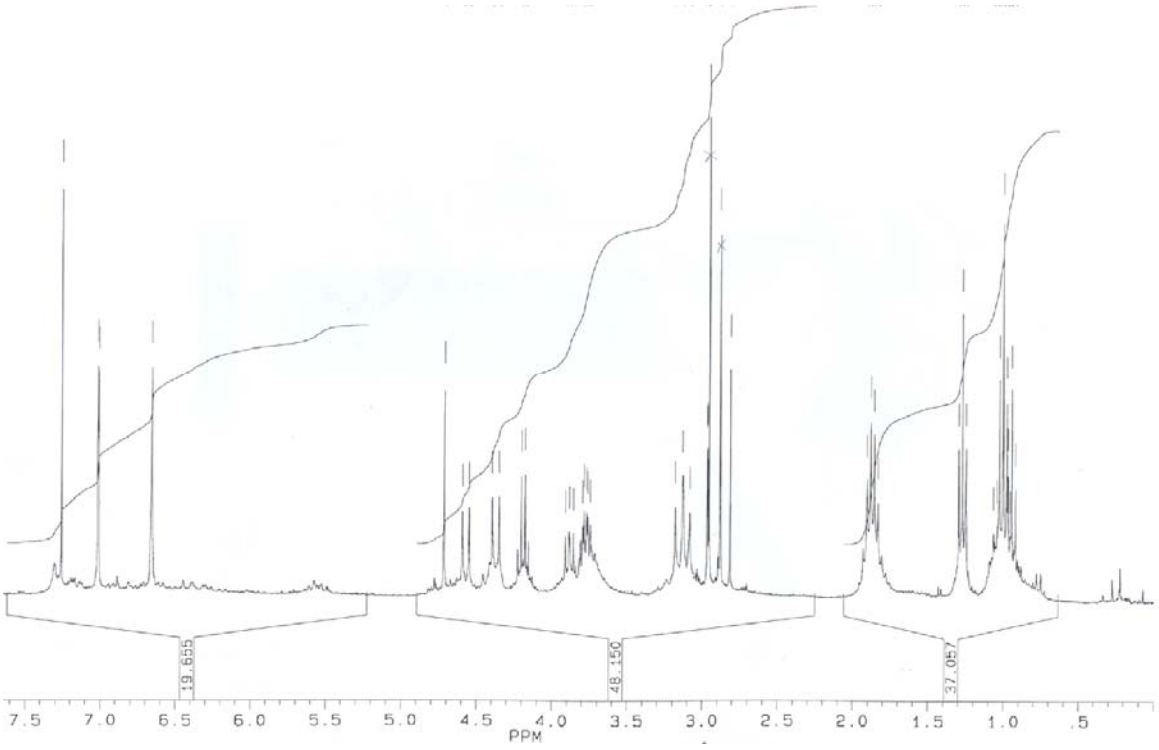

Fig. 10: ^{1}H NMR spectrum (300 MHz, $CDCl_3$, 300 K) of compound **20**

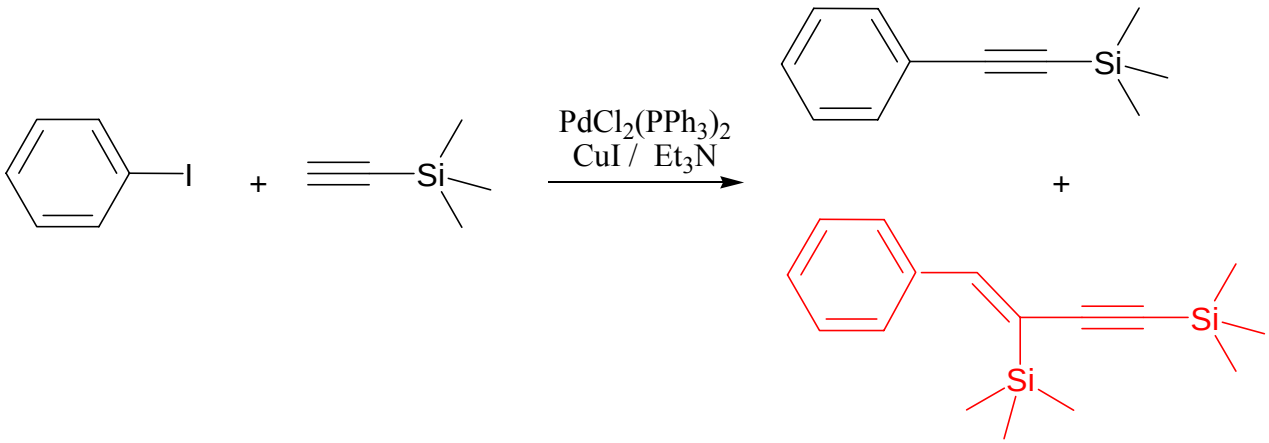

Scheme 9 Schematic representation of possible by-product (red colour) in *Sonogashira coupling*

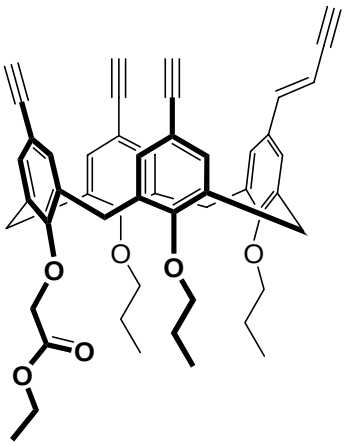

$[M+Na]^+$ m/z = 781.29

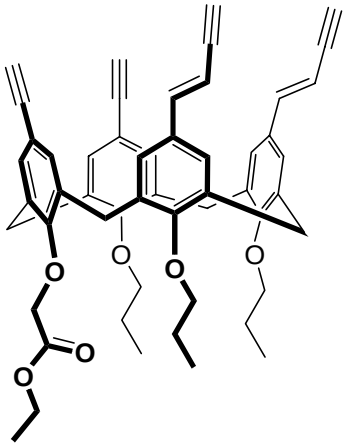

$[M+Na]^+$ m/z = 807.47

Fig. 11 By-products from Sonogashira coupling : alkene groups in difunctionalised products might be in vicinal or distal positions

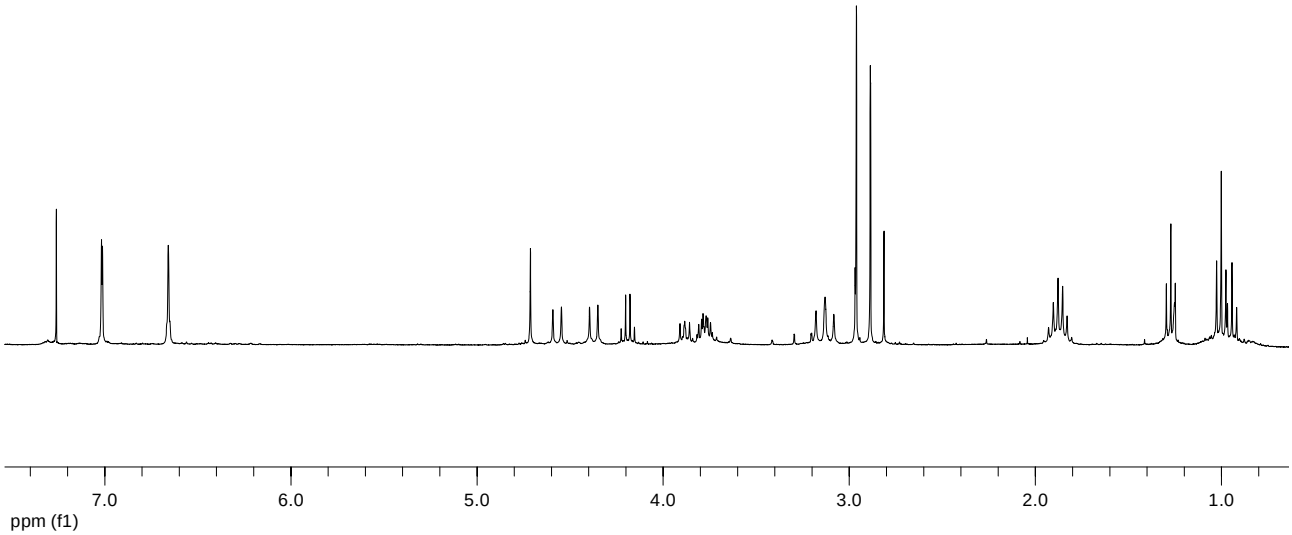

Fig. 12: ^{1}H NMR spectrum (300 MHz, $CDCl_3$, 300 K) of compound **20** after purification by flash chromatography. The spectrum shows the absence of signals around 5.5 ppm and clean signals for the aromatic and methylene protons.

The hydrolysis of the ester group in calixarene **20** was performed in THF/H_2O solution with potassium hydroxide and after 12 h reflux we obtained the compound **21** with 80% yield without further purification. In the ^{1}H-NMR spectrum we observed the disappearance of the signals of the ethyl group of the ester and a change in the aromatic region where two doublets respectively at δ = 6.55 and 6.50 ppm (J = 1.8 Hz) were observed. Moreover at δ = 7.32 ppm there is a singlet of four protons corresponding to the hydrogen atoms in meta position of the ring with the carboxylic group and the opposite one. The mass spectrum confirms the ester hydrolysis, showing the peak at m/z = 755.41 $[M+Na]^+$ corresponding to compound **21**.

In parallel, we synthesized the peracetylated 2-azido ethyl-*O*-galactoside (**Fig. 8**, compound **23**) as reported in literature[46 47] and according to scheme **10.** D-galactose was peracetylated with acetic anhydride and sodium acetate to get the corresponding peracetylate compound in quantitative yield. The 2-bromoethanol was mixed at 0° C with boron trifluoride in dichloromethane. The reaction was stirred at room temperature over night and monitored by TLC. After disappearance of the starting material the reaction was quenched and only the β-anomer compound **22** was obtained in 98 % yield without further purification. The bromine atom was then replaced with azide in DMF at 60° C and under nitrogen atmosphere to get compound **23** in high yield (the same procedure was used for synthesizing the corresponding glucose derivative **23a** in 95% yield)

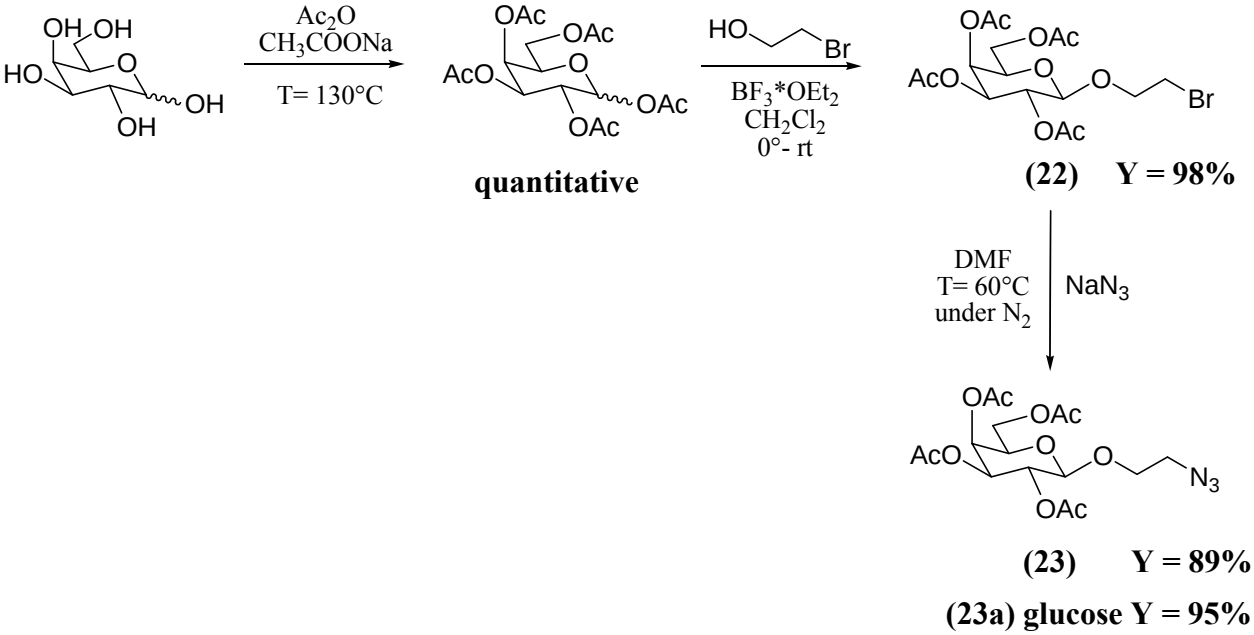

Scheme 10

Once obtained the sugar azide **23** and the tetra-acetylene calix[4]arene mono-acid **21,** we started to study their conjugation through "*Click Chemistry"*. Compound **21** was dissolved in toluene and copper iodide and DIPEA were added. The reaction was stirred at room temperature in the dark since copper iodide is light sensitive. After 24 h, TLC analysis of a sample still showed mainly the presence of the starting material. Attributing the low reactivity to the presence of the carboxylic group, which could have sequestered the copper catalyst, we added another aliquot of copper iodide and left the reaction for an additional day in the same conditions. The compound **24** was isolated after work-up and trituration with ethyl ether. The ^{1}H-NMR spectrum of **24** (**Fig. 13**) results rather complicated and very difficult to be interpreted. The presence of singlets between 1.96 and 2.15

ppm for the acetyl groups, of multiplets at 3.75-5.40 ppm together with two doublets around 3.40 ppm for the equatorial methylene protons and the aromatic signals clearly indicate that the sugar units are conjugated to the calixarene scaffold.

In the aromatic region, two doublets at 6.83 and 6.72 ppm and two singlets at 7.71 and 7.12 ppm, show the multiplicity expected for compound **24,** although one signal is unexpectedly shifted at quite low fields.

This unusual distribution of the aromatic signals could be probably due to a flattened cone conformation of the calix[4]arene induced by the formation of an intramolecular hydrogen bond between the carboxylic group and one oxygen atom bearing the propyl chain. Moreover, while for the triazole are expected at maximum three singlets, between 7.81 and 7.90 ppm there are, indeed, four signals. The spectrum is also quite broad and does not change significantly in DMSO-d_6 even at high temperature. One of the reasons of the complicated NMR spectrum could be that products of partial conjugation might also be present: by increasing the degree of conjugation at the upper rim, increases also the steric crowding and tetra conjugation might be slowed down. This could also explain the unusually long reaction times needed for a *"Click Chemistry"* reaction.

Another hypothesis made to explain the broadness and high multiplicity of the signals could be related to the presence of conjugation between the triazole and the phenol nuclei which slow the rate of rotation around arene-arene bonds.

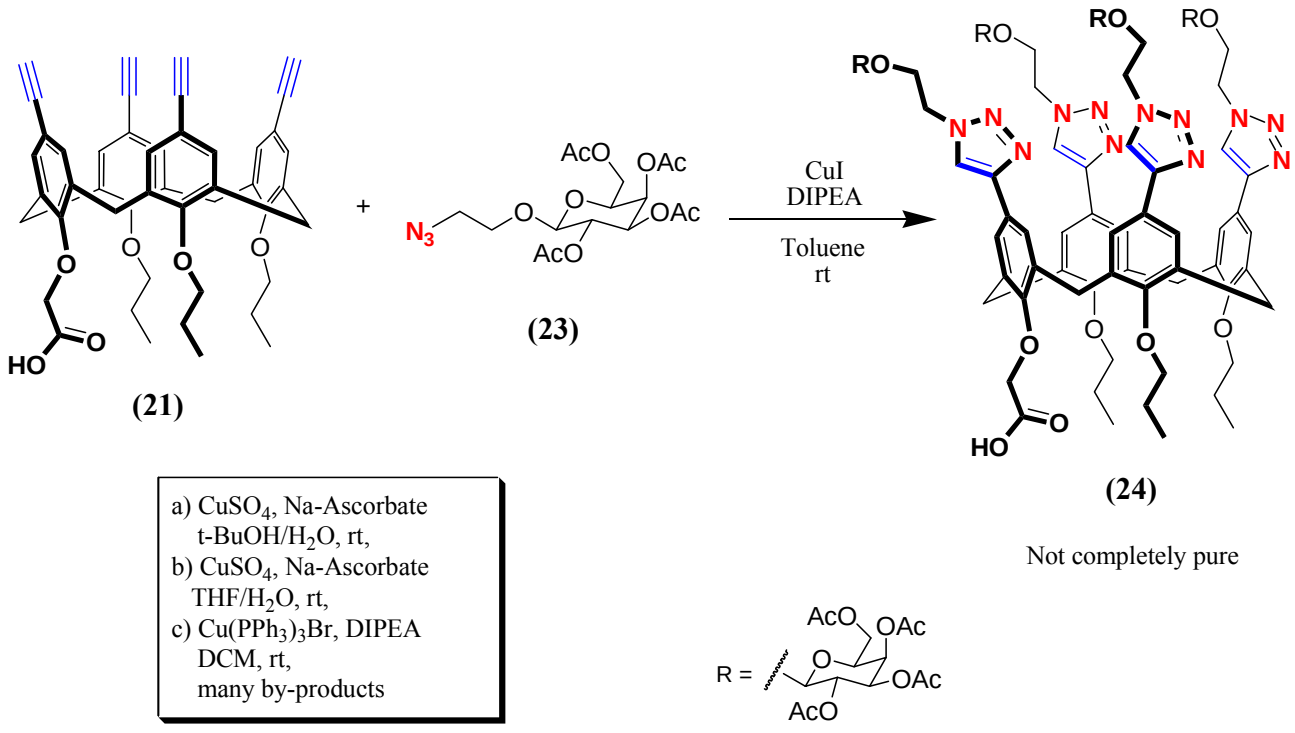

Scheme 11

To perform the reaction between compounds **21** and **23** we also used Cu(II) sulfate mixed organic/water solution or copper (I) with a coordination complex ($Cu(PPh_3)_3Br$) which is particular effective in organic solvents, like dichloromethane solubility but we did not obtain improvements. (**scheme 11** conditions a-c).

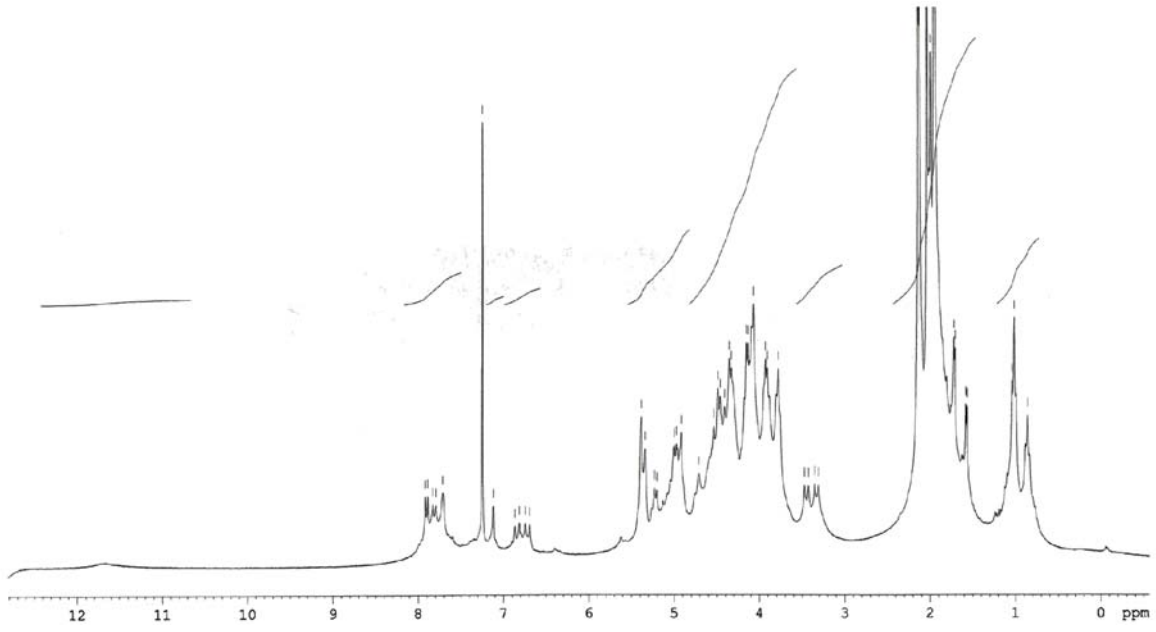

Fig. 13 ^{1}H NMR spectrum (300 MHz, $CDCl_3$, 300 K) of the compound **24**

The ESI mass spectrum (**fig. 14**) also confirms the presence of compound **24.** The cluster of peaks around 1200 a. u. can be in fact explained as doubly charge ions of the desired product: m/z = 1209.91 $[M + 2Na]^{2+}$; 1220.8 $[M + 3Na - H]^{2+}$; 1199.4 $[M + Na + H]^{2+}$; 1188.5 $[M + 2H]^{2+}$.

Despite of all these attempts, the amount of tetra-conjugated product was always quite modest. The reactivity of the p-alkynyl calix[4]arene **21** in the "*Click chemistry" conditions* seems rather low and long reaction times and high temperature are required to obtain a significant conversion. All these data brings us to hypothesize that the reaction follows also the thermal route producing a mixture of 1,4- and 1,5- disubstituted, triazoles which makes it difficult the purification of the compounds and gives complicated NMR spectra.

This low reactivity could derive from an increase of steric crowding at the upper rim of the macrocycle as soon as the number of triazole units increases. We have therefore decided to increase the distance between the triazoles and calixarene scaffold by introducing a linker (**Fig. 15**).

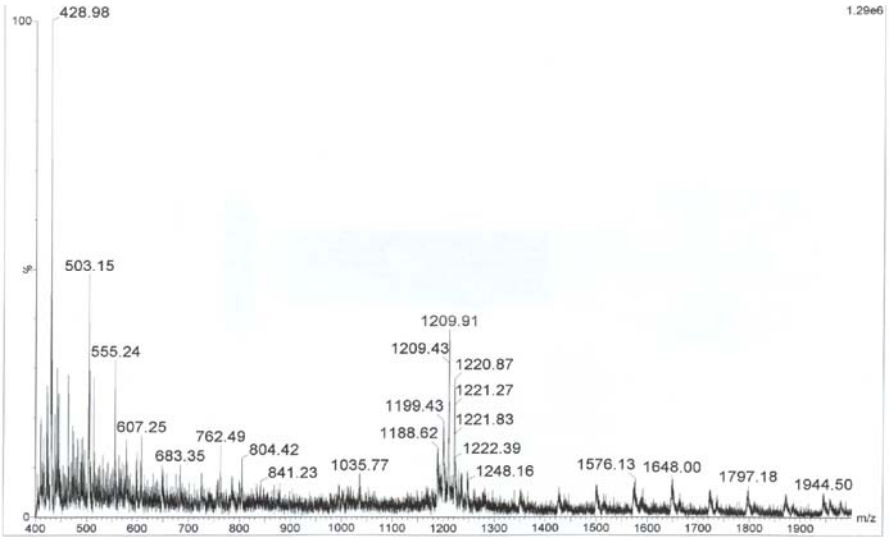

Fig. 14 ESI mass spectrum in CH_3OH with positive ionization mode of compound **24**

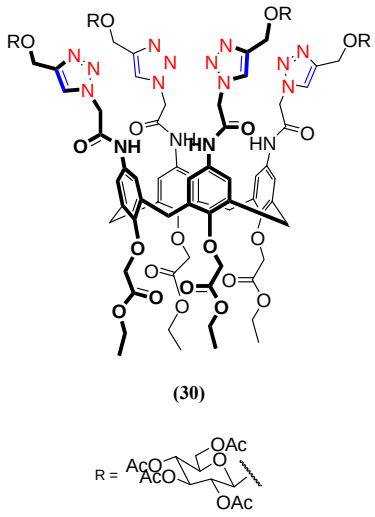

Fig. 15 new target with a linker between calix[4]arene and triazole

In the compound **30** we planned to have a spacer of three atoms which should be enough to eliminate the steric crowding at the upper rim of the calixarene during the *Click Chemistry* reaction. The new synthetic strategy to obtain compound **30** is reported in **scheme 12**.

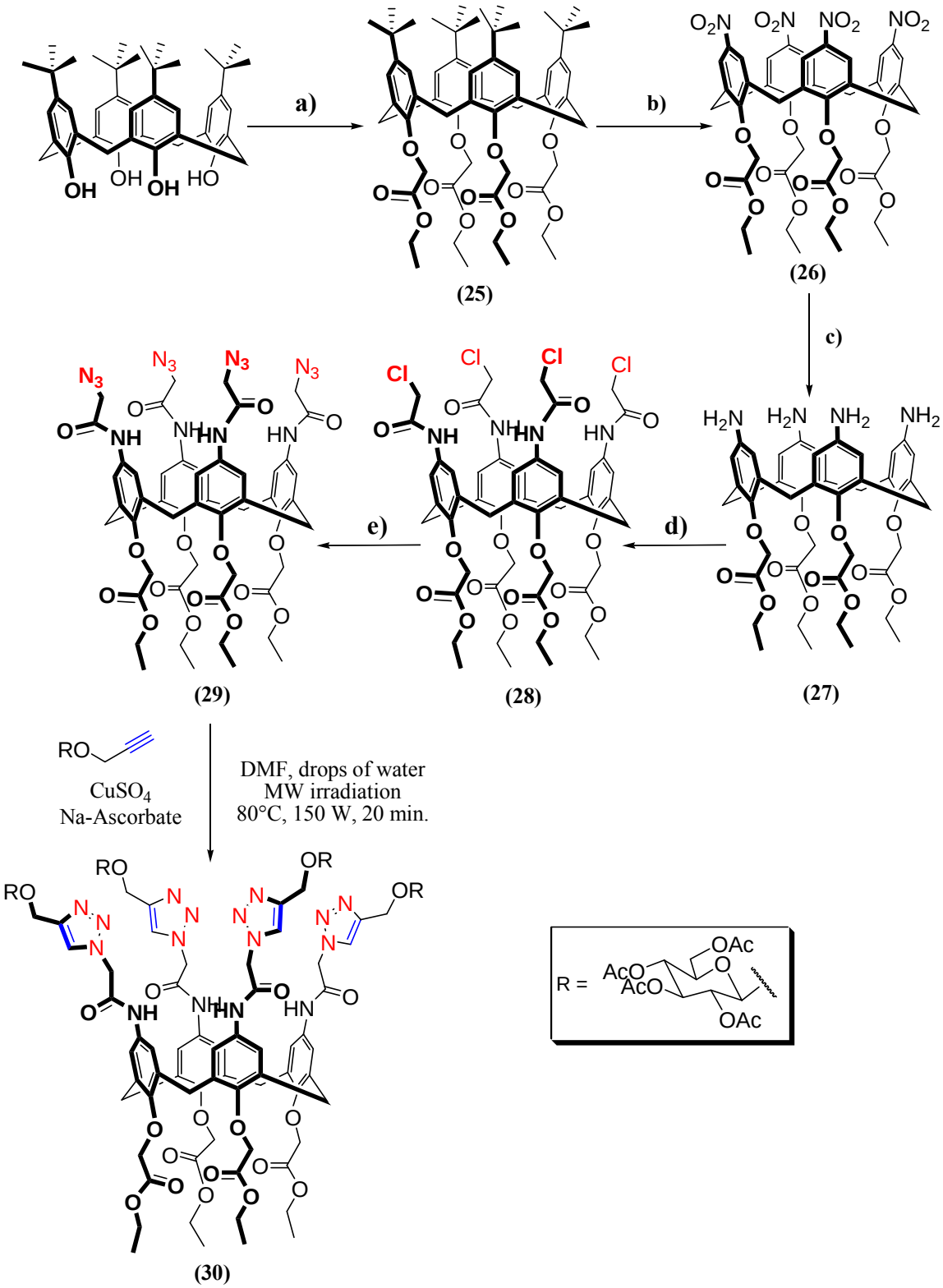

a) $BrCH_2COOEt$, NaH, THF dry, T = 67°C, 1h 30'; **(25),** Y = 87%. **b)** HNO_3 100%, CH_2Cl_2, CH_3COOH, rt, 24h; **(26),** Y = 60%. **c)** $NaBH_4$, $CoCl_2$ x $6H_2O$, CH3OH, N_2, overnight; **(27),** Y = 78%, **d)** $ClCH_2COCl$, DIPEA, DCM, rt, 1h 30'; **(28),** Y = 95%. **e)** NaN_3, TBAHS, $NaHCO_3$, DCM, r t, 2 days; **(29),** Y = 54%

Scheme 12

The p-tert-butyl calix[4]arene, as reported in literature[48] was deprotonated with a strong base such as sodium hydride, and then alkylated with α-bromo-ethyl acetate in dry THF. The reaction was stirred at 70° C for two hours. We slightly modified the procedure reported in literature. In fact we used 16 equivalents of NaH and 20 equivalents of α-bromo ethyl acetate instead of the 8 equivalents of each reagent. Compound **25** was obtained, after work-up and without further purification, in 87% yield. In the ^{1}H-NMR spectrum **Fig. 16** two doublets at δ = 4.85 ppm and 3.18 ppm (J = 13 Hz) are present, which are the signals characteristic of the methylene bridge protons in axial and equatorial positions respectively indicating only a cone conformation for the product. Beside the singlets at δ = 6.77 ppm for the aromatic protons and at δ = 1.07 ppm for the tert-butyl-groups, it is possible to assign the singlet at δ = 4.8 ppm to the ArO*CH*$_2$- groups and the quartet at δ = 4.2 ppm and the triplet at δ = 1.28 ppm to the ethyl ester group.

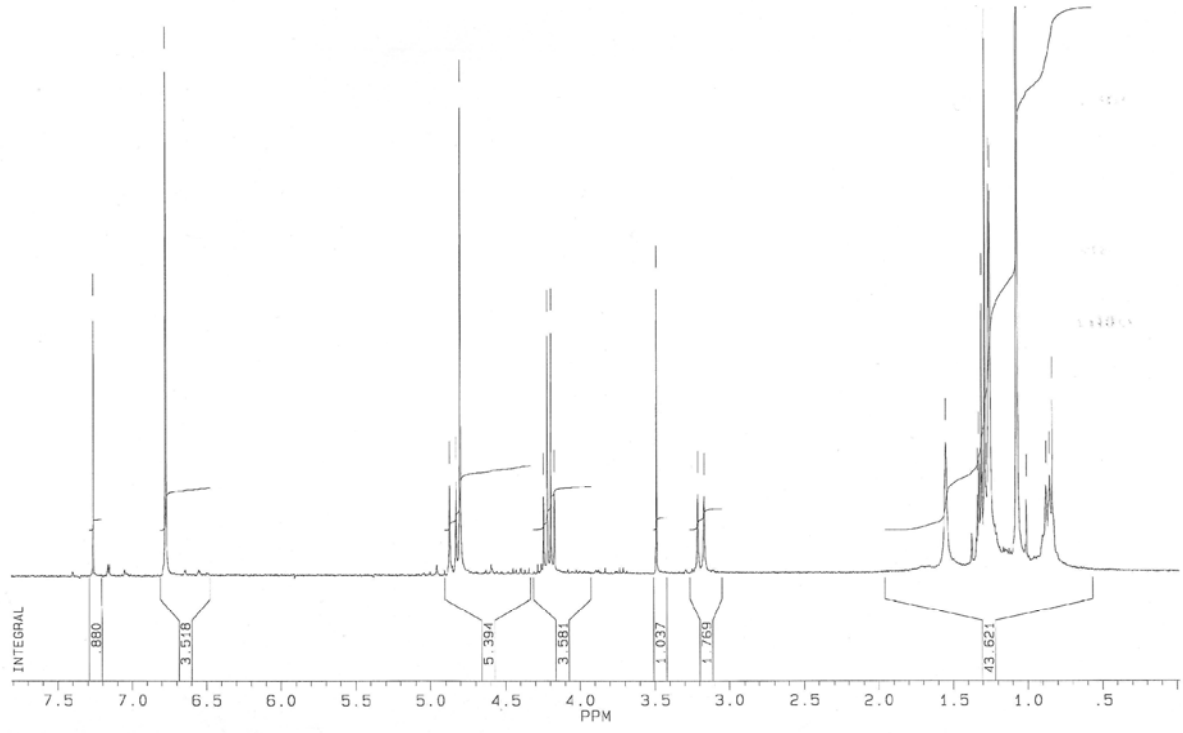

Fig. 16 ^{1}H-NMR spectrum ($CDCl_3$) of compound **25**

Compound **25** was then nitrated at the upper rim using a reaction which, due to the simultaneous removal of the tert-butyl groups is named ipso-nitration[49]. The corresponding tetra-nitro compound **26** was isolated in 45% yield. The reaction was carried out in the same conditions as reported in the **scheme 3** for compound **4.** In this case, however, we observed, after crystallization from methanol

of the crude compound, a small amount of the corresponding methyl ester, originated from the transesterification reaction, which took place during crystallization in slightly acidic condition. The mixture of ethyl and methyl esters were therefore treated with refluxing ethanol and a catalytic amount of concentrated sulfuric acid for 24 hours, to obtained the pure tetra-ethyl ester.

The reduction of the nitro groups to amine, (**c, scheme 12**) was carried out with a large excess of sodium borohydride and cobalt(II) dichloride hexahydrate at room temperature and overnight. Compound **27** was isolated in high yield but not in a very pure form. In fact in the ^{1}H-NMR spectrum (**Fig. 17**) all the signals are rather broad, included the peak of residual $CDCl_3$. We tried to record the spectrum in different solvents, like methanol-d_4 and DMSO-d_6 but we also observed very broad spectra as in $CDCl_3$. Probably, the broad signals observed should be attributed to the presence of traces of cobalt which is paramagnetic. Although the spectrum is quite difficult to be interpreted and even if peaks are rather broad, all expected signals are present. A positive test with ninhydrin reagent on the TLC plate also confirms the presence of amino groups.

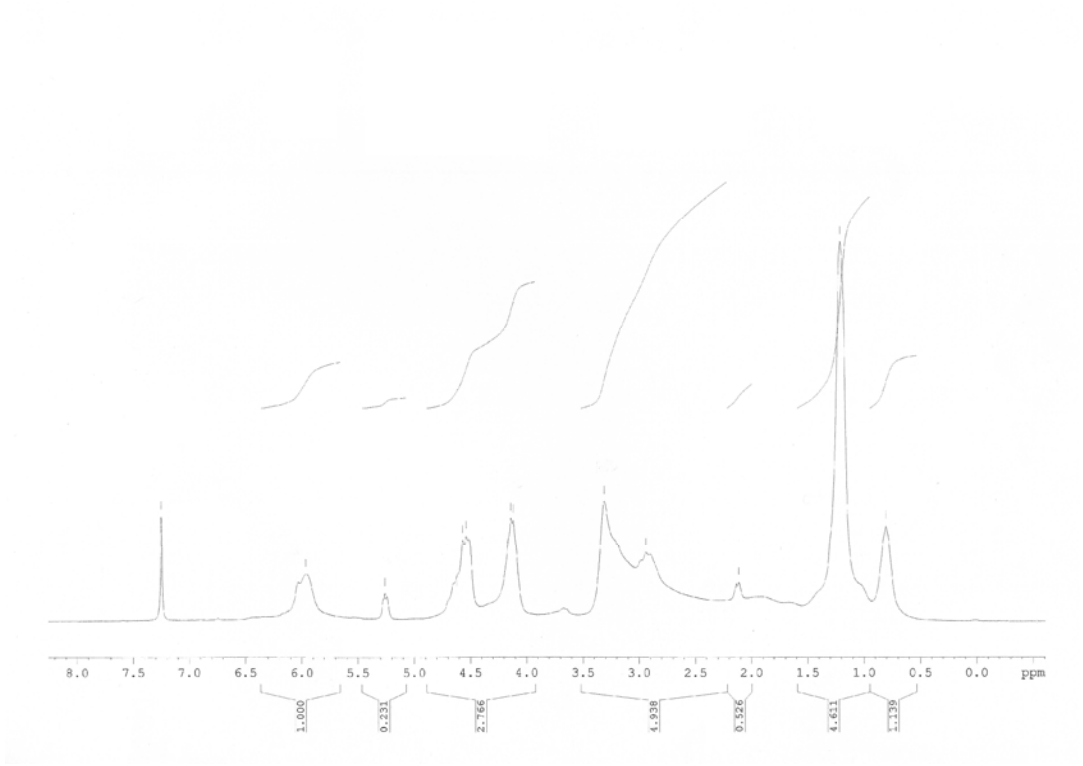

Fig. 17 ^{1}H-NMR spectrum (300 MHz $CDCl_3$) of compound **27**

This crude product 27 was therefore submitted to acylation reaction with α-chloro-acetyl chloride and N-ethyl-di-isopropyl amine. The mixture was stirred in dry dichloromethane at room temperature and under nitrogen atmosphere for 1h. After work-up the crude product was purified by flash chromatography to give the pure compound **28** (**scheme 12**) in 95 % yield. The ^{1}H-NMR spectrum was registered in a mixture of $CDCl_3$ and methanol-d_4 to avoid the formation of intra-and

intermolecular H-bonds, which broadens the spectrum. We could observe the characteristic singlet at δ = 3.82 ppm for the proton of the C(O)CH_2Cl group which confirms the success of the reaction.

To synthesize the tetra-azido derivative **29,** to be used in the final "*Click Chemistry*" step for conjugation of the sugar to the calixarene, we submitted compound **28** to the nucleophilic substitution of chlorine with azide group. The reaction was carried out under phase transfer-catalysis, with tetra-butyl ammonium hydrogen sulfate, sodium azide, in a mixture of a sodium hydrogen carbonate saturated aqueous solution and methylene chloride (**e, scheme 12**). The mixture was vigorously stirred at room temperature for two days.

It was rather difficult to monitor this reaction by TLC, since no chromatographic conditions could be found either on a direct or an inverse phase, to separate the two compounds. We therefore used Electrospray Mass Spectrometry (ESI-MS) to follow the reaction. The kinetics of this reaction is very slow; in literature it was reported the use of 12 equivalents of sodium azide but we had to use 40 equivalents for each chloride to be substituted. After the work-up we could obtain a crude product which was purified by crystallization in ethanol to get compound **29** in 52% yield. The latter compound was characterized by ESI-MS (**Fig. 18**) where the sodiated molecular peak at m/z = 1183.66 $[M+Na]^+$ was observed; in any case no peak of partially substituted compounds is present. The IR spectrum of this compound (**Fig. 19**) in a film on NaCl pellets shows the characteristic absorption at 2107 cm^{-1} which is typical of the azide group. On the other hand the ^{1}H-NMR spectrum was not very informative since not significant differences with the signals of the tetrachloro derivative **28** could be observed.

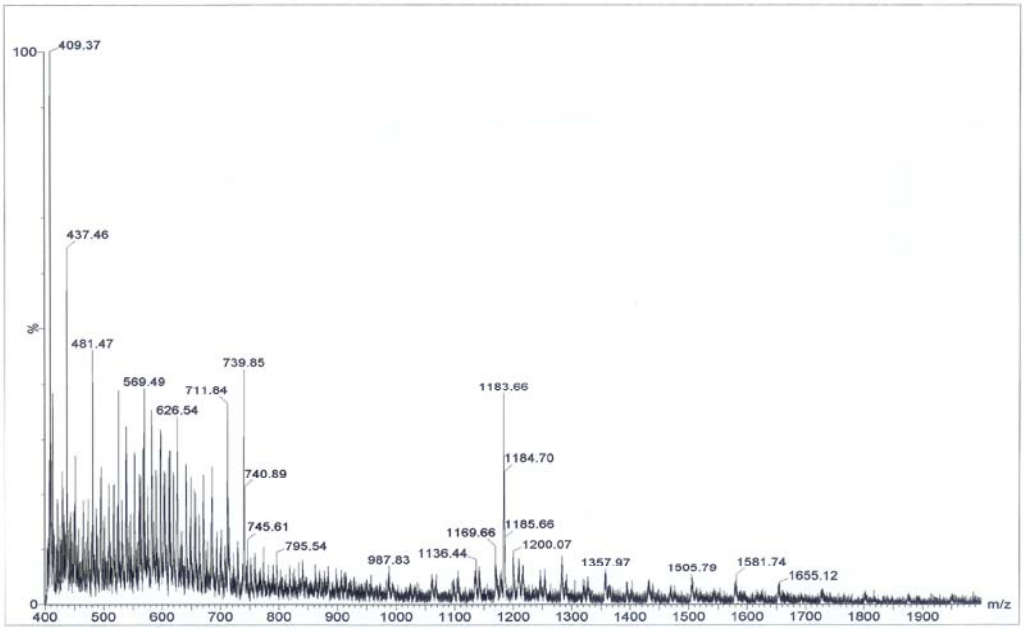

Fig. 18 ESI-MS spectrum in CH_3OH with positive ionization mode of compound **29**.

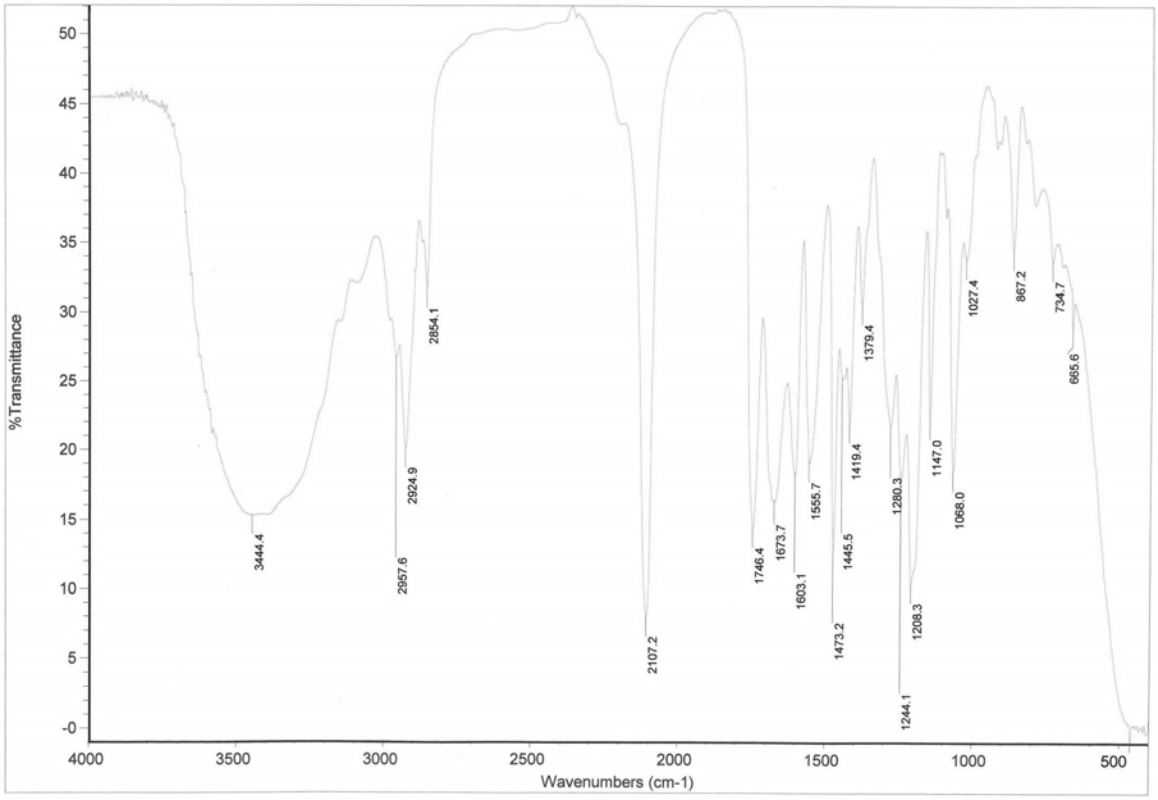

Fig. 19 Infrared spectrum (film on NaCl pellets) of compound **29**

The following *"Click Chemistry"* was carried out between compound **29** and the commercially available peracetylated 2-propynil-β-D-glucose (**31**). The reaction was carried out in microwave apparatus. Compound **29**, and an excess of peracetylated 2-propynil-β-D-glucose were mixed together with a catalytic amount of copper sulfate penta-hydrate and sodium ascorbate in DMF as solvent. The mixture was irradiated at 150 watt power (T = 80° C) for 20 minutes. After this time a TLC analysis indicated the complete conversion of the starting material. After quenching the reaction and work-up we could recover the unreacted sugar, used in excess, by trituration of the crude product in ethyl ether. We obtained quite pure the compound **30** in 84% yield without further purification. In parallel experiments under traditional heating, conditions we used the $Cu(PPh_3)_3Br$, a Cu(I) complex soluble in organic solvents[50], in methylene chloride or CuI in toluene, but without success. In both conditions we only obtained mixtures of compounds partially conjugated, which were very difficult separated.

The ^{1}H-NMR spectrum (**Fig. 20**) shows at δ = 8.03 ppm the signal of triazole protons (4H); at δ = 6.93 ppm the signal of the aromatic protons (8H). The sugar units give at δ = 5.04 ppm a triplet for H-4 which couples with H-3 (at δ = 5.24-5.21). H-3 is also coupled with H-2 (at δ = 4.95-4.70)

while the doublet for H-1 is superimposed to H-2. The four singlets at δ = 2.02, 1.99, 1.95, 1.94 are attributed to the protons of the acetyl groups of the sugar. The assignment of each of these signals was confirmed with the aid of a COSY spectrum (**Fig. 21**).

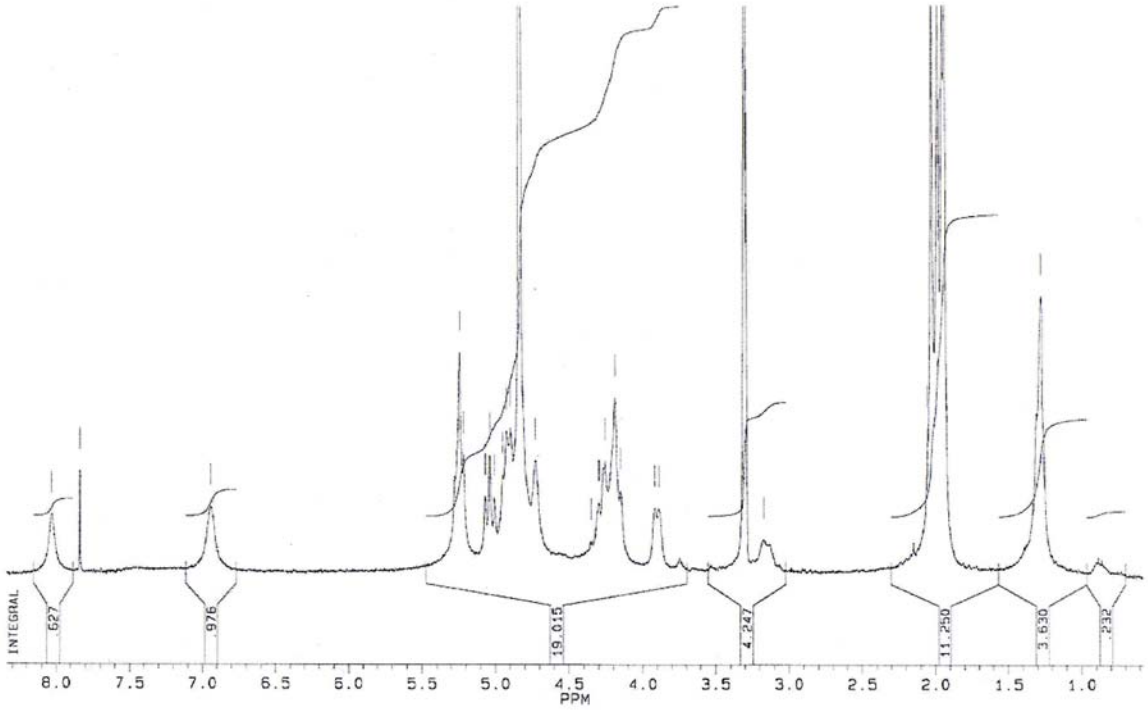

Fig. 20 ^{1}H-NMR (300 MHz in CD_3OD)spectrum of compound **30**.

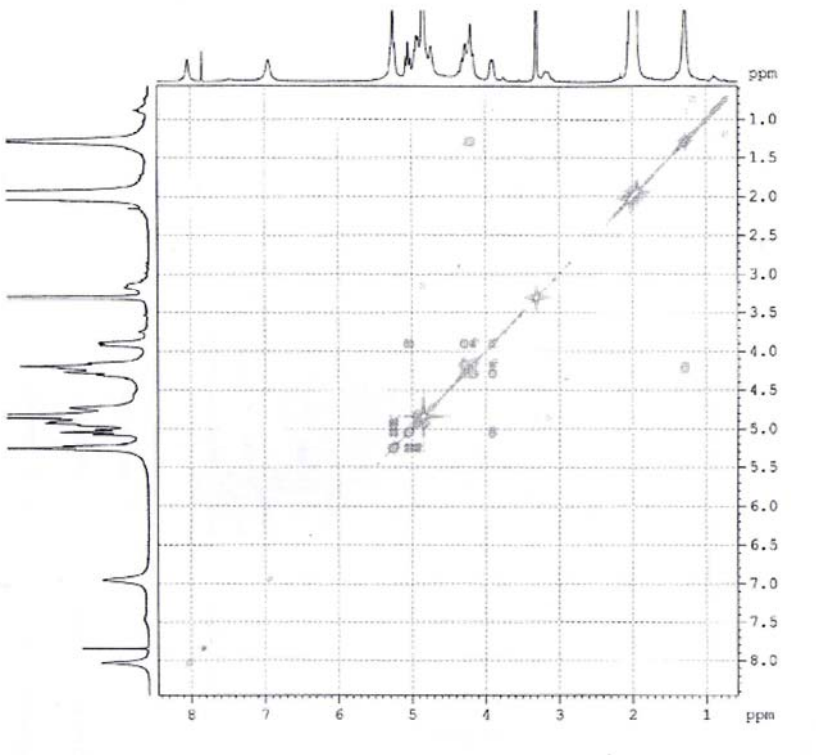

Fig. 21 H-COSY spectrum (300 MHz in CD_3OD) of compound **30**

For reason of time, compound **30** could not be linked to DOTA. However, we plan to selectively hydrolyse one of the four ester groups at the lower rim, as reported in literature[51] on similar tetraester derivatives, and to subsequently couple the resulting acid with DOTA-amine (**12**). Another possibility which could be explored is to hydrolyse all the four ethyl groups at the lower rim of the calix and to attach four DOTA-amine (**12**) units (**Fig. 21b**).

The latter conjugate, once complexed with Gd(III), should present a high concentration of paramagnetic ions and should improve sensitivity for this class of site-specific contrast agents.

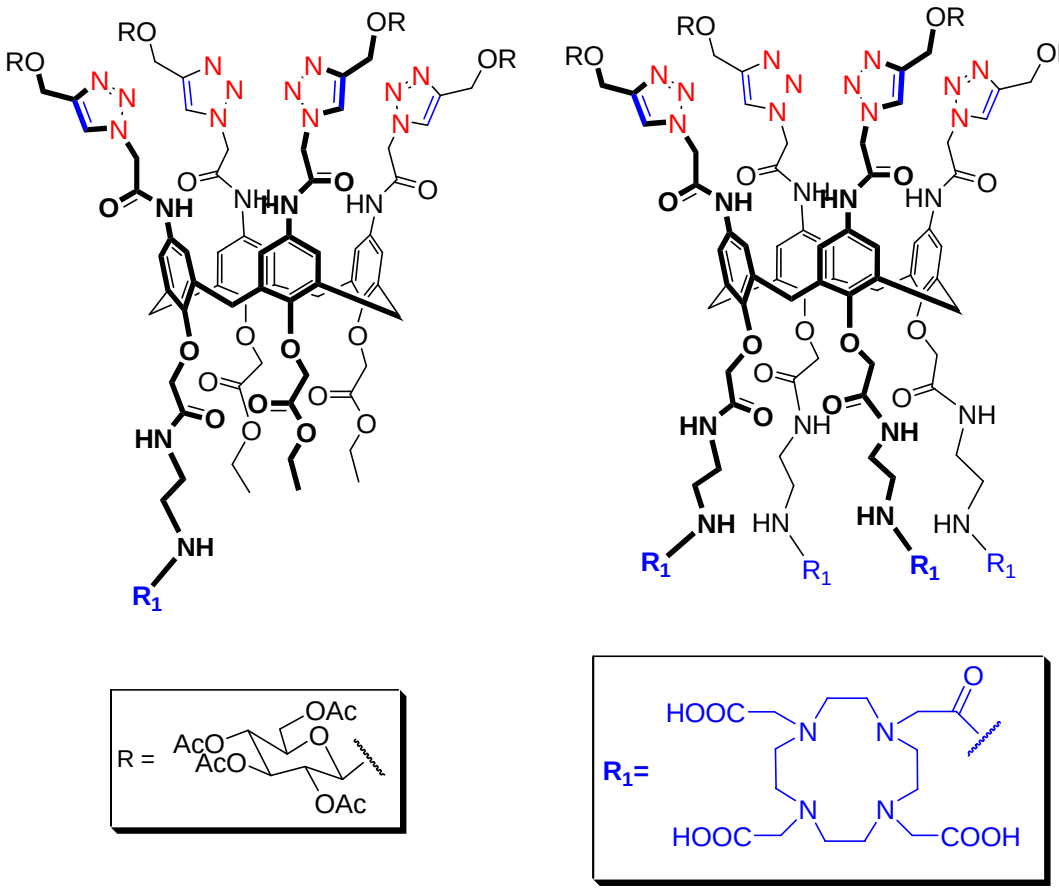

Fig. 21b compound 30 respectively one and four units of DOTA derivative

4.4 Synthesis of Gallic acid-DOTA conjugates

In parallel to the synthesis of polyglycosylated calixarene-DOTA conjugates we also prepared two potential contrast agents based on gallic acid as scaffold and having exposed galactose or glucose units (**Fig. 22**). We choose gallic acid since it bears three hydroxy groups to which three units of the same carbohydrate can be attached. Again we planned to take advantage of *"Click Chemistry"* to conjugate saccharide units to the trifunctional scaffold and use the carboxylic function to bind the DOTA derivative.

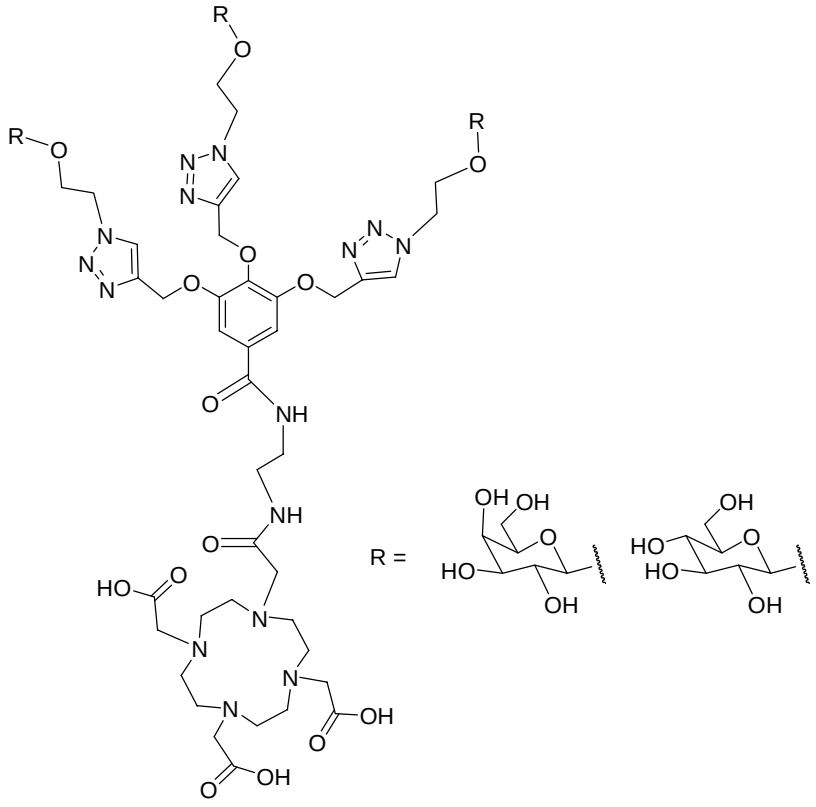

Fig. 22

Conjugation of sugar with "*Click Chemistry*" catalyzed by copper salts, should take place prior to the coupling of DOTA, since we verified that the functionalised azamacrocycle form extremely stable complexes with copper ions which are very difficult to dissociate.

Starting from gallic acid we synthesised the common intermediate **33** (**Scheme 13**) which was subsequently conjugated to galactose or glucose

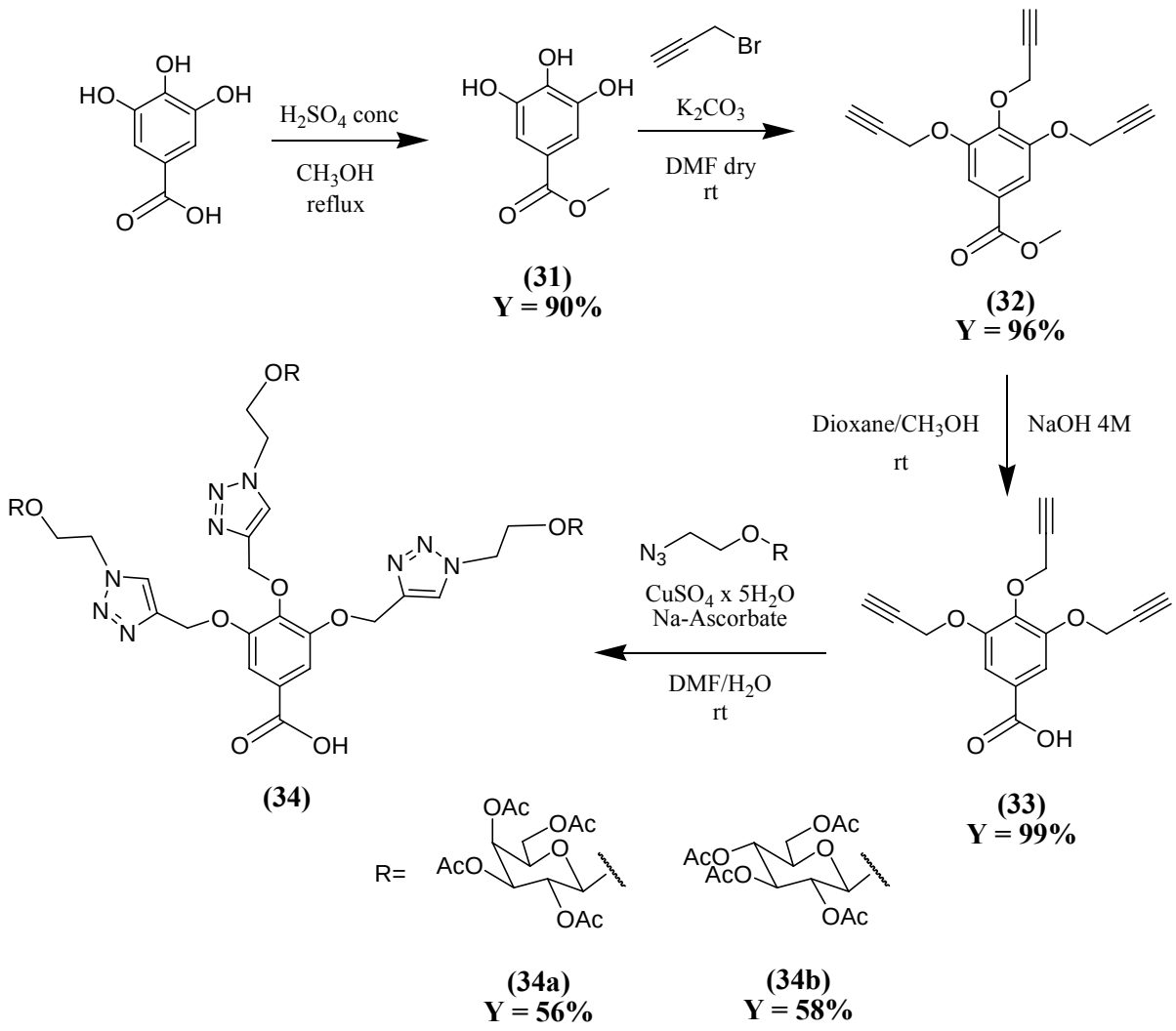

Scheme 13 Synthetic steps for conjugation of sugars on gallic acid.

Gallic acid was first protected as methyl ester, following the procedure reported in literature[52], which uses methanol and a catalytic amount of sulfuric acid at reflux to obtained compound **31** in 90% yield.

The alkylation of the hydroxy groups[53] was carried out using with an excess of propargyl bromide and potassium carbonate. Compound **32,** obtained in 96% yield, was then hydrolyzed[53] with sodium hydroxide in a mixture of dioxane/methanol at room temperature. Compound **33** was obtained in quantitative yield, without further purification.

At the same time the galactose-(**23a**) and the glucose-*O*-2-azido (**23b**) ethyl derivatives (see **scheme 10 chap. 4.1**) were synthesised as reported in literature[46, 47].

The *Click Chemistry* reactions between gallic acid derivative **33** and azido sugars **23a** and **23b** were carried out using the classic conditions[53] (**Scheme 14**); copper sulfate, sodium ascorbate in DMF/water as solvent in the dark and using conventional heating.

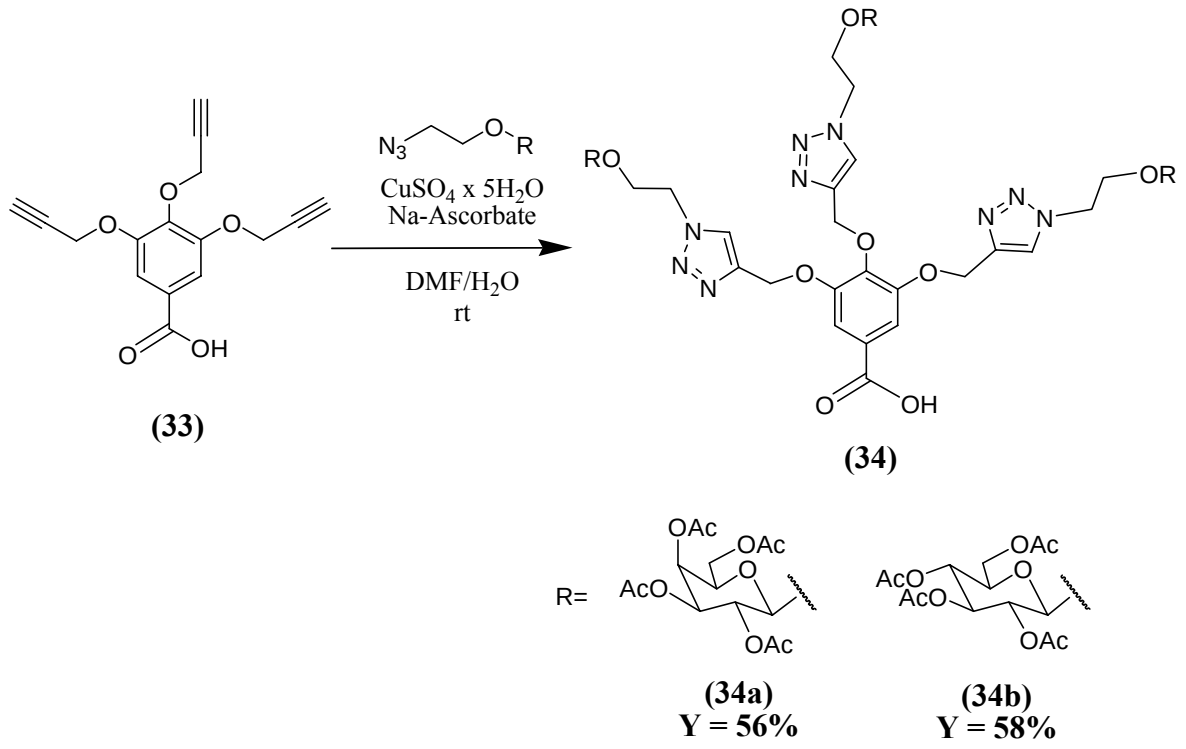

Scheme 14 *Click Chemistry* reaction on Gallic acid derivative.

In both reactions with galactose or glucose we encountered some problems; the reagents are not very soluble in the reaction media so we had to used a high stirring speed. Moreover, after 24 h TLC analysis still showed the presence of the starting material and an extra half equivalent of sugar and catalyst had to be added. After two more days, the starting material disappeared and the reaction was quenched. We tried to eliminate the copper salts with several washings of the organic phase with a phosphate buffer (pH = 7.00) but without success. Both compounds were purified by flash chromatography and the glycoconjugates **34a** and **34b** were obtained in 56 and 58% yield respectively.

These compounds were characterised by ESI-MS where we observed the doubly charged molecular peaks with two sodium ions $[M +2Na]^{2+}$ at m/z = 1581. The structure of compounds **34** was verified by ^{13}C and ^{1}H-NMR spectra while all the signals in the proton NMR spectra where unequivocally assigned using 2D-COSY. For compound **34a** in $CDCl_3$ the broad singlet at δ = 7.86 ppm correlates with signals at 5.23 ppm indicating they are due to the triazole and the $ArOCH_2$ protons. At δ = 7.47 the broad singlet of the aromatic protons are clearly visible indicating that the coupling took place. The methyne and methylene protons of the sugar are visible between 3.92 and 5.19 ppm. whereas the four singlets between 1.88 and 2.13 ppm are diagnostic of the acetyl groups. The expected ratio

between the signals of the sugar units and the gallic and $ArOCH_2$ units confirm the trifunctionalization. The coupling reaction between compounds **34a,** or **34b** and DOTA amino amide derivative **12** was carried out using O-Benzotriazole-N,N,N',N-tetramethyl-uronium-hexafluoro-phosphate (HBTU) and triethylamine in dry dichloromethane (**scheme 15**). In each case the reaction mixture was stirred at room temperature under nitrogen atmosphere for 24 h. After the work-up, the crude reaction product were purified by flash chromatography to obtained **35a** and **35b** in 84% and 55% yield, respectively.

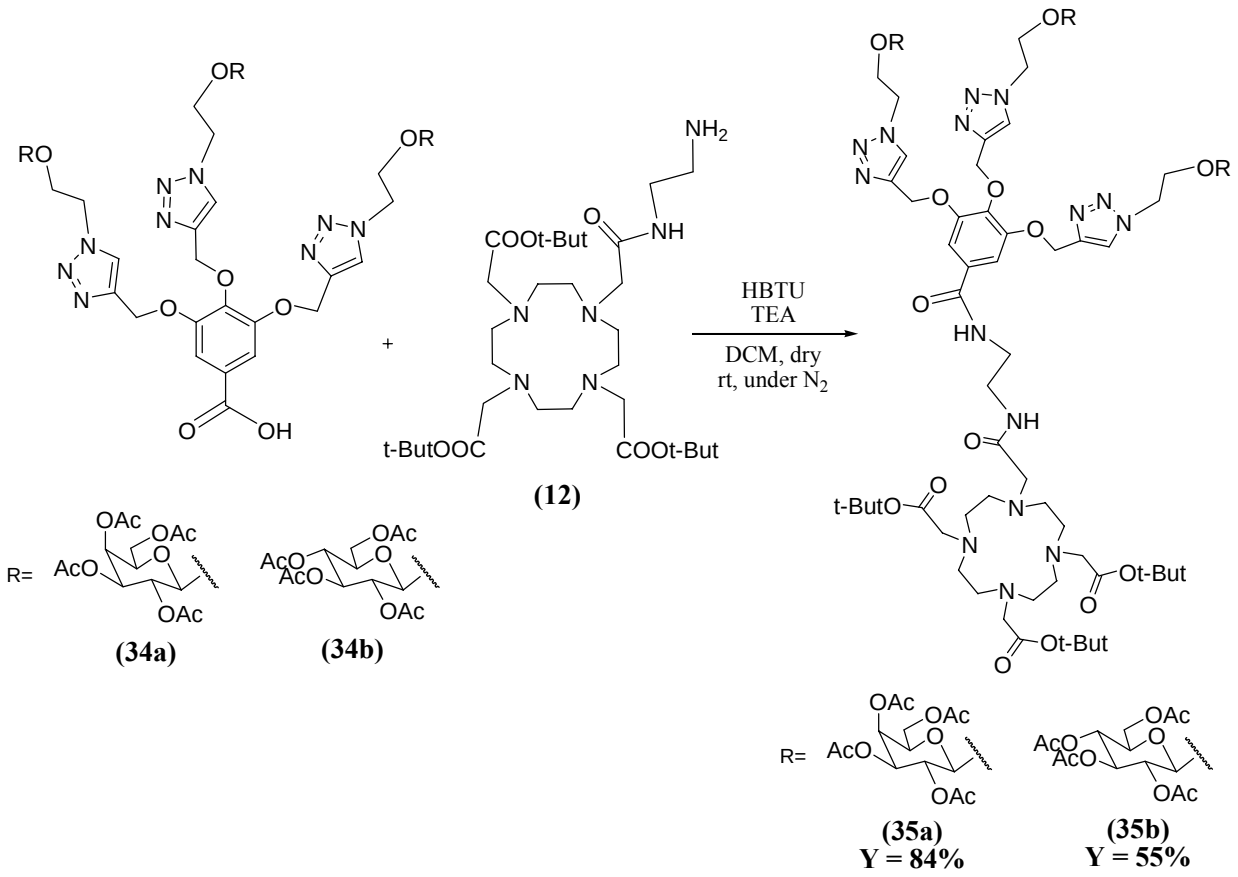

Scheme 15 Coupling reactions between gallic acid derivatives and DOTA amino-amide derivative

The 1H-NMR spectrum of compound **35a** registered in DMSO-d6 (**Fig. 23**) shows two broad singlets at δ = 7.92 and 8.11 ppm which are correlated with signals at 5.17 and 5.04 ppm indicating they are due to the triazole and the $ArOCH_2$ protons. Moreover, at δ = 8.22 and 8.43 ppm there are two broads singlets of the two –NH protons. Between δ = 3.92 and 5.25 ppm we observe the methylene protons of the sugar and the signals of the NCH_2CH_2O chain between triazole and sugar. Finally, significant is the presence at δ = 1.43 and 1.44 ppm of two singlets which are attributed to the tert-butyl groups of the macrocycle. The structures (**35a** and **35b**) were confirmed with electro-spray analysis where we observed peak at m/z = 1089.6 $[M+2Na]^{2+}$ and 2155.8 $[M+Na]^{+}$.

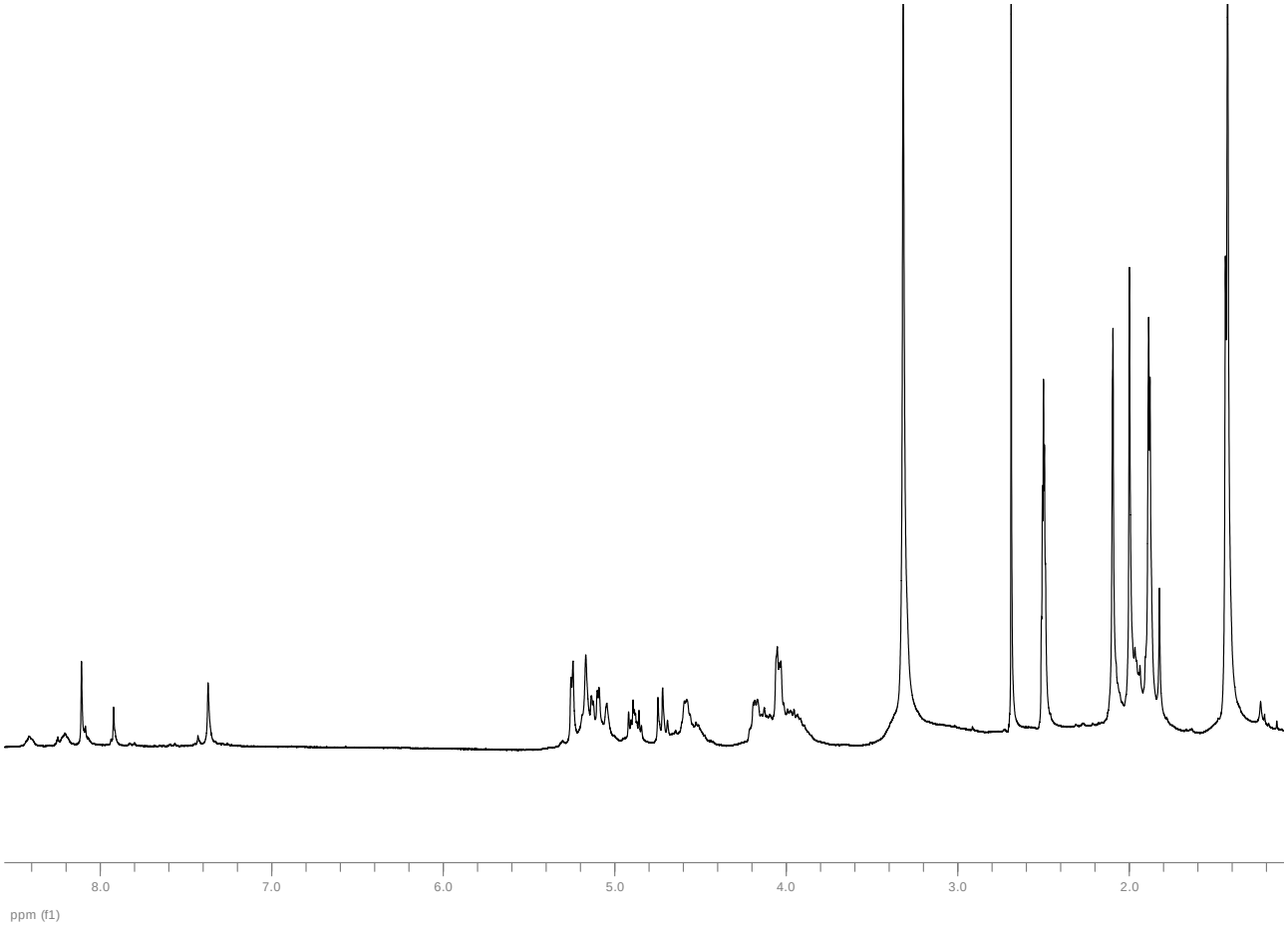

Fig.23 ^{1}H-NMR spectrum in DMSO-d6 (300 Mhz) of compound **35a**.

The removal of the tert-butylic groups of both compounds **35a** and **35b** was performed (**scheme 16**) following the classical conditions reported in literature[54], trifluoro acetic acid and triethyl-silane, in dichloromethane. The reactions were stirred at room temperature for 24 h, obtaining compounds **36a** and **36b** in 92 and 78% yield respectively, after solvent evaporation. The ^{1}H-NMR spectra showed the disappearance, in both compounds, of the signals of the tert-butyl groups around 1 ppm. Moreover we recorded the two-dimensional ^{1}H-^{1}H COSY in both compounds.

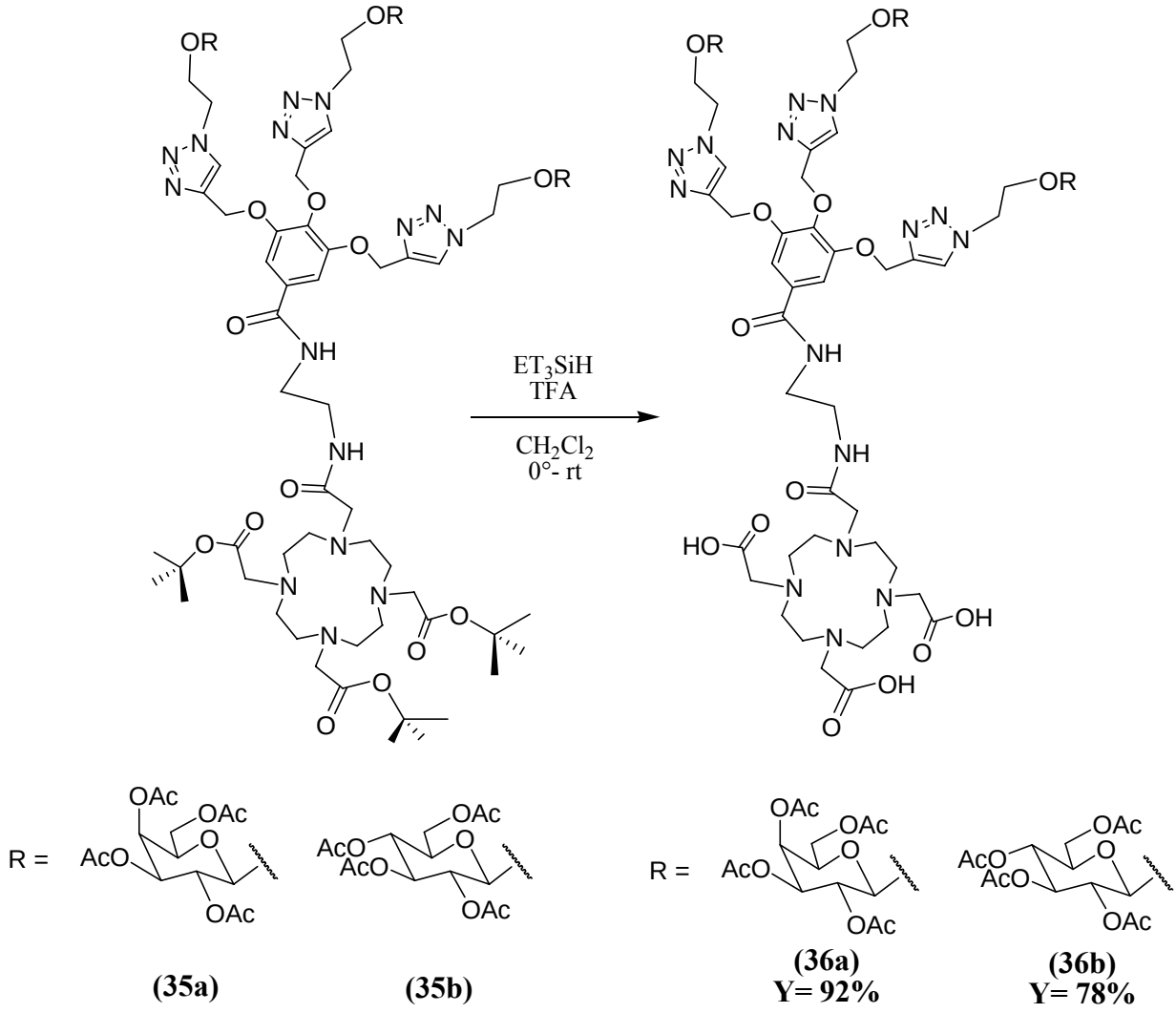

Scheme 16 Removal of the tert-butyl groups.

The last step consisted in the removal of the acetyl groups from the saccharide units. A solution of sodium methoxide in methanol was added to compounds **36a** and **36b** and the suspension stirred at room temperature for 3 h. The pH was slowly brought at neutrality by addition of a AMBERLITE IR 120 H^+ resin. After filtration of the resin, methanol was removed from the solution to give compound **37a** and **37b** in 98 and 81% yield respectively (**scheme 17**). The ^{1}H-NMR spectrum in D_2O showed the characteristic peaks of the triazole proton at low fields and all the other protons were identified by ^{1}H-^{1}H COSY analysis.

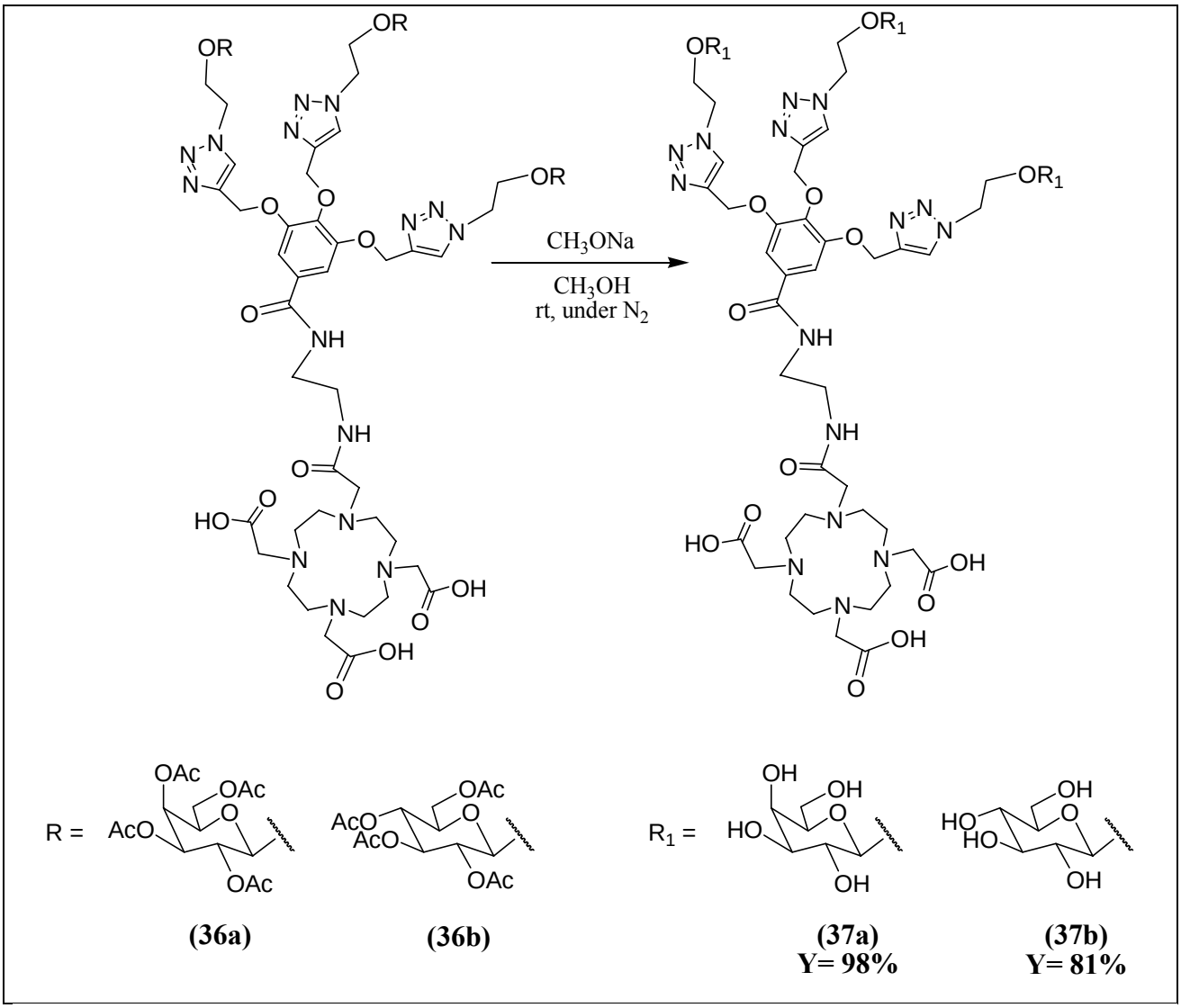

Scheme 17 Removal of the acetyl groups

In collaboration with Aime's group at the University of Torino we tested compounds **37a** and **37b** to estimate the complexation ability versus the gadolinium ion, the relaxometric properties of their Gd(III) complexes and to study the interaction all these polyglycosylated Gd complexes with two types of lectins, ConcanavalinA (ConA) and *Peanut Agglutinin* from *Arachis hypogea* (PNA). Herein we report our preliminary results (**Tab.1**).

The gadolinium complexes show a relaxivity at 20 MHz and 25° C of 7.8 $mM^{-1}s^{-1}$ for the compound **37a** and 8.5 $mM^{-1}s^{-1}$ for **37b (Tab 1),** which are comparable to values found for analogous complexes having similar molecular weight (cfr. Aglycone **38** in **tab 1**).

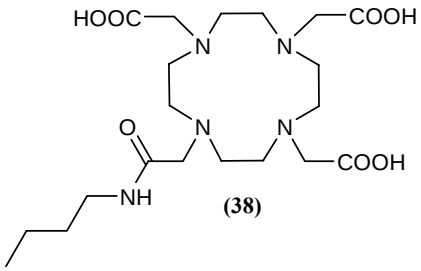

(38)

Fig. 24

The preliminary relaxometric studies carried out so far show that both compounds **37a** and **37b** form rather stable complexes with Gd(III) in water solution at different pH (results not shown) with a stability quite similar to those of other monoamide-Gd-DOTA.

Compound	**Relaxivity** 20 MHz, 25°C ($mM^{-1}s^{-1}$)	**PNA K ass** (M^{-1})	**ConA Kass** (M^{-1})	**Relaxivity of the ConcA adduct**
Galacto-gallic 37a	7.8 $mM^{-1}s^{-1}$	No interaction	9.8×10^{5} M^{-1}	15.5 $mM^{-1}s^{-1}$.
Gluco-gallic 37b	8.5 $mM^{-1}s^{-1}$	No interaction	3.9×10^{3} M^{-1}	38.8 $mM^{-1}s^{-1}$
Aglycone 38	5.06 $mM^{-1}s^{-1}$	Not measured	No interaction	_

Tab. 1 Preliminary results of relaxivity and complexation of compounds **37a, 37b** and aglycone **38**

The interaction of the Gd-**37a** and Gd-**37b** complexes with plant lectins was also studied by observing the variation of the relaxivity of a 0.1 mM solution of Gd(III) complexes with increasing amount of proteins.

ConA itself is paramagnetic, since it contains a Mn(II) ion. For this reason, the relaxivity of ConA alone was also measured at 20 MHz and 25°C resulting to be 7.1 mM^{-1} s^{-1}, which is a rather high value and comparable to that of the Gd(III) complexes. During the titration experiments of Gd **37a/b** with ConA, this contribution to relaxivity had therefore to be subtracted.

The curves for the galactose cluster complex Gd-37a and ConA or PNA are reported in **fig. 24** while those for the glucose cluster complex Gd-37b are reported in **fig. 25**

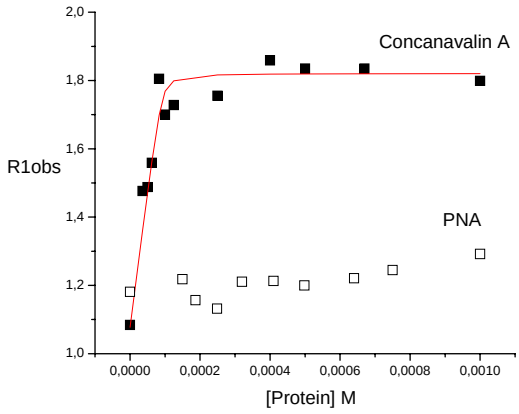

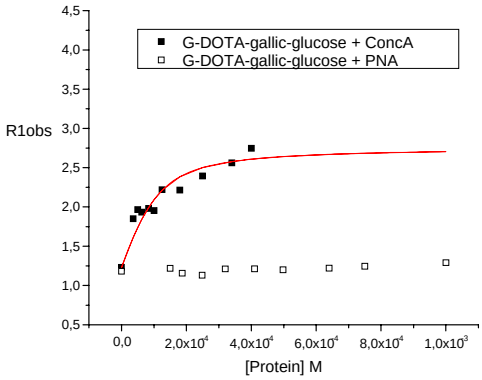

Fig. 24

Fig. 25

While it is clear that neither Gd-37an or Gd-37b interact with the galactose-selective lectin (PNA), both Gd-complexes seem to interact rather strongly with the glucose-selective lectin (ConA).

From these titration curves, the Kass and relaxivity of the Gd-37-ConA adduct could be calculated. While the relaxivity of the two adducts are quite similar, the affinity for ConA of the galactose-Gd-37a complex is unexpectedly nearly 250-fold higher than that of the corresponding complex of glucose Gd-37b. Rather unexpected is also the fact that a galactose sugar cluster is bound so firmly to a glucose-selective lectin. In order to exclude that this strong binding is simply originated by a Gd-protein interaction, we also titrated the Gd-38 complex with ConA. The linear trend of this titration curve (not shown) however clearly indicates a complete absence of interaction.

We are currently trying to confirm these Kass values using a different technique. However these preliminary results are quite encouraging, indicating that ligands 37a and 37b strongly complex Gd(III) ions with important relaxivities and are able, thanks to the presence of the sugar units, to interact with lectins.

4.5 Conclusions

In this chapter of the thesis, our efforts to synthesize new potential Site-Directed Contrast Agents for MRI, which exploit the cluster glycoside effect, are described. We used the strategy of coupling a tetraazacyclododecane-N,N',N'',N'''-tetraacetic acid (DOTA) to polyglycosylated calix[4]arene and gallic acid scaffolds. Several synthetic procedures were attempted to introduce glycosyl units on the calixarene macrocycles at the upper rim and it was finally found that the best one exploits the "Click Chemistry" approach through the formation of a triazole ring. Initially the calix[4]arene scaffold was adorned with four alkynyl groups at the upper rim and were coupled with sugar-azide derivatives, leading to useful intermediates but not to the final products. Subsequently, the complementary strategy of anchoring the azido group on the calixarene scaffold and the alkynyl moiety on the carbohydrate, was attempted. In this case it was found that the cycloaddition reactions leading to the simultaneous conjugation of four sugar units is very sensitive to the steric crowding which originates at the upper rim during the reaction. To obtain positive results in this conjugation method it was necessary to introduce a three-atom spacer between the macrocycle and the forming triazole units. In the case of the gallic acid scaffold the synthetic goal of having simultaneously on the same molecule a sugar clusters and a DOTA unit was completed. The Gd(III) complexes of these ligands were prepared and their stability and relaxivity properties studied in water solution, in collaboration with Prof. Aime's group in Torino. They show good stability and remarkable relaxivities, comparable with those of other DOTA derivatives reported in literature. However, thanks to the multivalent display of galactose and glucose units the complexes strongly interact with plant lectins such as Concanavalin A (ConA) and PeaNut Agglutinin (PNA) showing good perspective in the development of new "Site-Directed Contrast Agents".

4.6 Experimental section

General Methods: all moisture sensitive reactions were carried out under nitrogen atmosphere. Dry solvents were prepared according to standard procedures and stored over molecular sieves.

Melting points were determined under nitrogen sealed capillaries with an Electrothermal apparatus.

^{1}H and ^{13}C NMR spectra were recorded at 300 and 75 MHz, respectively, on Bruker AC300 and Bruker 300 Avance spectrometers, at 300 K unless otherwise specified. The reported *J* values are referred to H,H coupling constants, unless other specifications. Chemical shifts are reported as δ values in ppm using the solvent residual peak as internal standard. IR spectra were recorded on a Perkin Elmer 298 apparatus.

Mass spectra by chemical ionization (CI) and electrospray ionization (ESI) methods were recorded on a Finnigan Mat SSQ 710 spectrometer and on a Micromass ZMD spectrometer, respectively.

TLC were performed on silica gel Merck 60 F_{254} sheets and flash chromatography on 230-240 mesh Merck 60 silica gel.

For reasons of clarity and in order to reduce space, the names calix[4]arene was used instead of the original IUPAC name: pentacyclo[19.3.1.1.1.1]octaosa-1(25),3,5,7(28),9,11,13(27),15,17,19(26),-21,23-dodecane. The nomenclature IUPAC applied to the calixarene is complicated; in fact to expose a macrocycle very large denominations are required. Therefore here is used the international nomenclature proposed by Gutsche, where the numeration of the positions on the macrocycle is denominated as in the scheme below.

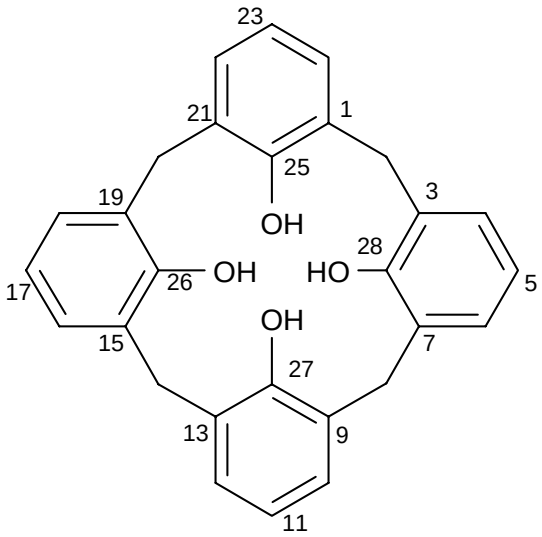

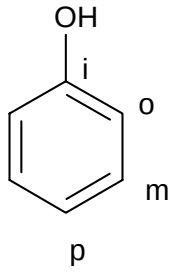

The internal positions of the aromatic rings are referred to the main hydroxy substituent, that is named with ipso, and the following are indicated as ortho, meta and para. The substituent in para is posed before the name of the calixarene.

Synthesis of 25-(ethoxycarbonylmethoxy)-p-tert-butylcalix[4]arene 2

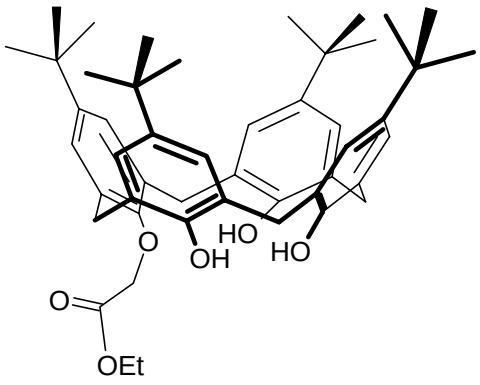

In the two-necked flask under nitrogen was dissolved cesium fluoride (840 mg; 5.5 mmol) in dry DMF (75 ml), then was added p-tert-butylcalix[4]arene (3 g; 4.62 mmol) and ethyl bromoacetate (5.12 ml 46 mmol). The reaction mixture was stirred under nitrogen at 40°C for 7 h and at room temperature for 60 h.

The reaction was monitored by TLC (SiO_2: eluent CH_2Cl_2/ether petroleum 3:1). When the starting material disappeared, the reaction was quenched with a 2M HCl solution (200 ml). The aqueous phase was extracted with CH_2Cl_2 (3 x 50 ml). The organic phase was washed with water (3 x 50 ml) and dried over sodium sulfate. The solvent was evaporated under reduced pressure to obtain a crude product as white solid. The crude product was purified by flash chromatography (SiO_2 : gradient cyclohexane:ethyl acetate = 95:5, 9:1, 8:2) to obtain the product **2** as white solid. **Yield:** 50%. **^{1}H NMR** (300 MHz, $CDCl_3$): δ(ppm) 10.23 (s, 1H, OH), 9.25 (s, 2H, OH), 7.09 (s, 2H, Ar), 7.05 (s, 2H, Ar), 7.04 (d, 2H, *J* = 2,3 Hz, Ar), 6.98 (d, 2H, *J* = 2.3 Hz, Ar), 4.89 (s, 2H, OCH_2CO), 4.48 (d, 2H, *J* = 13.3 Hz, ArCH_{2ax}Ar), 4.41 (q, 2H, *J* = 7.2 Hz, OCH_2CH_3), 4.30 (d, 2H, *J* = 13.3 Hz, ArCH_{2ax}Ar), 3.43 (d, 4H, *J* = 13.3 Hz, ArCH_{2eq}Ar), 1.38 (t, 3H, *J* = 7.2 Hz, OCH_2CH_3), 1.23, 1.20, 1.19 (s, 36H, $C(CH_3)_3$). **^{13}C NMR:** δ(ppm): 169.5 (s, CO), 149.9 and 148.2 (Ar ispo), (Ar), 72.0 (OCH_2COOEt), 61.9 (OCH_2CH_3), 34.2, 34.0, 33.9 ($C(CH_3)_3$), 33.0 and 32.5 (ArCH_2Ar), 31.5, 31.4, 31.2 ($C(CH_3)_3$), 14.2 (CH_3). **ESI-MS** (+) $C_{48}H_{62}O_6$ (734.45): m/z = 757.3 $[M+Na]^+$. **m. p.:** 275-276 °C

Synthesis of 25-(ethoxycarbonylmethoxy)-26,27,28-tripropyloxy-p-tert-butylcalix[4]arene 3

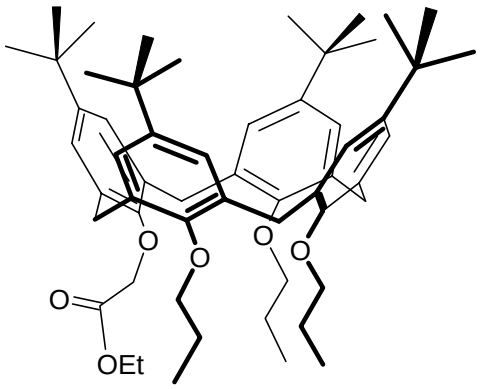

Compound **2** (0.430 g, 0.58 mmol) and DMF dry (4 ml) were stirred in a two-necked round bottomed flask under nitrogen atmosphere. Then sodium hydride (55-65% in oil, 0.140 g, 2.9 mmol) and iodopropane (0.493 g, 2.9 mmol) were added. The reaction mixture was stirred under nitrogen at room temperature for 24h. The reaction was monitored by TLC (SiO_2: eluent ethyl acetate/hexane = 6:4). After disappearance of the starting material, the reaction was quenched with 0.1M HCl (15 ml). The organic phase was extracted with dichloromethane (3 x 20 ml), dried over sodium sulfate and the solvent was evaporated under reduced pressure to obtain a crude product. This yellow solid was crystallized by acetonitrile to obtain a product **3** as white solid. Yield: 55%.

^{1}H NMR (300 MHz, $CDCl_3$) δ(ppm) 6.91 (s, 2H, Ar), 6.89 (s, 2H, Ar), 6.70-6.63 (m, 4H, Ar), 4.83 (d, 2H, J = 11.8 Hz, OCH_2CO), 4.62 (t, 2H, *J* = 12.9 Hz, ArCH_{2ax}Ar), 4.40 (d, 2H, *J* = 12.6 Hz, ArCH_{2ax}Ar), 4.10 (t, 2H, *J* = 6.8 Hz $OCH_2CH_3CH_3$), 3.85-3.65 (m, 6H, $OCH_2CH_2CH_3$, CH_3CH_2O), 3.16 (d, 2H, *J* = 12.9 Hz, ArCH_{2eq}Ar), 3.11 (d, 2H, *J* = 12.6 Hz, ArCH_{2eq}Ar), 2.19-2.05 (m, 2H, $OCH_2CH_2CH_3$), 2.05-1.88 (m, 4H, $OCH_2CH_2CH_3$), 1.30 (t, 3H, OCH_2CH_3), 1.18 (s, 18H, $C(CH_3)_3$), 0.98 (s, 18H, $C(CH_3)_3$), 1.10-0,90 (m, 12H, $OCH_2CH_2CH_3$).

^{13}C NMR (75 MHz, $CDCl_3$): δ(ppm): 170.9 (CO); 154.1; 153.5; 153.5 (Ar ipso); 144.9; 144.6; 144.3 (Ar para); 134.6; 134.1; 133.3; 133.1 (Ar ortho); 125.5; 125.1; 124.9; 124.8 (Ar meta); 76.8 ($OCH_2CH_2CH_3$); 70.9 (OCH_2CO); 60.2 (OCH_2CH_3); 33.8, 33.6 31.5, 31.4, 31.3, 30.9 ($C(CH_3)_3$, $C(CH_3)_3$ and $ArCH_2Ar$); 23.3 23.2 ($OCH_2CH_2CH_3$); 14.1; 10.4 10.0 ($OCH_2CH_2CH_3$).

ESI-MS (+) $C_{57}H_{80}O_6$ (860.6): m/z = 883.9 $[M+Na]^+$. **m. p.:** 189-191 °C

Synthesis of 25-(hydroxycarbonylmethoxy)-26,27,28-tripropyloxy-p-tert-butylcalix[4]arene 4

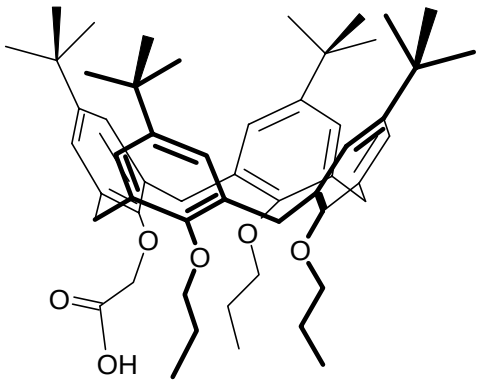

In a round-bottomed flask, 25-ethoxycarbonylmethoxy-26,27,28-tripropyloxy-p-tert-butylcalix[4]arene **3** (1.22 g; 1.42 mmol) was dissolved in THF/H_2O (60 ml, 5:1) and a solution of KOH (0.738 g; 13.2 mmol) in THF/H_2O (5:1) was added. The reaction mixture was stirred at reflux for 48h. The reaction was monitored by TLC (SiO_2: eluent, cyclohexane/ethyl acetate = 1:1). The reaction was quenched with 0.1M HCl until pH 3. the organic phase was extracted with CH_2Cl_2 (4 x 30 ml) and dried over sodium sulfate. The solvent was evaporated under reduced pressure to obtain a yellow solid after trituration by methanol. **Yield:** 82.5%.

^{1}H NMR (300 MHz, $CDCl_3$): δ(ppm): 7.15 (s, 2H, Ar), 7.13 (s, 2H, Ar), 6.59 (d, 2H, *J* = 2.4 Hz, Ar), 6.48 (d, 2H, *J* = 2.4 Hz, Ar), 4.64 (s, 2H, OCH_2COO), 4.45 (d, 2H, *J* = 12 Hz, $ArCH_{2ax}Ar$), 4.22 (d, 2H, *J* = 12 Hz, $ArCH_{2ax}Ar$), 3.78- 3.67 (m, 6H, *J* = 6.5 Hz, $OCH_2CH_2CH_3$), 3.22 (d, 2H, *J* = 12 Hz, $ArCH_{2eq}Ar$), 3.15 (d, 2H, *J* = 12 Hz, $ArCH_{2eq}Ar$), 1.93- 1.85 (m, 6H, *J* = 6,5 Hz, $OCH_2CH_2CH_3$), 1.34 (s, 18H, $C(CH_3)_3$), 0.98 (t, 6H, 7.5 Hz, $OCH_2CH_2CH_3$), 0.88 (t, 3H, 7.5 Hz, $OCH_2CH_2CH_3$), 0.83 (s, 18H, $C(CH_3)_3$). **^{13}C NMR** (75 MHz, $CDCl_3$): δ (ppm): 170.7 (CO), 154.1, 151.8, 151.0 (Ar-CO), 147.0, 145.0, 144.8 (Ar-CC), 135.4, 135.0, 132.6, 131.6 (Ar-CCH_2), 125.9, 125.3, 125.1, 124.5 (Ar-CH), 78.2 and 77.6 ($OCH_2CH_2CH_3$), 70.7 (OCH_2CO), 34.2, 34.1, 33.6 ($C(CH_3)_3$), 31.7, 31.6, 31.2, 31.0, 30.9, 29.7 ($C(CH_3)_3$ and $ArCH_2Ar$), 23.1 and 22.4 ($OCH_2CH_2CH_3$), 10.3, 9.8 ($OCH_2CH_2CH_3$). **ESI-MS** (+) $C_{55}H_{76}O_6$ (832.56): m/z = 877.5 $[M+2Na]^+$. **m. p.:** 226.6-228 °C.

Synthesis of 5,11,17,23-tetranitro-25-(hydroxycarbonylmethoxy)-26,27,28-tripropyloxy-calix[4]arene 5

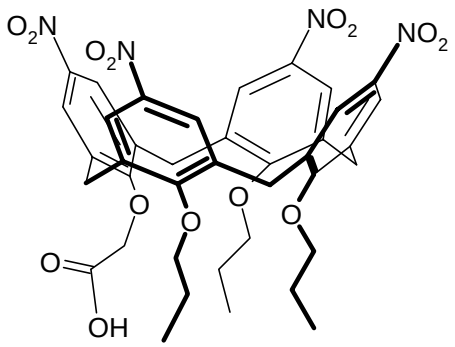

In a round-bottomed flask, compound **4** (241 mg, 0.29 mmol) was dissolved in CH_2Cl_2 (4 ml) and glacial acetic acid (4 ml), the solution cooled to 0°C and added dropwise of 100% HNO_3 (1.35 ml). The black coloured reaction mixture was stirred at room temperature for 72h. The reaction was monitored by TLC (SiO_2: eluent cyclohexane/ethyl acetate 6/4) and then quenched at 0°C (ice bath) with water (20 ml). The organic layer was extracted with $CHCl_3$ (3 x 20 ml), washed with water till neutral pH, dried over sodium sulfate and the solvent was evaporated under reduced pressure to obtain a yellow solid. **Yield:** 81%.

^{1}H NMR (300 MHz, $CDCl_3$): δ(ppm): 8.01 (s, 4H, Ar), 7.25-7.20 (m, 4H, Ar), 4.87 (s, 2H, OCH_2COO), 4.58 (d, 2H, *J* = 14.4 Hz, $ArCH_{2ax}Ar$), 4.54 (d, 2H, *J* = 14.4 Hz, $ArCH_{2ax}Ar$), 4.04 (t, 2H, *J* = 7.8 Hz,), 3.90 (t, 2H, *J* = 7.8 Hz, $OCH_2CH_2CH_3$), 3.53 (d, 2H, *J* = 14.4 Hz, $ArCH_{2eq}Ar$), 3.44 (d, 2H, *J* = 14.4 Hz, $ArCH_{2eq}Ar$), 2.00-1.78 (m, 6H, $OCH_2CH_2CH_3$), 1.05 (t, 6H, *J* = 7.2 Hz, $OCH_2CH_2CH_3$), 0.94 (t, 3H, *J* = 7.5 Hz, $OCH_2CH_2CH_3$). **^{13}C NMR** (75 MHz, $CDCl_3$): δ(ppm): 10.1-10.5 ($OCH_2CH_2CH_3$); 23.38 and 23.4 ($OCH_2CH_2CH_3$); 31.5 and 31.8 ($ArCH_2Ar$); 71.3 (OCH_2CO); 79.1 ($OCH_2CH_2CH_3$); 123.9, 124.2, 125.0, 125.4 (Ar meta); 134.2; 135.0; 135.8; 136.6 (Ar ortho); 143.9 and 144.3 (Ar para); 160.2 and 162.5 (Ar ipso); 169.2 (CO). **ESI-MS** (+) $C_{39}H_{40}N_4O_{14}$ (788.25): m/z = 787.1 $[M-H]^-$ **m. p.:** 267- 268 °C.

Synthesis of N, N', N'', N'''-tetratosyl-1,4,7,10-tetraazacyclododecane 8

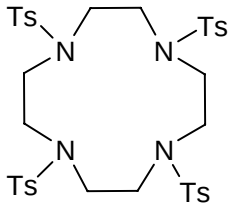

In a two-necked flask under nitrogen atmosphere, a suspension of dry potassium carbonate (1.13 g; 8.15 mmol) in dry DMF (50 ml) was added of compound **7** (3.0 g; 3.92 mmol). The suspension was stirred at room temperature under nitrogen for 15 min. Then the reaction mixture was added dropwise of a solution of triethylenetetramine tetratosylated **6** (1.45 g; 8.15 mmol) in dry DMF (20 ml). The suspension was stirred at room temperature under nitrogen for 24h and heated at 70°C for 3h.

The solvent was then evaporated under reduced pressure and the brown solid was transferred in water and extracted with CH_2Cl_2 (3 x 50 ml). The combined organic layers were dried over sodium sulfate. The solvent was evaporated under reduced pressure to obtain a crude product as brown liquid. This residue was crystallized from toluene to obtain a white solid. **Yield:** 67%

^{1}H NMR (300 MHz, $CDCl_3$): δ(ppm): 7.68 (d, 8 H, Ar), 7.33 (d, 8 H, Ar), 3.42 (s, 16 H, NCH_2), 2.44 (s, 12 H, CH_3). **^{13}C NMR** (75 MHz, $CDCl_3$): δ(ppm): 143.9, 129.8, 127.6 (Ar), 52.3 (CH_2), 21.5 (CH_3). **ESI-MS** (+) $C_{36}H_{44}N_4O_8S_4$ (788.2): m/z = 811.2 $[M+Na]^+$. **m. p.:** > 260 °C.

Synthesis of 1,4,7,10-tetraazacyclododecane 9

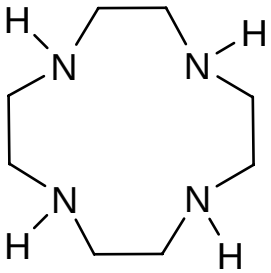

To a sample of compound **8** (2.06 g; 2.61 mmol) in a round-bottomed flask was added concentrated sulfuric acid (5.5 ml). The black coloured suspension was stirred at 130°C under nitrogen atmosphere for 36h. The solution was then cooled in an iced bath and ether (15 ml) slowly added. The resulting precipitate was filtered, washed with ethyl ether and dried at a vacuum pump. The solid was then dissolved in water (50 ml) and the solution cooled with an iced bath. A concentrated

NaOH solution was added until a precipitate started to form (impurity). This precipitate was filtered off and the filtrate was extracted with chloroform (4 x 20 ml). The combined organic layers were dried over sodium sulfate. The solvent was evaporated under reduced pressure to obtain a white solid. **Yield:** 54%

^{1}H NMR (300 MHz, $CDCl_3$): δ (ppm): 2.67 (s, 36H, NCH_2CH_2N). **^{13}C NMR** (75 MHz, $CDCl_3$): δ (ppm): 45.9. **ESI-MS** (+) $C_8H_{20}N_4$ (172.17): m/z = 174.0 [M+1]. **m. p.** 113-114 °C.

Synthesis of N,N',N''-tris(butoxycarbonylmethyl)-1,4,7,10-tetraazacyclododecane 10

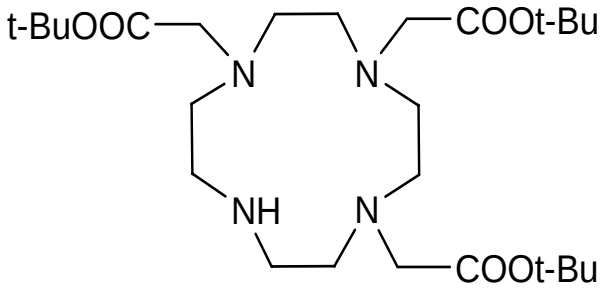

In a two-necked flask, to a solution of compound **9** (40.6 mg, 0.23 mmol) in dry CH_3CN (2.3 ml) was added under nitrogen atmosphere sodium hydrogen carbonate (65 mg, 0.77 mmol). This suspension was cooled to 0°C with an iced bath and tert-butylbromoacetate (0.126 ml, 0.77 mmol) added dropwise. The reaction mixture was stirred at room temperature for 48h and monitored by TLC (SiO_2 eluent dichloromethane/methanol, 92:2). The inorganic salts were filtered off and the solvent evaporated under reduced pressure to obtain a crude yellow product. This solid was crystallized by toluene to obtain the product as a white solid. **Yield:** 62%

^{1}H NMR (300 MHz, $CDCl_3$): δ (ppm): 10.0 (s, 1H, NH), 3.36 (s, 4H, CH_2COO), 3.28 (s, 2H, CH_2COO), 3.09- 2.87 (m, 16 H, NCH_2), 1.46, 1.45, 1.44 (3s, 27 H, $C(CH_3)_3$). **^{13}C NMR** (300 MHz, $CDCl_3$):δ (ppm): 170.4 and 169.5 (CO), 81.6 and 81.56 ($C(CH_3)_3$), 58.1 (NCH_2CO), 51.2, 51.1, 49.1 and 47.4 (NCH_2CH_2N), 28.1 ($C(CH_3)_3$). **ESI-MS** (+) $C_{26}H_{50}N_4O_6$ (514.37): m/z = 515.3 [M+1]. **m. p.** 187.8-190 °C.

Synthesis of N-(ethoxycarbonylmethyl)-N',N'',N'''-tris(butoxycarbonylmethyl)-1,4,7,10-tetraazacyclododecane 11

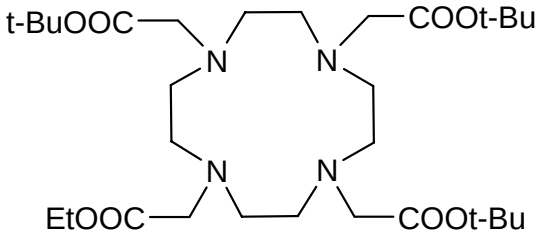

In a two-necked flask under nitrogen atmosphere, a solution of compound **10** (0.38 mg; 0.75 mmol) in dry CH_3CN (20 ml) was added of potassium carbonate (96.8 mg; 0.7 mmol) and ethyl bromoacetate (0.075 ml). The reaction mixture was stirred at room temperature for 72h and monitored by TLC (SiO_2, eluent dichloromethane/methanol 94:6). After completion of the reaction, the solid phase was filtered off and the filtrate evaporated under reduced pressure to obtain a white product after trituration with ethyl ether.

Yield: 92%. **^{1}H NMR** (300 MHz, $CDCl_3$): δ (ppm): 4.14 (bq, 2H, $COOCH_2$), 3.60-2.10 (bs, 24H, NCH_2CO and NCH_2CH_2N), 1.45, 1.44 (s, 27H, $C(CH_3)_3$), 1.26 (t, J = 7.2 Hz, 3H, $COOCH_2CH_3$).

^{13}C NMR (75 MHz, $CDCl_3$):δ (ppm): 173.4, 172.8, 172.7 (CO), 82.0 ($C(CH_3)_3$), 61.2 ($COCH_2CH_3$), 55.5 54.6 (NCH_2CO), 52.4 48.6 (NCH_2CH_2N), 27.7 ($C(CH_3)_3$), 13.9 ($COCH_2CH_3$).

ESI-MS (+) $C_{30}H_{56}N_4O_8$ (600.41): m/z = 623.4 $[M+Na]^+$. **m. p.** : 170-172 °C.

Synthesis of N-[(2-amino-ethylamino)carbonylmethyl]-,N',N'',N'''-tris(buthoxycarbonylmethyl)-1,4,7,10-tetraazacyclododecane 12

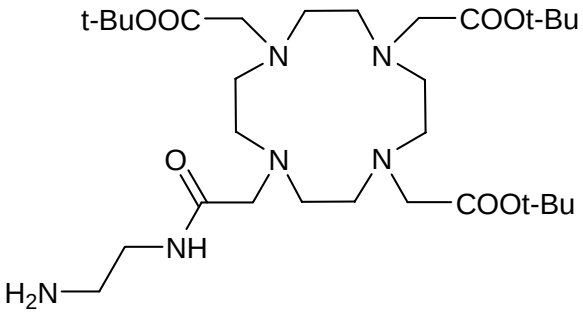

Compound **11** (0.4 g; 0.6 mmol) in neat ethylendiamine (3.5 ml) were stirred in a round-bottomed flask at room temperature for 72 h. Unreacted ethylendiamine was eliminated under reduced pressure to obtain a yellow oil. **Yield:** 79%

^{1}H NMR (300 MHz, $CDCl_3$): δ (ppm): 8.76 (t,1H, NH), 3.36 (q, 2H, NCH_2CH_2NCO), 2.90 (t, 2H, NCH_2CH_2NCO), 3.46- 2.16 (m, 30H, NCH_2), 1.45 (s, 27H, $C(CH_3)_3$).
^{13}C NMR (75 MHz, $CDCl_3$): δ (ppm): 172.3 172.2 (CO), 81.7, 81.6 ($C(CH_3)_3$), 55.9, 55.5, 55.4 (NCH_2CO), 51.3, 48.5 (NCH_2CH_2N), 40.1 and 36.6 ($NHCH_2CH_2NH_2$), 27.9 ($C(CH_3)_3$). **ESI-MS** (+) $C_{30}H_{58}N_6O_7$ (614.44): m/z = 637.5 $[M+Na]^+$.

Synthesis of tetranitrocalix[4]arene-DOTA-tri-tert-butyl ester 13

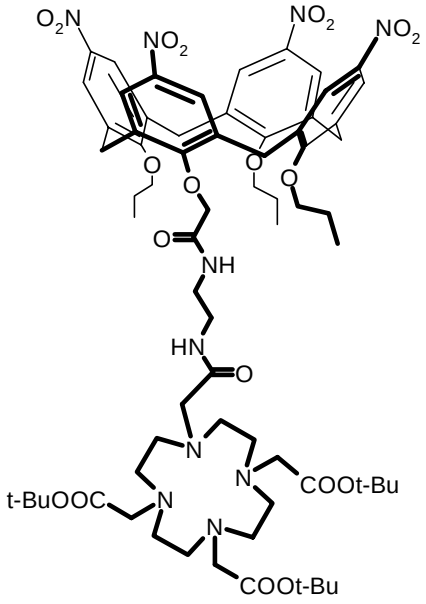

To a stirring solution of compound **12** (72.9 mg; 0.115 mmol) and **5** (100 mg; 0.127 mmol) and DCM (8 ml) in a two-necked flask under nitrogen atmosphere, was added HOBt (17.4 mg; 0.128 mmol) and a solution of DCC (26.5 mg; 0.13 mmol) in DCM (2 ml). The reaction mixture was stirred at 0°C for 15 min and then allowed to return to room temperature and stirred for 24h. The reaction was monitored by TLC (SiO_2, eluent dichloromethane/methanol 96:4). The salts were filtered off and the filtrate evaporated under reduced pressure. The residue was taken with ethyl acetate and washed with brine and a saturated solution of potassium hydrogen carbonate. The solvent was evaporated under reduced pressure to obtain a crude product as orange solid. Compound **13** was obtained pure by flash-chromatography (SiO_2, eluent dichloromethane/methanol 96:4) tas an orange solid. **Yield:** 62%
^{1}H NMR (300 MHz, $CDCl_3$): δ (ppm): 8.85 and 8.80 (2 bs, 1 H of each NH), 7.80 (d, 2H, J = 2.7 Hz, Ar), 7.76 (d, 2H, J = 2.7 Hz, Ar), 7.36 (s, 2H, Ar), 7.29 (s, 2H, Ar), 4.87 (d, 2H, J = 14.4 Hz, $ArCH_{2ax}Ar$), 4.84 (s, 2H, OCH_2CO), 4.54 (d, 2H, J = 14.1 Hz, $ArCH_{2ax}Ar$), 4.20-4.10 (m, 2H, $OCHHCH_2CH_3$), 4.05-3.95 (m, 2H, $OCHHCH_2CH_3$), 3.88 (t, 2H, J = 7.2 Hz, $OCH_2CH_2CH_3$), 3.53

(d, 2H, *J* = 14.4 Hz, ArCH_{2eq}Ar), 3.35 (d, 2H, *J* = 14.1 Hz, ArCH_{2eq}Ar), 3.30 and 3.00-2.00 (bs, 26H, NHCH_2CH_2NH, NCH_2CH_2N, NCH_2CO), 2.00-1.85 (m, 6H, $OCH_2CH_2CH_3$), 1.45 (s, 9H, $C(CH_3)_3$), 1.40 (s, 18H, $C(CH_3)_3$), 1.04 (t, 3H, *J* = 7.5 Hz, $OCH_2CH_2CH_3$), 0.95 (t, 6H, *J* = 7.5 Hz, $OCH_2CH_2CH_3$). **^{13}C NMR** (75 MHz, $CDCl_3$): δ (ppm): 172.3, 171.5, 168.1 (CO), 162.5, 161.2, 161.1 (Ar ipso), 142.7, 142.6, 142.5 (Ar para), 136.4, 135.8, 135.4, 135.0 (Ar ortho), 124.6, 124.0, 123.5, 123.3 (Ar meta), 81.9, 81.8, ($C(CH_3)_3$), 77.8, 77.7, 73.8 ($OCH_2CH_2CH_3$), 56.0, 55.6, 55.5, (NCH_2CO), 52.2, 51.5, 48.7, 47.9 (NCH_2CH_2N), 39.1, 38.9 ($NHCH_2CH_2NH$), 31.8, 31.1 ($ArCH_2Ar$), 29.6, 27.9, 27.8 ($C(CH_3)_3$), 23.2, 23.1 ($OCH_2CH_2CH_3$), 10.3, 9.9 ($OCH_2CH_2CH_3$). **ESI-MS** (+) $C_{69}H_{95}N_{10}O_{20}$ (1383.67): m/z = 1407.6 $[M+Na]^+$. **m. p.** 186.5-189 °C.

Synthesis of 2,3,4,6-tetra-O-acetyl-α-D-galactopyranosyl-bromide

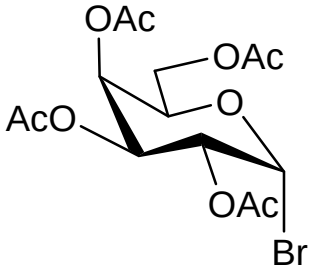

To a solution of peracetylated D-galactose (1.62 g; 3.94 mmol) in dry DCM (16 ml) was added an HBr solution in glacial acetic acid (33% w/v, 11 ml). The yellow solution was stirred at room temperature for 18h. The solvent was evaporated under reduced pressure, to obtain a crude product as brown oil which was purified by TLC (SiO_2, eluent: cycloexane/ ethyl acetate 1:1), to give a white foam. **Yield:** 97%.

^{1}H NMR (300 MHz, $CDCl_3$): δ (ppm): 6.69 (d, 1H, J = 1.2 = 3.6 Hz, H-1), 5.51 (dd, 1H, J = 4.3 = 3.6 Hz, J = 4.5 = 1.1 Hz, H-4), 5.40 (dd, 1H, J = 2.3 = 10.6 Hz, J = 2.1 = 3.6 Hz, H-2), 5.04 (dd, 1H, J = 3.2 = 10.6, Hz, J = 3.4 = 3.6 Hz, H-3), 4.51-4.46 (m, 1H, H-5), 4.18 (dd, 1H, J6,6 = 11.4 Hz, J6,5 = 6.4 Hz, H-6), 4.10 (dd, 1H, J = 6.6 = 11.4 Hz, J = 6.5 = 6.7 Hz, H-6'), 2.14, 2.10, 2.05, 2.00 (4s, 3H, of each CH_3CO). **^{13}C NMR** (75 MHz, $CDCl_3$): δ (ppm): 170.1, 169.9, 169.7, 169.6 (4s, CO), 88.1 (d, C-1), 71.0 (d, C-5), 67.9 (d, C-3), 67.7 (d, C-2), 66.9 (d, C-4), 60.1 (t, C-6), 20.6, 20.5, 20.4 (3q, CH_3CO). **m. p.** 84-85°C. **$[\alpha]_D$** = + 266.8 (c = 0.5, $CHCl_3$).

Synthesis of 2,3,4,6-tetra-O-acetyl-β-D-galactopyranosylazide

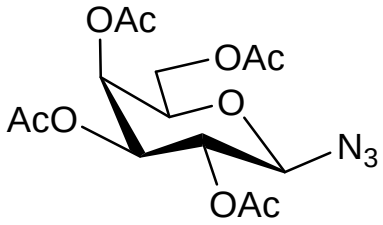

To a solution of 2,3,4,6-tetra-O-acetyl-α-D-galactopyranosyl-bromide (793 mg, 1.93 mmol) in DCM (15 ml) was added sodium azide (376 mg; 5.79 mmol), TBAHS (655 mg; 1.93 mmol) and a saturated solution of sodium hydrogen carbonate (15 ml). This suspension was stirred at room temperature for 5h monitoring it by TLC (SiO_2, eluent: toluene/ethyl acetate 2:1). The reaction was diluted with dichloromethane, the organic phase was extracted and washed several times with a $NaHCO_3$ aqueous solution, water, brine and dried over sodium sulfate. The solvent was evaporated under reduced pressure to obtain a pure white solid. **Yield:** 96%.

^{1}H NMR (300 MHz,$CDCl_3$):δ(ppm): 5.33 (dd, 1H, $J_{4,3}$=3.2 Hz, $J_{4,5}$=0.7 Hz, H_4); 5.07 (dd, 1H, $J_{2,3}$= 10.3 Hz, $J_{2,1}$= 8.5 Hz, H_2); 4.97 (dd, 1H, $J_{3,2}$= 10.3 Hz, $J_{3,4}$= 3.2 Hz, H_3); 4.55 (d, 1H, $J_{1,2}$=8.5 Hz, H_1); 4.09-4.07 (m, 2H, H_6, $H_{6'}$); 3.96 (ddd, 1H, $J_{5,6'}$= 7.1 Hz, $J_{5,4}$= 0.6 Hz, H_5); 2.07, 1.99, 1.96, 1.90 (4s, 3H of each CH_3CO). **^{13}C NMR** (75 MHZ,$CDCl_3$): δ(ppm): 170.3-169.3 (4s,CO); 88.2 (d,C_1); 72.8 (d, C_5) 70.7 (d, C_3); 68.0 (d, C_2); 66.8 (d, C_4); 61.2 (t, C_6); 20.7, 20.6, 20.5 (q,CH_3CO). **m. p.**: 103-104 °C**. $[\alpha]_D$** = -14.0 (c=1, $CHCl_3$).

Synthesis of 2,3,4,6-tetra-O-acetyl-β-D-galactopyranosylamine

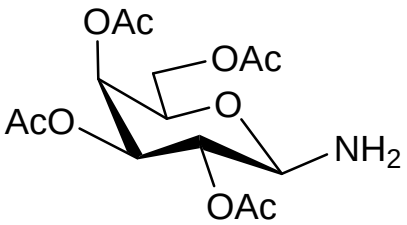

To a solution of 2,3,4,6-tetra-O-acetyl-β-D-galactopyranosylazide (706 mg; 1,89 mmol) in acetonitrile (100 ml) was added a catalytic amount of Palladium hydroxide on carbon. The suspension was hydrogenated in a Parr apparatus under pressure (2 atm) for 6h. The reaction was monitored by TLC (SiO_2, eluent: toluene/ethyl acetate 6:4). After disappearance of the starting

material, the reaction was quenched, palladium filtered off and the solvent evaporated under reduced pressure to obtain a yellow solid. **Yield:** 74%.

^{1}H NMR (300 MHz,$CDCl_3$): δ(ppm): 5.37 (dd, 1H, $J_{4,3}$=3.0 Hz, $J_{4,5}$= 1.2 Hz, H_4); 5.01 (dd, 1H, $J_{3,2}$= 10.0 Hz, $J_{3,4}$= 3.3 Hz, H_3); 4.96 (dd, 1H, $J_{2,3}$= 10.0 Hz, $J_{2,1}$= 7.8 Hz, H_2); 4.11 (d, 1H, $J_{1,2}$= 7.8 Hz, H_1); 4.08-4.01 (m, 2H, H_6, $H_{6'}$); 3.85 (ddd, 1H, $J_{5,6'}$= 6.8 Hz, $J_{5,6}$= 6.5Hz, $J_{5,4}$= 1.2 Hz, H_5); 2.09, 2.02, 1.99, 1.95 (4s, 3H each, CH_3CO). **^{13}C NMR** (75 MHZ,$CDCl_3$): δ(ppm): 170.5, 170.3, 170.2 (3s, CO); 85.4 (d, C_1); 71.6 (d, C_5); 71.4 (d, C_3); 69.9 (d, C_2); 67.7 (d, C_4), 61.8 (t, C_6); 21.0, 20.8, 20.7 (q, CH_3CO). **p.m.**: 73-75°C **$[\alpha]_D$** = +39.3 (c=0.6, $CHCl_3$)**.**

Synthesis of 2,3,4,6-tetra-O-acetyl-β-D-galactosyl-isothiocyanate

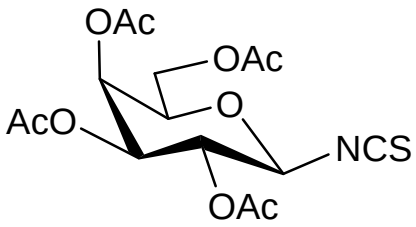

To a solution of 2,3,4,6-tetra-O-acetyl-β-D-galactopyranosylamine (608 mg; 1.75 mmol) in $CHCl_3$ (13 ml) were added water (5.5 ml), calcium carbonate (525 mg; 5.25 mmol) and thiophosgene (302.5 mg; 2.63 mmol). The reaction mixture was stirred at room temperature for 6h and followed by TLC (SiO2: eluent: toluene/ethyl acetate 6:4). Calcium carbonate was filtered off and the dichloromethane added. The organic phase was washed with water (4 x 20 ml), dried over sodium sulfate and the solvent evaporated under reduced pressure to obtain a yellow syrup . **Yield:** 90%.

^{1}H NMR (300 MHz,$CDCl_3$) : δ(ppm): 5.39 (dd, 1H, $J_{4,3}$= 3.3 Hz, $J_{4,5}$= 1.1 Hz, H_4); 5.31 (dd,1 H, $J_{2,3}$= 10.2 Hz, $J_{2,1}$= 8.6 Hz, H_2); 5.01 (dd, 1H, $J_{3,2}$= 10.2 Hz, $J_{3,4}$= 3.3 Hz, H_3); 4.97 (d, 1H, $J_{1,2}$= 8.6 Hz, H_1); 4.13-4.11 (m, 2H, H_6, $H_{6'}$); 3.95 (ddd, 1H, $J_{5,6}$= 6.4 Hz, $J_{5,6'}$= 6.2 Hz, $J_{5,4}$= 1.1 Hz, H_5); 2.16, 2.12, 2.04, 1.97 (4s, 3H of each CH_3CO). **^{13}C NMR** (75 MHz,$CDCl_3$) : δ(ppm): 170.2, 169.9, 169.8, 169.0 (4s, CO); 143.7 (s, CS); 83.9 (d, C_1), 72.9 (d, C_5); 70.5 (d, C_3); 69.2 (d, C_2); 66.7 (d, C_4); 61.1 (t, C_6); 20.54, 20.48, 20.39 (3q, CH_3CO). **m.p.** : 94°C **$[\alpha]_D$** = +33.9 (c=1, CH_2Cl_2).

Synthesis of 25-(ethoxycarbonylmethoxy)calix[4]arene 16

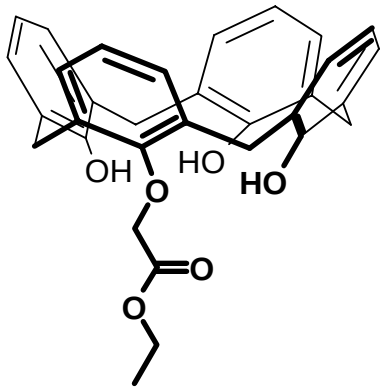

To a suspension of tetrahydroxy calix[4]arene (3.0 g; 7.06 mmol) in dry DMF (120 ml) were added under nitrogen cesium fluoride (1.29 g, 8.47 mmol) and ethyl bromoacetate (7.86 ml, 7.06 mmol). The reaction mixture was stirred at 40°C for 24h and monitored by TLC (SiO_2, eluent petroleum-ether/dichloromethane 3:1). After completion of the reaction, water (100 ml) was added and the mixture extracted with ethyl acetate (3 x 100 ml). The combined organic layers were dried over sodium sulfate and the solvent was evaporated under reduced pressure to obtain compound xx as a white solid after flash chromatography (SiO_2, eluent petroleum-ether/dichloromethane 3:1, 2:8, 1:9). **Yield:** 68.5%.

^{1}H NMR (300 MHz,$CDCl_3$) : δ(ppm): δ = 9.86 (s, 1H, OH); 9.14 (s, 2H, OH); 7.10 (d, 2H, *J* = 7.8 Hz, Ar-H); 7.10 – 6.95 (m, 6H, Ar-H); 6.89 (dd, 1H, *J* = 7.6 Hz, Ar-H); 6.66 (q, 3H, Ar-H); 4.89 (s, 2H, OCH_2CO); 4.48 (d, 2H, *J* = 9.0 Hz, $ArCH_{2ax}Ar$); 4.45 (q, 2H, *J* = 7.2 Hz, OCH_2CH_3); 4.30 (d, 2H, *J* = 13.8 Hz, $ArCH_{2ax}Ar$); 3.45 (d, 4H, *J* = 13.8 Hz, $ArCH_{2eq}Ar$); 1.43 (t, 3H, *J* = 6.9 Hz, CH_3).

^{13}C NMR, see literature data (Sasaky, A. Murahashi, N. Yamada, H. Morikawa, A. *Biol. Pharm. Bull*., **1995**, 18 (5), 740-746).

ESI-MS (+) $C_{32}H_{30}O_6$ m/z = 533.19 $[M+Na]^+$.

Synthesis of 25-(ethoxycarbonylmethoxy)-26,27,28-tripropyloxycalix[4]arene 17

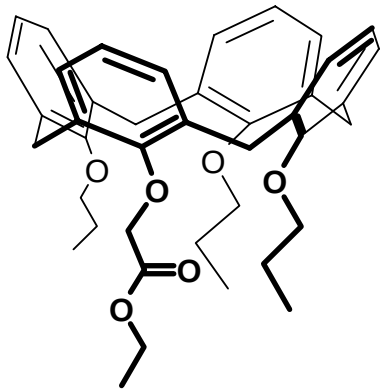

To a solution of compound **16** (2.46 g; 4.81 mmol) in dry DMF (35 ml) at 0°C, sodium hydride (0.96 g; 24 mmol) and propyl iodide (4.1 g; 24 mmol) were added under nitrogen atmosphere. The suspension was stirred at room temperature for 24h and the reaction monitored by TLC (SiO_2, eluent cycloexane/ ethyl acetate 8:2). The reaction was quenched with 0.1M HCl and extracted with ethyl acetate (3 x 100 ml). The combined organic layers were dried over sodium sulfate and the solvent was evaporated under reduced pressure to obtain compound **17** as a colourless oil after purification by cartridge Flashvach chromatography (SiO_2, eluent cycloexane/ethyl acetate 98:2). **Yield:** 89%.

^{1}H NMR (300 MHz,$CDCl_3$) : δ (ppm): 6.84 – 6.75 (m, 4H, Ar-H); 6.75 – 6.67 (m, 2H, Ar-H); 6.44 (s, 6H, Ar-H); 4.74 (s, 2H, OCH_2CO); 4.65 (d, 2H, *J* = 13.5 Hz, $ArCH_{2ax}Ar$); 4.45 (d, 2H, *J* = 13.2 Hz, $ArCH_{2ax}Ar$); 4.20 (q, 2H, *J* = 7.2 Hz, OCH_2CH_3); 3.89 (t, 2H, *J* = 7.5 Hz, $OCH_2CH_2CH_3$); 3.88 – 3.76 (m, 4H, $OCH_2CH_2CH_3$); 3.21 (d, 2H, *J* = 13.5 Hz, $ArCH_{2eq}Ar$); 3.16 (d, 2H, *J* = 13.5 Hz, $ArCH_{2eq}Ar$); 1.95-1.87 (m, 6H, $CH_2CH_2CH_3$); 1.29 (t, 3H, *J* = 7.2 Hz, CH_2CH_3); 1.03 (t, 6H, *J* = 7.5 Hz, $OCH_2CH_2CH_3$); 0.97 (t, 3H, *J* = 7.5 Hz, $OCH_2CH_2CH_3$). **^{13}C NMR (75 MHz, $CDCl_3$):** δ (ppm): 170.3 (CO); 157.2, 156.1, 156.0 (Ar ipso); 135.9, 135.6, 134.4, 134.3 (Ar meta); 128.8, 128.5, 128.8, 127.9 (Ar ortho); 122.6, 122.2, 122.1 (Ar para); 76.9 (OCH_2CH_2); 70.5 (OCH_2CO); 60.4 ($COCH_2CH_3$); 31.4, 31.0 (Ar-CH_2-Ar); 23.4 ($CH_2CH_2CH_3$); 14.3 (OCH_2CH_3); 10.7, 10.3 ($CH_2CH_2CH_3$); **ESI-MS:** (+) $C_{30}H_{38}N_6O_7$ m/z = 637.55 $[M+Na]^+$.

Synthesis of 5,11,17,23-tetraiodo-25-(ethoxycarbonylmethoxy)-26,27,28-tripropyloxy-calix[4]arene 18

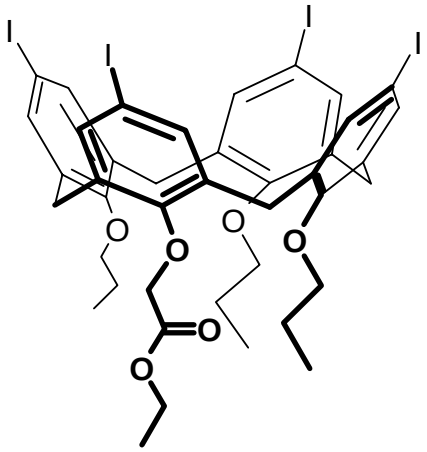

To a solution of compound **17** (200 mg, 0.31 mmol) in $CHCl_3$ (30 ml) silver acetate (305 mg, 1.38 mmol) was added. The reaction mixture was stirred at 60°C for 30 min and then iodine (351 mg, 1.38 mmol) was added and the suspension stirred at 60°C for 1h. The reaction was monitored by TLC (SiO_2, eluent cycloexane/ethyl acetate 99:1) and then quenched by filtration of the inorganic salts which were eliminated. The filtrate was washed with 20% sodium thiosulfate solution until the water colour turns to yellow. The organic phase was washed again with water (2 x 60 ml) and dried over sodium sulfate to obtain compound **18** as a yellow foam. **Yield:** 88%.

^{1}H NMR (300 MHz,$CDCl_3$) : δ(ppm): 7.20 (s, 2H, Ar-H); 7.19 (s, 2H, Ar-H); 6.43 (s, 4H, Ar-H); 4.70 (s, 2H, OCH_2CO); 4.50 (d, 2H, *J* = 13.5 Hz, $ArCH_{2ax}Ar$); 4.28 (d, 2H, *J* = 13.2 Hz, $ArCH_{2ax}Ar$); 4.17 (q, 2H, *J* = 7.2 Hz, OCH_2CH_3); 3.86 (t, 2H, *J* = 7.8 Hz, $OCH_2CH_2CH_3$); 3.82-3.67 (m, 6H, OCH_2CH_2); 3.10 (d, 2H, *J* = 14.4 Hz, $ArCH_{2eq}Ar$); 3.05 (d, 2H, *J* = 13.8 Hz, $ArCH_{2eq}Ar$); 1.95 – 1.80 (m, 6H, $CH_2CH_2CH_3$); 1.27 (t, 3H, *J* = 5.1 Hz, CH_2CH_3); 0.99 (t, 6H, *J* = 7.2 Hz, $CH_2CH_2CH_3$); 0.93 (t, 3H, J = 7.5 Hz, $CH_2CH_2CH_3$). **^{13}C NMR (75 MHz, $CDCl_3$):** δ (ppm): 169.4 (CO); 156.9, 156.0, 155.0 (Ar ipso); 140.8, 138.0, 137.4, 137.2, 137.1, 136.7, 133.4, 128.3, 123.5 (Ar); 86.2, 85.7 (Ar para); 76.5 (OCH_2CH_2); 71.1 (OCH_2CO); 60.6 ($COCH_2CH_3$); 31.7, 30.2, 29.6 ($ArCH_2Ar$); 23.1, 22.9 ($CH_2CH_2CH_3$); 14.2 (OCH_2CH_3); 10.3, 10.2 ($CH_2CH_2CH_3$). **ESI-MS:** (+) $C_{30}H_{58}N_6O_7I_4$ m/z = 1163.07 $[M+Na]^+$

Synthesis of 5,11,17,23-tetrakis[trimethylsilylacetylene]-25-(ethoxycarbonylmethoxy)-26,27,28-tripropyloxycalix[4]arene 19

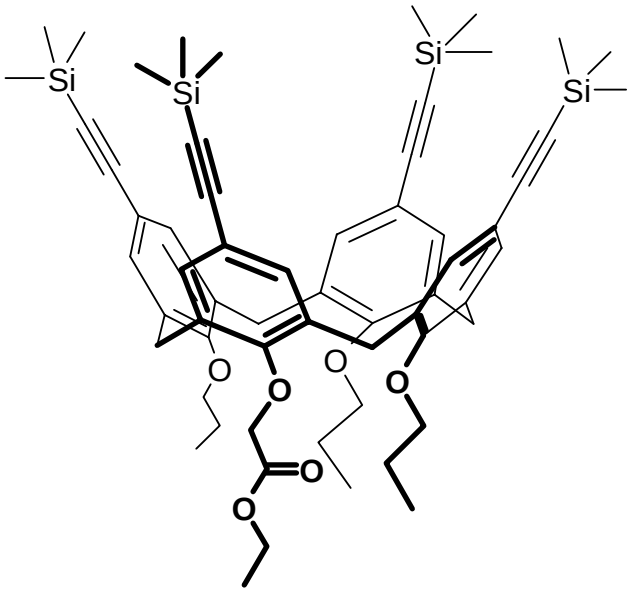

In a sealed tube under argon atmosphere, a solution of compound **18** (2.95 g, 2.6 mmol) in degassed TEA (80 ml) was added of $PdCl_2(PPh_3)_3$ (3% mol; 0.055 g, 0.078 mmol), CuI (5% mol; 0.025 g, 0.13 mmol) and trimethylsilylacetylene (1.52 g; 15.6 mmol). The solution was stirred at 80°C under argon atmosphere for 48h and monitored by TLC (SiO2; eluent petroleum ether/ethyl acetate 99:1). Then was quenched with 0.01M HCl until neutral pH. The organic phase was extracted with ethyl acetate (3 x 100 ml), washed with water until the pH is neutral, dried over sodium sulfate and the solvent evaporated under reduced pressure to obtain a brown foam. The crude product of reaction was purified by flash chromatography (SiO_2; eluent petroleum ether/ethyl acetate 96:4, 9:1) to obtain compound **19** as yellow solid. **Yield:** 56%.

^{1}H NMR (300 MHz,$CDCl_3$) : δ(ppm) = 7.08 (s, 2H, Ar-H); 7.07 (s, 2H, Ar-H); 6.80 (s, 4H, Ar-H); 4.80 (s, 2H, OCH_2CO); 4.54 (d, 2H, *J* = 13.2 Hz, $ArCH_{2ax}Ar$); 4.34 (d, 2H, *J* = 12.9 Hz, $ArCH_{2ax}Ar$); 4.15 (q, 2H, *J* = 5.4 Hz, OCH_2CH_3); 3.88 (t, 3H, *J* = 7.8 Hz, OCH_2CH_2); 3.88 – 3.68 (m, 6H, OCH_2CH_2); 3.15 (d, 2H, *J* = 14.4 Hz, $ArCH_{2eq}Ar$); 3.10 (d, 2H, *J* = 13.2 Hz, $ArCH_{2eq}Ar$); 1.94 - 1.80 (m, 6H, $CH_2CH_2CH_3$); 1.26 (t, 3H, *J* = 5.7 Hz, OCH_2CH_3); 1.04 - 0.94 (m, 9H, $CH_2CH_2CH_3$). **^{13}C NMR (75 MHz, $CDCl_3$):** δ (ppm): 157.3 (CO); 156.3 (Ar ipso); 135.5, 134.6, 133.5, 132.8, 132.6, 132.4, 132.3 (Ar); 117.2 (Ar para); 105.5, 105.3 (*C*CSi); 92.7 (C*C*Si); 77.3, 77.2 (OCH_2CH_2); 70.5 ($COCH_2O$); 60.5 (OCH_2CH_3); 31.2, 30.7 ($ArCH_2Ar$); 23.1 ($CH_2CH_2CH_3$); 14.2 (OCH_2CH_3); 10.4, 10.0 ($CH_2CH_2CH_3$); 0.2 ($Si(CH_3)_3$). **ESI-MS:** (+) $C_{61}H_{80}O_6Si_4$ m/z = 1044.20 $[M+Na]^+$.

Synthesis of 5,11,17,23-tetraacetylene-25-(ethoxycarbonylmethoxy)-26,27,28-tripropyloxycalix[4]arene 20

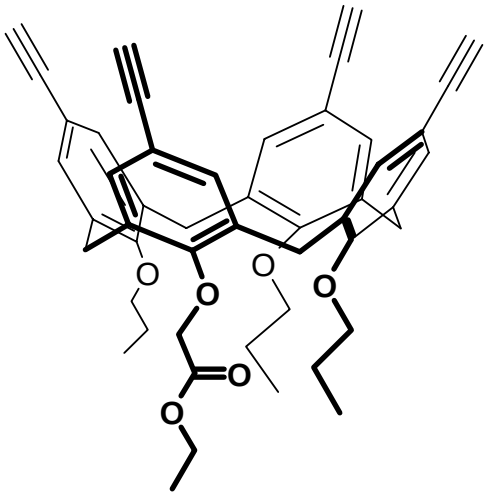

To a solution of compound **19** (0.153 g, 0.15 mmol) and dry DMF (15 ml) in a Schlenk tube under nitrogen atmosphere was added potassium fluoride (0.521 g, 8.98 mmol). The suspension was stirred at 60°C for 24h. The reaction was monitored by TLC (SiO_2; eluent cycloexane/ethyl acetate 8:2) and then quenched with 0.1M HCl (20 ml). The product was extracted with ethyl acetate (3 x 20 ml), dried over sodium sulfate and solvent evaporated under reduced pressure to obtain compound **20** as brown foam. **Yield:** 98%.

^{1}H NMR (300 MHz,$CDCl_3$) : δ(ppm): δ = 7.018, 7.013 (2s, 2H for each, Ar-H); 6.65 (s, 4H, Ar-H); 4.71 (s, 2H, OCH_2CO); 4.56 (d, 2H, *J* = 13.8 Hz, $ArCH_{2ax}Ar$); 4.37 (d, 2H, *J* = 13.5 Hz, $ArCH_{2ax}Ar$); 4.18 (q, 2H, *J* = 7.2 Hz, OCH_2CH_3); 3.88 (t, 2H, *J* = 7.5 Hz, OCH_2CH_2); 3.90 – 3.74 (m, 6H, OCH_2CH_2); 3.15 (d, 2H, *J* = 14.7 Hz, $ArCH_{2eq}Ar$); 3.10 (d, 2H, *J* = 14.1 Hz, $ArCH_{2eq}Ar$); 2.96, 2.81 (2s, 4 H, HCC); 2.00 - 1.90 (m, 6H, $CH_2CH_2CH_3$); 1.27 (t, 3H, *J* = 7.2 Hz, CH_2CH_3); 1.06-0.91 (m, 9H, $CH_2CH_2CH_3$). **^{13}C NMR (75 MHz, $CDCl_3$):** δ (ppm): δ = 172.9 (CO); 156.8 (Ar ipso); 135.0, 133.8, 132.7, 132.5, 132.0, 129.0, 128.2, 125.2 (Ar); 116.0 (Ar ortho); 83.8, 83.7 (*C*CH); 77.1, 76.1 (C*C*H); 76.0, 75.7 (OCH_2CH_2); 70.3 (OCH_2CO); 60.5 (OCH_2CH_3); 30.9, 29.6 ($ArCH_2Ar$); 23.1, 21.4 ($CH_2CH_2CH_3$); 14.1 (OCH_2CH_3); 10.0, 9.3 ($CH_2CH_2CH_3$). **ESI-MS:** (+) $C_{58}H_{72}O_6$ m/z = 755.41 $[M+Na]^+$.

Synthesis of 5,11,17,23-tetracetylene-25-(hydroxycarbonylmethoxy)-26,27,28-tripropyloxycalix[4]arene 21

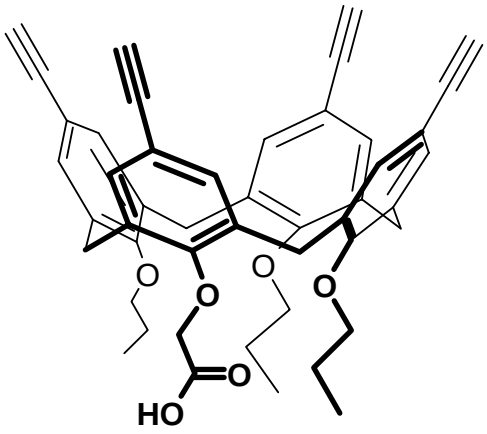

To a solution of compound **20** in THF/H_2O (25 ml 5:1 v/v) was added a solution of potassium hydroxide (0.308 g, 0.61 mmol) in THF/H_2O (10 ml 5:1 v/v). The reaction mixture was stirred at reflux for 12 h and the reaction monitored by TLC (SiO_2; eluent cycloexane/ethyl acetate 8:2), then quenched with 1M HCl until the pH 3. The product was extracted with dichloromethane (3 x 30 ml), the organic layer washed with water and dried over sodium sulfate. The solvent was evaporated under reduced pressure to obtain compound **21** as a brown foam. **Yield:** 80%.

^{1}H NMR (300 MHz,$CDCl_3$): δ(ppm): 7.32 (s, 4H, Ar); 6.55 (d, 2H, *J* = 1.8 Hz, Ar); 6.50 (d, 2H, *J* = 1.8 Hz, Ar); 4.83 (s, 2H, OCH_2CO); 4.38 (d, 2H, *J* = 13.2 Hz, $ArCH_{2ax}Ar$); 4.24 (d, 2H, *J* = 13.8 Hz, $ArCH_{2ax}Ar$); 4.05 – 3.95 (m, 2H, OCH_2CH_2); 3.77-3.15 (m, 6H, OCH_2CH_2); 3.27 (d, 2H, *J* = 13.8 Hz, $ArCH_{2eq}Ar$); 3.15 (d, 2H, *J* = 12.8 Hz, $ArCH_{2eq}Ar$); 3.10, 2.77 (2s, 4 H, HCC) 2.00 – 1.75 (m, 6H, $CH_2CH_2CH_3$); 1.00 (t, 6H, *J* = 7.2 Hz, CH_2CH_3); 0.85 (t, 3H, *J* = 7.5 Hz, CH_2CH_3). **^{13}C NMR (75 MHz, $CDCl_3$): δ (ppm):** 170.1 (CO); 157.6, 156.6, 154.0 (Ar ipso); 136.2, 134.7, 133.5, 133.2, 132.9, 132.4, 132.0, 131.9 (Ar); 118.8, 117.4, 116.6 (Ar para); 83.8, 83.0 (*C*CH); 78.5, 77.2 (C*C*H); 76.3 (OCH_2CH_2); 71.4 (OCH_2CO); 30.9, 30.2 ($ArCH_2Ar$); 22.9, 22.6 ($CH_2CH_2CH_3$); 10.3, 9.7 ($CH_2CH_2CH_3$). **ESI-MS:** (+) $C_{58}H_{72}O_6$ m/z = 755.41 $[M+Na]^+$

Synthesis of tetra-O-acetyl-1-β-(2-bromoethyloxy)-galactose 22

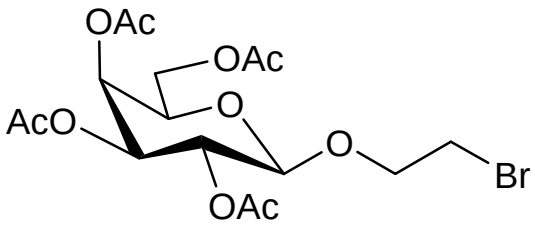

To a solution of peracetylated D-galactose (2.5 g, 6.40 mmol) and dry DCM (25 ml) in a two-necked flask under nitrogen atmosphere, was added at 0° C 2-bromoethanol (8.7 mmol, 0.625 ml) and boron trifluoride (25.6 mmol, 3.2 ml). The solution was stirred at room temperature overnight. The reaction was monitored by TLC (SiO2, eluent toluen/ethyl acetate 7:3) and quenched with water (20 ml) and an aqueous solution of sodium chloride. The organic phase was separated, washed with water until neutral pH and dried over sodium sulfate. The solvent was evaporated under reduced pressure to obtain pure compound **22** as a yellow syrup. **Yield:** 99%.

^{1}H NMR (300 MHz,$CDCl_3$) : δ(ppm): δ = 5.38 (dd, 1H, *J* = 3.2 Hz, *J* = 0.9 Hz, H_4); 5.23 (dd, 1H, *J* =10.5 Hz, *J* = 7.8 Hz, H_2); 5.01 (dd, 1H, *J* = 10.5 Hz, *J* = 3.3, H_3); 4.51 (d, 1H, *J* = 7.8 Hz, H_1); 4.21 – 4.06 (m, 3H, H_{6ab} and OCH*H*CH_2); 3.91 (td, 1H, *J* = 6.6, *J* = 0.9 Hz, H5); 3.88 – 3.76 (m, 1H, OC*H*HCH_2); 3.55 – 3.44 (m, 2H, CH_2Br); 2.14, 2.07, 2.04, 1.99 (4s, 12 H, CH_3CO_2).

ESI-MS: (+)$C_{16}H_{23}O_{10}Br$ m/z = 479.13 $[M+2Na]^+$, 477.13 $[M+Na]^+$

For other physico-chemical data see: Sasaky, A. Murahashi, N. Yamada, H. Morikawa, A. *Biol. Pharm. Bull.*, **1995**, 18 (5), 740-746).

Synthesis of tetra-O-acetyl-1-β-(2-azidoethyloxy)-galactose 23

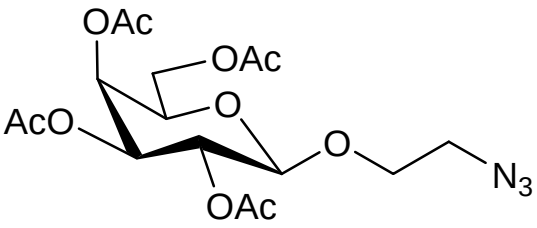

To a solution of compound **22** (2.94 g, 6.46 mmol) and dry DMF (40 ml) in a two-necked flask, was added sodium azide (0.855 g, 13.5 mmol) under nitrogen atmosphere. The suspension was stirred at 60°C for 24h. The reaction was monitored by TLC (SiO2, eluent toluene/ethyl acetate 7:3) was and then quenched with water (50 ml). The product was extracted with ethyl acetate (3 x 30 ml), the combined organic layers dried over sodium sulfate and the solvent evaporated under reduced pressure to obtain compound **23** as yellow oil. **Yield:** 90%.

^{1}H NMR (300 MHz, $CDCl_3$) : δ(ppm): 5.39 (dd, 1H, *J*= 3.3 Hz, *J* = 0.9 Hz, H_4); 5.24 (dd, 1H, *J* = 10.5 Hz, *J* = 7.8 Hz, H_2); 5.01 (dd, 1H, *J* = 10.5 Hz, *J* = 3.3, H_3); 4.55 (d, 1H, *J* = 8.4 Hz, H_1); 4.25 – 3.98 (m, 3H, H_{6ab} and OCH*H*CH_2); 3.91 (td, 1H, *J* = 6.6 Hz, *J* = 0.9 Hz, H_5); 3.72 – 3.64 (m, 1H, OC*H*HCH_2); 3.55 – 3.44 (m, 1H, CH*H*Br); 2.14, 2.07, 2.04, 1.97 (4s, 12 H, CH_3CO_2).

For other physico-chemical data see: Sasaky, A. Murahashi, N. Yamada, H. Morikawa, A. *Biol. Pharm. Bull*., **1995**, 18 (5), 740-746).

Synthesis of compound 24

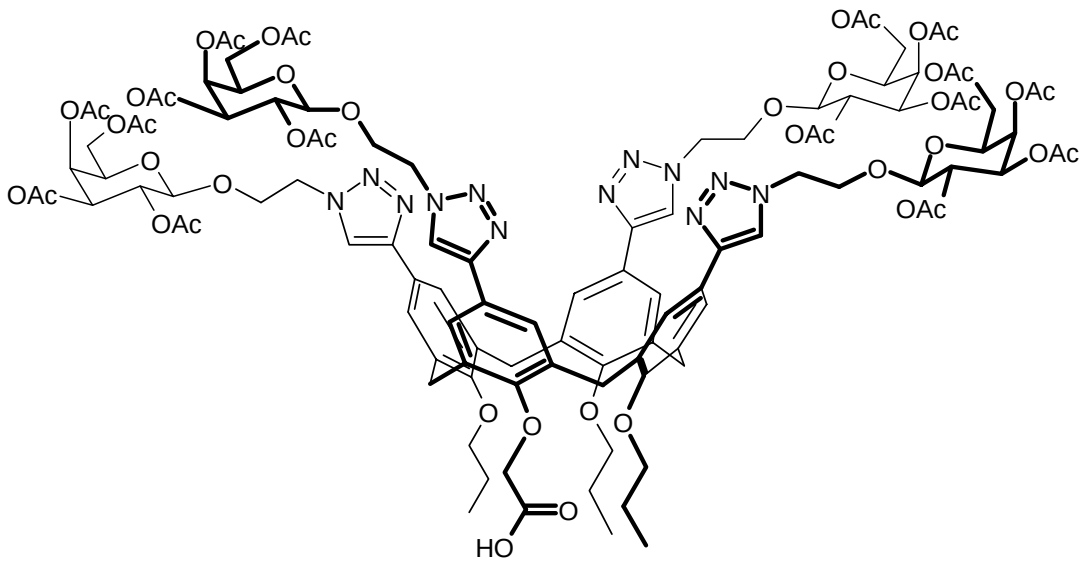

To a mixture of compound **21** calix (77.3 mg, 0.11 mmol) and compound **23** azide (100.6 mg, 0.24 mmol) in THF/H_2O (4 ml 2:1) copper sulfate (5% mol) and sodium ascorbate (50% mol) were added. The reaction mixture was sonicated in an ultrasound cleaning bath for two minutes, then magnetically stirred in the dark at room temperature for 72h. The reaction was monitored by TLC (SiO_2, eluent DCM/MeOH, 94:6). The reaction was quenched with water (10 ml), the product extracted with ethyl acetate (3 x 15 ml) and the organic layers washed with 1M phosphate buffer at pH 7 (2 x 10 ml), dried over sodium sulfate and concentrated under vacuum. The residue was triturateed with ethyl ether to obtain a compound **24** as white solid (to eliminate **Yield:** 34% not pure)

Selected physico-chemical data

^{1}H NMR (300 MHz,$CDCl_3$) : δ(ppm): 11.70 (bs, 1H, COOH); 7.91 (d, 2H, *J* = 7.8 Hz, NCHC); 7.81 (d, 2H, *J* = 10.8 Hz, NCHC); 3.45 (d, 2H, *J* = 13.8 Hz, $ArCH_{2eq}Ar$); 3.33 (d, 2H, *J* = 13.2 Hz, $ArCH_{2eq}Ar$); 2.14, 2.05, 2.00, 1.96 (4s, 48 H, $COCH_3$); 1.03, 0.87 (2m, 12 H, $CH_2CH_2C\mathit{H}_3$).

ESI-MS: (+) $C_{111}H_{136}O_{46}N_{12}$ m/z = 1209.91 $[M+2Na]^{2+}$

Synthesis of 25,26,27,28-tetrakis(ethoxycarbonylmethoxy)-5,11,17,23-tetra-tert-butyl calix[4]arene 25

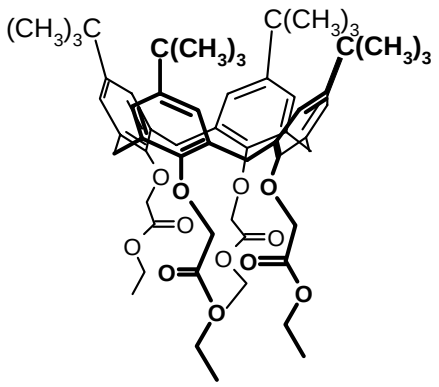

To a solution of para-tert-butyl-calix[4]arene (5 g, 7.7 mmol) and dry THF (100 ml) in a three-necked flask was added NaH at 55% (5.39 g, 123 mmol) under nitrogen atmosphere. The solution was stirred at room temperature for 20 minutes. Ethyl bromoacetate (7.13 ml, 61.6 mmol) was then added and the reaction mixture stirred at 70° C for two hours. The reaction was monitored by TLC (SiO_2, eluent: DCM/hexane 1:1). The reaction was quenched with 1N HCl (100 ml) and the separated organic phase was washed with water until neutral pH. The solvent was evaporated under reduced pressure to obtain compound **25** as beige solid. **Yield** 87 %.

^{1}H-NMR (300 MHz, $CDCl_3$): δ (ppm) = 6.77 (s, 8H, Ar); 4.85 (d, J= 12 Hz, 4H, Ar-C*H*$_2$-Ar ax); 4.8 (s, 8H, Ar-OCH_2); 4.2 (q, J= 6 Hz, 8H, OCH_2); 3.18 (d, J=12 Hz, 4H, Ar-C*H*$_2$-Ar eq); 1.28 (m, 12H, CH_3); 1.07(s, 36H, CH_3 del *t*-Bu).

For other physico-chemical data see: Iwamoto, K. Shinkai, S. *J. Org. Chem.* **1992**, 57, 7066-7073.

Synthesis of 25,26,27,28-tetrakis(ethoxycarbonylmethoxy)-5,11,17,23-tetranitrocalix[4]arene 26

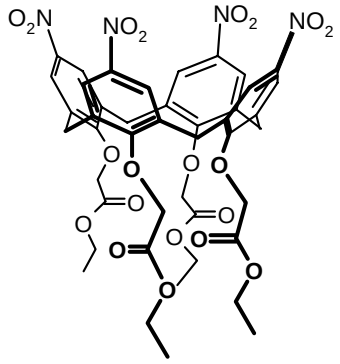

To a cooled (0°C) solution of compound **25** (3 g, 3.02 mmol) and DCM (30 ml) in a round-bottomed flask, were added acetic acid (100 ml) and concentrated HNO_3 (19 ml, 301 mmol). The solution was stirred at room temperature for 5 h and monitored by TLC (SiO_2, eluent: ethyl acetate/hexane 6:4). Then it was quenched with water (100 ml) and the product extracted in the organic phase with DCM (2 x 50 ml) and then washed with water until neutral pH. The solvent was evaporated under reduced pressure to obtain a brown solid. **Yield** 45%.

^{1}H-NMR (300 MHz, $CDCl_3$): δ (ppm) = 7.62 (s, 8H, Ar); 5.05 (d, J=15 Hz, 4H, Ar-C*H*$_2$-Ar ax); 4,77 (s, 8H, Ar-OC*H*$_2$); 4.24 (q, J = 6 Hz, 8H, OCH_2); 3.52 (d, J=15 Hz, 4H, Ar-C*H*$_2$-Ar eq); 1.31 (t, J=3 Hz, 12H, CH_3). **ESI-MS**: (+) $C_{44}H_{44}N_4O_{20}$ m/z= 971.39 $[M+Na]^+$.

For other physico-chemical data see: Verboom, W. Durie, A. Egberink, R. J. M. Asfari, Z. Reinhoudt, D. N. *J. Org. Chem.* **1992,** 57, 1313-1316.

Synthesis of 25,26,27,28-tetrakis(ethoxycarbonylmethoxy)-5,11,17,23-tetraaminocalix[4]arene

27

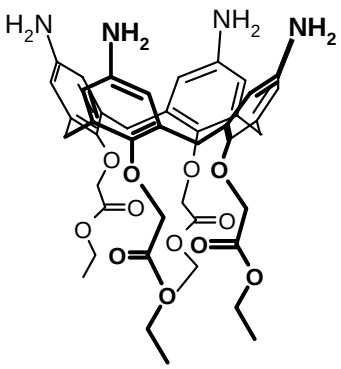

In a two necked round bottomed flask, under nitrogen atmosphere, compound **26** (1.29 g, 1.34 mmol) was dissolved in methanol (64.68 ml). Then Co(II) chloride hexahydrate (2.14 g, 9 mmol) and $NaBH_4$ (1.68 g, 44.4 mmol) were added in small aliquots. The suspension was stirred at room temperature overnight. The reaction was monitored by TLC (SiO_2, eluent: ethyl acetate/methanol 9:1). After disappearance of the starting material, the reaction was quenched by addition of dichloromethane (20 ml). The organic phase was separated and washed with 1N HCl (30 ml) and NH_4OH (28%, 40 ml) until pH 10. The solvent was evaporated under reduced pressure to obtain **27** as brown solid. **Yield** 55%.

^{1}H-NMR (300 MHz, $CDCl_3$ drops of CD_3OD):

δ (ppm)= 5.95 (bs, 8H, Ar); 4.57-4,54 (bs, 12H, Ar-C*H*$_2$-Ar Ax and Ar-OCH_2); 4.14-4.12 (bs, 8H, CH_2); 2.94 (bs, 4H, Ar-C*H*$_2$-Ar eq); 1.21 (bs, 12H, CH_3).

Synthesis of 25,26,27,28-tetrakis(ethoxycarbonylmethoxy)-5,11,17,23-tetrakis(N-2-chloroacetamide)calix[4]arene 28

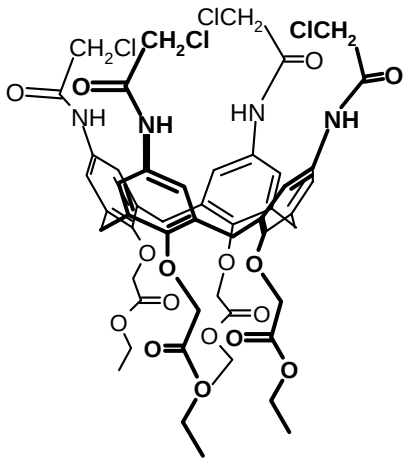

To a solution of **27** (0.71 g, 0.74 mmol) and diisopropylamine (DIPEA, 1.3 ml, 7.37 mmol) in dry dichloromethane (35 ml), was added 2-chloro-acetyl chloride (0.59 ml, 7.37 mmol) under nitrogen atmosphere. The solution was stirred at room temperature for 1 h. The reaction was monitored by TLC (SiO_2, eluent: THF/DCM 7:3) and then quenched with 0.5 M HCl (15 ml). The reaction was diluted with DCM (20 ml) and washed with water (4 x 10 ml) until neutral pH. The solvent was evaporated under reduced pressure to obtain product **28** as dark solid after preparative layer chromatography (SiO_2, eluent: THF/DCM 1:1). **Yield** 95%.

^{1}H-NMR (300 MHz, $CDCl_3$ drops of CD_3OD): δ (ppm) = 6.71 (s, 8H, Ar); 4.63 (d, J=15 Hz, 4H, Ar-C*H*$_2$-Ar ax); 4.51 (s, 8H, Ar-OC*H*$_2$); 3.98 (q, J = 6 Hz, 8H, OCH_2); 3.82 (s, 8H, CH_2Cl); 3.01 (d, J=15 Hz, 4H, Ar-C*H*$_2$-Ar eq); 1.07 (t, J = 6 Hz, 12H, CH_3).

^{13}C-NMR (300 MHz, $CDCl_3$ drops of CD_3OD): δ (ppm) = 169.8 (*C*OOEt), 167.8 (*C*OCH_2Cl); 152.8 (Ar-ipso); 134.6 (Ar-para); 131.7 (Ar-ortho); 121.1 (Ar-meta); 71.2 (Ar-O*C*H$_2$); 60.6 (OCH_2CH_3); 42.8 (CO*C*H$_2$Cl); 31.4 (Ar-*C*H$_2$-Ar); 14.0 (CH_2CH_3).

m. p. = 96-99°C

Synthesis of 25,26,27,28-tetrakis(ethoxycarbonylmethoxy)-5,11,17,23-tetrakis(N-2-azidoacetamide)calix[4]arene 29

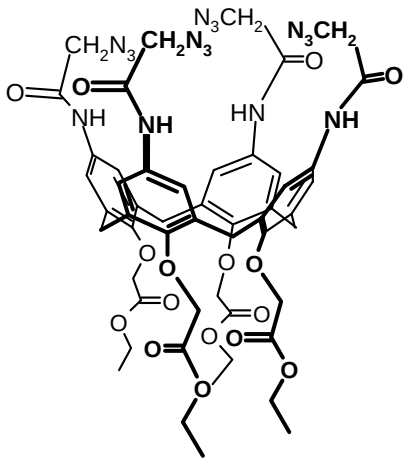

To a solution of compound **28** (1.16 g, 1.03 mmol) in DCM (30 ml) were added tetrabutyl ammonium hydrogen sulfate (TBAHS, 1.39 g, 4.10 mmol), sodium azide (2.67 g, 41 mmol) and a saturated aqueous $NaHCO_3$ solution (30 ml). The suspension was stirred at room temperature for 2 days. The reaction was monitored by ESI-MS analysis and quenched with water (15 ml). The organic phase was separated and washed with a saturated $NaHCO_3$ solution (3 x 10 ml), HCl 1M (4 x 15 ml) and again water until neutral pH. The solvent was evaporated under reduced pressure to obtain a beige solid compound **29** after crystallization by ethanol. **Yield** 52%.

^{1}H-NMR (300 MHz, $CDCl_3$): δ (ppm) = 6.84 (s, 8H, Ar); 4.87 (d, J = 12 Hz, 4H, Ar-C*H*$_2$-Ar ax); 4.71 (s, 8H, Ar-OCH_2); 4.19 (q, J = 9 Hz, 8H, OCH_2); 4.04 (s, 8H, CH_2N_3); 3.27 (d, J = 12 Hz, 4H, Ar-C*H*$_2$Ar eq); 1.23 (t, J = 9 Hz, 12H, CH_3). **^{13}C-NMR** (300 MHz, $CDCl_3$): δ (ppm)= 169.8 (*C*OOEt); 164.8 (*C*OCH_2N_3); 153.1 (Ar-ipso); 134.8 (Ar-para), 131.4 (Ar-ortho); 121.5 (Ar-meta); 71.3 (Ar-O*C*H_2CO); 60.5 (OCH_2); 52.7 (CH_2N_3); 31.5 (Ar-*C*H_2-Ar); 14.1 (CH_2*C*H_3). **ESI-MS**: (+) $C_{52}H_{56}N_{16}O_{16}$ m/z = 1183.66 $[M+Na]^+$, 1200.07 $[M+K]^+$. **m. p.** = 144-147 °C

Synthesis of compound 30

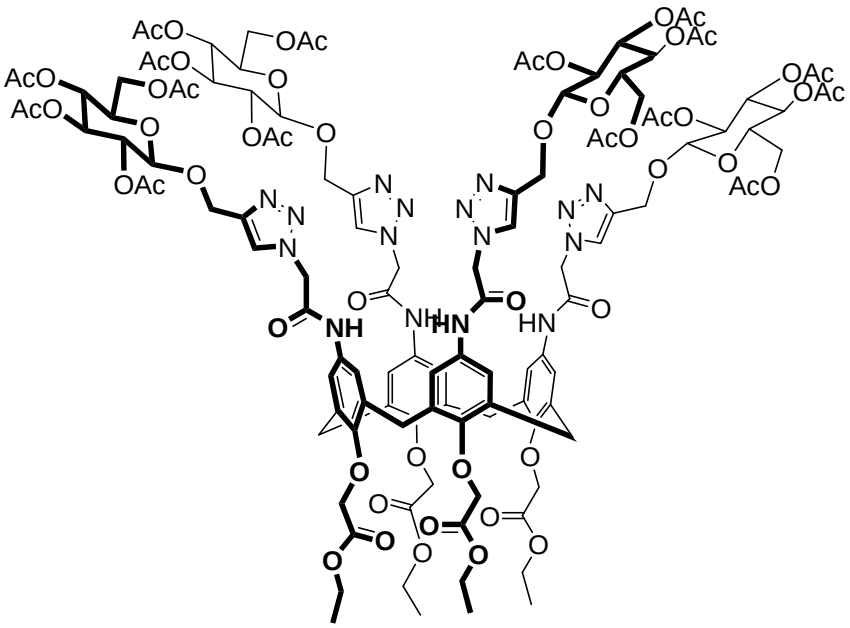

In a test tube were added compound **29** (0.05 g, 0.0043 mmol), peracetylated 2-propynil-β-D-glucose (0.099 mg, 0.258 mmol), copper sulfate pentahydrate (6.5 mg, 0.026 mmol), sodium ascorbate (10.3 mg, 0.052 mmol) and DMF with 10 drops of water. The suspension was stirred under microwave irradiation in the dark at 80°C, 150 W for 20 minutes. The reaction was monitored by TLC (SiO_2, eluent: ethyl acetate 100% plus 4 drops of glacial acetic acid). The reaction was quenched with water (10 ml), the product extracted in ethyl acetate (4 x 20 ml),the organic phase dried over sodium sulfate and the solvent evaporated under reduced pressure. The carbohydrate excess was recovered by trituration of the crude product with ethyl ether to obtain the compound **30** as brown solid. **Yield** 84%.

^{1}H-NMR (300 MHz, $CDCl_3$): δ (ppm) = 8.03 (bs, 4H, CH tr); 6.94 (bs, 8H, Ar); 5.24-5.21 (m, 20H, OCH_2CO, $OCCH_2N$, H-3); 5.04 (t, J=18 Hz, 4H, H-4); 4.95-4.70 (m, 16H, H-2, H-1, Ar-C*H*$_2$-Ar ax); 4.72 (bs, 8H, OCH_2-tr); 4.34-4.15 (m, 16H, H-6, H-6' and OC*H*$_2$$CH_3$); 3.95-3.85 (m, 4H, H-5); 3.20-3.09 (bs, 4H, Ar-C*H*$_2$-Ar eq); 2.02, 1.99, 1.95 and 1.94 (4s, 12H each, CH_3CO); 1.27 (bs, 12H, CH_2CH_3). **ESI-MS:** (+) $C_{120}H_{144}N_{16}O_{56}$ m/z = 1376.8 $[M+Na]^{++}$, 925 $[M+Na]^{+++}$

m. p. = 99-103 °C

Synthesis of methyl-3,4,5-trihydroxybenzoate 31

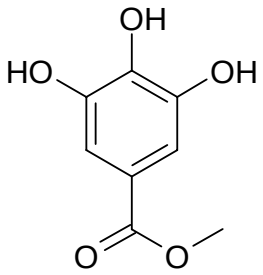

To a solution of gallic acid (0.500 g, 2.9 mmol) in methanol (15 ml) was added a catalytic amount of conc. sulfuric acid (two drops) and the stirring mixture was refluxed overnight. The reaction was quenched with 2N NaOH till neutral pH. Methanol was distilled off and the residue dissolved in ethyl acetate, washed with brine (3 x 20 ml) and water until the pH is neutral. The organic phase was dried over sodium sulfate, the solvent was evaporated under reduced pressure to obtain compound **31** as white solid. **Yield:** 86%.

Physic-chemistry date see: Brouwer, A. J. Mulders, S. J. E. Liskamp, R. M. J. *Eur. J. Org. Chem*. **2001**,1903-1915.

Synthesis of methyl-3,4,5-tripropargyloxybenzoate 32

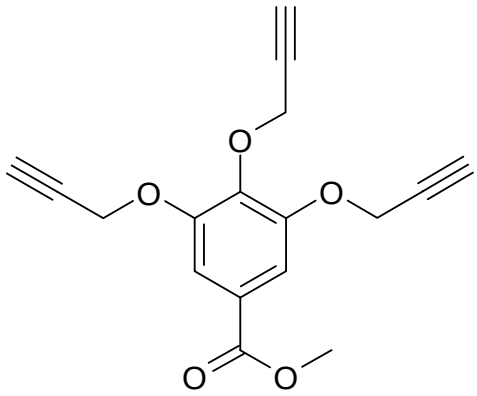

Methyl 3,4,5-trihydroxy benzoate (0.457 g, 2.48 mmol) was dissolved in dry DMF (5 ml) and anhydrous K_2CO_3 (1.30 g, 9.30 mmol) was added under nitrogen atmosphere. To this suspension was added dropwise a solution of propargylbromide (0.831 ml, 9.30 mmol). The mixture was stirred at room temperature for 24h. The reaction was monitored by TLC (SiO_2; eluent cyclohexane/ethyl acetate 2:8). Then, DMF was distilled off under vacuum and the brown solid was solubilised in ethyl acetate (20 ml) and washed with water (3 x 20 ml), 1M $KHSO_4$ (3 x 20 ml) and

brine (3 x 20 ml). The organic phase was dried over sodium sulfate, the solvent was removed under reduce pressure to obtain compound **32** as white solid. **Yield** 91%.

^{1}H NMR (300 MHz,$CDCl_3$) : δ (ppm): 7.46 (s, 2H, H-Ar); 4.82 (d, 2H, J = 2.45 Hz, C*H*$_2$-propargyl); 4.79 (d, 4H, J = 2.40 Hz, C*H*$_2$-propargyl); 3.90 (s, 3H, COOC*H*$_3$); 2.53 (t, 2H, J = 2.39, $CH_2C{\equiv}CH$); 2.45 (t, 1H, J = 2.40 Hz $CH_2C{\equiv}CH$);

^{13}C NMR (75 MHz, $CDCl_3$): δ (ppm): 166.2 (C=O); 151.2, 141.0, 125.7, 109.8 (Ar); 78.6 77.9 ($OCH_2C{\equiv}CH$); 76.13, 75.5 (C≡CH); 60.3, 56.9 (OCH_2); 52.3 (OCH_3).

ESI-MS: (+)$C_{17}H_{14}O_5$ m/z = 321.2 $[M+Na]^+$.

Synthesis of 3,4,5-tripropargyloxybenzoate 33

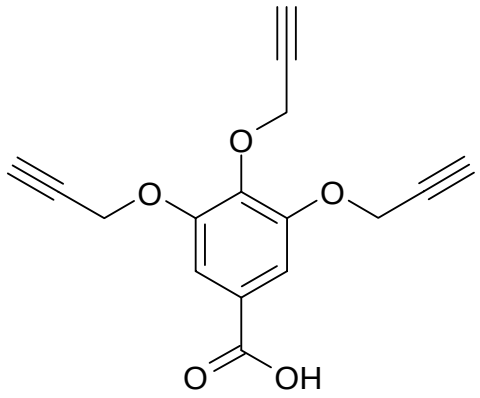

To a solution of compound **32** (672.6 mg 2.25 mmol) in a dioxane/methanol 15:1 mixture (4 ml) was added an aqueous 4M NaOH solution (2 ml). The solution was stirred to room temperature overnight and monitored by TLC (SiO_2; eluent cycloexane /ethyl acetate 4:6). After complete conversion of starting material, the reaction was quenched with 1N HCl until neutral pH. The solution was evaporated to obtain a solid that was dissolved in ethyl acetate. The solution was washed with 1M $KHSO_4$ solution (3 x 50 ml) and brine (3 x 50 ml). The organic phase was separated and dried over sodium sulfate, the solvent was evaporated under reduced pressure to obtain a white solid pure. **Yield:** 96%.

^{1}H NMR (300 MHz,CD_6CO): δ(ppm): 7.53 (s, 2H, H-Ar); 4.93 (d, 4H, J = 2.42 Hz OC*H*$_2$C≡CH); 4.82 (d, 2H, J = 2.49 Hz OC*H*$_2$C≡CH); 3.13 (t, 2H, J = 2.38 Hz $OCH_2C{\equiv}CH$); 3.00 (t, 1H, J = 2.42 Hz $OCH_2C{\equiv}CH$); **^{13}C NMR** (75 MHz, acetone-d6): δ (ppm): 166.9 (CO); 152.4, 141.8, 126.8, 110.6 (Ar); 79.8, 79.3 ($OCH_2C{\equiv}CH$); 77.5, 76.9 ($OCH_2C{\equiv}CH$); 60.5, 57.5 ($OCH_2C{\equiv}CH$).

ESI-MS: (+)$C_{16}H_{12}O_5$ m/z = 284 $[M+Na]^+$

Synthesis of compound 34a

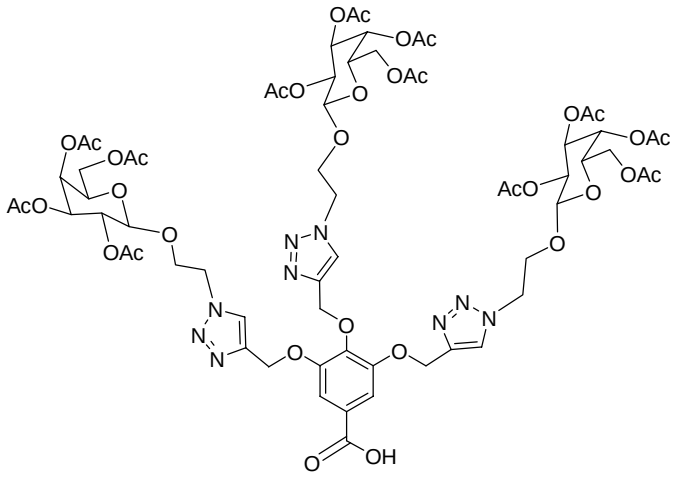

To a suspension of **33** (300 mg, 1.06 mmol) and **23** (1.72 g, 4.13 mmol) in DMF/H_2O 1:1, was added copper sulfate pentahydrate (13.23 mg, 0.05 mmol) and sodium ascorbate (105 mg, 0.53 mmol). The mixture was allowed to react in the dark under vigorously stirring. The reaction was monitored by TLC (SiO_2 ; eluent: cycloexane/ethyl acetate 1:9). After complete conversion of starting material the reaction was quenched with water (20 ml) to obtain a white solid that was purified by flash chromatography (SiO_2 ; eluent: cycloexane/ethyl acetate 3:7, 2:8, 100% acetone) to obtain compound **34a** as white foam. **Yield** 56%.

^{1}H NMR (300 MHz,$CDCl_3$): δ(ppm): 7.86 (bs, 3H, H-Tr); 7.47 (bs, 2H, H-Ar); 5.37 (d, J = 3.0 Hz, H-4); 5.23 (bs, 6H, OC*H_2*Tr); 5.20-5.10 (m, 3H, H-2); 5.00-4.96 (m, 3H, H-3); 4.60-4.52 (m, 6H, N*CH_2*CH_2O); 4.50 (d, 1H, J = 7.8 Hz, H-1); 4.49 (d, 2H, J = 8.1 Hz, H-1); 4.35-4.20 (m, 3H, NCH_2C*H_2*O); 4.20-4.04 (m, 6H, H-6, H-6'); 4.04-3.84 (m, 6H, NCH_2C*H_2*O, H-5); 2.14, 2.04, 1.96, 1.94 (4s, 9H, each, COC*H_3*). **^{13}C NMR** (75 MHz, $CDCl_3$): δ(ppm) 170.3, 170.1, 169.9, 169.6, 151.9, 144.0, 143.2, 141.9, 125.0, 124.6, 109.6, 100.9, 100.8, 70.8, 70.5, 68.3, 67.8, 67.4, 66.9, 66.2, 62.8, 61.6, 61.1, 50.0, 49.7, 20.6. **ESI-MS:** (+) $C_{64}H_{81}N_9O_{35}$ m/z = 1581.0 $[MNa + Na]^+$.

Synthesis of compound 35a

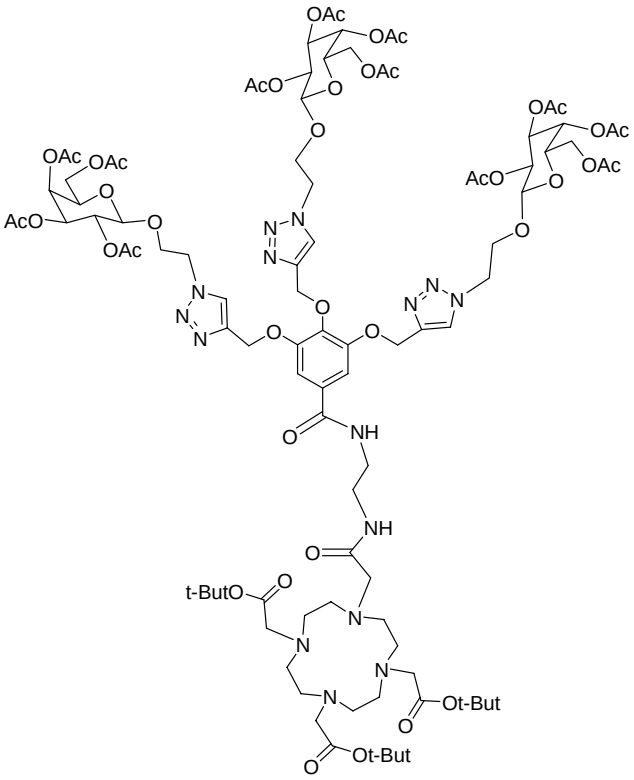

To a stirring solution of compound **34a** (200 mg, 0.13 mmol) and DCM (10 ml) in a two-necked flask under nitrogen atmosphere, was added HBTU (74 mg; 0.19 mmol), DOTA amino derivative **12** (80 mg, 0.13 mmol) and TEA (0.036 ml 0.26 mmol,). The reaction mixture was stirred at room temperature for 24h. The reaction was monitored by TLC (SiO_2, eluent dichloromethane/methanol 9:1). The reaction was quenched with water (15 ml) the organic phase extracted with dichloromethane (3 x 10 ml), and dried on sodium sulphate. The solvent was evaporated under reduced pressure to obtain a crude product as orange. Compound **35a** was obtained pure by flash-chromatography (SiO_2, eluent dichloromethane/methanol 96:4) as an white solid. **Yield:** 84%.

^{1}H NMR (300 MHz, DMSO-d_6): δ(ppm): 8.42 (bs, 1H, CON*H*); 8.21 (bs, 1H, CON*H*); 8.11 (s, 2H, H-Tr); 7.92 (s, 1H, H-Tr); 7.37 (s, 2H, H-Ar); 5.25 (d, J = 3.3 Hz, 3H, H-4); 5.17 (bs, 4H, OCH_2Tr); 5.15-5.07 (m, 3H, H-3); 5.05 (bs, 2H, OCH_2Tr); 4.96-4.83 (m, 3H, H-2); 4.73 (d, J = 8.1 Hz, 2H, H-1); 4.71 (d, J = 8.1, Hz, 1H, H-1); 4.64-4.55 (m, 3H, NC*H*HCH$_2$O); 4.55-4.41 (m, 3H, NC*H*HCH$_2$O); 4.30-4.15 (m, 3H, H-5); 4.16-4.08 (m, 3H, NCH$_2$C*H*HO); 4.08-4.01 (m, 6H, H-6 H-6'); 4.00-3.81 (m, 3H, NCH$_2$C*H*HO); 2.09, 2.00, 1.89, 1.88 (4s, 9H each, OCOCH_3); 1.44 (s, 9H, COOC(CH_3)$_3$); 1.43 (s, 18H, COOC(CH_3)$_3$). **^{13}C NMR** (75 MHz, DMSO-d_6): δ(ppm) 172.3, 172.0, 171.4, 169.7, 169.3, 168.9, 151.4, 143.1, 142.3, 129.8, 124.5, 106.8, 99.5, 80.9, 80.8, 69.9, 69.8,

68.1, 67.1, 65.5, 62.3, 61.1, 55.8, 55.2, 49.2, 49.0, 38.1, 27.5, 27.4, 27.3, 20.3, 20.2, 20.1, 20.0. **ESI-MS:** (+) $C_{94}H_{137}N_{15}O_{41}$ m/z = 1089.6 $[M + 2Na]^{2+}$, 2155.8 $[M + Na]^{+}$.

Synthesis of compound 36a

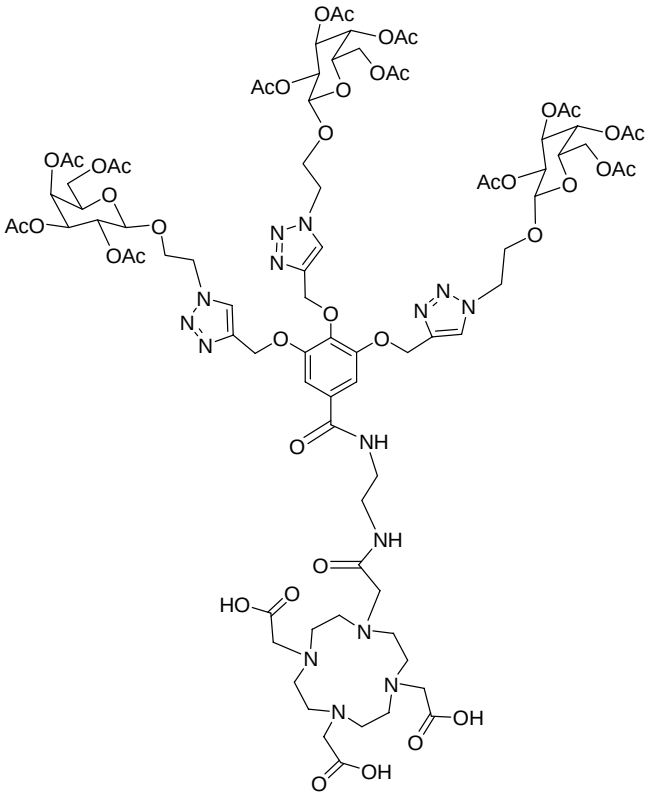

To a solution of compound **35a** (232.8 mg 0.11 mmol) in dichloromethane (1.5 ml) was added, at 0°C, triethylsilane (0.088 ml 0.55 mmol,) and trifluoroacetic acid (0.111 ml, 1.49 mmol) The mixture was stirred at room temperature for 24 h and monitored by TLC (SiO_2; eluent dichloromethane/methanol 9:1). After complete conversion of starting material, the solvent was evaporated under reduced pressure and the crude was washed several times with chloroform and ethyl ether until to obtained compound **36a** as white solid without further purification. **Yield** 92%.
^{1}H NMR (300 MHz, $CDCl_3$): δ(ppm): 11.40 (bs, 3H, COO*H*); 7.95 (bs, 3H, H-Tr); 7.30 (bs, 2H, H-Ar); 5.38 (bs, 3H, H-4); 5.28-5.16 (m, 6H, OCH_2Tr); 5.16-5.09 (m, 3H, H-2); 5.04-4.91 (m, 3H, H-3); 4.63 (bs, 6H, NCH_2CH$_2$O); 4.50 (d, 3H, J = 7.8 Hz, H-1); 4.34-3.76 (m, 15H, NCH$_2$CH_2O, H-6, H-6', H-5); 3.68-2.48 (multiplets and bs, 28H, NCH_2CH_2N, NCH_2CONH, NCH_2CH_2-crown, NCH_2COOH); 2.13, 2.02, 1.95, 1.91 (4s, 9H each, OCOCH_3). **^{13}C NMR** (75 MHz, $CDCl_3$): δ(ppm) 170.5, 170.2, 170.0, 169.8, 160.6, 160.1, 159.6, 152.7, 125.2, 117.1, 113.3,100.7, 70.8, 70.5, 68.4, 66.9, 61.8, 61.1, 50.7, 38.7, 29.6, 20.5. **ESI-MS:** (+) $C_{82}H_{113}N_{15}O_{41}$ m/z = 1035.1 $[MNaK+2Na]^{2+}$, 1014 $[MNa+2Na]^{2+}$.

Synthesis of compound 37a

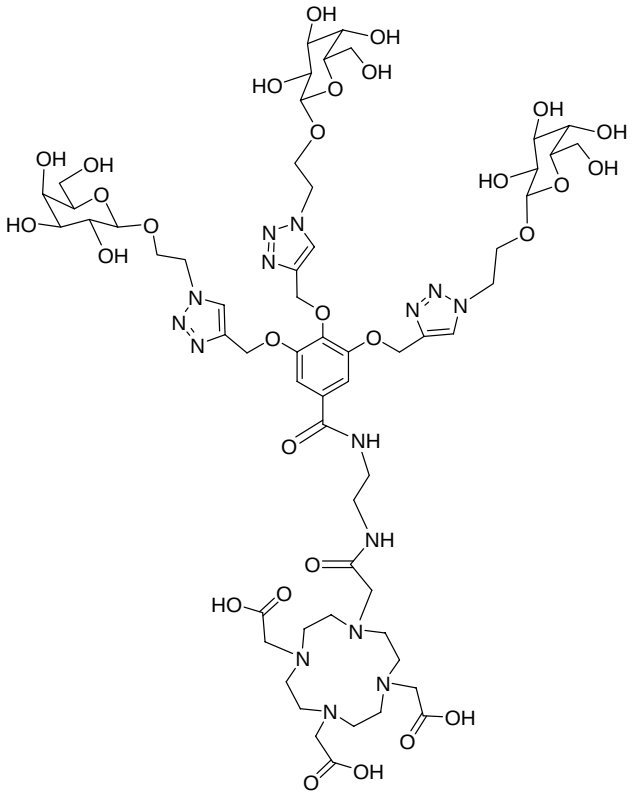

To a solution of compound **36a** (199 mg 0.10 mmol) in methanol (25 ml) was added, a solution of sodium methoxide until pH is 8-9. The solution was stirred at room temperature for 2h. The reaction was monitored by TLC (SiO_2; eluent ethyl acetate/iso-propanol/water 5:2:1. After complete conversion of starting material, the reaction was quenched by addition of AMBERLITE IR 120 H^+ resin until neutral pH. The resin was filtered, washing with methanol and the solvent was evaporated under reduced pressure to obtained product as beige solid without further purification. **Yield** 98%.

^{1}H NMR (300 MHz, D_2O): δ(ppm): 8.20 (bs, 2H, H-Tr); 7.88 (bs, 1H, H-Tr); 7.34 (bs, 2H, H-Ar); 5.26 (bs, 4H, OCH_2Tr); 5.13 (bs, 2H, OCH_2Tr); 4.80-4.67 (m, 4H, NCH_2CH_2O); 4.67-4.52 (m, 2H, NCH_2CH_2O); 4.43-4.29 (m, 5H, H-1, NCH_2CH_2O); 4.29-3.95 (m, 4H, NCH_2CH_2O); 3.92 (d, J = 3.2 Hz, H-4); 3.82-2.62 (multiplets and bs, 43H, H-5, H-3, H-6, H-6', H-2, $NHCH_2CH_2NH$, NCH_2CO, NCH_2COOH, NCH_2CH_2N-crown). **^{13}C NMR** (75 MHz, D_2O): δ(ppm) 172.6, 155.0, 146.1, 129.4, 110.6, 106.4, 78.4, 75.9, 74.2, 73.9, 72.6, 72.3, 71.8, 71.3, 68.5, 65.4, 64.2, 54.5, 53.8, 53.6, 42.9, 41.6. **ESI-MS:** (+) $C_{58}H_{89}N_{15}O_{29}$ m/z = 753.01 $[M+2Na]^{2+}$, 731.05 $[M+2H]^{2+}$, 1482.7 $[M+Na]^+$.

Synthesis of compound 34b

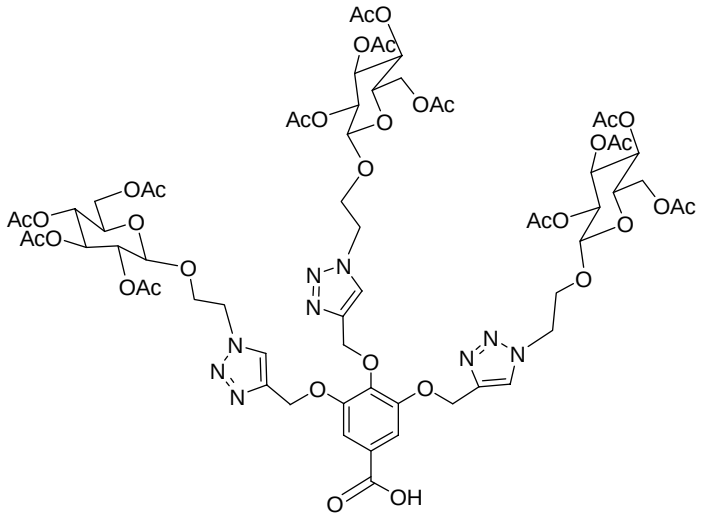

To a suspension of **33** (300 mg, 1.06 mmol) and peracetylated glucose-*O*-2-azido **23a** (1.46 g, 3.49 mmol) in DMF/H_2O 1:1, was added copper sulfate pentahydrate (25 mg, 0.10 mmol) and sodium ascorbate (105 mg, 0.53 mmol). The mixture was allowed to react in the dark under vigorously stirring. The reaction was monitored by TLC (SiO_2 ; eluent: cycloexane/acetone 2:8, 0.1% of acetic acid). After complete conversion of starting material the reaction was quenched with water (20 ml) to obtain a white solid that was purified by flash chromatography (SiO_2 ; eluent: cycloexane/ethyl acetate 3:7, 2:8, 100% acetone) to obtain compound **34b** as white foam. **Yield** 56%.

^{1}H NMR (300 MHz, $CDCl_3$): δ(ppm):7.87 (bs, 2H, H-Tr); 7.82 (bs. 1H, H-Tr); 7.47 (bs, 2H, H-Ar); 5.28 (bs, 6H, OC*H_2*Tr); 5.23-4.93 (m, 9H, H-3, H-4, H-2); 4.65-4.48 (m, 6H, NC*H_2*CH_2O); 4.53 (d, J = 8.1 Hz, 3H, H-1); 4.45-3.85 (m, 12H, NCH_2C*H*HO, H-6, H-6') 3.80-3.60 (m, 3H, H-5); 2.06, 2.00, 1.97, 1.92 (4s, 9H each, OCOC*H_3*). **^{13}C NMR** (75 MHz, $CDCl_3$): δ(ppm) 170.6, 170.1, 169.4, 151.9, 144.0, 143.2, 141.7, 125.1, 124.6, 109.5, 100.5, 100.4, 72.4, 71.8, 70.8, 70.7, 68.1, 67.6, 66.1, 62.8, 61.7, 50.0, 49.7, 20.7, 20.5. **ESI-MS:** (+) $C_{64}H_{81}N_9O_{35}$ m/z = 790.2 $[M+2Na]^{2+}$, 801.7 $[MNa+2Na]^{2+}$, 1558.4 $[M+Na]^+$.

Synthesis of compound 35b

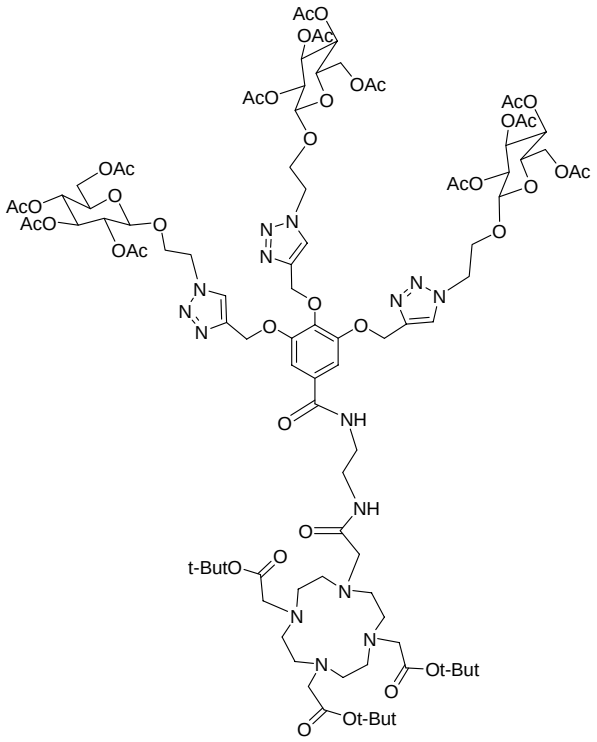

To a stirring solution of compound **34b** (400 mg, 0.26 mmol) and DCM (20 ml) in a two-necked flask under nitrogen atmosphere, was added HBTU (148 mg; 0.39 mmol), DOTA amino derivative **12** (160 mg, 0.26 mmol) and TEA (0.072 ml 0.52 mmol,). The reaction mixture was stirred at room temperature for 24h. The reaction was monitored by TLC (SiO_2, eluent dichloromethane/methanol 9:1). The reaction was quenched with water (20 ml) the organic phase extracted with dichloromethane (3 x 10 ml), and dried on sodium sulphate. The solvent was evaporated under reduced pressure to obtain a crude product as orange. Compound **35b** was obtained pure by flash-chromatography (SiO_2, eluent dichloromethane/methanol 96:4) as an white solid. **Yield:** 55%.

^{1}H NMR (300 MHz, $CDCl_3$): δ(ppm): 7.95 (bs, 1H, H-Tr); 7.90 (bs, 2H, H-Tr); 7.28 (bs, 2H, H-Ar); 7.09 (bs, 1H, N*H*CO) 6.71 (bs, 1H, N*H*CO) 5.23 (bs, 4H, OCH_2Tr); 5.20 (bs, 2H, OCH_2Tr); 5.18-4.90 (m, 9H, H-3, H-4, H-2); 4.63-4.50 (m, 6H, NCH_2CH_2O, H-1); 4.32-3.92 (m, 12H, NCH_2CH_2O, H-6, H-6'); 3.80-3.68 (m, 3H, H-5); 2.08, 2.00, 1.97, 1.93 (4s, 9H each, $OCOCH_3$); 1.45 (s, 18H, $OC(CH_3)_3$); 1.44 (s, 9H, $OC(CH_3)_3$). **^{13}C NMR** (75 MHz, $CDCl_3$): δ(ppm): 172.3, 171.8, 170.7, 170.0, 169.5, 169.4, 152.0, 144.3, 143.5, 129.9, 124.9, 124.5, 107.1, 100.5, 100.3, 82.0, 72.6, 71.8, 71.7, 70.7, 68.2, 67.5, 66.4, 62.9, 61.7, 55.8, 55.6, 49.8, 49.5, 38.6, 27.9, 20.7, 20.6. **ESI-MS:** (+) $C_{94}H_{137}N_{15}O_{41}$ m/z = 1089.4 $[M + 2Na]^{2+}$.

Synthesis of compound 36b

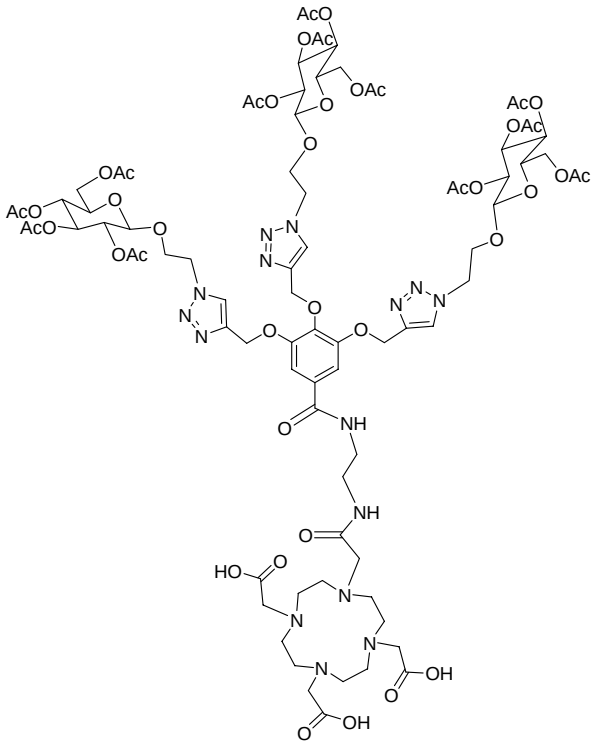

To a solution of compound **35b** (300 mg 0.14 mmol) in dichloromethane (3 ml) was added, at 0°C, triethylsilane (0.112 ml 0.70 mmol,) and trifluoroacetic acid (0.470 ml, 5.74 mmol) The mixture was stirred at room temperature for 24 h and monitored by TLC (SiO_2; eluent dichloromethane/methanol 9:1). After complete conversion of starting material, the solvent was evaporated under reduced pressure and the crude was washed several times with chloroform and ethyl ether until to obtained compound **36b** as white solid without further purification. **Yield** 78%.
^{1}H NMR (300 MHz, $CDCl_3$): δ(ppm): 7.93 (bs, 3H, H-Tr); 7.30 (bs, 2H, H-Ar); 5.25-4.80 (m, 15H, OCH_2Tr, H-4, H-3, H-2); 4.80-4.45 (m, 9H, NCH_2CH_2O, H-1); 4.40-2.35 (multiplets and bs, 43H, H-5, NCH_2CH_2O, $CONHCH_2CH_2NHCO$, NCH_2CO, NCH_2COOH, NCH_2CH_2N-crown); 2.05, 2.00, 1.97, 1.89 (4s, 9H each, $OCOCH_3$). **^{13}C NMR** (75 MHz, $CDCl_3$): δ(ppm): 170.7, 170.1, 169.5, 165.8, 100.4, 72.4, 71.8, 70.8, 68.3, 65.8, 61.7, 40.1, 38.6, 20.7, 20.5. **ESI-MS:** (+) $C_{82}H_{113}N_{15}O_{41}$ m/z = 1035.2 $[MNaK+2Na]^{2+}$, 1013.3 $[MNa+2Na]^{2+}$ 1005.3 $[M+2Na]^{2+}$.

Synthesis of compound 37b

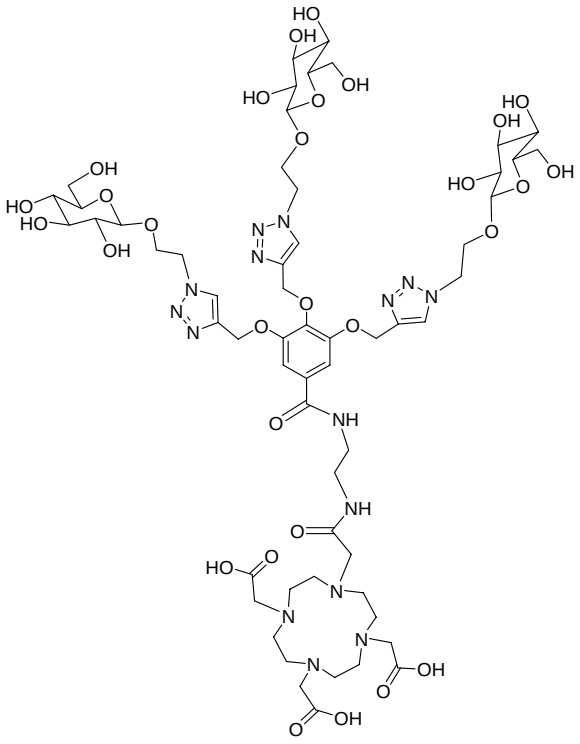

To a solution of compound **36b** (215.6 mg 0.11 mmol) in methanol (30 ml) was added, a solution of sodium methoxide until pH is 8-9. The solution was stirred at room temperature for 2h. The reaction was monitored by TLC (SiO_2; eluent ethyl acetate/iso-propanol/water 5:2:1. After complete conversion of starting material, the reaction was quenched by addition of AMBERLITE IR 120 H^+ resin until neutral pH. The resin was filtered, washing with methanol and the solvent was evaporated under reduced pressure to obtained product as beige solid without further purification. **Yield** 81%.

^{1}H NMR (300 MHz, D_2O): δ(ppm): 8.17 (bs, 2H, H-Tr); 7.83 (bs, 1H, H-Tr); 7.30 (bs, 2H, H-Ar); 5.25 (bs, 4H, OCH_2Tr); 5.09 (bs, 2H, OCH_2Tr); 4.69 (bs, 4H, NCH_2CH_2O); 4.56 (bs, 2H, NCH_2CH_2O); 4.45-4.35 (m, 3H, H-1); 4.30-3.93 (m, 6H, NCH_2CH_2O); 3.90-3.75 (m. 3H, H-6'); 3.68-2.68 (multiplrts and bs, 43H, H-5, H-3, H-6, H-4, H-2, $CONHCH_2CH_2NHCO$, $NHCOCH_2N$, CH_2COOH $NHCH_2CH_2NH$-crown). **^{13}C NMR** (75 MHz, D_2O): δ(ppm); 172.4, 154.9, 146.0, 141.7, 133.6, 129.5, 129.4, 110.5, 105.7, 79.2, 78.8, 76.2, 72.9, 71.3, 65.3, 64.0, 53.7, 53.5, 42.9, 41.6, 33.5. **ESI-MS:** (+) $C_{58}H_{89}N_{15}O_{29}$ m/z = 760.9 $[M+K+Na]^{2+}$, 783.3 $[MNa+Na+K]^{2+}$.

4.7 References

[1] R. A. Moats, S. E. Fraser, T. J. Meade, *Angew. Chem., Int. Ed. Engl.*, **1997**, *36*, 726

[2] A. Y. Louie, M.M. Huber, E. T. Ahrens, U. Rothbacher, R. Moats, R. E. Jacobs, S. E. Fraser, T. J. Meade *Nat. Biotechnol.* **2000**, *18***,** 321-325

[3] J. A. Duimstra, F. J. Femia, T. J. Meade, *J. Am. Chem. Soc.*, **2005**, *127*, 12847-12855.

[4] S. Laurent, E. L. Vander, Y. Fu, R. N. Muller *Bioconjug. Chem.*, **2004**, *15*, 99-103.

[5] J. J. Lundquist, E. J. Toone *Chem. Rev.*, **2002**, 102, 555-578.

[6] H. Lis, N. Sharon *Chem. Rev.*, **1998**, 98, 637-674.

[7] J.P. André, C.F.G.C. Geraldes, J.A. Martins, A.E. Merbach, M.I.M. Prata, A.C. Santos, J.J.P. de Lima, E. Toth *Chem. Eur. J.* **2004**, *10*, 5804–5816.

[8] P. Baıa, J.P. Andre´, C.F.G.C. Geraldes, J.A. Martins, A.E. Merbach, E. Toth *Eur. J. lnorg. Chem.* **2005**, 2110–2119.

[9] M.I.M. Prata, A. C. Santos, S. Torres, J.P. Andre´, J.A. Martins, M. Neves, M. L. Garcia-Martin, T. B. Rodrigues, P. Lopez-Larrubia, S. Cerdan, C.F.G.C. Geraldes *Contrast Media Mol. Imag.* **2006**, *1*, 246-258.

[10] M. Takahashi, Y. Hara, K. Aoshima, H. Kurihara, T. Ashikawa, M. Yamashita *Tetrahedron Lett.* **2000**, *41*, 8485-8488.

[11] D. A. Fulton, E. M. Elemento, S. Aime, L. Chaabane, M. Botta, D. Parker *Chem. Commun.* **2006**, 1064-1066.

[12] R. Huisgen, *Angew. Chem., Int. Ed. Engl.* **1963**, 2, 565.

[13] Tome, A. C. Storr, R. C. Gilchrist, T. L. *Science of Synthesis* Eds.; Thieme: New York, **2004,** vol. 13, pp. 415-601.

[14] Krivopalov, V. P. Shkurko, O. P. *Russ. Chem. Rev.* **2005,** 74, 339.

[15] Huisgen, R. *Pure Appl. Chem.* **1989,** 61, 613.

[16] Huisgen, R. *In 1,3-Dipolar Cycloaddition Chemestry;* Padwa, A., Ed.; Wiley: New York, **1984,** Vol. 1, pp.1-176.

[17] Himo, F. Lovell, T. Hilgraf, R. Rostovtsev, V. V. Noodleman, L. Sharpless, K. B. Fokin, V. V. *J. Am. Chem. Soc.* **2005,** 127, 210.

[18] Rostovtsev, V. V. Green, L. G. Fokin, V. V: Sharpless, K. B. *Angew. Chem. Int. Ed.* **2002,** 41, 2596.

[19] Perez-Balderas, F. Ortega-Munoz, M. Morales-Sanfrutos, J. Hernandez-Mateo, F. Calvo-Flores, F. G. Calvo-Asin, J. A. Isac-Garcia, J. Santoyo-Gonzalez, F. *Org. Lett.* **2003,** 5, 1951.

[20] Malkoch, M. Schleicher, K. Drocknmuller, E. Hawker, C. J. Russel, T. P. Wu, P. Fokin, V. V. *Macromolecules* **2005,** 38, 3663.

[21] Wu, P. Feldman, A. K. Nugent, A. K. Hawker, C. J. Scheel, A. Voit, B. Pyun, J. Frèket, J. M. J. Sharpless, K. B. Fokin, V. V. *Angew. Chem. Int. Ed.* **2004,** 43, 3928.

[22] Rostovtsev, V. V. Green, L. G. Fokin, V. V. Sharpless, K. B. *Angew. Chem.* **2002,** 114, 2708-2711.

[23] Tornoe, C. W. Christensen, C. Meldal, M. *J. Org. Chem.* **2002,** 67, 3057-3062.

[24] S. Aime, E. Gianolio, F. Uggeri, S. Tagliapietra, A. Barge, G. Cravotto *J. Inorg. Biochem.* **2006**, *100*, 931–938.

[25] W. J. M. Mulder, G. J. Strijkers, A. W. Griffioen, L. van Bloois, G. Molema, G. Storm, G. A. Koning, K. Nicolay *Bioconjugate Chem.* **2004,** *15,* 799-806

[26] Sansone, F.; Chierici, E.; Casnati, A.; Ungaro, R. *Org. Biomol. Chem.* **2003,** *1*, 1802-1809.

[27] Sansone, F.; Baldini, L.; Casnati, A.; Ungaro, R. *Supramol. Chem.* **2008,** *20*, 161-168.

[28] André, S.; Sansone, F.; Kaltner, H.; Casnati, A.; Kopitz, J.; Gabius, H. J.; Ungaro, R. *Chembiochem* **2008,** *9*, 1649-1661.

[29] Schädel, U.; Sansone, F.; Casnati, A.; Ungaro, R. *Tetrahedron* **2005,** *61*, 1149-1154.

[30] Dondoni, A.; Marra, A.; Scherrmann, M. C.; Casnati, A.; Sansone, F.; Ungaro, R. *Chem. Eur. J.* **1997,** *3*, 1774-1782.

[31] Marra, A.; Scherrmann, M. C.; Dondoni, A.; Casnati, A.; Minari, P.; Ungaro, R. *Angew. Chem. Int. Engl. Ed.* **1994,** *33*, 2479-2481.

[32] Arena,G. Cali, R. Lombardo, G. G. Rizzarelli, E. Sciotto, D. Ungaro, R. Casnati, A., *Supramol. Chem.* **1992,** 1, 19-24.

[33] Casnati, A.. Ferdani, R. Pochini, A. Ungaro, R *J. Org. Chem.* **1997** 62,6236.

[34] Parker D. *Macrocycle Synthesis A Pratical Approach* Ed. by D. Parker Department of Chemistry, University of Durham, UK, Oxford Universiry Press **1996.**

[35] Michael. Lattman, Suman K. Chopra, Alan H. Cowley, Atta M. Arif *Organometallics* vol. 5 No. 4, **1986,** 677–683

[36] Dadabhoy, A. Faulkner, S. Sammes, P. G. .*J. Chem. Soc. Perkin Trans.* 2, **2002**, 348-357

[37] (a) Husigen, R. In *1,3-Dipolar Cycloaddition Chemistry* ; Pdwa, A. Ed.; Wiley: New York, **1984** ; pp. 1-176. (b) Pdwa, A. In *Comprehensive Organic Synthesis;* Trost, B. M., Ed. Prgamon: Oxford, **1991**; vol. 4, pp. 1069-1109. (c) Fan, W.-Q. ; Katritzky, A. R. In *Comprehensive Heterocyclic Chemistry II;* Katritzky, A. R., Rees, C. W., Scriven, E. F. V., Eds.; Pergamon: Oxford, **1996**; vol. 4, pp 101-126.

[38] Kolb, H. C.; Finn, M. G.; Sharpless, K. B. *Angew. Chem. Int. Ed.* 2001, , **2004,** 40

[39] (a) Tornøe, C. W.; Christensen, C.; Meldal, M. *J. Org. Chem.* **2002,** 67, 3057. (b) Rostovtsev, V. V.; Green, L. G.; Fokin, V. V.; Sharpless, K. B. *Angew. Chem. Int. Ed.* **2002**, 41, 2596. (c) For study on the mechanism of the Cu(I)-mediated cycloaddition, see; Rodionov, V. O.; Fokin, V. V.; Finn, M. G. *Angew. Chem., Int. Ed.* **2005**, 44, 2210.

[40] Fernandez-Megia, E. Correa, J. Rodriguez-Meizioso, I. Riguera, R. *Macromolecules* **2006,** 39, 2113-2120.

[41] Dondoni A. Marra A. *J. Org. Chem.*, **2006**, *71* (20), 7546–7557.

[42] Da Silva, E.; Coleman, A. W.; *Tetrahedron* 59 **2003** 7357-7364.

[43] Arduini, A. Pochini, A. Sicuri, A. R. Secchi, A. Ungaro, R. *Gazzetta chimica italiana,* **1994**, 124, 129-132

[44] Kenkichi Sonogashira, *Journal of Organometallic Chemistry*, **2002**, 653, 46-49

[45] Yi-Jen Chen, Gene-Hsaing Lee, Shie-Ming Peng, Chen-Yu Yeh, *Tetrahedron letters* , **2005**, 46, 1541-1544

[46] Jan Dahmén, Torbjörn Frejd, Gunnar Grönberg, Thomas Lave, Göran Magnusson, Ghazi Noori *Carbohydrate Research* **1983**, 116, 303.

[47] Sasaky, A.. Murahashi, N. Yamada, H Morikawa, A. *Biol. Pharm. Bull*., **1995**, 18 (5), 740-746.

[48] Iawamoto, K. Shinkai, S. *J. Org. Chem.* **1992**, 57, 7066-7073.

[49] Regayeg, M. Vocanson, F. Duport, A. Blondeau, B. Perrin, M. Fort, A. Lamartire, R. *Materials Science & Engineering c* **2002**, 21, 131-135.

[50] Gujadhur, R. Venkataraman, D. Kintigh, J. T. *Tetrahedron lett.* **2001,** 42, 4791-4793.

[51] Böhmer, V. Vogt, W. Harris, S. J. Leonard, R. G Collins, E. M. Deasy, M.. McKervey, M. A Owens, M. *J. Chem. Soc., Perkin Trans. 1*, 1990, 431 - 432

[52] Brouwer A. J. Mulders, S. J. E. Liskamp, R. M. J. *Eur. J. Org. Chem.* **2001**, 1903-1915.

[53] Dirk T. S. Rijkers, G. Wilma van Esse, Remco Merkx, Arwin J. Brouwer, Hans J. F. Jacobs, Roland J. Pieters and Rob M. J. Liskamp *Chem. Comm.* **2005**, 4581-4583.

[54] João P. André, Carlos F. G. C. Geraldes, José A. Martins, André E. Merbach, Maria I. M. Prata, Ana C. Santos, João J. P. de Lima, Éva Tóth *Chem. Eur. J.* **2004**, 10, 5813